UNIVERSIDAD DE MÁLAGA
Facultad de Ciencias
Departamento de Microbiología

Programa de Doctorado en Biología Celular y Molecular

TESIS DOCTORAL

La matriz extracelular de la biopelícula en la ecología de dos especies de *Pseudomonas* asociadas a plantas

Zaira María Heredia Ponce

Abril 2021

Directores:
Antonio de Vicente Moreno
José Antonio Gutiérrez Barranquero

AUTOR: Zaira María Heredia Ponce

https://orcid.org/0000-0002-8707-6168

EDITA: Publicaciones y Divulgación Científica. Universidad de Málaga

DECLARACIÓN DE AUTORÍA Y ORIGINALIDAD DE LA TESIS PRESENTADA PARA OBTENER EL TÍTULO DE DOCTOR

Dña. Zaira María Heredia Ponce

Estudiante del programa de doctorado en Biología Celular y Molecular de la Universidad de Málaga, autora de la tesis presentada para la obtención del título de doctor por la Universidad de Málaga, titulada:

La matriz extracelular de la biopelícula en la ecología de dos especies de *Pseudomonas* asociadas a plantas

Realizada bajo la tutorización de Antonio de Vicente Moreno y dirección de Antonio de Vicente Moreno y José Antonio Gutiérrez Barranquero

DECLARO QUE:

La tesis presentada es una obra original que no infringe los derechos de propiedad intelectual ni los derechos de propiedad industrial u otros, conforme al ordenamiento jurídico vigente (Real Decreto Legislativo 1/1996, de 12 de abril, por el que se aprueba el texto refundido de la Ley de Propiedad Intelectual, regularizando, aclarando y armonizando las disposiciones legales vigentes sobre la materia), modificado por la Ley 2/2019, de 1 de marzo.

Igualmente asumo, ante la Universidad de Málaga y ante cualquier otra instancia, la responsabilidad que pudiera derivarse en caso de plagio de contenidos en la tesis presentada, conforme al ordenamiento jurídico vigente.

En Málaga, a 19 de febrero de 2021.

Fdo.: Zaira María Heredia Ponce

Facultad de Ciencias

Departamento de Microbiología

TESIS DOCTORAL

La matriz extracelular de la biopelícula en la ecología de dos especies de *Pseudomonas* asociadas a plantas

Zaira María Heredia Ponce

Abril 2021

COMITÉ EVALUADOR

Presidente

Jesús M. Murillo Martínez

Departamento de Agronomía, Biotecnología y Alimentación

Universidad Pública de Navarra

Secretario

Cayo J. Ramos Rodríguez

Departamento de Biología Celular, Genética y Fisiología

Universidad de Málaga

Vocal

Jos M. Raaijmakers

Department of Microbial Ecology (NIOO-KNAW)

Universidad de Leiden

Sustitutos

Emilia López Solanilla

Centro de Biotecnología y Genómica de Plantas (CBGP-INIA)

Universidad Politécnica de Madrid

Alejandro Pérez García

Departamento de Microbiología

Universidad de Málaga

Gabriella Pessi Ahrens

Department of Plant and Microbial Biology

Universidad de Zúrich

UNIVERSIDAD DE MÁLAGA

Facultad de Ciencias

Departamento de Microbiología

D. JUAN JOSÉ BORREGO GARCÍA, director del Departamento de Microbiología de la Universidad de Málaga

INFORMA QUE:

Dña. Zaira María Heredia Ponce ha realizado en los laboratorios de este departamento el trabajo experimental conducente a la elaboración de la presente Memoria de Tesis Doctoral

Y para que así conste, y tenga los efectos que correspondan, en cumplimiento de la legislación vigente, expido el siguiente informe.

En Málaga, a 16 de febrero del 2021

DPTO. DE MICROBIOLOGÍA - UNIVERSIDAD DE MÁLAGA

Fdo. D. Juan José Borrego García

UNIVERSIDAD DE MÁLAGA

Facultad de Ciencias

Departamento de Microbiología

D. ANTONIO DE VICENTE MORENO, catedrático del Departamento de Microbiología de la Universidad de Málaga y **D. JOSÉ ANTONIO GUTIÉRREZ BARRANQUERO**, profesor sustituto interino del Departamento de Microbiología de la Universidad de Málaga

INFORMAN QUE:

Dña. Zaira María Heredia Ponce ha realizado bajo la dirección de ambos el trabajo experimental conducente a la elaboración de la presente Memoria de Tesis Doctoral.

Y para que así conste, y tenga los efectos que correspondan, en cumplimiento de la legislación vigente, expiden el siguiente informe.

En Málaga, a 19 de febrero del 2021

Fdo. D. Antonio de Vicente

D. José Antonio Gutiérrez

El presente trabajo fue apoyado por las siguientes fuentes de financiación:

Proyecto de Excelencia de la Junta de Andalucía. Código del proyecto: P12-AGR-1473. Título: "Profundizando en la biología y el control de las dos enfermedades críticas del cultivo del mango en Andalucía". Investigador principal: Dr. Antonio de Vicente Moreno.

Ayudas a proyectos I+D+I en el marco del Programa Operativo FEDER. Código del proyecto: UMA18-FEDERJA-046. Título: "Estudio de una comunidad microbiana sintética como modelo de interacción multitrófica durante el control biológico en la rizosfera frente a hongos fitopatógenos". Investigadores principales: Dr. Francisco M. Cazorla López y Dr. Cayo J. Ramos Rodríguez.

Plan Nacional de I+D+I. Código del proyecto: AGL2014-52518-CR-1-R. Título: "Aprendiendo de las interacciones multitróficas en la rizosfera de aguacate para avanzar en el control biológico contra *Rosellinia necatrix*". Investigador principal: Dr. Francisco M. Cazorla López.

Plan Nacional de I+D+I. Código del proyecto: AGL2017-83368-C2-1-R. Título: "Estrategias de control biológico eficientes contra *Rosellinia necatrix* de la genómica funcional al campo". Investigador principal: Dr. Francisco M. Cazorla López.

Dña. Zaira María Heredia Ponce fue apoyada por las siguientes fuentes de financiación:

Contrato para "Formación de Profesorado Universitario (FPU)" del Ministerio de Educación, Cultura y Deporte. Código FPU15-03644 (2016-2021).

Ayudas D2 para la realización de estancias de investigadores de la UMA en centros de investigación de calidad del Plan Propio de Investigación, Transferencia y Divulgación Científica de la Universidad de Málaga. Desde el 2 de septiembre de 2018 al 1 de diciembre de 2018 (Convocatoria de marzo del 2018) y desde el 26 de agosto del 2019 hasta el 22 de noviembre de 2019 (Convocatoria de marzo del 2019).

AGRADECIMIENTOS

En primer lugar, quiero agradecer a la Universidad de Málaga y al Departamento de Microbiología por proporcionarme las instalaciones para realizar mi Tesis Doctoral. Mi profundo agradecimiento a las tres personas principales implicadas en esta Tesis, mis dos directores Antonio de Vicente y José Antonio Gutiérrez Barranquero, y a mi tercer "director" Francisco Cazorla, por ofrecerme la oportunidad de hacer la tesis en este grupo de investigación, por toda la ayuda y orientación recibida durante estos años, así como por todo lo que he aprendido de vosotros.

Un reconocimiento especial a todos mis compañeros de laboratorio, tanto a los más lejanos como a los más cercanos. Desde el equipo BacBio, donde comencé a dar mis primeros pasos en investigación, hasta "los de genética", los del edificio de I+D+I ("la Torre"), tanto "los de micro" como "los de bioquímica" y en especial a mis compañeros del Laboratorio 1. Estoy agradecida por todos los momentos que hemos pasado juntos, cada conversación, seminario, comida de grupo y congreso que hemos compartido. Quiero destacar a Sandra, Guti, Eva, Rafa, Carmen y France, con los que he convivido a diario en los últimos años, y a Marisa por todos los momentos que hemos compartido juntas, desde el principio. Quiero destacar también la labor esencial de las técnicos Irene, Yandira y Saray. A ti también María, por todo lo que hemos aprendido juntas durante tu trabajo final de grado y de máster, y por ver mi propio reflejo en ti cuando comencé.

Este párrafo va dedicado exclusivamente a Guti, mi director de tesis y compañero de laboratorio. Ha sido un placer compartir contigo todo este tiempo y te estoy eternamente agradecida, no sólo por todo lo que has trabajado conmigo y todo lo que me has ayudado, que ha sido muchísimo, sino por las largas charlas, los infinitos audios de whatsapp en época de pandemia y por animarme a seguir durante todo este tiempo. Eres de esas personas a las que gusta tener cerca porque de ti se puede aprender.

My deepest thanks to Professor Leo Eberl for allowing me to perform two research short-stays at your lab. Both stays were two wonderful experiences in which I fell in love with your research group and Switzerland forever. I also want to thank all the members of your group and people that I have met during the stays for making me feel welcomed, for all the help and support and for everything that I have learned

from you. Specially, I want to thank Gabriela Purtschert and Aurèlian Bailly for their constant assistance and patience.

Y por último a ti, mi amor. Porque contigo no he compartido sólo el tiempo que ha durado mi tesis, sino además toda la carrera y el máster. Has sido un pilar fundamental durante todos estos años y te estoy profundamente agradecida por tu apoyo incondicional, por levantarme el ánimo, por creer en mí cuando ni yo misma lo he hecho, por escuchar pacientemente cada ensayo previo a una charla en público, cada hipótesis y cada problema que he encontrado en el camino, y por todo el tiempo que has invertido en ayudarme a encontrar soluciones. Y respecto a lo personal, no tengo palabras para expresar lo agradecida que estoy por haberte encontrado en mi camino. Eres un compañero de vida ejemplar y siempre serás mi más preciada casualidad. Te quiero mucho.

A Paco,

"Si hay algo verdaderamente cierto es que lo ignoro todo o casi todo. Y me da rabia, porque hubo un tiempo en el que una mente despierta podría haber adquirido todo el saber de la época. Pero ahora ya no es posible. Ya no hay más que pequeños sabios que lo saben todo sobre casi nada. Y yo soy uno de ellos"

Jean Dausset

INDEX

RESUMEN

- **Antecedentes**

Las biopelículas están formadas por grupos de microorganismos adheridos entre sí y a superficies a través de una matriz extracelular producida por ellos mismos que está compuesta principalmente de polisacáridos, proteínas, lípidos y ADN extracelular (Costerton & Lewandowsky, 1995; Costerton *et al.*, 1999; Høiby *et al.*, 2010). Las células que forman parte de las biopelículas se conocen como células sésiles, las cuales difieren de las células planctónicas, que son aquellas que tienen un estilo de vida libre (Marshall, 2006). Estudios recientes indican que la mayor parte de las bacterias se encuentra formando biopelículas (Flemming & Wuertz, 2019; Bar-On & Milo *et al.*, 2019). Las bacterias forman biopelículas tanto en superficies artificiales como naturales, incluyendo el suelo, tejidos internos y externos de todos los organismos vivos, las rocas y el agua, etcétera (Flemming & Wuertz, 2019). Comparado con el estilo de vida planctónico, el estilo de vida de la biopelícula confiere varios beneficios a las células integrantes, como son la mayor protección frente a agentes antimicrobianos y depredadores, tolerancia a las condiciones medioambientales cambiantes y una mayor capacidad de colonización (Jefferson, 2004; Høiby *et al.*, 2010; Yin *et al.*, 2019).

Las bacterias pertenecientes al género *Pseudomonas* están entre los grupos bacterianos más estudiados, ya que su interacción con organismos vivos tiene frecuentemente una gran importancia ecológica y múltiples aplicaciones biotecnológicas (Silby *et al.*, 2011). Dentro del género *Pseudomonas*, la especie *Pseudomonas aeruginosa* constituye uno de los modelos más importantes a nivel mundial para el estudio de la formación de biopelículas y la patogénesis, debido a su relevancia clínica (Diggle & Whiteley, 2020). La matriz extracelular de *P. aeruginosa* se ha estudiado en profundidad y, hasta ahora, se conoce que está compuesta por tres polisacáridos diferentes: alginato, Psl (del inglés, "*polysaccharide synthesis loci*") y Pel (del inglés, *"pellicle loci"*) (Franklin *et al.*, 2011). El papel de estos polisacáridos en la formación de biopelículas desde un punto de vista clínico, relacionado con la resistencia a antibióticos y frente a los mecanismos de defensa del hospedador, se ha analizado en numerosos estudios (Hentzer *et al.*, 2001; Wozniak *et al.*, 2003; Stapper *et al.*, 2004; Leid *et al.*, 2005; Ma *et al.*, 2006, 2012; Colvin *et al.*, 2011; Billings *et al.*, 2013; Ciofu *et al.*, 2019). Cabe resaltar que *P. aeruginosa* es una bacteria ubicua, pero que además puede

actuar como un patógeno de plantas (Elrod & Braun, 1942; Walker *et al.*, 2004). Sin embargo, la importancia biológica de la producción de los polisacáridos alginato, Psl y Pel en un entorno diferente al clínico no ha sido estudiada.

Las bacterias asociadas a plantas forman biopelículas durante la interacción con sus huéspedes (Danhorn & Fuqua, 2007; Bogino *et al.*, 2013) y, dependiendo de si dichas bacterias son patógenas o beneficiosas, siempre que la interacción planta-bacteria sea compatible, el resultado puede ser completamente diferente. Así, en el caso de las bacterias fitopatógenas, éstas pueden promover el desarrollo de enfermedades en las plantas generando graves pérdidas económicas en el sector agrícola; en el caso de bacterias beneficiosas, éstas pueden estimular el crecimiento de las plantas, favorecer la disponibilidad de nutrientes en el suelo e inducir la respuesta inmune (Kennelly *et al.*, 2007; Mercado-Blanco & Bakker, 2007). Por ejemplo, la formación de biopelículas por parte de las bacterias fitopatógenas *Erwinia amylovora*, *Ralstonia solanacearum*, *Xantomonas citri*, *Xylella fastidiosa* y *Pseudomonas syringae* contribuye a la adhesión y colonización de los tejidos vegetales, afectando posteriormente a la virulencia (Yu *et al.*, 1999; Marques *et al.*, 2002; Rigano *et al.*, 2007; Koczan *et al.*, 2009, 2011; Killiny *et al.*, 2013; Arrebola *et al.*, 2015; Mori *et al.*, 2016). Por otro lado, la formación de biopelículas por parte de bacterias beneficiosas como *Bacillus subtilis*, *Pseudomonas fluorescens*, *Pseudomonas putida* y *Pseudomonas chlororaphis* también contribuye a la adhesión y colonización de los tejidos vegetales, favoreciendo el desarrollo de sus actividades beneficiosas (Gal *et al.*, 2003; Chen *et al.*, 2013; Calderón *et al.*, 2013, 2014, 2019; Sun *et al.*, 2017). De este modo, la interacción de las bacterias asociadas a planta con sus huéspedes a través de la formación de biopelículas tiene consecuencias ecológicas muy relevantes para la agricultura.

Las bacterias pertenecientes al género *Pseudomonas* son uno de los grupos bacterianos más comunes en las superficies de las plantas (Hirano & Upper, 2000; Lugtenberg *et al.*, 2001). Las diferentes especies de *Pseudomonas* patógenas de plantas se encuentran usualmente en la filosfera, siendo *P. syringae* la más estudiada ya que puede infectar a un número elevado de cultivos, produciendo graves pérdidas (Kennelly *et al.*, 2007). Esta promiscuidad se debe al hecho de que *P. syringae* posee un amplio repertorio de factores de virulencia y de mecanismos de adaptación que posibilitan la infección y que promueven la persistencia en la planta. En cuanto a los

factores de virulencia, *P. syringae* presenta el sistema de secreción tipo III, proteínas efectoras de dicho sistema, apéndices móviles, fitotoxinas, bombas de expulsión de compuestos tóxicos, polisacáridos, enzimas degradadoras de la pared celular y la actividad nucleadora de hielo (Ichinose *et al.,* 2013). La filosfera es un ambiente altamente inestable, ya que está expuesta a una alta variabilidad de los factores ambientales (Danhorn & Fuqua, 2007; Hirano & Upper, 2000; Leveau, 2019). En este sentido, la presencia de genes de resistencia a luz ultravioleta y a metales pesados, como el cobre, desempeñan un papel fundamental en la supervivencia y fitness epifítico de *P. syringae* (Sundin *et al.,* 1996; Cazorla *et al.,* 2002; Arrebola *et al.,* 2015; Gutiérrez-Barranquero *et al.,* 2013, 2017, 2019; Aprile *et al.,* 2021).

Por otro lado, las bacterias beneficiosas para las plantas se encuentran principalmente asociadas a la rizosfera. *P. fluorescens*, y especies relacionadas pertenecientes al complejo *P. fluorescens*, incluyen cepas de un gran interés para la agricultura ya que frecuentemente poseen características relevantes como son la actividad promotora de crecimiento en las plantas y el control biológico, principalmente frente a hongos fitopatógenos de suelo (Couillerot *et al.,* 2009). Las fluctuaciones de los factores ambientales que tienen lugar en la rizosfera son débiles en comparación con la filosfera (Dong *et al.,* 2019). Sin embargo, tampoco se ha de considerar a la rizosfera como un ambiente estable, ya que las condiciones pueden cambiar de manera abrupta en rangos de distancia extremadamente pequeños, y por tanto las bacterias que habitan en la rizosfera también deben poseer mecanismos de adaptación que les permitan sobrevivir a estos cambios (Fageria & Stone, 2006; Thies & Grossman, 2006).

- **Modelos de estudio**

La necrosis apical del mango (NAM) es una enfermedad causada por la bacteria fitopatógena *P. syringae* pv. syringae (Pss) y es el principal factor limitante del cultivo del mango (*Mangifera indica*) en el área mediterránea (Cazorla *et al.,* 1998). Los síntomas iniciales de la NAM consisten en necrosis de las yemas vegetativas de los árboles de mango, que rápidamente se extienden a las hojas a través de los peciolos (Kenelly *et al.,* 2007). Las cepas de Pss aisladas de mango presentan la capacidad de producir una toxina antimetabolito denominada mangotoxina (Arrebola *et al.,* 2003), siendo esta toxina uno de los factores de virulencia más relevantes a la

hora de producir síntomas necróticos en los árboles de mango (Arrebola *et al.*, 2009). Las condiciones ambientales tienen una gran influencia en el inicio y el desarrollo de la enfermedad, ya que los niveles más altos de NAM coinciden usualmente con periodos fríos y húmedos (Cazorla *et al.*, 1998).

P. syringae transita entre un estilo de vida epífito y patógeno durante su interacción con las plantas, el cual parece depender principalmente de las condiciones ambientales (Hirano & Upper, 2000; Xin *et al.*, 2018). La cepa *P. syringae* pv. syringae UMAF0158 (PssUMAF0158) fue elegida por nuestro grupo de investigación como cepa de referencia en la que desarrollar estudios que permitieran elucidar el papel de la mangotoxina en virulencia y el fitness epifítico (Arrebola *et al.*, 2007, 2009; Carrión *et al.*, 2012, 2014). El proyecto de secuenciación del genoma completo de PssUMAF0158 reveló la presencia de diversas regiones genómicas codificantes para diferentes factores de virulencia, así como de un clúster de genes implicado en la producción del polisacárido celulosa (Martínez-García *et al.*, 2015). La síntesis de celulosa está implicada en la formación de biopelículas en la cepa PssUMAF0158, la adhesión a la superficie de las hojas de mango y, a su vez, influye en la transición entre el estilo de vida epífito y patógeno, ya que el mutante en la producción de celulosa mostró ser más virulento que la cepa silvestre y la virulencia de la cepa sobreproductora de celulosa era mínima (Arrebola *et al.*, 2015). Por consiguiente, se concluyó que la formación de biopelículas, a través de la producción de polisacáridos como la celulosa, podría estar relacionada con la transición entre los estilos de vida epífito y patógeno de las cepas de Pss asociadas a mango (Arrebola *et al.*, 2015; Gutiérrez-Barranquero *et al.*, 2019). Sin embargo, además del polisacárido celulosa, se desconoce qué otros componentes pueden formar parte de la matriz extracelular de las cepas de Pss asociadas a mango y el papel que éstos podrían desempeñar en la formación de biopelículas y patogénesis. Según resultados previos, podría existir una relación entre los factores ambientales, la formación de biopelículas y el hecho de manifestar un estilo de vida epífito o patógeno sobre la planta huésped (Cazorla *et al.*, 1998; Arrebola *et al.*, 2015). También se desconoce si los factores ambientales pueden o no influir la formación de biopelículas en Pss.

Por otro lado, la especie *Pseudomonas chlororaphis* es un miembro común de la rizosfera de muchas plantas que posee una serie de características relevantes

relacionadas con la biofertilización, fitoestimulación y el control biológico (Bloemberg & Lugtenberg, 2001; Arrebola *et al.*, 2019). La cepa *P. chlororaphis* PCL1606 (PcPCL1606) fue aislada de la rizosfera de un árbol de aguacate sano rodeado de árboles afectados por la podredumbre blanca radicular producida por el hongo fitopatógeno de suelo *Rosellinia necatrix* en una finca localizada en Algarrobo (Málaga). PcPCL1606 presenta una importante actividad antagonista frente a diferentes hongos fitopatógenos y ha mostrado una actividad de control biológico importante frente a la podredumbre blanca radicular del aguacate causada por el hongo *R. necatrix* y la podredumbre del cuello y raíz de tomate causada por el hongo *Fusarium oxysporum* (Cazorla *et al.*, 2006). Sin embargo, la cepa PcPCL1606, aunque confiere protección frente a enfermedades fúngicas, es un miembro inusual de la especie *P. chlororaphis*, ya que no produce fenazinas y no promueve el crecimiento de las plantas (Arrebola *et al.*, 2019). La actividad antagonista de PcPCL1606 está principalmente asociada a la producción del compuesto 2-hexil 5-propil resorcinol (HPR), ya que una cepa mutante en el gen *darB* (Δ*darB*), defectiva en la síntesis de HPR, mostró una menor capacidad de control biológico con respecto a la cepa silvestre utilizando tanto el sistema *R. necatrix*-aguacate como *F. oxysporum*-tomate (Calderón *et al.*, 2013). Aparte de mostrar actividad antagonista frente al crecimiento de hongos fitopatógenos, el compuesto HPR parece actuar en PcPCL1606 como una molécula señal ya que la cepa Δ*darB*, no productora de HPR, también mostró estar afectada en la colonización de las raíces de plántulas de aguacate y en la formación de biopelículas (Calderón *et al.*, 2014, 2019). Todo esto sugiere que la reducción del control biológico en la cepa mutante PcPCL1606 Δ*darB* podría realmente deberse a un proceso multifactorial liderado por la ausencia de HPR, en el que no solo la ausencia del compuesto antifúngico *per se*, sino también la reducción en colonización debido a una alteración en la producción de biopelículas, podrían explicar el fenotipo defectivo en su capacidad de control biológico. De hecho, la formación de biopelículas en las raíces ha sido descrita como un prerrequisito para conferir fitoprotección en otras especies de pseudomonas de suelo, incluida *P. chlororaphis* (Bloemberg & Lugtenberg, 2001; Chin-A-Woeng *et al.*, 2007; Lugtenberg & Kamilova, 2009). Además, se ha descrito a la formación de biopelículas como una característica relevante de la cepa PcPCL1606 durante su interacción con planta (Calderón *et al.*, 2019). Sin embargo, hasta el momento no se ha estudiado el papel

que podrían desempeñar los diferentes componentes de la matriz extracelular de *P. chlororaphis* en la formación de biopelículas y en la ecología de esta especie bacteriana.

Como se ha comentado en el apartado anterior, la especie *P. aeruginosa* constituye un modelo para el estudio de la formación de biopelículas dentro del género *Pseudomonas* (Diggle & Whiteley, 2020). En general, algunas regiones genómicas que codifican para componentes de la matriz extracelular de *P. aeruginosa* también están presentes en bacterias fitopatógenas y beneficiosas de plantas, tales como los exopolisacáridos alginato y Psl, así como la fimbria tipo Fap (Blanco-Romero *et al.*, 2020). Particularmente, en el caso de Psl, a pesar de que se ha descrito la presencia de la región genómica que lo codifica en diferentes especies del género *Pseudomonas* asociadas a plantas aparte de en *P. aeruginosa* (Mann & Wozniak, 2012), el papel que este polisacárido podría desempeñar en la formación de biopelículas y la ecología de estas bacterias durante la interacción con la planta no se ha estudiado hasta el momento.

Teniendo en cuenta todos estos antecedentes y que el estilo de vida de biopelícula parece ser muy relevante para la ecología bacteriana tanto de la cepa PssUMAF0158 como de PcPCL1606 durante sus interacciones con planta, en esta tesis doctoral se han abordado tres objetivos fundamentales:

1. Determinar el papel que poseen otros componentes de la matriz extracelular, además de la celulosa, en la formación de biopelículas (y/o fenotipos relacionados) y la ecología la bacteria fitopatógena *P. syringae* pv. syringae.

2. Determinar el papel que podrían desempeñar determinados factores ambientales, tales como la temperatura y la luz, en la formación de biopelículas en cepas de *P. syringae* pv. syringae.

3. Determinar el papel que poseen ciertos componentes de la matriz extracelular en la formación de biopelículas (y/o fenotipos relacionados) y la ecología del agente de control biológico *P. chlororaphis* PCL1606.

- **Resultados y discusión**

El polisacárido alginato es un copolímero acetilado de ácido D-manurónico y L-glucurónico (Evans & Linker, 1973). En *P. aeruginosa* PAO1, el polisacárido alginato está codificado en un operón de doce genes que se corresponde con la región genómica PA3540-PA3551 (Wozniak *et al.,* 2003). Durante el proceso de infección desarrollado en pacientes con fibrosis quística (FQ), *P. aeruginosa* se transforma en una variante mucoide caracterizada por la sobreproducción de este polisacárido (Fegan *et al.,* 1990; Terry *et al.,* 1991; Lyczak *et al.,* 2002). La sobreproducción de alginato tiene fines protectores, pues se ha demostrado que incrementa la resistencia de *P. aeruginosa* frente a agentes antimicrobianos, depredadores y frente a los sistemas de defensa del hospedador (Simpson *et al.,* 1988; Hentzer *et al.* 2001). La alta frecuencia en la que ocurre esta conversión al fenotipo mucoide, así como las capacidades protectoras descritas para este polisacárido, llevó a considerar al alginato como el componente principal de la matriz extracelular de *P. aeruginosa*. Sin embargo, estudios realizados en cepas no mucoides de *P. aeruginosa*, tales como PAO1 y PA14, las cuales son capaces de colonizar eficientemente los pulmones de pacientes con FQ, han demostrado que este polímero, aunque no es esencial para la constitución de la biopelícula, sí que forma parte de la matriz extracelular y puede llegar a influir en su arquitectura (Wozniak *et al.,* 2003; Stapper *et al.,* 2004; McIntyre-Smith *et al.,* 2010; Ghafoor *et al.,* 2011).

Tal y como se había observado previamente en *P. aeruginosa*, el polisacárido alginato no es esencial para la constitución de la biopelícula formada por la cepa fitopatógena PssUMAF0158, pues el mutante afectado en la producción de este polisacárido (PssUMAF0158 Δ*alg8*) aún mantenía la capacidad de formar biopelículas (Capítulo 1). Sin embargo, este polisacárido sí que forma parte de la arquitectura tridimensional de la misma, ya que la biopelícula formada por la cepa PssUMAF0158 Δ*alg8* redujo significativamente su área y volumen en cámaras de flujo continuo en comparación con la cepa silvestre (Capítulo 1). Este resultado contrasta con otros datos publicados previamente, en el que la variante no productora de alginato derivada de la cepa *P. syringae* PG4180.muc formó biopelículas que eran indistinguibles de las formadas por la cepa silvestre PG4180.muc (Laue *et al.,* 2006). Trabajos previos han indicado que el polisacárido

alginato está implicado en la virulencia de *P. syringae* (Rudolph *et al.,* 1994; Fett *et al.,* 1989; Yu *et al.,* 1999). Por ejemplo, el mutante en la producción de alginato de la cepa *P. syringae* pv. syringae 3525 estaba afectado significativamente en la colonización de las hojas de frijol (huésped) y tomate (no huésped) y, aunque era capaz de generar síntomas, éstos eran menos severos que los desarrollados por la cepa silvestre (Yu *et al.,* 1999). En contraposición a estos resultados, la cepa mutante PssUMAF0158 Δ*alg8* no mostró diferencias en virulencia respecto a la cepa silvestre PssUMAF0158 en ensayos de virulencia usando foliolos de tomate (Capítulo 1). El polisacárido alginato tampoco mostró ser esencial para la constitución de la biopelícula del agente de biocontrol PcPCL1606 (Capítulo 3). En línea con este resultado, el mutante en la producción de alginato de la cepa beneficiosa para plantas *P. fluorescens* SBW25 también retuvo la capacidad de formar biopelículas en cámaras de flujo continuo, aunque tal y como se ha mencionado previamente para PssUMAF0158 y *P. aeruginosa* PAO1, esta poseía un volumen menor que la formada por la cepa silvestre SBW25 (Noirot-Gros *et al.,* 2019).

En *P. aeruginosa* PAO1 se describió por primera vez el polisacárido Psl, que estaba codificado por un operón de 15 genes (*pslA-O*) correspondiente a la región genómica PA2231-PA2245 (Friedman & Kolter, 2004; Jackson *et al.,* 2004; Matsukawa & Greenberg 2004). Sin embargo, trabajos posteriores han revelado que los tres últimos genes del supuesto operón (*pslMNO*) realmente constituyen una unidad transcripcional independiente (Goodman *et al.,* 2004; Hickman *et al.,* 2005; Starkey *et al.,* 2009) y no son necesarios para producir Psl (Byrd *et al.,* 2009). Excepto en la cepa *P. aeruginosa* PA14, la cual no produce Psl debido a que carece de los genes *pslA-D* (Friedman & Kolter, 2004), el clúster *psl* está presente en múltiples cepas de *P. aeruginosa*, y en algunas de ellas se ha demostrado que juega un papel muy relevante en el estilo de vida de la biopelícula (Ghafoor *et al.,* 2011; Blanco-Romero *et al.,* 2020). Varios estudios han demostrado la implicación del polisacárido Psl de *P. aeruginosa* en la adhesión a superficies bióticas y abióticas, la arquitectura de la biopelícula, la movilidad y en la protección frente a diferentes estreses (Ma *et al.,* 2006; Colvin *et al.,* 2012; Billings *et al.,* 2013; Wang *et al.,* 2013, 2014; Periasamy *et al.,* 2015). Como se ha comentado anteriormente, varias pseudomonas ambientales poseen en sus genomas un clúster de genes similar al que codifica para

Psl en *P. aeruginosa* (Mann & Wozniak, 2012; Blanco-Romero *et al.,* 2020). Generalmente, el clúster de tipo *psl* que se encuentra en estas cepas o bien carece de ortólogos que codifican para los genes *pslMNO* o éstos se encuentran presentes en otras regiones del genoma. La bacteria fitopatógena PssUMAF0158 contiene un clúster de tipo *psl* que carece de los genes *pslCLMNO*, y entre los genes de tipo *pslJ* y *pslK* contiene un gen que codifica para una presunta acetiltransferasa que podría desempeñar una función relacionada a la de la aciltransferasa codificada por *pslL* en *P. aeruginosa* (Capítulo 1). Además, el clúster de tipo *psl* de PssUMAF0158 está conservado entre los filogrupos asociados a planta del complejo *P. syringae* (Capítulo 1). Por otro lado, el agente de control biológico PcPCL1606 también posee un clúster de tipo *psl* que carece de los genes *pslLMNO* y también posee un gen entre los genes de tipo *pslJ* y *pslK* que codifica para una presunta acetiltransferasa, similar a la de la cepa PssUMAF0158 (Capítulo 3). Sin embargo, utilizando como referencia a las cepas incluidas en el trabajo de Garrido-Sanz *et al.,* (2017), la presencia del clúster de tipo *psl* de PcPCL1606 dentro del complejo *P. fluorescens* mostró una gran variabilidad (Capítulo 3). No obstante, este clúster mostró estar presente en todas las cepas de *P. chlororaphis* incluidas en dicho estudio, lo que sugiere que el polisacárido de tipo Psl podría ser relevante para la formación de biopelículas en esta especie (Capítulo 3).

El primer estudio en el que se describió la composición de Psl reveló que este polisacárido estaba constituido principalmente por galactosa y manosa (Ma *et al.,* 2007). Dos años más tarde, el estudio estructural de Psl reveló que este polisacárido consistía en repeticiones de una subunidad pentasacarídica compuesta por manosa, glucosa y ramnosa en una ratio 3:1:1 (Byrd *et al.,* 2009). Curiosamente, el monosacárido galactosa no fue detectado en el análisis estructural, a pesar de haberse descrito previamente como un componente mayoritario (Ma *et al.,* 2007). Estas diferencias encontradas respecto a la composición de Psl ha llevado a los autores de estos trabajos a sugerir que la composición de Psl podría variar en la misma cepa dependiendo de las condiciones de cultivo y sustratos que se utilicen en el laboratorio. Sea como fuere, lo que parece ser consistente entre ambos estudios es que el monosacárido manosa es un componente clave de la estructura de Psl en *P. aeruginosa*. Los estudios preliminares llevados a cabo en esta tesis doctoral con las

cepas PssUMAF0158 y PcPCL1606 sugieren que los polisacáridos de tipo Psl producidos por estas cepas también podrían contener manosa (Capítulo 1 y 3).

El polisacárido de tipo Psl producido por PssUMAF0158 y PcPCL1606 mostró ser un componente importante de la arquitectura tridimensional de las biopelículas formadas por estas cepas (Capítulo 1 y 3). Así, la cepa PssUMAF0158 Δ*pslE*, afectada en la síntesis del polisacárido tipo Psl, mostró un fenotipo alterado en la formación de biopelículas comparado con el de la cepa silvestre PssUMAF0158 consistente en agregados celulares esparcidos sobre la superficie de las cámaras de flujo continuo (Capítulo 1) que se correlacionaba con el fenotipo de biopelícula de algunas cepas mutantes en la producción de Psl de *P. aeruginosa* (Colvin *et al.*, 2012). Por otro lado, la cepa mutante PcPCL1606 Δ*pslE*, afectada en la producción del polisacárido de tipo Psl, también mostró estar alterada en la producción de biopelículas (Capítulo 3), con un fenotipo similar al descrito en la cepa no productora de Psl derivada de *P. aeruginosa* PAO1 (Jackson *et al.*, 2004; Matsukawa & Greenberg, 2004). En PAO1, el mutante afectado en la producción del polisacárido Psl también poseía un defecto en la interacción con superficies, tanto de tipo biótico como abiótico (Jackson et al., 2004; Matsukawa & Greenberg, 2004; Ma *et al.*, 2006). En línea con estos resultados, los mutantes defectivos en la producción del polisacárido de tipo Psl de las cepas PssUMAF0158 y PcPCL1606 también mostraron la implicación de este polisacárido en la adhesión a superficies. La cepa PssUMAF0158 Δ*pslE* mostró estar afectada en la adhesión inicial a la superficie de las hojas de mango en comparación con la cepa silvestre PssUMAF0158 (Capítulo 1) y la cepa PcPCL1606 Δ*pslE* mostró estar afectada en la adhesión inicial a pocillos de poliestireno y a la superficie de la raíz de plántulas de aguacate en comparación con la cepa silvestre PcPCL1606 (Capítulo 3). El polisacárido de tipo Psl también mostró tener un papel en la movilidad tipo *swarming* de la cepa PssUMAF0158, probablemente mediado por la producción de surfactantes (Capítulo 1). La relación observada entre la producción de Psl y la movilidad tipo *swarming*, mediada por la producción de ramnolípidos (RHL), ha sido descrita previamente en *P. aeruginosa* (Wang *et al.*, 2014). No obstante, la conexión observada entre la formación de biopelículas mediada por Psl, la producción de RHL y la movilidad tipo *swarming* en *P. aeruginosa* (Wang *et al.*, 2014) no coincide con la observada en PssUMAF0158 (Capítulo 1). Así, la no producción de Psl en *P. aeruginosa* causaba

un incremento en la movilidad tipo *swarming* debido a un incremento en la producción de RHL, al existir una competencia por el monosacárido ramnosa entre Psl y RHL (Wang *et al.,* 2014). Por el contrario, la no producción del polisacárido de tipo Psl en PssUMAF0158 causa una reducción en la movilidad tipo *swarming*, probablemente mediada por una reducción en la producción de surfactantes, ya que el gen *rhlA* mostraba una menor expresión en el mutante que en la cepa silvestre PssUMAF0158 (Capítulo 1).

La formación de biopelículas mediada por el polisacárido de tipo Psl influye en la ecología bacteriana de las cepas PssUMAF0158 y PcPCL1606 sobre el huésped vegetal. Así, tal y como se había descrito previamente con respecto a la celulosa en PssUMAF0158 (Arrebola *et al.,* 2015), la reducción en la formación de biopelícula de PssUMAF0158 causada por una alteración en la producción del polisacárido de tipo Psl parece predisponer a esta cepa a manifestar un estilo de vida patógeno en planta, ya que el mutante mostró ser más virulento que la cepa silvestre (Capítulo 1). Por el contrario, la reducción en la formación de biopelícula de PcPCL1606 causada por una alteración en la producción del polisacárido de tipo Psl disminuyó la actividad de control biológico de esta bacteria frente a la podredumbre blanca radicular del aguacate causada por el hongo *R. necatrix* (Capítulo 3). La alteración en la adhesión inicial a superficie abiótica y a raíz de aguacate, así como en la actividad de control biológico, también se ha observado en el mutante defectivo en la producción de la fibra amiloide de tipo Fap (Capítulo 3). De este modo, los defectos en adhesión inicial a la raíz y/o en la formación de biopelículas podrían causar una alteración en la actividad de control biológico al proporcionar al hongo un mayor acceso hacia la raíz de la planta, o incluso al estar impidiendo la transferencia efectiva de los agentes antimicrobianos, como se ha sugerido previamente en estudios llevados a cabo en *P. chlororaphis* (Chin-A-Woeng *et al.,* 2007).

La celulosa es un polímero de residuos de D-glucosa unidos por enlaces glicosídicos de tipo β-1,4 que en *P. fluorescens* SBW25 está codificada por un operón de diez genes correspondiente a la región genómica PFLU0300-PFLU0309 (Spiers *et al.,* 2003). La celulosa constituye un componente relevante de la matriz extracelular de las biopelículas de muchas pseudomonas ambientales, entre las que se encuentran algunas patógenas y beneficiosas para las plantas (Ude *et al.,* 2006; Spiers *et al.,*

2013). La especie *P. aeruginosa* no contiene la región genómica que codifica para este polisacárido (Blanco-Romero *et al.,* 2020) y, además, no se ha detectado su producción en las cepas modelo *P. aeruginosa* PAO1 y PA14 (Spiers *et al.,* 2013). No obstante, PAO1 y PA14 producen el polisacárido Pel, un polímero parcialmente acetilado de N-acetilgalactosamina y N-acetilglucosamina unidos por enlaces glicosídicos de tipo β-1,4 que recuerda mucho a la celulosa (Friedman & Kolter, 2004; Jennings *et al.,* 2015). El polisacárido Pel podría desempeñar roles estructurales en la biopelícula de *P. aeruginosa* similares a los de la celulosa en otras pseudomonas ambientales, ya que está igualmente implicado en la formación de biopelículas flotantes (Friedman & Kolter, 2004; Mann & Wozniak, 2012). A diferencia de la bacteria fitopatógena PssUMAF0158, el agente de control biológico PcPCL1606 no produce celulosa (Capítulo 3), mientras que la celulosa es el componente principal de la biopelícula de la bacteria fitopatógena PssUMAF0158 y está muy implicado en su ecología; la adhesión a la superficie de las hojas de mango y, al igual que se ha observado para el polisacárido tipo Psl, también parece tener un papel importante en la transición entre los estilos de vida epífito y patógeno de Pss en la interacción con planta (Capítulo 1; Arrebola *et al.,* 2015).

La transición entre los estilos de vida epífito y patógeno de cepas de Pss asociadas a mango podría estar influenciada por factores ambientales, ya que los síntomas más severos de la NAM se observan principalmente en periodos fríos y húmedos (Cazorla *et al.,* 1998). Las cepas de Pss aisladas de mango forman un filotipo diferenciado del resto de cepas de Pss aisladas de otros hospedadores, asociadas estrechamente con la producción de mangotoxina (Gutiérrez-Barranquero *et al.,* 2013). Recientemente, se ha descrito que dentro de este filotipo diferenciado se encuentran al menos 9 subgrupos filogenéticos diferentes (Aprile *et al.,* 2021). Gracias a la disponibilidad de un elevado número de genomas secuenciados de diferentes cepas de Pss de mango pertenecientes a los diferentes subgrupos filogenéticos, se conoce que los polisacáridos alginato, celulosa y Psl están presentes en todas las cepas que se han analizado hasta el momento (datos no publicados). El estudio filogenético de estos polisacáridos ha mostrado cierta incongruencia respecto a la historia evolutiva de su hospedador, observándose de manera relevante una distribución en base al nivel de producción del polisacárido celulosa (Capítulo 2). Todas las cepas de Pss eran productoras de celulosa, pero a diferentes niveles de

producción (Capítulo 2). La formación de biopelículas mediada por la producción de polisacáridos, principalmente celulosa, en cepas de Pss aisladas de mango, ha mostrado estar influenciada por factores ambientales como la temperatura y sobre todo la luz (Capítulo 2). Algunos de estos datos se correlacionan parcialmente con otros observados previamente en *P. aeruginosa* PAO1, en la que la formación de biopelículas mediada por la producción de polisacáridos sufre una disminución entre los 20 y 25ºC y un ligero aumento entre los 25 y los 37ºC (Kim *et al.,* 2020). Además, tal y como se ha descrito en PAO1, las estructuras de biopelícula más complejas se observaron a 20ºC (Capítulo 2). Por último, la luz blanca incrementó la producción de polisacáridos en cepas de Pss aisladas de mango (Capítulo 2) al igual que en *P. syringae* pv. tomato DC3000, en la cual se describió que la luz blanca producía un incremento en la expresión del gen *algD* y la adhesión a hoja (Río-Álvarez *et al.,* 2014).

Por lo tanto, de los resultados obtenidos en esta tesis doctoral se puede concluir de forma sintética que:

- Un polisacárido de tipo Psl forma parte de la arquitectura de la biopelícula de la bacteria fitopatógena *Pseudomonas syringae* pv. syringae UMAF0158 y el agente de control biológico *Pseudomonas chlororaphis* PCL1606.

- La formación de biopelículas, a través de la síntesis de celulosa y de un polisacárido similar a Psl, juega un papel relevante en la ecología de la bacteria fitopatógena PssUMAF0158 durante su interacción con la planta, participando en la formación de biopelículas, en la adhesión a las hojas e influyendo en la transición entre los estilos de vida epífito y patógeno.

- Los factores ambientales, particularmente la luz blanca, influyen en la formación de biopelículas al controlar la síntesis de polisacárido en cepas de *P. syringae* pv. syringae (Pss) aisladas de mango. Además, niveles más bajos de producción de polisacáridos parecen estar asociados a una mayor virulencia de Pss.

- Un polisacárido de tipo Psl y una putativa fibra amiloide juegan papeles relevantes en la ecología del agente de biocontrol *P. chlororaphis* PCL1606,

al estar implicados ambos en la adhesión temprana a diferentes superficies, como la raíz de aguacate, y estar relacionada su producción con la eficacia de la actividad de control biológico.

INTRODUCTION

Part of the information included in the introduction has been published:

Zaira Heredia-Ponce, Antonio de Vicente, Francisco M. Cazorla & José Antonio Gutiérrez Barranquero. Beyond the wall: exopolysaccharides in the biofilm lifestyle of plant-associated *Pseudomonas*. ***Microorganisms*** (2021) 9, 445.

Bacterial biofilms are matrix-enclosed bacterial populations that are adherent to each other and to surfaces and/or interfaces and are mainly composed of polysaccharides, proteins, lipids and extracellular DNA (Costerton & Lewandowsky, 1995; Costerton *et al.*, 1999; Høiby *et al.*, 2010). The cells forming biofilms are called sessile cells, which differ from their non-encased free-swimming counterparts, the planktonic cells (Marshall, 2006). The extracellular matrix is self-produced by the cells and acts as a protective barrier from external stressors, including ultraviolet (UV) radiation, extreme temperature and pH, high salinity and pressure, poor nutrients, antibiotics, etc. (Yin *et al.*, 2019).

Approximately 6% of the global biomass on Earth corresponds to bacteria and archaea (Bar-on & Milo *et al.*, 2019) and to date, depending on the habitat, it is estimated that around 40-80% of them reside in biofilms (Flemming & Wuertz, 2019). Biofilms can be found almost everywhere and in both natural and artificial environments, including the soil, internal and external tissues of all living organisms, rocks and water, among others (Figure 1.I).

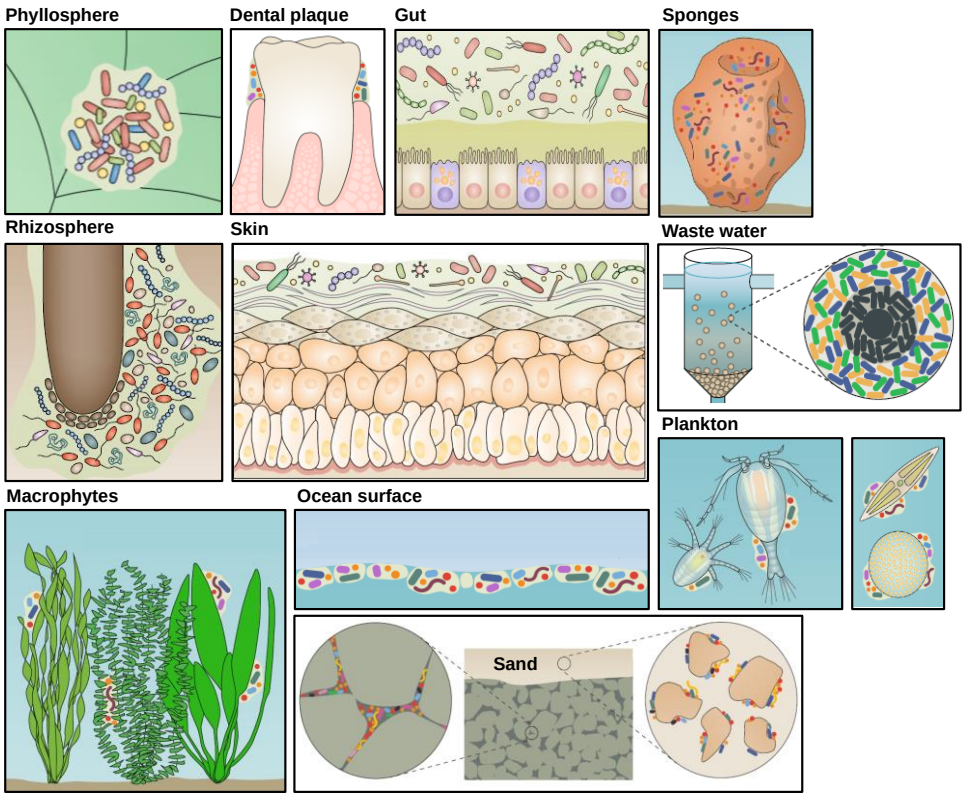

Figure 1.I. Examples of different environments colonized by biofilms (images obtained from Flemming and Wuertz, 2019).

Depending on the bacteria involved, biofilms can have negative or positive consequences, such as causing diseases, reducing product yield and/or quality in the food industry, cleaning-up environmental pollutants (bioremediation), contribute to biological control and promote nutrient cycling, among others (Singh *et al.*, 2006; Del Pozo *et al.*, 2011; Zeriouh *et al.*, 2014; Percival *et al.*, 2015; Pandit *et al.*, 2019; Vishwakarma, 2019; Caro-Astorga *et al.*, 2020). For instance, *P. aeruginosa* can cause nosocomial infections in patients with cystic fibrosis by colonizing their lungs, leading to chronic inflammation and lung tissue damage (Høiby *et al.*, 2010). The biofilm structure formed by *P. aeruginosa*, which confers protection against host defence and antibiotics, together with the multidrug resistance phenotype of this bacterium, makes these infections very difficult to treat (Abdulhaq *et al.*, 2020). Biofilm formation in medical devices, such as those formed in catheters and cardiac pacemakers by staphylococci, causes serious health problems that can lead to death (Hall-Stoodley *et al.*, 2004; Hogan *et al.*, 2016). Biofilm formation on equipment and food of food processing plants leads to a reduction in product quality or even to foodborne diseases (Vishwakarma *et al.*, 2019). Biochemical and physiological activities within biofilms enhance degradation and immobilization of toxic compounds, leading to an efficient bioremediation of contaminated sites (Singh *et al.*, 2006). Furthermore, biofilm formation can cause both significant problems and benefits in the agricultural sector, such as plant diseases that lead to a reduction in production and/or food quality (Kenelly *et al.*, 2007; Koczan *et al.*, 2009; Killiny *et al.*, 2013) and the promotion of plant growth, biocontrol activity, enhancement of plant-defences, nutrient solubilization and nutrient cycling (Zeriouh *et al.*, 2014; Pandit *et al.*, 2019; Cámara-Almirón *et al.*, 2020).

The ability to form biofilms is a universal attribute of bacteria, but the most studied models are *Escherichia coli*, *Pseudomonas aeruginosa*, *Bacillus subtilis* and *Staphylococcus aureus* (López *et al.*, 2010; Romero *et al.*, 2010; Franklin *et al.*, 2011; Sharma *et al.*, 2016). Particularly, the *Pseudomonas* genus is among the most studied bacterial groups for several reasons: 1) it harbours species with the ability to colonize a wide variety of environments, such as soil, fresh water, marine habitats, animals and plants, due to the high metabolic and physiologic diversity found in this group of microorganisms; 2) it has ecological relevance due to its interactions with living organisms and 3) it has potential biotechnological applications for production

of small molecules, enzymes and biopolymers of commercial interest. Therefore, members of *Pseudomonas* are of great importance for agriculture, bioremediation, public health and environmental studies.

1. Biofilms: a multicellular mode of growth

The environmental signals that trigger biofilm formation appear to be low conserved, differing from one species to another (Stanley & Lazazzera, 2004) but generally, the presence of high nutrients is required, as biofilms will not form where nutrients are lacking (Hunt *et al.*, 2004). Bacteria form biofilms because they benefit from this mode of growth (Jefferson, 2004). Living within a biofilm confers three main advantages to their inhabitants compared to the planktonic lifestyle: 1) defence, as protection against predators and tolerance towards biotic and abiotic stresses increase during the biofilm mode of growth; 2) colonization, a mechanism that allows the permanence in a favourable niche and 3) community benefits, including the division of metabolic tasks, gene transfer and some altruistic behaviour of their inhabitants.

Natural biofilms profoundly differ from their laboratory-produced equivalents but under laboratory settings four types of biofilms have been observed (Figure 2.I): 1) submerged, which can form under dynamic conditions, as in flow-cell chambers, or under static conditions; 2) floating biofilms or pellicles, which form at the air-liquid interfaces of static cultures; 3) 'microwell plates" biofilms, which are attached to the interfaces of microwell plates under static culture conditions; 4) bacterial colonies, which form on the surface of agar-solidified medium (modified from Branda *et al.*, 2005).

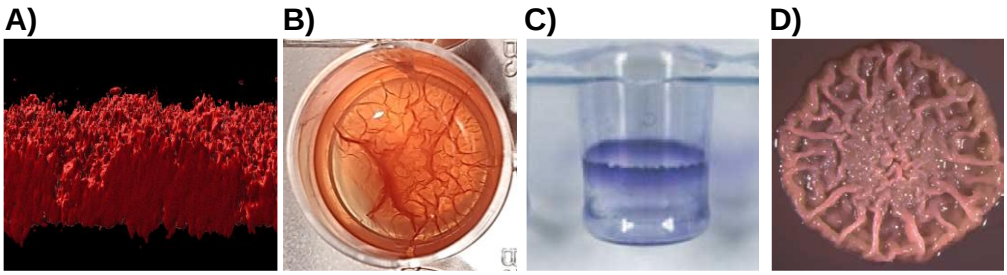

Figure 2.I. Types of biofilms formed under laboratory settings. A) Flow cell biofilm formed by *Pseudomonas syringae* pv. syringae UMAF0158 (PssUMAF0158) strain that constitutively express the dsRed fluorescent protein and visualized using confocal laser scanning microscopy (CLSM); B) Pellicle biofilm formed by PssUMAF0158 strain in TPG medium containing Congo red (CR) dye at 20ºC; C) "Microwell plates" biofilms formed by *Escherichia coli* strains under standing-culture conditions and visualized using crystal violet; D) Biofilms formed by *Pseudomonas aeruginosa* strains on agar plates containing CR dye. Figure modified from Branda *et al.*, 2005.

2. Stages of biofilm formation

Since the first studies biofilm formation has been divided in three general stages: attachment, proliferation/maturation and dispersion (Figure 3.I). These stages seem to be well-conserved among a remarkable range of prokaryotes (Hall-Stoodley *et al.*, 2004). However, the description of these stages is mostly based on phenotypic observations rather than in an actual knowledge of the molecular mechanisms underlying the transition through all the stages (Monds & O'Toole, 2009).

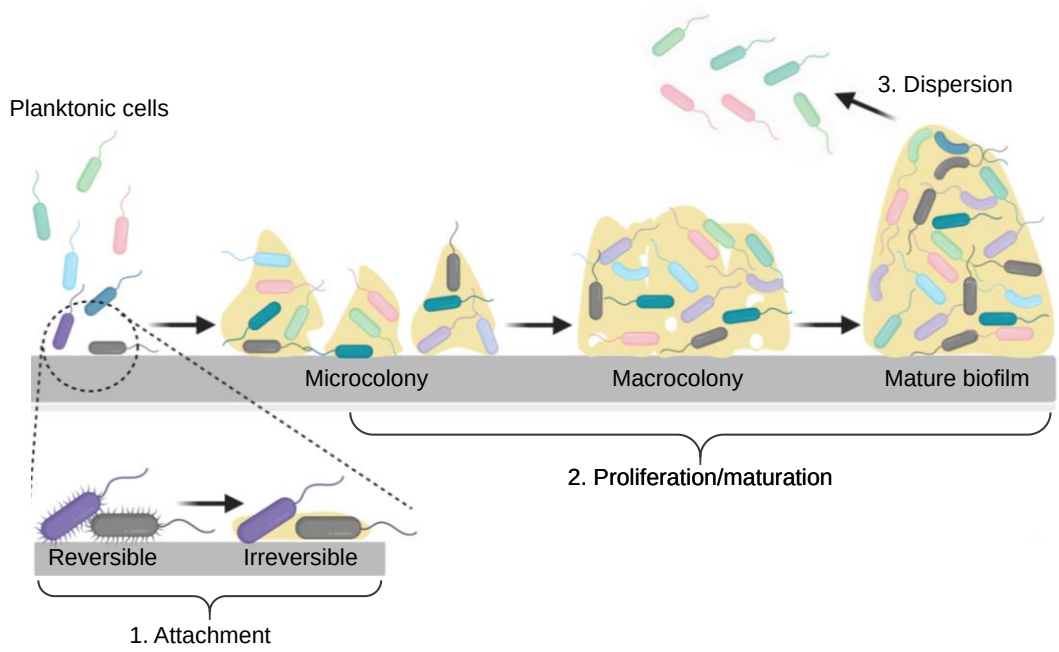

Figure 3.I. Stages of biofilm formation. The three main stages leading to biofilm formation are attachment (reversible and irreversible), proliferation/maturation (microcolony, macrocolony and mature biofilm) and dispersion. Image created with BioRender.com.

The attachment stage begins when cells turn from a planktonic to a sessile lifestyle by interacting with a surface (Figure 3.I) and consists of two phases: an adsorption or reversible phase, which is characterized by a loose or transient association with a surface and cells are readily able to detach; and an irreversible phase, which is characterized by a strong and stable association with a surface. Adsorption is frequently mediated by extracellular appendages such as flagella, pili and fimbriae; the irreversible phase is often mediated by polysaccharides and proteins that attach the bacteria to the surfaces (Hoffman *et al.,* 2015). Attachment to surfaces is not solely governed by bacterial factors but also by environmental factors. Examples are the charge, hydrophobicity and roughness of the surfaces involved (Palmer *et al.,* 2007), as well as their availability of nutrients and protection sites (Bogino *et al.,* 2013; Danhorn & Fuqua, 2007; Schlechter *et al.,* 2019).

The proliferation/maturation stage begins after irreversible attachment (Figure 3.I) and is characterized by the production of an extracellular matrix that eventually will define the final architecture of the community (Costerton, 1999). The maturation stage consists of three sequential phases: microcolony formation, macrocolony formation and mature biofilm. The exact point at which one phase finishes and the next begins is poorly understood and has led some authors to establish their own parameters. For example, in Cárcamo-Oyarce *et al.,* (2015), an aggregate size of eight cells was defined as threshold for considering the cells from free to colony-associated. In theory, but very difficult to precisely illustrate, the microcolony stage starts when a group of irreversible attached bacteria produce an extracellular matrix. The macrocolony stage starts when a cell from any microcolony overlaps with a cell from another microcolony. Both microcolonies would eventually merge and constitute a macrocolony. Similarly, a mature biofilm is constituted when all the macrocolonies are merged.

The bacterial release from biofilms to the surrounding media can be accomplished actively, via desorption, or passively, through external perturbations that disrupt biofilm structure (Kaplan, 2010). Desorption consists in the active degradation and release of the biofilm extracellular matrix components by the action of enzymes or other active compounds produced by the cells (Boyd & Chakrabarty, 1994; Lee *et al.,* 1996; Boles *et al.,* 2005). Desorption is induced upon environmental signals, including alterations in the availability of nutrients and minerals, oxygen and

temperature changes, and also upon bacteria-derived signals, like quorum sensing and other small molecules (McDougald *et al.*, 2012). Biofilm disruption is mediated by external forces, including fluid shear, abrasion or grazing (Choi & Morgenroth, 2003; Ymele-Leki & Ross, 2007). Regardless of the mechanism used, the result is bacterial dispersion (Figure 3.I), which allows the translocation of the cells to a new location and the formation of new biofilms.

3. Common architectural aspects of biofilms

A unifying attribute of biofilms is the presence of an extracellular matrix that represents the 90% of their mass (Flemming & Wingender, 2010). The extracellular matrix substances are extremely complex, dynamic and diverse and generally correspond to polysaccharides, proteins, nucleic acids and lipids (Sutherland, 2001). However, polysaccharides are frequently the main components in many different bacteria (Christensen, 1989; Limoli *et al.*, 2015; Karygianni *et al.*, 2020). The extracellular matrix is mainly produced by cells within biofilms, but it is also plausible that environmental organic and inorganic components could be incorporated, although this field has not been investigated and remains largely unknown.

Another common aspect of the biofilm structure are nutrient and oxygen gradients (Figure 4.I). There is a lower availability of these substances when increasing in depth within biofilms (Christensen, 1989) because diffusion, which is the predominant process for the transport of nutrients and oxygen within biofilms, is dramatically reduced during a sessile mode of growth (Stewart, 2003). Water channels in the biofilm structure act as conduits that facilitate nutrient and oxygen exchange and movement of waste products between the internal parts of the biofilms and the environment, or even between different zones within a biofilm (Costerton & Lewandowsky, 1995; Hall-Stoodley *et al.*, 2004).

The gradients found within biofilms create microenvironments that lead into spatially heterogeneous growth of the cells, different patterns of gene expression and, therefore, different metabolic activities and physiological features of bacteria depending on their position within the community (Stewart, 2003; Paula *et al.*, 2020). The result is bacteria specialization (An & Parsek, 2007; Spormann, 2008), for instance, different intracellular levels of c-di-GMP correlate with cell

differentiation into motile or matrix-producing cells in *P. aeruginosa* (Armbruster *et al.*, 2019).

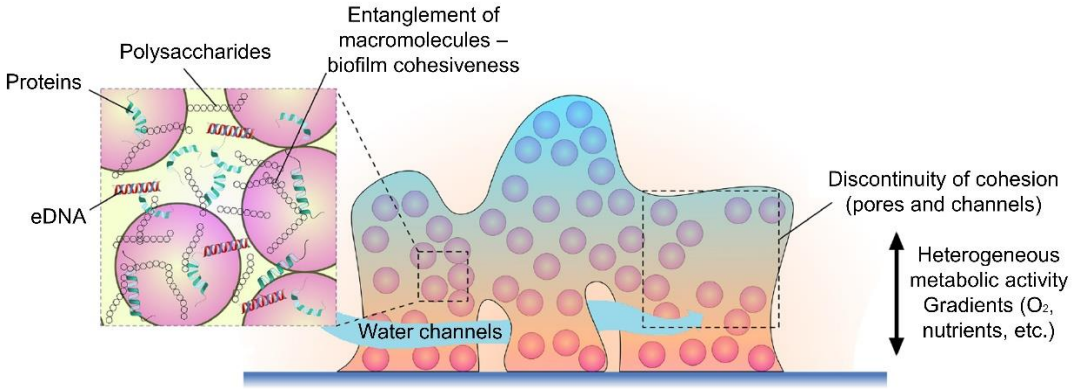

Figure 4.I. Physical heterogeneities of bacterial biofilms. Biofilms are made of bacteria surrounded by extracellular matrix components (exopolysaccharides, proteins, extracellular DNA – eDNA-, lipids and other cellular components). Oxygen and nutrient gradients result in metabolic heterogeneity. Figure obtained from Boudarel *et al.*, 2018.

4. Ecological importance of biofilm formation by plant-interacting bacteria

Plant-associated bacteria can develop a biofilm lifestyle during their interactions with plants (Danhorn & Fuqua, 2007; Bogino *et al.*, 2013). Depending on whether the biofilms are formed by pathogenic or beneficial strains, the ecological outcome resulting from the interaction can be completely different. In the context of plant-pathogenic bacteria, the biofilm formed by *Erwinia amylovora*, the causal agent of fire blight disease in different plant species of the *Rosaceae* family, plays critical roles in the pathogenesis of this bacterium (Koczan *et al.*, 2009, 2011). During fire blight disease, *E. amylovora* forms biofilms, which mainly contains amylovoran and levan polysaccharides, that physically block the vascular system of plants (Figure 5A.I; Sjulin & Beer, 1978; Koczan *et al.*, 2009). The mutant defective in amylovoran synthesis was nonpathogenic and died rapidly following inoculation and the mutant defective in levan synthesis was not detected in the xylem vessels and its movement into apple shoots was reduced (Koczan *et al.*, 2009). Besides, mutants in some cell surface attachment structures, such as type I fimbriae, flagella, type IV pili and curli, also decreased *E. amylovora* virulence *in planta*, which indicates these appendages could also be necessary for the colonization of the xylem vessels (Koczan *et al.*, 2011).

Ralstonia solanacearum, the causal agent of bacterial wilt disease, requires biofilm structures for the colonization of the plant and ultimately for its virulence. Thus, a mutant in the *lecM* gene, which encodes a lectin, reduced biofilm formation *in vitro* and colonization of the intercellular spaces of tomato leaves and was impaired in virulence (Mori *et al.,* 2016). *Xanthomonas citri*, which produces canker disease in citrus plants, forms biofilms that favour its epiphytic fitness and disease development in plants. Thereby, *X. citri* pv. citri *gumB* mutant strain, which was unable to produce the polysaccharide xanthan, exhibited reduced biofilm formation, survival and symptom development on lemon leaves (Rigano *et al.,* 2007). Similarly, *Xylella fastidiosa*, which causes economically important diseases in several host plants, produces exopolysaccharides that play roles in virulence (Figure 5B.I), as these are required for bacterial movement within plants (Marques *et al.,* 2002; Killiny *et al.,* 2013). The Gum polysaccharide mutant of *X. fastidiosa* was also impaired in plant-to-plant transmission through insects (Killiny *et al.,* 2013). The extracellular matrix of *P. syringae*, which can infect almost all economically important crops, influences transition between pathogenic and epiphytic lifestyles of this bacterium in plants (Yu *et al.,* 1999; Arrebola *et al.,* 2015).

In the context of plant-beneficial bacteria, *Bacillus subtilis*, a gram-positive bacterium that acts as a biocontrol agent of several plant pathogens, requires genes involved in biofilm formation for conferring plant protection (Chen *et al.,* 2013). The production of biofilm extracellular matrix components in *B. subtilis*, such as those encoded by *tapA-sipW-tasA* and *epsA-O* operons, are critical for the colonization of the plant roots, which is a prerequisite for conferring plant protection (Figure 5C.I; Chen *et al.,* 2013). In agreement with this, *Pseudomonas fluorescens*, an important rhizobacterium that promotes plant health and nutrition, requires biofilm formation for the colonization of plant surfaces (Gal *et al.,* 2003). A cellulose exopolysaccharide mutant in the *P. fluorescens* SBW25 strain was compromised in the colonization of the rhizosphere and the phyllosphere of sugar beet compared to the wild-type strain (Gal *et al.,* 2003). Phenotypes linked to biofilm formation have also been observed to favour bacteria-plant root interactions and biocontrol activity in *Pseudomonas chlororaphis* and *Pseudomonas putida* species (Calderón *et al.,* 2013, 2014, 2019; Sun *et al.,* 2017).

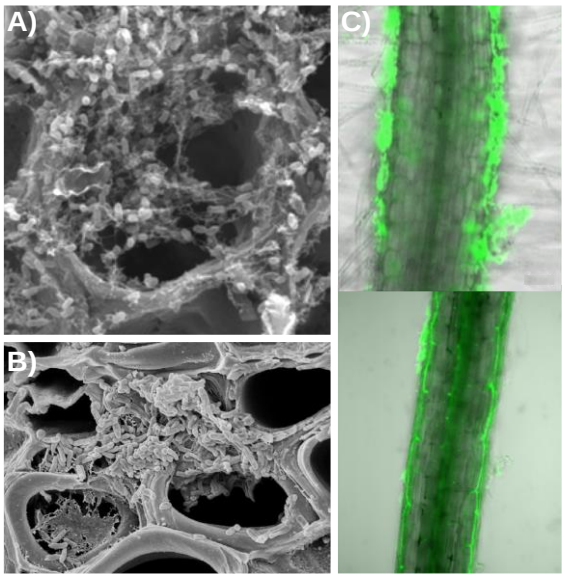

Figure 5.I. Examples of biofilm formation by plant interacting bacteria. A) Scanning electron micrograph of *Erwinia amylovora* biofilm within the xylem vessels of apple tree (image obtained from Koczan *et al.,* 2009); B) Scanning electron micrograph of *Xylella fastidiosa* biofilm within the xylem vessels of orange tree (image of E. W. Kitajima); C) Biofilm formation on the tomato root surfaces by the GFP-tagged *Bacillus subtilis* 3610 wild-type (up) and derived exopolysaccharide mutant (down; images obtained from Chen *et al.,* 2013).

5. *Pseudomonas aeruginosa*: a model bacterium for the study of biofilm formation within the *Pseudomonas* genus

The *P. aeruginosa* species is a ubiquitous bacterium that can also act as an opportunistic pathogen of humans which has long been used as a model bacterium for the study of biofilm formation and pathogenesis within the *Pseudomonas* genus due to its relevance in the clinical environment (Diggle & Whiteley, 2020). Particularly, *P. aeruginosa* PAO1 and PA14 are the reference strains used to perform biofilm studies. The *P. aeruginosa* extracellular matrix components (EMC) consist of exopolysaccharides – such as alginate, Psl ("*polysaccharide synthesis loci*") and Pel ("*pellicle loci*") (Franklin *et al.,* 2011)- proteins - such as CdrA and the Fap fibre (Blanco-Romero *et al.,* 2020)- and extracellular DNA (eDNA; Whitchurch *et al.,* 2002). The role that these EMC play in the biofilm architecture of *P. aeruginosa* and the impact of their synthesis in the clinical setting, such as protection against antibiotics and host defence, have been explored in multiple studies (Hentzer *et al.,* 2001; Whitchurch *et al.,* 2002; Wozniak *et al.,* 2003; Stapper *et al.,* 2004; Leid *et al.,* 2005; Ma *et al.,* 2006; Colvin *et al.,* 2011; Ma *et al.,* 2012; Billings *et al.,* 2013; Dueholm *et al.,* 2013b; Reichhardt *et al.,* 2018; Ciofu & Tolker-Nielsen, 2019). Although *P. aeruginosa* produces infections in humans, there are also some examples of this bacterium acting as a plant pathogen (Elrod & Braun, 1942; Walker *et al.,* 2004). However, the biological significance of these EMC in a nonclinical context has not been studied.

Alginate is a copolymer made of O-acetylated D-mannuronic and L-glucuronic acid residues joined by β-1,4 linkages (Figure 6.I; Evans & Linker, 1973). In *P. aeruginosa* PAO1, the alginate polysaccharide is encoded on a twelve gene operon that corresponds to the PA3540-PA3551 genomic region (Wozniak *et al.*, 2003). During infections in cystic fibrosis (CF) patients, *P. aeruginosa* undergoes a switch into a mucoid phenotype characterized by alginate overproduction (Fegan *et al.*, 1990; Terry *et al.*, 1991; Lyczak *et al.*, 2002). Alginate overexpression increases the resistance of *P. aeruginosa* to antimicrobial treatments, predators and host defences (Simpson *et al.*, 1988; Hentzer *et al.*, 2001). The high frequency in which this conversion occurs, and the protective capacities described for alginate, suggested that alginate was the main exopolysaccharide of the *P. aeruginosa* extracellular matrix. However, studies performed on nonmucoid *P. aeruginosa* strains (e.g., PAO1 and PA14), the truly predominant phenotype and the one responsible for the colonization of the lungs of CF patients, have shown that alginate is not critical for biofilm constitution but it is a component of the *P. aeruginosa* extracellular matrix and can influence its biofilm architecture (Wozniak *et al.*, 2003; Stapper *et al.*, 2004; McIntyre-Smith *et al.*, 2010; Ghafoor *et al.*, 2011).

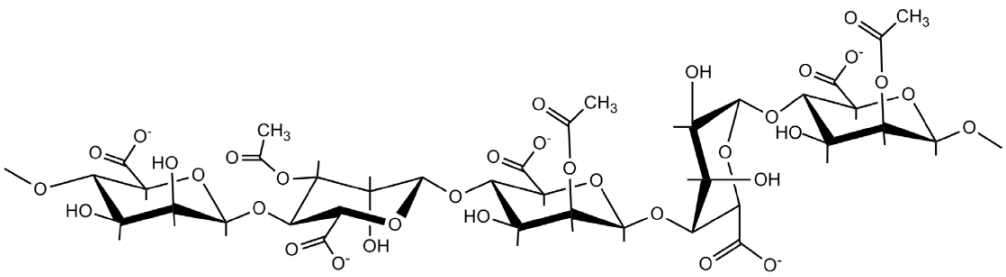

Figure 6.I. Structure of alginate polysaccharide. Alginate is a copolymer made of O-acetylated D-mannuronic and L-glucuronic acid residues joined by β-1,4 linkages. Image obtained from Franklin *et al.*, 2011.

The Psl polysaccharide was discovered in *P. aeruginosa* by three different research groups at the same year (Friedman & Kolter, 2004; Jackson *et al.*, 2004; Matsukawa & Greenberg 2004) and the most recent study has determined that its structure consists of a repeating pentasaccharide subunit of D-mannose, D-glucose and L-rhamnose in a 3:1:1 ratio (Figure 7.I; Byrd *et al.*, 2009). In *P. aeruginosa*, Psl was formerly described to be encoded by the 15-gene operon *pslA-O* (Friedman & Kolter, 2004; Jackson *et al.*, 2004; Matsukawa & Greenberg 2004). However, later

works have revealed that the last three genes of the operon (*pslMNO*) constitute an independent transcriptional unit (Goodman *et al.*, 2004; Hickman *et al.*, 2005; Starkey *et al.*, 2009) and are not truly required to produce Psl (Byrd *et al.*, 2009). Except for the case of the *P. aeruginosa* PA14 strain, which does not produce Psl due to the absence of the *pslA-D* genes (Friedman & Kolter, 2004), the *psl* gene cluster is present in multiple strains of *P. aeruginosa*, where it plays key roles in their biofilm lifestyles (Ghafoor *et al.*, 2011; Blanco-Romero *et al.*, 2020). Several studies have proven the involvement of Psl in adhesion to biotic and abiotic surfaces, biofilm architecture, motility and protection against stressors (Ma *et al.*, 2006; Colvin *et al.*, 2012; Billings *et al.*, 2013; Wang *et al.*, 2013; Wang *et al.*, 2014; Periasamy *et al.*, 2015). Although the existence of a *psl*-like gene cluster was reported in some environmental nonaeruginosa *Pseudomonas* years ago (Mann & Wozniak, 2012), its role in biofilm formation has not been assessed.

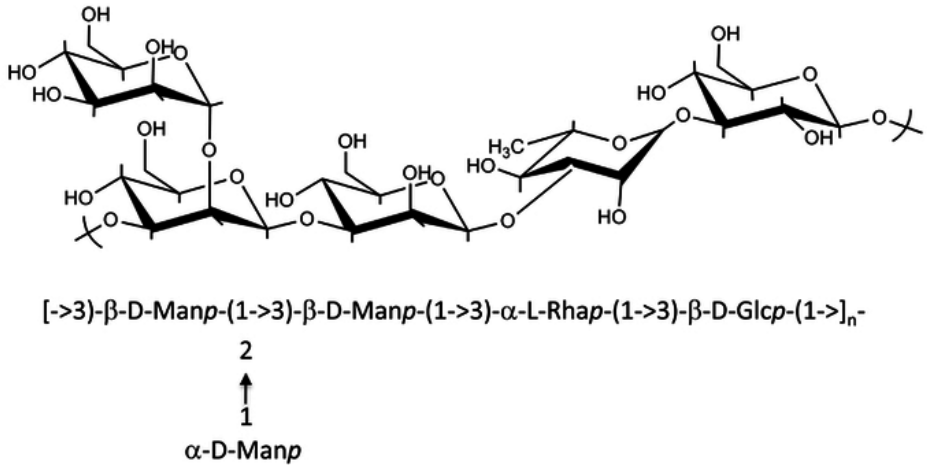

Figure 7.I. Structure of Psl polysaccharide. Psl structure consists of a pentasaccharide subunit of D-mannose, D-glucose and L-rhamnose in a 3:1:1 ratio. Image obtained from Franklin *et al.*, 2011.

The Pel polysaccharide is encoded in PAO1 and PA14 by a seven-gene operon (Friedman & Kolter, 2004; Mann & Wozniak, 2012) and consists of a partially acetylated polymer of 1→4 glycosidic linkages of N-acetylgalactosamine and N-acetylglucosamine residues (Jennings *et al.*, 2015). The Pel polysaccharide is involved in the formation of pellicle biofilms and is particularly relevant for biofilm formation in *P. aeruginosa* PA14 strain, as it does not produce Psl (Friedman & Kolter, 2004; Colvin *et al.*, 2011; Mann & Wozniak, 2012). The Psl and Pel polysaccharides can serve redundant structural functions in mature biofilms of those *P. aeruginosa* strains that can produce both polysaccharides (Colvin *et al.*, 2012). In

PA14 strain, Pel is crucial for maintaining cell-to-cell interactions within biofilms and enhances antibiotic resistance (Colvin *et al.*, 2011). However, the genomic region encoding Pel is poorly conserved among environmental *Pseudomonas* (Mann & Wozniak, 2012; Blanco-Romero *et al.*, 2020).

6. Biofilm formation by plant interacting *Pseudomonas*

Bacteria belonging to the *Pseudomonas* genus are common inhabitants of plant surfaces (Hirano & Upper, 2000; Lugtenberg *et al.*, 2001). The role played by *Pseudomonas* in the agricultural industry is remarkable, as several economically important activities are derived from their interaction with plants. Among these activities, there are harmful diseases that involve severe economic losses and beneficial activities such as plant growth stimulation, the promotion of plant health and nutrient availability in soils and induction of plant immune defences (Kennelly *et al.*, 2007; Mercado-Blanco & Bakker, 2007). Some of the extracellular matrix components, mainly exopolysaccharides, that are required for biofilm formation and pathogenesis in *P. aeruginosa* find their equivalents in pathogenic and beneficial plant-interacting *Pseudomonas* (Blanco-Romero *et al.*, 2020) such as the alginate, Psl and Pel exopolysaccharides and the Fap system. Interestingly, the roles that Psl and Pel play in biofilm formation and ecology of environmental *Pseudomonas*, including plant-interacting *Pseudomonas*, have not been assessed.

6.1. Biofilm formation by pathogenic plant-interacting *Pseudomonas*: the case study of *P. syringae*

The *P. syringae* complex harbours most of the phytopathogens within the *Pseudomonas* genus (Bull *et al.*, 2010). The *P. syringae* species *sensu stricto* is a model for the study of plant-bacteria interactions because of its ubiquity (Lindow & Brandl, 2003) and that it can infect almost all economically important crops (Kennelly *et al.*, 2007). *P. syringae* is a phytopathogenic bacterium but is not always found causing disease. It is currently known that *P. syringae* undergoes between epiphytic and pathogenic stages in plants mostly depending on environmental conditions (Cazorla *et al.*, 1998; Hirano & Upper, 2000; Xin *et al.*, 2018). *P. syringae* possesses a great diversity of virulence factors that engage in plant infection, as well as adaptation mechanisms that improve bacterial survival over the plant surfaces. Generally, *P. syringae* produces a type III secretion system (T3SS), effector proteins, motility appendages, phytotoxins, multidrug efflux pumps, plant

hormones, cell wall-degrading enzymes and ice nucleation activity (Ichinose *et al.,* 2013). Copper- and UV radiation-resistance genes, as well as exopolysaccharide production, play fundamental roles in *P. syringae* fitness and survival (Sundin *et al.,* 1996; Cazorla *et al.,* 2002; Arrebola *et al.,* 2015; Gutiérrez-Barranquero *et al.,* 2013, 2017, 2019; Aprile *et al.,* 2021).

P. syringae is able to produce a number of biofilm matrix polysaccharides, including alginate, levan and cellulose (Osman *et al.,* 1986; Fakhr *et al.,* 1999; Preston *et al.,* 2000; Li & Ullrich *et al.,* 2001; Arrebola *et al.,* 2015; Pérez-Mendoza *et al.,* 2019). As previously observed in *P. aeruginosa* (Wozniak *et al.,* 2003), alginate plays non-essential structural roles in *P. syringae* biofilms, as the alginate-deficient derivative of the *P. syringae* pv. glycinea PG4180 mucoid strain (PG4189.muc) still retained the ability to form biofilms in flow-cell chambers (Laue *et al.,* 2006). Alginate is overproduced in some strains of *P. syringae* upon exposure to copper bactericides, which are usually applied to reduce the disease incidence caused by some plant-pathogens (Kidambi *et al.,* 1995). Previous works have indicated that alginate polysaccharides are involved in the pathogenic interaction of *P. syringae* with plants (Rudolph *et al.,* 1994; Fett *et al.,* 1989; Yu *et al.,* 1999). For instance, the alginate mutant of *P. syringae* pv. syringae 3525 strain, the causal agent of bacterial brown spot on bean, is significantly impaired in the colonization of bean (host) and tomato (non-host) leaves, and although it retains the ability to generate symptoms, the symptoms are less severe than those induced by the wild-type (Yu *et al.,* 1999). However, these results have not been observed in other *P. syringae* strains (Peñaloza-Vázquez *et al.,* 1997; Willis *et al.,* 2001; Schenk *et al.,* 2008).

Levan is a β-2,6 linked fructose polymer that is highly branched through β-2,1 linkage and is synthetized from sucrose by levansucrases (Osman *et al.,* 1986). The presence of levansucrases has been reported in the *Pseudomonas* genus, including the *P. syringae, P. fluorescens, P. chlororaphis and P. corrugata* species (Blanco-Romero *et al.,* 2020). However, levan production has been mainly detected in strains belonging to the *P. syringae* and *P. fluorescens* species (Fett *et al.,* 1989; Li & Ullrich, 2001). Studies regarding the synthesis, spatial distribution and function of this polysaccharide within biofilms have essentially been conducted in the PG4180 strain (Osman *et al.,* 1986; Li & Ullrich, 2001; Laue *et al.,* 2006). The PG4180.muc levan-deficient derivative still retained the ability to form biofilms (Laue *et al.,*

2006). To study the spatial distribution of levan within biofilms, Laue and collaborators stained PG4180.muc mature biofilms with the fluorescently labelled Concavalin A (ConA lectin) lectin, which binds to levan polysaccharide. The results determined that levan accumulated in cell-free spaces within biofilms, which led the authors hypothesize this polysaccharide could function as a carbohydrate reservoir under starvation (Laue *et al.,* 2006).

Finally, cellulose is a polymer of D-glucose residues joined by β-1,4 glycosidic linkages and is considered a relevant biofilm matrix molecule in many environmental *Pseudomonas* species (Ude *et al.,* 2006; Spiers *et al.,* 2013). Previous studies reported that several plant-pathogenic *Pseudomonas* can produce cellulose, including *P. syringae*, *P. asplenii*, *P. marginalis*, *P. corrugata* and *P. savastanoi* (Ude et al., 2006; Spiers *et al.,* 2013; Blanco-Romero *et al.,* 2020). However, most studies regarding its structural roles within biofilms and biological significance have been conducted on *P. syringae*. The *P. syringae* pv. syringae UMAF0158 (PssUMAF0158) strain, the causal agent of bacterial apical necrosis (BAN) on mango trees (Arrebola *et al.,* 2015), and *P. syringae* pv. tomato DC3000 (PtoDC3000), responsible for bacterial speck disease on tomato plants (Pérez-Mendoza *et al.,* 2014), produce cellulose as the main exopolysaccharide of their biofilms. The biofilm structures formed by PssUMAF0158 and PtoDC3000 in microwell plates are highly similar, consisting of pellicles with wrinkles on the surface that are weakly attached to the walls of the culture vessels (Pérez-Mendoza *et al.,* 2014; Arrebola *et al.,* 2015). Despite the structural similarities found *in vitro*, the biological performance of cellulose seems to differ in both strains. Cellulose allows PssUMAF0158 adhesion to mango leaves and its production intimately affects the epiphytic and pathogenic stages of this strain over the plant surface (Arrebola *et al.,* 2015). Hence, the incidence and severity of necrotic symptoms developed by PssUMAF0158 on tomato leaflets are lower in the wild-type than in the cellulose mutants (Δ*wssB* and Δ*wssE* strains) and practically nonexistent in the cellulose-overproducing strain (Arrebola *et al.,* 2015). These results led to propose a lifecycle for PssUMAF0158 over the mango tree, in which biofilm formation would be mainly needed during the epiphytic phase, when bacteria are more exposed to the external environment and protection against its challenging conditions becomes crucial for survival (Gutiérrez-Barranquero *et al.,* 2019). Interestingly, the link

observed between cellulose production and PssUMAF0158 transition through epiphytic and pathogenic stages over the mango plant surface has not been reported in PtoDC3000. The disease symptoms developed in tomato by PtoDC3000 wild-type strain were not different from those of its Δ*wssBC*-derived mutant (Prada-Ramírez *et al.,* 2016). Furthermore, in disagreement with PssUMAF0158, cellulose overproduction in PtoDC3000 does not lead to a significant impact on virulence (Pérez-Mendoza *et al.,* 2014). However, the infection assays were performed using different tomato cultivars and inoculation approaches, which could eventually account for different results.

6.2. Biofilm formation by beneficial plant-interacting *Pseudomonas*: the case study of *P. fluorescens*

Beneficial plant-interacting *Pseudomonas* are frequently present in soil communities (Janssen, 2006; Mercado-Blanco & Bakker, 2007). Generally, species belonging to the *P. fluorescens* complex are among the most studied as they frequently show agricultural, biotechnological and ecological interest (Garrido-Sanz *et al.,* 2017). Particularly, the *P. fluorescens* and *P. chlororaphis* species stand out because of their potential use as biocontrol agents (Ganeshan & Kumar, 2005; Cazorla *et al.,* 2006; Anderson & Kim, 2020). Root colonization results in the formation of biofilm structures on the roots (Morris & Monier, 2003). Usually, biocontrol agents can form biofilms, and increasing evidence strongly suggest that the biofilm-forming ability should be considered in assessing their potential beneficial performance (Pandin *et al.,* 2017).

Biofilm formation by beneficial plant-interacting bacteria provide advantages for both plant and bacteria. On the one hand, they can increase plant yield by improving mineral uptake and phytohormone production, inducing the competitive suppression of pathogens and triggering plant-induced systemic resistance (Rudrappa *et al.,* 2008). On the other hand, biofilms allow the attachment of the cells to a nutrient source and confer protection against plant defences and environmental fluctuations (Danhorn & Fuqua, 2007; Bogino *et al.,* 2013). Furthermore, the biofilms produced by rhizospheric bacteria enhance soil aggregation, which improves the water-holding capacity, fertility and porosity of the soils, leading to an increase in agricultural productivity (Davey & O'Toole, 2000; Lynch & de Leij, 2012; Sandhya & Ali, 2015; Costa *et al.,* 2018).

Members belonging to the *P. fluorescens* complex and *P. putida* species can produce alginate and cellulose polysaccharides (Conti *et al.,* 1994; Bianciotto *et al.,* 2001; Spiers *et al.,* 2003, 2005; Blanco-Romero *et al.,* 2020). Alginate plays minor structural roles in the biofilms of *P. fluorescens* and *P. putida* (Nilsson *et al.,* 2011; Noirot-Gros *et al.,* 2019). The alginate mutant of *P. fluorescens* SBW25 still forms biofilms in flow-cell chamber experiments but they are thinner than those formed by the wild-type strain (Noirot-Gros *et al.,* 2019). This result was consistent with the flow-cell chamber phenotype of the *P. aeruginosa* PAO1 alginate mutant, which showed significantly lower surface coverage and volume values than the wild-type strain (Ghafoor *et al.,* 2011). Alginate has been described as the primary polysaccharide that promotes hydration under desiccating stress in *P. putida* (Nielsen *et al.,* 2011; Schnider-Keel *et al.,* 2001; Chang *et al.,* 2007). In fact, alginate slightly contributes to the biofilm architecture of *P. putida* under water-limiting conditions (Chang *et al.,* 2007). The functions performed by alginate polysaccharide in both *P. fluorescens* and *P. putida* strains *in vivo* seem to be more relevant than those *in vitro*. For instance, the CHA211 and CHA213M mucoid variants of the *P. fluorescens* CHA0 strain, which overproduce alginate, enhance their biofilm formation abilities on carrot roots compared to the wild-type strain (Bianciotto *et al.,* 2001). The genomic region located upstream of the *algD* gene of *P. putida* KT2440 is active during the colonization of maize roots, which suggests that this polysaccharide could be a fitness determinant for the rhizosphere colonization ability of this bacterium (Ramos-Gonzalez *et al.,* 2005).

Previous studies reported that some beneficial plant-interacting *Pseudomonas* can also produce cellulose (Ude *et al.,* 2006; Spiers *et al.,* 2013; Blanco-Romero *et al.,* 2020). In particular, cellulose is involved in the formation of floating biofilms or pellicles in many strains of the *P. fluorescens* and *P. putida* species (Spiers *et al.,* 2003; Ude *et al.,* 2006; Armitano *et al.,* 2014; Ardré *et al.,* 2019). Within the *Pseudomonas* genus, *P. fluorescens* SBW25 (SBW25) strain has been traditionally used as the model strain for the study of bacterial cellulose (Spiers *et al.,* 2003). In SBW25, cellulose polysaccharide is encoded on a ten-gene operon (*wssA-J*) that corresponds to the PFLU0300-PFLU0309 genomic region (Spiers *et al.,* 2003). Biofilm experiments on SBW25 have determined that the gradients occurring within a static microcosm immediately select for the emergence of variants that occupy

different niches (Rainey & Travisano, 1998). Among those variants, the air-liquid (A-L) interface is colonized by Wrinkly Spreader (WS) pellicles, an SBW25-derived mutant that overproduces cellulose compared to the wild-type equivalent (Spiers *et al.,* 2002). In *P. putida* mt2 and KT2440 strains, cellulose plays minor roles in biofilm formation *in vitro* (Nielsen *et al.,* 2011; Nilsson *et al.,* 2011). Instead, the role of cellulose exopolysaccharide in *P. putida* seems to be more directed towards conferring protection, as water-limiting conditions and increasing osmolarity highly induce cellulose expression of *P. putida* mt2 (Nielsen *et al.,* 2011; Svenningsen *et al.,* 2018). In addition, the cellulose mutant of the *P. putida* mt2 accumulates significantly more reactive oxygen species (ROS) than the wild-type strain upon exposure to matric and copper stressors (Svenningsen *et al.,* 2018). During plant-bacteria interaction, cellulose exopolysaccharide of SBW25 contributes to the ecological performance of this strain in the rhizosphere and phyllosphere of sugar beet (Gal *et al.,* 2003). Thus, a cellulose-defective mutant of SBW25 (SM13) was competed against the wild-type in the rhizosphere, phyllosphere and bulk soil surrounding the rhizosphere of sugar beet seedlings, and the results showed no significant differences between the fitness of SM13 relative to the wild-type in bulk soil, but significant differences were found in the rhizosphere and phyllosphere, especially in the phyllosphere (Gal *et al.,* 2003). Something similar has been reported in the *P. putida* mt2 strain, in which the cellulose mutant is impaired in the colonization of the maize rhizosphere during competition with the wild-type equivalent (Nilsson *et al.,* 2011). These studies indicate that while the cellulose operon does not seem to be critical under laboratory conditions in *P. fluorescens* and *P. putida,* its roles in these species seem to be more pronounced *in vivo*.

7. *P. syringae* pv. syringae UMAF0158 and *P. chlororaphis* PCL1606 as reference strains for the study of biofilm formation

The bacterial apical necrosis (BAN) disease of mango trees (*Mangifera indica*) is the most limiting factor for mango crop in the Mediterranean area (Cazorla *et al.,* 1998). BAN symptoms consist of necrosis of vegetative buds that rapidly expand on leaves (Kenelly *et al.,* 2007). Sometimes, necrotic lesions can extend through the leaf petiole to the stem and, eventually, kill or severely debilitate the trees (Cazorla *et al.,* 1998; Kenelly *et al.,* 2007). *P. syringae* pv. syringae (Pss) was described as the causal agent of BAN disease (Cazorla *et al.,* 1998) and mangotoxin, an

antimetabolite toxin that was present in all the Pss strains isolated from mango (Arrebola *et al.,* 2003), was intimately associated with the development of necrotic symptoms (Arrebola *et al.,* 2009). Weather conditions play a fundamental role in *P. syringae* disease development, as it has also been described that the highest disease severity of BAN always coincides with cool and wet time periods (Cazorla *et al.,* 1998).

Initially, the *P. syringae* pv. syringae UMAF0158 (PssUMAF0158) strain was chosen by our research group as model strain to elucidate the role of mangotoxin in virulence and bacterial fitness in planta (Arrebola *et al.,* 2007, 2009; Carrión *et al.,* 2012, 2014). PssUMAF0158 was isolated from a necrotic bud of a mango tree located in Algarrobo, Malaga (South Spain; Arrebola *et al.,* 2003). The genome-sequencing project of PssUMAF0158 revealed the presence of several virulence factors (Table 1.I) and a gene cluster related to cellulose production (Martínez-García *et al.,* 2015). Cellulose biosynthesis is involved in PssUMAF0158 biofilm formation, attachment to the mango leaf surfaces and influences transition between epiphytic and pathogenic stages in plants in *P. syringae* (Arrebola *et al.,* 2015). Thus, the mutants defective in cellulose production are more virulent than the wild-type strain and virulence in the cellulose overproducing strain is practically abolished (Arrebola *et al.,* 2015). Therefore, biofilm formation has proven to be a very important trait for the ecology of this bacterium during its interaction with the mango host plant.

Table 1.I. Summary of putative virulence-associated genes in the PssUMAF0158 strain. Table modified from Martínez-García *et al.,* (2015).

Virulence factors	Products
Toxins	Syringomycin, syringopeptin, mangotoxin, syringolin A
PCWDEs	Pectin lyase, xylanase, cellulase, lipoyl synthase
Siderophores	Achromobactin, pyoverdine
Adhesion proteins	Cellulose synthase, filamentous haemagglutinin, fimbrial proteins, adhesion proteins AttC/AttG
Detoxifying compounds	Copper oxidase, catalase/hydroperoxidase, proline iminopeptidase, ferritin, cytochrome C oxidase
Phytohormones	Auxin
EPSs	Alginate, cellulose

PCWDEs (plant-cell-wall degrading enzymes); EPS (exopolysaccharides).

On another front, *P. chlororaphis* is a common inhabitant of the root environment of many plants that possesses traits related to biofertilization, phytostimulation and biocontrol (Bloemberg & Lugtenberg, 2001; Arrebola *et al.,* 2019). *P. chlororaphis* PCL1606 (PcPCL1606) strain was isolated from the rhizosphere of a healthy avocado (*Persea americana*) tree located in Algarrobo, Malaga (South Spain) and showed antagonistic activity against several phytopathogenic fungi, including *Rosellinia necatrix* and *Fusarium oxysporum* (Cazorla *et al.,* 2006). PcPCL1606 showed biocontrol activity against white root rot and foot and root rot diseases in the avocado-*R. necatrix* and tomato-*F. oxysporum* pathosystems, respectively (Cazorla *et al.,* 2006). The compound 2-hexyl 5-propyl resorcinol (HPR) is responsible of PcPCL1606 antagonistic activity, as the *darB* mutant (Δ*darB*), which is defective in HPR synthesis, shows impairment in biocontrol activity using both pathosystems (Calderón *et al.,* 2013). However, PcPCL1606 is an unusual member of the *P. chlororaphis* species because it does not produce phenazines and does not promote plant growth *per se* (Table 2.I; Arrebola *et al.,* 2019). Apart from its antagonistic activity, the compound HPR seems to function as a signal molecule because the PcPCL1606 Δ*darB* strain (impaired in HPR production) is also impaired in avocado root colonization and biofilm formation (Calderón *et al.,* 2014, 2019). The impairment in biofilm formation and reduction in avocado root colonization observed in the PcPCL1606 Δ*darB* mutant suggests that the reduction in biocontrol

activity could be due to a conjunction of events, mainly to the impairment in HPR production, but also to the impairment in biofilm formation and root colonization, as the last two processes have been formerly described to be prerequisites for conferring plant protection (Bloemberg & Lugtenberg, 2001; Chin-A-Woeng *et al.*, 2007; Lugtenberg & Kamilova, 2009). Therefore, biofilm formation might be an important trait for the ecology of PcPCL1606 during its interaction with their host plant roots.

Table 2.I. Detection of genes of compounds present in the PcPCL1606 strain. Data obtained from Calderón *et al.*, (2015).

Antimicrobial antibiotic volatiles[a]						
HPR	DAPG	PRN	HCN	PHZ	PLT	Rhizoxins
+	-	+	+	-	-	-
Cyclic-peptides		**Siderophores**				**Toxins**
Orfamide	Viscosin	Pyoverdine	Pyochelin	Achromobactin	Hemophore	FitD
-	-	+	+	+	-	+

[a]HPR = 2-hexyl, 5-propyl resorcinol; DAPG = 2,4-diacetylphloroglucinol; PRN = pyrrolnitrin; HCN = hydrogen cyanide; PHZ = phenazine and PLT = pyoluteorin.

In this dissertation, the biological role of several extracellular matrix components (EMC) in the biofilm lifestyle and ecology of the two plant-interacting bacteria PssUMAF0158 (pathogenic) and PcPCL1606 (beneficial) have been assessed. The results highlight the role played by the Psl exopolysaccharide, which to date had been only studied in *P. aeruginosa*, in the biofilm architecture and ecology of PssUMAF0158 and PcPCL1606 during their interaction with their plant hosts.

OBJECTIVES

Biofilm formation could be related to the transition between epiphytic and pathogenic lifestyles in *Pseudomonas syringae* pv. syringae (Pss) associated with the mango host (Arrebola *et al.,* 2015; Gutiérrez-Barranquero *et al.,* 2019). Furthermore, previous evidences indicate that there could be a connection between environmental factors and biofilm formation in Pss strains associated with the mango host (Cazorla *et al.,* 1998; Arrebola *et al.,* 2015). On the other hand, the decrease in biocontrol activity of *Pseudomonas chlororaphis* PCL1606 Δ*darB* mutant compared to the wildtype strain against the white root rot disease caused by *Rosellinia necatrix* (Calderón *et al.,* 2013) could be due to a combination of factors, in which not only the absence in antifungal metabolite production but also the impairment in root colonization due to a defect in biofilm formation could contribute to its decrease in biocontrol activity.

With this background, biofilm formation by different *Pseudomonas* strains could be relevant in the phyllosphere and rhizosphere ecosystems and for epipythic-pathogenic transition and biocontrol activity. Therefore, the following objectives were raised:

1. To determine the role that the extracellular matrix components play in biofilm formation (and/or related phenotypes) and ecology of the phytopathogenic bacterium *P. syringae* pv. syringae.

2. To determine the role that environmental factors, such as temperature and light, play in biofilm formation in *P. syringae* pv. syringae strains.

3. To determine the role that extracellular matrix components play in biofilm formation (and/or related phenotypes) and ecology of the biocontrol agent *P. chlororaphis* PCL1606.

La formación de biopelículas podría estar relacionada con la transición entre el estilo de vida epífito y patógeno en las cepas de *Pseudomonas syringae* pv. syringae (Pss) aisladas de mango (Arrebola *et al.,* 2015; Gutiérrez-Barranquero *et al.,* 2019). Además, evidencias previas sugieren que podría existir una relación entre los factores ambientales y la formación de biopelículas en las cepas de Pss (Cazorla *et al.,* 1998; Arrebola *et al.,* 2015). Por otro lado, la reducción de la actividad de biocontrol de la cepa mutante *Pseudomonas chlororaphis* PCL1606 Δ*darB* (Calderón *et al.,* 2013) en comparación con la de la cepa silvestre frente a la podredumbre blanca radicular del aguacate causada por el hongo *Rosellinia necatrix* podría deberse a una combinación de factores, en la que no solo la ausencia de producción de antifúngicos, sino también fallos en colonización de la raíz debidos a las alteraciones en la formación de biopelículas, podrían contribuir a la reducción en dicha actividad de biocontrol.

Con estos antecedentes, la formación de biopelículas en diferentes cepas de *Pseudomonas* podría ser relevante tanto en la filosfera como en rizosfera, en particular para la transición entre las fases epífita-patógena y la actividad de biocontrol. Por lo tanto, los siguientes objetivos fueron propuestos:

1. Determinar el papel que los componentes de la matriz extracelular poseen en la formación de biopelículas (y/o fenotipos relacionados) y la ecología de la bacteria fitopatógena *P. syringae* pv. syringae.

2. Determinar el papel que los factores ambientales, como la temperatura y la luz, poseen en la formación de biopelículas en cepas de *P. syringae* pv. syringae.

3. Determinar el papel que los componentes de la matriz extracelular poseen en la formación de biopelículas (y/o fenotipos relacionados) y en la ecología del agente de biocontrol *P. chlororaphis* PCL1606.

EXPERIMENTAL PROCEDURES

1. Bacterial strains and growth conditions

The bacterial strains and plasmids used are listed in Table 1.C1 for Chapter 1 and Table 1.C3 for Chapter 3. For standard maintenance, *Pseudomonas syringae* strains and derived extracellular matrix mutants were grown in King's B medium (KB; King *et al.*, 1954) at 25ºC and *Pseudomonas chlororaphis* PCL1606 wild-type and derived extracellular matrix mutants were grown in tryptone-peptone-glycerol medium (TPG; Calderón *et al.*, 2014) at 25ºC. *Escherichia coli* was used as a host for the mutation and complementation plasmids and was routinely grown in lysogenic broth (LB) at 37ºC. The antibiotics used for the selection of *P. syringae* pv. syringae UMAF0158 (PssUMAF0158) and *P. chlororaphis* PCL1606 (PcPCL1606) derivatives were kanamycin 50 mg/L (Km_{50}), gentamycin 50 mg/L (Gm_{50}) and tetracycline 25 mg/L (Tc_{25}). PcPCL1606 was hyper-resistant to ampicillin, but PssUMAF0158 derivatives can be selected at ampicillin 500 mg/L (Amp_{500}). The antibiotics used for the selection of *E. coli* derivatives were kanamycin 50 mg/L (Km_{50}), ampicillin 100 mg/L (Amp_{100}) and gentamycin 10 mg/L (Gm_{10}). TPG medium was used for the *in vitro* experiments. Pseudomonas Isolation Agar (PIA; Difco) was used for PcPCL1606 fluorescent tagging by triparental conjugation. PssUMAF0158 could not grow on PIA medium, thus KB medium supplemented with nitrofurantoin 100 mg/L (nft_{100}), which does not allow *E. coli* growth, was used for PssUMAF0158 fluorescent tagging by triparental conjugation. Flow-cell chamber experiments were performed using AB minimal medium (Clark & Maaløe, 1967) supplemented with 0.3 mM glucose and 0.005% yeast extract for PssUMAF0158 and with 0.3 mM citrate for PcPCL1606.

Table 1.C1. Bacterial strains and plasmids used in Chapter 1.

Strains or plasmids	Relevant characteristics	Reference
Bacterial strain		
Pseudomonas syringae pv. syringae UMAF0158	Wild-type, isolated from mango (Malaga)	Arrebola *et al.*, 2003
PssUMAF0158 *Δalg8*	Alginate deletional mutant; Km^R	This study
PssUMAF0158 *ΔwssE*	Cellulose deletional mutant; Km^R	This study
PssUMAF0158 *ΔpslE*	Psl-like deletional mutant; Km^R	This study
PssUMAF0158 *Δalg8,wssE*	Double deletional mutant; Km^R	This study
PssUMAF0158 *Δalg8,pslE*	Double deletional mutant; Km^R	This study

PssUMAF0158 *Δ*wssE,pslE	Double deletional mutant; Km^R	This study
PssUMAF0158 *Δalg8*,wssE,pslE	Triple deletional mutant; Km^R	This study
PssUMAF0158 *Δalg8* + pBBR1MCS5*alg8*	Alginate complemented strain; Km^R, Gm^R	This study
PssUMAF0158 *ΔwssE* + pBBR1MCS5*wssE*	Cellulose complemented strain; Km^R, Gm^R	This study
PssUMAF0158 *ΔpslE* + pBBR1MCS5*pslE*	Psl-like complemented strain; Km^R, Gm^R	This study
PssUMAF0158 wild-type dsRed	PssUMAF0158 wt with the pMP4662-dsRed plasmid; Tc^R	This study
PssUMAF0158 wild-type GFP	PssUMAF0158 wt with the pMP4655-GFP plasmid; Tc^R	This study
PssUMAF0158 *ΔwssE* dsRed	Cellulose deletional mutant with the pMP4662-dsRed plasmid; Km^R; Tc^R	This study
PssUMAF0158 deletional mutant GFP	PssUMAF0158 deletional mutant (*Δalg8*, *ΔwssE* or *ΔpslE*) with the pMP4655-GFP plasmid; Km^R, Tc^R	This study
PssUMAF0158 *Δalg8* + pBBR1MCS5*alg8* GFP	Chromosomally-tagged alginate mutant strain with the *alg8* complementation plasmid; Km^R, Gm^R	This study
PssUMAF0158 *ΔwssE* + pBBR1MCS5*wssE* GFP	Chromosomally-tagged cellulose mutant strain with the *wssE* complementation plasmid; Km^R, Gm^R	This study
PssUMAF0158 *ΔpslE* + pBBR1MCS5*pslE* GFP	Chromosomally-tagged Psl-like mutant strain with the *pslE* complementation plasmid; Km^R, Gm^R	This study
PssUMAF0158 wt + pBBR1MCS5	PssUMAF0158 wild-type strain with the pBBR1MCS5 plasmid; Gm^R	This study
PssUMAF0158 wt + pBBR1MCS5*pslE*	PssUMAF0158 wild-type with the *pslE* complementation plasmid; Gm^R	This study
E. coli DH5α	*E. coli [F' Φ80lacZ ΔM15 Δ(lacZYA-argF)U169 deoR recA endA1 hsdR17 (rK-mK+)phoA supE44 lambda- thi-1]*	Hanahan *et al.*, 1983
E. coli S17-1 λpir pTNS3	Helper strain for Tn7 transposition; Amp^R	Norris *et al.*, 2010
E. coli S17-1 λpir mini-Tn7-Km-GFP	Donor strain with mini-Tn7-Km harboring GFP; Km^R, Amp^R	Bao *et al.*, 1991

Plasmid	Relevant characteristics	Source
pGEM-T *easy*	3 kb cloning vector; Amp^R	Promega, Madison, WI
pMP4655	14,2 kb cloning vector harboring GFP; Tc^R	Bloemberg *et al.*, 2000
pMP4662	14,2 kb cloning vector harboring dsRed; Tc^R	Bloemberg *et al.*, 2000
pGEM-T-KmFRT-HindIII	Contains Km^r from pKD4 and HindIII sites; Amp^R, Km^R	Matas *et al.*, 2014
pFPL2	Contains a flipase gene; Amp^R	Modified from Hoang *et al.*, 1998
pBBR1MCS-5	4.7 kb broad-host-range cloning vector; Gm^R	Kovach *et al.*, 1995

Table 1.C3. Bacterial strains and plasmids used in Chapter 3.

Strains or plasmids	Relevant characteristics	Reference
Bacterial strain		
Pseudomonas chlororaphis PCL1606	Wild-type, isolated from Spanish avocado rhizosphere (Malaga)	Cazorla *et al.*, 2006
PcPCL1606 *Δalg8*	Alginate deletional mutant; Km^R	This study
PcPCL1606 *ΔpslE*	Psl-like deletional mutant; Km^R	This study
PcPCL1606 *ΔfapBC*	Fap-like deletional mutant; Km^R	This study
PcPCL1606 *Δalg8,pslE*	Double deletional mutant; Km^R	This study
PcPCL1606 *Δalg8,fapBC*	Double deletional mutant; Km^R	This study
PcPCL1606 *ΔpslE,fapBC*	Double deletional mutant; Km^R	This study
PcPCL1606 *Δalg8,pslE,fapBC*	Triple deletional mutant; Km^R	This study
PcPCL1606 *Δalg8* + pBBR1MCS5*alg8*	Alginate complemented strain; Km^R, Gm^R	This study
PcPCL1606 *ΔpslE* + pBBR1MCS5*pslEF*	Psl-like complemented strain; Km^R, Gm^R	This study
PcPCL1606 *ΔfapBC* + pBBR1MCS5*fapBC*	Fap-like complemented strain; Km^R, Gm^R	This study
PcPCL1606 wild-type mCherry	Chromosomally-tagged mCherry-PcPCL1606 wt; Gm^R	This study
PcPCL1606 wild-type GFP	Chromosomally-tagged GFP-PcPCL1606 wt; Gm^R	This study

PcPCL1606 *ΔpslE* mCherry	Chromosomally-tagged GFP-PcPCL1606 deletional mutant; Km^R, Gm^R	This study
E. coli DH5α	*E. coli [F' Φ80lacZ ΔM15 Δ(lacZYA-argF)U169 deoR recA endA1 hsdR17 (rK-mK+)phoA supE44 lambda- thi-1]*	Hanahan *et al.*, 1983
E. coli S17-1 pUX-BF13	Helper strain for Tn7 transposition; Amp^R	Bao *et al.*, 1991
E. coli S17-1 mini-Tn7-GFP	Donor strain carrying mini-Tn7 PA1/04/03-GFP; Gm^R, Amp^R	Norris *et al.*, 2010
E. coli S17-1 mini-Tn7-mCherry	Donor strain carrying mini-Tn7 PA1/04/03-mCherry; Gm^R, Amp^R	Norris *et al.*, 2010
Plasmid	**Relevant characteristics**	**Source**
pGEM-T *easy*	3 kb cloning vector; Amp^R	Promega, Madison, WI
pGEM-T-KmFRT-HindIII	Contains Km^r from pKD4 and HindIII sites; Amp^R, Km^R	Matas *et al.*, 2014
pFPL2 - Gm	Contains a flipase gene; Amp^R, Gm^R	Hoang *et al.*, 1998
pBBR1MCS-5	4.7 kb broad-host-range cloning vector; Gm^R	Kovach *et al.*, 1995

2. Strain manipulation and tagging

PssUMAF0158 and PcPCL1606 knockout extracellular matrix mutants were generated according to the protocol described in Zumaquero *et al.*, 2010. Specific primers are listed in Table S1 for Chapter 1 and Table S2 for Chapter 3. The transformants were selected on KB medium containing kanamycin. To assess whether each transconjugant integrated the plasmid into the chromosome or engaged in allelic exchange, two approaches were performed depending on the strain. In PssUMAF0158, the resulting colonies were grown in KB+Km_{50} and KB+Amp_{500} and those resistant to kanamycin but sensitive to ampicillin were assessed by PCR using primers that amplify a fragment within the selected gene. In PcPCL1606, the resulting colonies were directly assessed by PCR using primers that amplify a fragment within the selected gene. Those colonies that did not show amplification of the selected gene were subsequently assessed by southern blot using probes that matched within the selected gene and the Km cassette. To create the doubles and

triple mutants, the kanamycin cassette was removed using a pFPL2 plasmid ($Amp^{R)}$, which in the case of PcPCL1606, due to its natural resistance to ampicillin, it was modified by introducing the gentamycin cassette present in the pBBR1MCS5 plasmid using primers containing the XbaI and BamHI restriction sequences (pFPL2-Gm; Table S2). The complementation plasmids were constructed using specific primers that included the amplification of the fifty base pairs upstream of the selected gene to include their own ribosome biding site (*rbs*). The resulting amplicons were then cloned into the pBBR1MCS5 plasmid and fully sequenced to discard any possible mutations.

In PssUMAF0158, fluorescent tagging of the wild-type and derived extracellular matrix mutants was performed by electroporation (Choi *et al.*, 2006) using the pMP4655 (GFP) and pMP4662 (dsRed) plasmids. Fluorescent tagging of the PssUMAF0158 complemented strains was performed by triparental conjugation (Lambertsen *et al.*, 2004) of the Km^S mutant strains using a donor and helper strains (Table 1.C1). Then, the complementation plasmid was introduced in the tagged strains by electroporation (Choi *et al.*, 2006). In PcPCL1606, fluorescent tagging of the wild-type and derived extracellular matrix mutants was performed by triparental conjugation (Lambertsen *et al.*, 2004) using a donor and a helper strain (Table 1.C3). Briefly, the *E. coli* donor, *E. coli* helper and recipient strains were grown overnight at an appropriate temperature (37ºC for *E. coli* and 25ºC for *Pseudomonas*). Then, the bacterial suspensions were washed (1x) with 0.85% NaCl solution. Subsequently, 200 µl of each donor and helper and 100 µl of the recipient strain were mixed, plated in LB-agar and incubated overnight at 25ºC. The conjugation spots were subsequently resuspended in 0.85% NaCl solution, serial diluted 10-fold and spread on plates to avoid *E. coli* growth (PIA for PcPCL1606 and $KB+nft_{100}$ for PssUMAF0158). The plates were incubated 48 h at 25ºC for single fluorescent colonies to appear.

3. Bioinformatic analyses

Nucleotide and protein sequence searches were performed with the Pseudomonas Genome Database (https://www.pseudomonas.com/) and the National Center for Biotechnology Information (NCBI) database (https://www.ncbi.nlm.nih.gov/). Putative protein domain searches were carried out using Protein Family Software (PFAM) (https://pfam.xfam.org/).

4. Phylogenetic analyses

The nucleotide sequence of the complete *psl*-like gene cluster of the strains included in Table S3, along with partial combined sequences of *gyrB* and *rpoD* housekeeping genes, were used for phylogenetic comparison in Chapter 1. The combined nucleotide sequences of the genes belonging to the *psl*-like gene cluster of the *P. syringae* pv. syringae (Pss) strains included in Table 1.C2, along with the combined sequences of *gyrB*, *rpoD*, *gapA* and *cts* housekeeping genes, were used for phylogenetic comparison in Chapter 2. Finally, the nucleotide sequence of the complete *psl*-like gene cluster of the strains included in Table S4, along with the combined sequences of *gyrB* and *rpoD* housekeeping genes, were used for phylogenetic comparison in Chapter 3.

To identify the presence of the *psl*-like gene cluster in the genomes of different strains belonging to the *P. syringae* complex, the *psl*-like gene cluster of PssUMAF0158 was used for megablast searches in BLASTN against the complete genome of 34 plant-related strains belonging to different phylogroups within the *P. syringae* complex (Table S3). To identify the presence of the *psl*-like gene cluster in the genomes of different Pss strains, the *psl*-like gene cluster of PssUMAF0158 was used for megablast searches in BLASTN against the draft genomes of 19 Pss strains mainly isolated from the mango host (Table 1.C2). To identify the presence of the *psl*-like gene cluster in the *P. fluorescens* complex, the *psl*-like gene cluster of PcPCL1606 was used for megablast and discontiguous megablast searches in BLASTN against the genomes of 50 strains belonging to the different phylogenetic groups included in the P. *fluorescens* complex (Table S4).

Sequence alignment was performed using Clustal Omega (Larkin *et al.*, 2007) and phylogenetic trees were constructed using MEGAX software with Jukes Cantor's algorithm and maximum likelihood (ML) statistical method. The confidence level for the branching points was determined using 1,000 bootstrap replicates. *P. aeruginosa* PAO1 (Chapter 1 and 3) and *P. syringae* pv. syringae B728a and *P. syringae* pv. tomato DC3000 (Chapter 2) were used as outgroups.

5. Cellulose staining

Cellulose production within the biofilms and bacterial colonies was assayed using calcofluor dye. For this purpose, two different experimental approaches were applied. For biofilm staining, PssUMAF0158 and its derived cellulose mutant were grown in flow-cell chambers supplied with AB minimal medium supplemented with 0.3 mM glucose and 0.005% (w/v) yeast extract. After 12 h of incubation, the flow was stopped and 100 µL of a 1 mg/mL calcofluor solution was gently injected into the chamber. After 20 min of staining, the flow was restarted, and the unbound dye was cleared for another 20 min. Subsequently, images were obtained, analysed and prepared as previously indicated. For the detection of the cells, a 532 nm wavelength was used for the excitation of the dsRed fluorophore and emission was monitored at 570-700 nm. Calcofluor was excited with a 405 nm wavelength and emission was monitored at 450-495 nm. For colony staining, 10 µl of an overnight culture (OD_{600nm} = 0.5 a.u, which corresponds to 10^8 CFU/mL) was spotted onto a TPG plate with 20 µg/ml calcofluor dye. Samples were incubated at 25ºC for 48 h and images of the colonies under UV irradiation were recorded to assess the presence or absence of cellulose. Two independent experiments and at least three technical replicates per experiment and strain were performed.

6. Lectin staining of Psl-like components

The putative presence of a Psl-like polysaccharide within the PssUMAF0158 and PcPCL1606 extracellular matrixes was assayed using the dsRed/mCherry-tagged wild-types and the dsRed/mCherry-tagged *ΔpslE* mutant strains, respectively, as well as the FITC-tagged *Musa paradisiaca* lectin (BanLec; Glycomatrix), which binds to mannose residues (Singh *et al.*, 2014). First, the biofilms were grown in flow-cell chambers as mentioned below. BanLec was used at a final concentration of 100 µg/ml, as previously described for lectins (Neu & Lawrence, 1999). Forty-eight hours postinoculation, the flow was stopped and 100 µl of a 100 µg/ml lectin solution was gently injected into the chamber, to avoid complete wash out of the biofilms. After 20 min of staining, the flow was restarted to allow the clearance of the unbound protein for 20 min before microscopic observation. Subsequently, the images were recorded and analysed with the Leica Application Suite (Mannheim, Germany) and IMARIS software package (Bitplane, Switzerland). To detect the cells, the 532-nm laser was used for mCherry fluorophore excitation and emission

was monitored at 570-700 nm. The FITC-tagged BanLec was excited with the 488-nm laser and emission was monitored at 450-500 nm.

7. RNA isolation and quantitative reverse transcription experiments (qRT-PCR)

PssUMAF0158 and respective mutants were grown overnight with shaking in liquid TPG medium at 25°C. For RNA extractions of biofilms grown on plates, the cultures were adjusted to an OD of 0.5 a.u. at 600 nm (10^8 CFU/ml) and a 10 µl aliquot was transferred to a TPG plate, which was then incubated at 25ºC. Three colonies were collected, resuspended in a sterile 0.85% NaCl solution and centrifuged at 11,000 xg for 2 min. For RNA extractions of biofilms grown on liquid medium, the cultures were adjusted to an OD of 0.5 a.u. at 600 nm (10^8 CFU/ml) and a 100 µl aliquot was transferred to 900 µl of TPG and incubated without shaking (static culture) at 25ºC. Three pellicles were collected by centrifugation at 11,000 xg for 2 min. Total RNA was extracted from the pellets using an RNA isolation kit (Macherey-Nagel). The total RNA concentration was determined with a NanoDrop 2000 spectrophotometer (Thermo Fisher Scientific, Waltham, MA, USA), and RNA integrity was assessed by agarose gel electrophoresis. The absence of genomic DNA contamination was checked by PCR amplification of RNA samples using specific primers that amplify the syringomycin B gene (Table S1), which is mainly found in the syringae pathovar. Subsequently, DNA-free total RNA was converted to cDNA using Superscript III reverse transcriptase (Invitrogen, Carlsbad, CA, USA) and random primers according to the manufacturer's instructions. The qRT-PCR assays were conducted in a CFX384 Touch Real-Time PCR detection system (Bio-Rad, Hercules, CA, USA) using SyBrGreen Supermix (Bio-Rad). The reaction was developed as follows: 2 min at 95°C (polymerase activation); 1 s at 95°C; and 5 s at 60°C. The last two steps were repeated 50 times. Three independent RNA extractions and at least two technical replicates per extraction were assessed. The expression of *gyrB* and *rpoD* genes were used for normalization of qRT-PCR data. Gene-specific primers (Table S1) were designed using Primer3 (Thornton & Basu, 2015).

8. Exopolysaccharide extractions

Exopolysaccharide extractions were performed to determine the composition of the Psl-like exopolysaccharide of PssUMAF0158 strain. For that purpose, the following strains were used: *P. aeruginosa* PAO1, as a positive control of Psl production, PssUMAF0158 *Δalg8,wssE* double mutant, unaffected in Psl-like exopolysaccharide production, and PssUMAF0158 *ΔpslE*, impaired in Psl-like exopolysaccharide production. Exopolysaccharides were extracted from cells and supernatants using the following method. Precultures of the strains mentioned above were grown overnight on TPG broth. Then, 100 µl of the overnight cultures (OD 0,5 a.u. at 600 nm, which corresponds to 10^8 CFU/ml) was inoculated into 900 µl of TPG broth in microwell plates. The microwell plates were statically incubated at 25ºC (*P. syringae*) or 37ºC (*P. aeruginosa*) for 24 h. Starting from 250 ml, the cells were separated from supernatants by centrifugation at 8000 x g for 10 min. On the one hand, the harvested cells were washed with 10 ml of distilled water and resuspended in 30 ml of PBS buffer. Then, cell suspensions were sonicated four times at 60% amplitude for 1 minute and centrifuged to obtain the soluble fractions. On the other hand, the supernatants were concentrated in a rotary evaporator at 60ºC up to a final volume of 50 ml. The proteins present in the cells- and supernatant-derived suspensions were precipitated with a 100% TCA solution, using 250 µl of 100% TCA per 1 ml of suspension. After a centrifugation step to remove proteins, exopolysaccharides were precipitated adding 5 volumes of iced-cold isopropanol under continuous stirring and then kept at 4ºC overnight for precipitation. The crude exopolysaccharide was collected by centrifugation at 8000 x g, 10 min. The pellets were dialyzed against distilled water overnight (Spectra/Por® dialysis membrane, molecular weight cutoff 3.5 kD) and the resulting solution was filtered and applied onto a size exclusion chromatography (SEC) column (Hiprep™ 16/60 Sephacryl™ S-300HR, Sigma) eluting with MQ water. Aliquots of each fraction were analysed by the phenol sulfuric acid method (Dubois *et al.,* 1956). Briefly, 40 µl aliquots of each fraction were mixed with 10 µl of water-saturated phenol and 100 µl of sulfuric acid in 96 microwell plates. The mixture was heated up to 60ºC for 30 min, cooled off and then absorption at 490 nm was monitored in a microplate reader (FLUOstar Omega reader, BMG LabTech). Each fraction (x-axis) was plotted against absorbance (y-axis) and those carbohydrates-containing fractions that conformed a peak were pooled together and applied onto an anion exchange chromatography (AEC;

HiTrap® DEAE FF 1 ml, Sigma) eluting with a NaCl gradient (maximum concentration 1M). Once more, aliquots of each fraction were analysed by the phenol sulfuric method, and each fraction (x-axis) was plotted against absorbance (y-axis), as described above. Carbohydrates-containing fractions that conformed a peak were again pooled and lyophilized for further analysis. Neutral EPS samples present on PAO1 supernatant that included a molecular mass of approximately 6.5 kDa were analysed as controls of Psl presence and composition, as previously described (Kocharova *et al.*, 1998; Ma *et al.*, 2007).

9. Sugar composition analysis (GC-MS)

Extracted samples (1-2 mg) of EPS were hydrolyzed with 1 mL of HCl/MeOH 3 N (sigma Aldrich) into a 3 ml reacti-vial (Thermo) at 80°C for 24 h. The mixture was evaporated under N_2 stream at 50°C. The residue was washed three times with MeOH and dried again under N_2 stream. Sililation of hydrolyzed samples were carried out with 300 µl of Tri-Sil reactive (Pierce, Thermo) for 1 h at 80°C. Excess of the reactive were eliminated by N_2 stream and 1.5 ml of Hexane was added followed by centrifugation. Recovered supernatant was filtered, dried under N_2 stream and 150 µl of Hexane (LC-MS grade, Sigma) was added for Gas chromatography analysis. A Zebrón ZB-5 capillary column (30 m × 0.25 mm ID × 0.25 µm df, Phenomenex) was used to separate monosaccharides. Carrier gas flow was set at 1.2 ml/min and injection volume at 1 µl in split mode. The initial column temperature was set at 80°C for 2 min followed by a temperature gradient of 10 °C/min until 180°C and a 5°C/min gradient until 250°C and then the temperature was kept for 2 min. Ionization in mass spectrometer was performed by electron impact (EI) at 70 eV and ion source temperature at 230°C. Full scan was set between 50-650 m/z.

10. Flow-cell assays and biofilm visualization

To assess the differences between wild-types and corresponding mutants regarding biofilm architecture, flow-cell chambers were used (Christensen *et al.*, 1999). The flow-cell chamber disinfection was carried out for 4 h using a 0.5% hypochlorite solution. Thereafter, the system was washed with sterile distilled water overnight. Biofilms were grown in flow-cells supplied with AB minimal medium supplemented with 0.3 mM glucose and 0.005% yeast extract for PssUMAF0158 and with 0.3 mM citrate for PcPCL1606 strain (Clark & Maaloe, 1967). Briefly, fresh GFP-tagged

wild-types and GFP-tagged extracellular matrix mutants were inoculated as single colonies into 5 ml of TPG tubes and incubated overnight at 200 rpm and 25ºC. Then, the cultures were adjusted to a low cell density (OD of 0.01 a.u at 600 nm, which corresponds to 10^6 CFU/ml) with 0.85% NaCl solution and 300 µl was injected into each channel with a small syringe. After inoculation, the flow remained stopped for 1 h to allow attachment of the cells to the channels. The medium flow was kept at a constant rate of 1.3 µl/min by a peristaltic pump (Watson-Marlow 205S). The incubation temperature was 25ºC. A minimal of two independent experiments and at least two technical replicates per experiment and strain were performed. Microscopic inspection and image acquisition were performed using a confocal laser scanning microscope (Leica; DM5500Q) equipped with a 40/1.3 and a 63/1.4 oil objective as well as detector and filter sets for the monitoring of GFP (488 nm for excitation and emission in 501-540 nm). The captured images were analysed with the Leica Application Suite (Mannheim, Germany) and the IMARIS software package (Bitplane, Switzerland) to quantify area and volume values.

11. Competition experiments during biofilm formation

For the competition experiments during biofilm formation, flow-cell chamber experiments were assembled and performed as above described. The channels were inoculated with a 1:1 mixture of differentially tagged wild-type and extracellular matrix mutants, previously grown at a low cell density (OD of 0.01 a.u. at 600 nm, which corresponds to 10^6 CFU/ml). Images were recorded and analysed with the Leica Application Suite (Mannheim, Germany) and IMARIS software package (Bitplane, Switzerland). The 532-nm laser was used for mCherry/dsRed fluorophore excitation and emission was monitored at 570-700 nm. The 488-nm laser was used for GFP fluorophore excitation and emission was monitored at 450-500 nm. Three independent experiments and at least two technical replicates per experiment and strain were performed.

12. YEM assays

Yeast extract medium (YEM; 0,5 g of yeast extract, 4 g of mannitol and 15 g of agar per litre) was used to visualize EPS production by Pss strains. Precultures were grown overnight in LB medium at 25ºC and adjusted at 10^8 CFU/ml (optical density of 1 a.u. at 600 nm wavelength). Plate inoculations were performed using a cotton swab. After 3 days of growth, EPS production appeared as a mucoid growth on YEM plates.

13. Congo red assays

Two different approaches were performed. 1) For plate Congo red (CR) binding assays, 10 µl of an overnight culture at 10^8 CFU/ml (optical density of 0,5 a.u. at 600 nm wavelength) was spotted onto a TPG plate with 20 µg/ml of CR. The samples were incubated at 25ºC for 48 h (Chapter 1) and at 25ºC for 6 days (Chapter 2) and then images were recorded. Each strain was assayed in triplicate and three different experiments were performed. 2) For pellicle CR binding, a modified version of the described protocol was performed (Ma *et al.*, 2006). Briefly, 100 µl of an overnight culture (10^8 CFU/ml) was inoculated into 900 µl of TPG medium with 20 µg/ml CR. The samples were incubated 16 h without shaking (static culture) at 25ºC in the dark (Chapter 1); 24 h without shaking at 15, 20, 25 or 30ºC in the dark (Chapter 2) and 24 h at 25ºC under constant white light exposure using fluorescent tubes in a growth chamber (Ibercex) (Chapter 2).

For the quantification of CR binding, the biofilms were centrifuged at 18,000 x g to separate the cells (biofilm and non-biofilm formers) from liquid culture and absorbance of the supernatant of each sample at 490 nm was determined. Free CR exhibits an absorption spectrum from 490 to 530 nm (Jagusiak *et al.*, 2017). To calculate CR binding in the pellicle, the supernatant absorbance values of the tested strains were first relativized to those of the control medium with CR for each independent experiment. Then, the relativized data is processed so that the CR binding values of the negative control are cero. Finally, to calculate the fold-change, the obtained values were normalized relative to the wild-type average. Each strain was assayed in triplicate and three different experiments were performed.

14. Motility assays

For swarming motility analysis, bacteria were stab inoculated in the centre of a 0.5% agar plate with KB medium diluted 20-fold in distilled water. In PssUMAF0158 strain, swarming patterns occur as migrating and branching tendrils from the point of inoculation. After 48 h of incubation at 25ºC, the area of swarming was measured using Quantity One 1D Analysis Software. Three independent experiments and three technical replicates per experiment and strain were performed.

15. Bacterial attachment assay

The attachment assays were conducted as previously described (McCarthy *et al.*, 2014; Gutiérrez-Barranquero *et al.*, 2015) with slight modifications. Five hundred microliters of the wild-type strain and its derivative extracellular matrix mutant at an OD of 0.25 a.u. at 600 nm (approx. 10^8 CFU/ml) were inoculated in 24-microwell plates. To ensure that there were no differences in bacterial concentration at the time of inoculation, cell counts of the bacterial suspensions were performed. After 4, 6 or 8 h of incubation at 25ºC, cultures were removed and washed with distilled water. Five hundred microliters of 0.1% crystal violet (Panreac) was added to each well, followed by an incubation period of 15 min. Then, the crystal violet was removed, and the wells were vigorously washed with tap water. The plates were subsequently dried at 37ºC for 2 h. Finally, 500 µl of 96% EtOH were added to each well and incubated under agitation at room temperature for 15 min. One hundred microliters was then collected from each well and added to a clean 96-well plate for absorbance measurements at 595 nm. Finally, the fold change data were obtained by normalizing the absorbance values relative to the wild-type average of each independent experiment.

16. Bacterial adhesion to mango leaves

The adhesion assays were performed as formerly described (Arrebola *et al.*, 2015) with some modifications. Overnight bacterial cultures were adjusted to 10^8 CFU/ml. Drops (10 µl) of each strain were inoculated onto 2x2 cm pieces of mango leaves that had been previously disinfected. After 4 h, the leaf pieces were gently washed in 1 ml of sterile 0.85% NaCl solution to remove unattached cells, vigorously vortexed for 30 s in 1 ml of sterile 0.85% NaCl solution to release adhered cells, diluted and plated onto KB plates to determine bacterial numbers. For data normalization, all the cell counts obtained in each experiment were normalized relative to the wild-type

average. From two to three technical replicates per strain and experiment and at least four independent experiments were performed.

17. Bacterial adhesion to avocado roots

The avocado roots were disinfected in 1% v/v household bleach for 20 min, washed in distilled water and immersed in GFP-tagged bacterial cultures at a final concentration of 10^8 CFU/ml for 20 min, as previously described (Calderón *et al.*, 2013). Then, each root was washed again by immersion in distilled water to remove the free and weakly attached bacteria and transplanted into pots filled with vermiculite. After 4 h of incubation, the plants were removed from the pots, and superficial root samples were randomly collected with a scalpel and placed on glass slides for examination. The fluorescently-labelled bacteria attached to the roots were visualized by confocal laser scanning microscopy (CLSM) using a Zeiss LSM 880 microscope. Three independent experiments, each with three avocado seedlings per strain, were performed.

18. Tomato virulence assays

Virulence experiments were carried out as previously described (Arrebola *et al.*, 2009, 2015; Carrión *et al.*, 2014). Detached tomato leaflets (*Solanum lycopersicum* Mill.) of cv. Hellfrucht Frühstamm were maintained *in vitro* at 22ºC using Murashige and Skoog medium (MS; Sigma Aldrich). Each leaflet was disinfected, washed, air-dried and inoculated with six 10 µl drops at different points. Inoculations were carried out by piercing with a sterile entomological pin through 10 µl droplets on the leaflet surface. The development of necrotic symptoms was determined after 6 days. For measurement, necrotic areas were digitally analysed using Quantity One 1D Analysis Software. Relative virulence was calculated normalizing the necrotic area values of the tested strains to the wild-type average of each experiment. In parallel, inoculated leaflets were processed for the estimation of the total bacterial population. Tomato leaflets were homogenized in sterile 0.85% NaCl solution, and bacterial counts were determined by plating 10-fold serial dilutions on KB plates with appropriate antibiotics. Between 3-4 leaflets per strain and experiment and three independent experiments were performed to estimate the induced necrotic area.

19. Biocontrol assays against avocado white root rot

The biocontrol assays against avocado white root rot disease were performed as previously described (Cazorla *et al.*, 2006). The roots of 6-month-old avocado plants obtained from Brokaw nurseries (Brokaw España, S.L., Vélez-Málaga, Spain) were disinfected with 1% v/v household bleach for 20 min, washed with distilled water and inoculated as previously described (Calderón *et al.*, 2013). For the inoculation process, the roots of the avocado plants were immersed either in a suspension of the bacterial isolate (10^8 CFU/ml) or in sterile TPG medium (controls) for 20 min. Excess bacteria were removed from the roots, and the seedlings were transplanted into pots containing potting soil (Jongkind Grond B.V., Aalsmeer, The Netherlands) and subsequently infected with *Rosellinia necatrix* using eight colonized wheat grains per pot (Freeman *et al.*, 1986). The plants that were not inoculated but were infected served as negative controls for biocontrol activity. Furthermore, the plants that were neither inoculated nor infected served as environmental controls. Two independent experiments, each with at least 7 avocado seedlings per strain, were performed. Aerial symptoms were recorded on a scale from 0 to 3 (from 0 – not affected – to 3 – dead plant). The disease index was calculated using the previously described formula (Cazorla *et al.*, 2006) and to minimize the variability inherent to the experiments with plants all values were normalized to the wild-type average for each independent experiment.

CHAPTER 1

Biological role of EPS from *Pseudomonas syringae* pv. syringae UMAF0158 extracellular matrix, focusing on a Psl-like polysaccharide

Most of the results included in this chapter have been published:

Zaira Heredia-Ponce, José Antonio Gutiérrez-Barranquero, Gabriela Purtschert-Montenegro, Leo Eberl, Francisco M. Cazorla & Antonio de Vicente. Biological role of EPS from *Pseudomonas syringae* pv. syringae UMAF0158 extracellular matrix, focusing on a Psl-like polysaccharide; ***npj Biofilms and Microbiomes*** 6, 37 (2020)

1. Summary

Pseudomonas syringae is a phytopathogenic model bacterium that is used worldwide to study plant-bacteria interactions and biofilm formation in association with a plant host. Within this species, the syringae pathovar is the most studied due to its wide host range, affecting both, woody and herbaceous plants. In particular, *P. syringae* pv. syringae (Pss) has been previously described as the causal agent of bacterial apical necrosis on mango trees. Pss exhibits major epiphytic traits and virulence factors that improve its epiphytic survival and pathogenicity. The cellulose exopolysaccharide has been described as a key component in the development of the biofilm lifestyle of the *P. syringae* pv. syringae UMAF0158 strain (PssUMAF0158). PssUMAF0158 contains two additional genomic regions that putatively encode for exopolysaccharides such as alginate and a Psl-like polysaccharide. To date, the Psl polysaccharide has only been studied in *Pseudomonas aeruginosa*, in which it plays an important role during biofilm development. However, its function in plant-associated bacteria is still unknown. To understand how these polymers contribute to the biofilm matrix of PssUMAF0158, knockout mutants of genes encoding these putative exopolysaccharides were constructed. Flow-cell chamber experiments revealed that cellulose and the Psl-like polysaccharide constitute a basic scaffold for biofilm architecture in this bacterium. Curiously, the Psl-like polysaccharide of PssUMAF0158 plays a role in virulence similar to what has been described for cellulose. The impaired swarming motility of the Psl-like exopolysaccharide mutant suggests that this exopolysaccharide may play a role in the motility of PssUMAF0158 over the mango plant-surface. Finally, chemical analysis revealed that the Psl-like polysaccharide could be similar in composition to the archetypal *P. aeruginosa*.

2. Introduction

Pseudomonas syringae is a model bacterium for the study of plant-microbial interactions, as it causes diseases in woody and herbaceous plants worldwide. Based mainly on host isolation and host range, *P. syringae* is divided into more than 60 pathovars (Young, 2010), among which pathovar syringae shows the largest host range, causing disease in over 180 plant species (Kennelly *et al.,* 2007). *P. syringae* shows two interconnected lifestyles while interacting with the plant: an epiphytic phase, in which it survives on the surface while coping with harsh environmental conditions, and a pathogenic phase, in which it enters and colonizes internal plant tissue, leading to the development of an infection (Kennelly *et al.,* 2007; Xin *et al.,* 2018; Gutiérrez-Barranquero *et al.,* 2019). The *P. syringae* pv. syringae (Pss) UMAF0158 strain (PssUMAF0158) is a mango tree pathogen that is considered a model for the study of the transition between the epiphytic and pathogenic lifestyles depending on environmental conditions (Cazorla *et al.,* 1998).

P. syringae harbours a diverse weaponry of virulence factors, including the type III secretion system (T3SS) and its effectors, phytotoxins, phytohormones, ice nucleation activity, plant cell wall-degrading enzymes and exopolysaccharides (Xin *et al.,* 2018). The ability to produce exopolysaccharides has been previously related to virulence in several phytopathogenic bacteria (Fett & Dunn, 1989; Yu *et al.,* 1999; de Pinto *et al.,* 2003; Arrebola *et al.,* 2015). *P. syringae* is able to produce a number of biofilm matrix polysaccharides, including alginate, levan and cellulose (Osman *et al.,* 1986; Fakhr *et al.,* 1999; Preston *et al.,* 2000; Li & Ullrich *et al.,* 2001; Arrebola *et al.,* 2015; Pérez-Mendoza *et al.,* 2019). Alginate is a copolymer of O-acetylated β-1,4-linked D-mannuronic acid and L-glucuronic acid that has been widely studied in *P. syringae* (Fakhr *et al.,* 1999; Kidambi *et al.,* 1995; Preston *et al.,* 2000; Laue *et al.,* 2006) and *Pseudomonas aeruginosa* (Hentzer *et al.,* 2001; Wozniak *et al.,* 2003; McIntyre-Smith *et al.,* 2010). Generally, the role of alginate during biofilm formation in these two species has been considered nonessential (Wozniak *et al.,* 2003; Laue *et al.,* 2006; McIntyre-Smith *et al.,* 2010). However, several studies have shown that alginate plays a role in the epiphytic fitness and virulence in some *P. syringae* strains (Yu *et al.,* 1999; Helmann *et al.,* 2019), as well as in biofilm structure, antibiotic resistance and protection against the human immune system in mucoid strains of *P. aeruginosa* (Hentzer *et al.,* 2001; Pier *et al.,*

2001; Leid *et al.,* 2005). The polysaccharide levan is a β-2,6 polyfructan that shows extensive branching through β-2,1 linkages (Laue *et al.,* 2006) whose synthesis is catalysed by levansucrases (Osman *et al.,* 1986; Li & Ullrich, 2001). Levan does not play a role in biofilm architecture and it has been speculated to consist of a storage molecule that may protects cells against starvation (Laue *et al.,* 2006). Cellulose is a polymer composed of β-D-glucose units that constitutes one of the main components of the biofilm matrix produced by many bacteria (Zogaj *et al.,* 2001; Solano *et al.,* 2002; Jahn *et al.,* 2011; Serra *et al.,* 2013) and its biosynthesis has proven to be important for biofilm formation by Pss (Arrebola *et al.,* 2015; Farias *et al.,* 2019).

The PssUMAF0158 genome sequencing project revealed the presence of a gene cluster related to cellulose biosynthesis (Martínez-García *et al.,* 2015). This gene cluster was identified as being closely related to the lifestyle of PssUMAF0158 on the mango tree surface (Arrebola *et al.,* 2015). Cellulose overexpression reduces virulence whereas cellulose-deficient mutants increase the area of necrosis (Arrebola *et al.,* 2015). This suggests that cellulose could act as a switch in the transition between epiphytic and pathogenic phases, decreasing cellulose biosynthesis and thus, biofilm formation, in the pathogenic phase (Gutiérrez-Barranquero *et al.,* 2019). In addition to alginate and cellulose, a region that putatively encodes a Psl-like exopolysaccharide was found in the PssUMAF0158 genome in this study. The Psl polysaccharide, composed of D-mannose, D-glucose and L-rhamnose (Byrd *et al.,* 2009), has thus far only been studied in *P. aeruginosa* (Friedman & Kolter, 2004; Jackson *et al.,* 2004; Matsukawa & Greenberg, 2004), where it plays essential roles in biofilm formation, adhesion, motility and protection against a variety of stresses (Ma *et al.,* 2006; Ghafoor *et al.,* 2011; Billings *et al.,* 2013; Wang *et al.,* 2013, 2014; Periasamy *et al.,* 2015). Although the presence of a *psl* cluster has been reported in a few species of the *Pseudomonas* genus, including the plant-associated *P. syringae* pv. syringae B728a and *P. syringae* pv. phaseolicola 1448a strains, the putative roles that this polysaccharide could play in biofilm formation in these bacteria have not been examined yet (Records & Gross, 2010; Mann & Wozniak, 2012).

Biofilm formation could play an important role in the PssUMAF0158 lifestyle during its interaction with the mango tree surface, so further research regarding its biofilm components and how they establish interactions with each other to promote

epiphytic survival is needed. In this study, in addition to cellulose, whose roles in biofilm formation and virulence have been previously reported, we have identified two genomic regions that putatively encode alginate and Psl-like exopolysaccharides. Thus, the main aim of this work is to elucidate the roles that these exopolysaccharides play in biofilm formation and architecture, as well as virulence, during interaction with the mango plant.

3. Results

Bioinformatic analysis revealed that alginate- and *psl*-like encoding clusters were present in the *Pseudomonas syringae* pv. syringae UMAF0158 genome. The presence of the alginate and *psl*-like gene clusters has never been assessed in PssUMAF0158 strain. An *in silico* analysis was performed to identify the genome regions that may be encoding these exopolysaccharides in PssUMAF0158. Using the alginate operon sequence of *P. syringae* pv. syringae B728a as a model, the Psyrmg_RS21275-Psyrmg_RS21330 region was identified in PssUMAF0158 (Table S5). There is high conservation pattern between the proteins encoded by these regions. The Psyrmg_RS06720-Psyrmg_RS06770 genomic region of PssUMAF0158 has been found to be similar to the *psl* operon of *P. aeruginosa* PAO1, although with some differences (Table S6). The PslM-like and PslO-like proteins were missing, although they are not required to produce the polysaccharide (Byrd *et al.,* 2009). PslC-like and PslN-like proteins seemed to be encoded somewhere else on the chromosome at Psyrmg_RS00890 and Psyrmg_RS04445 (Table S6). The PslL acyltransferase of PAO1 shares no identity with any protein encoded by the genome of PssUMAF0158. However, the Psyrmg_RS06765 gene, located within the *psl*-like cluster, encodes for an acetyltransferase. The identity between the proteins was over fifty percent and most of the domains were conserved (Tables S7 and S8). The cellulose operon of *P. syringae* pv. tomato DC3000 was previously reported to be orthologous to the Psyrmg_RS20465-Psyrmg_RS20500 region in PssUMAF0158 (Arrebola *et al.,* 2015). There is high conservation pattern between the proteins encoded by these cellulose production *loci* (Table S9).

Phylogenetic analysis revealed that a *psl*-like gene cluster was present on strains of the *Pseudomonas syringae* complex that interact with plants. To elucidate the evolutionary history of the *psl*-like gene cluster within the *P. syringae* complex, a total of 34 strains belonging to phylogenetic groups 1, 2, 3, 4, 5, 6, 7, 10 and 11, mainly related to plants, were selected and used for the analysis (Table S3). The partial combined sequences of the *rpoD* and *gyrB* housekeeping genes clearly supported the reported phylogenetic distribution in the different phylogenetic subgroups included in the analysis (Berge *et al.,* 2014; Figure 1A.C1). Therefore, the phylogenetic distribution of the strains from the different phylogenetic groups regarding the *psl*-like gene cluster indicated that this cluster followed a similar

evolutionary history to that of the housekeeping genes and demonstrated that it has been stably and vertically inherited by this group of microorganisms (Figure 1B.C1).

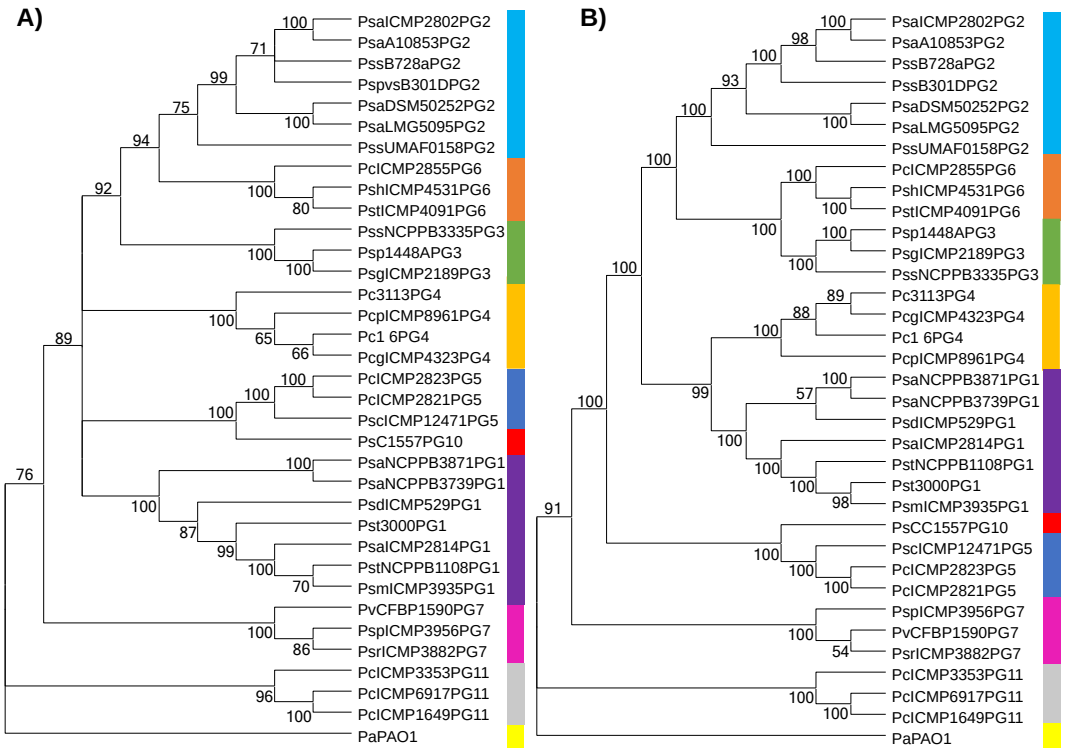

Figure 1.C1. Phylogenetic analysis of the *psl*-like exopolysaccharide genomic cluster in plant-associated phylogroups of the *P. syringae* complex. A) Neighbour-joining tree generated with MEGA10 using partial combined sequences of the *rpoD* and *gyrB* genes; B) Neighbour-joining tree generated with MEGA10 using the *psl*-like cluster nucleotide sequence. Both analyses included 34 strains belonging to 1 (purple), 2 (light blue), 3 (green), 4 (dark yellow), 5 (dark blue), 6 (orange), 7 (pink), 10 (red) and 11 (gray) phylogenetic groups within the *P. syringae* complex (Table S3). The *P. aeruginosa* PAO1 *psl* operon sequence was used as an outgroup (light yellow).

Involvement of the Psl-like exopolysaccharide in the virulence of *P. syringae* pv. syringae UMAF0158. Virulence experiments were performed on tomato leaflets, which are a more reliable plant model for pathogenicity than mango leaves (Arrebola *et al.*, 2009, 2015). At day six postinoculation, the overall necrotic area was estimated, and the results demonstrated significant differences between PssUMAF0158 wild-type and mutant defective in Psl-like exopolysaccharide production (Figure 2A,B.C1). The cellulose mutant was included as a positive control of virulence (Arrebola *et al.*, 2015). No significant differences in virulence were found between the wild-type and the *Δalg8* mutant (Figure 2A,B.C1). Moreover, the bacterial counts between PssUMAF0158 wild-type and *ΔpslE* mutant were similar (Figure 2C.C1), which indicates that the greater virulence observed in

the *ΔpslE* mutant was not due to an increase in the ability to grow on the leaflet surface.

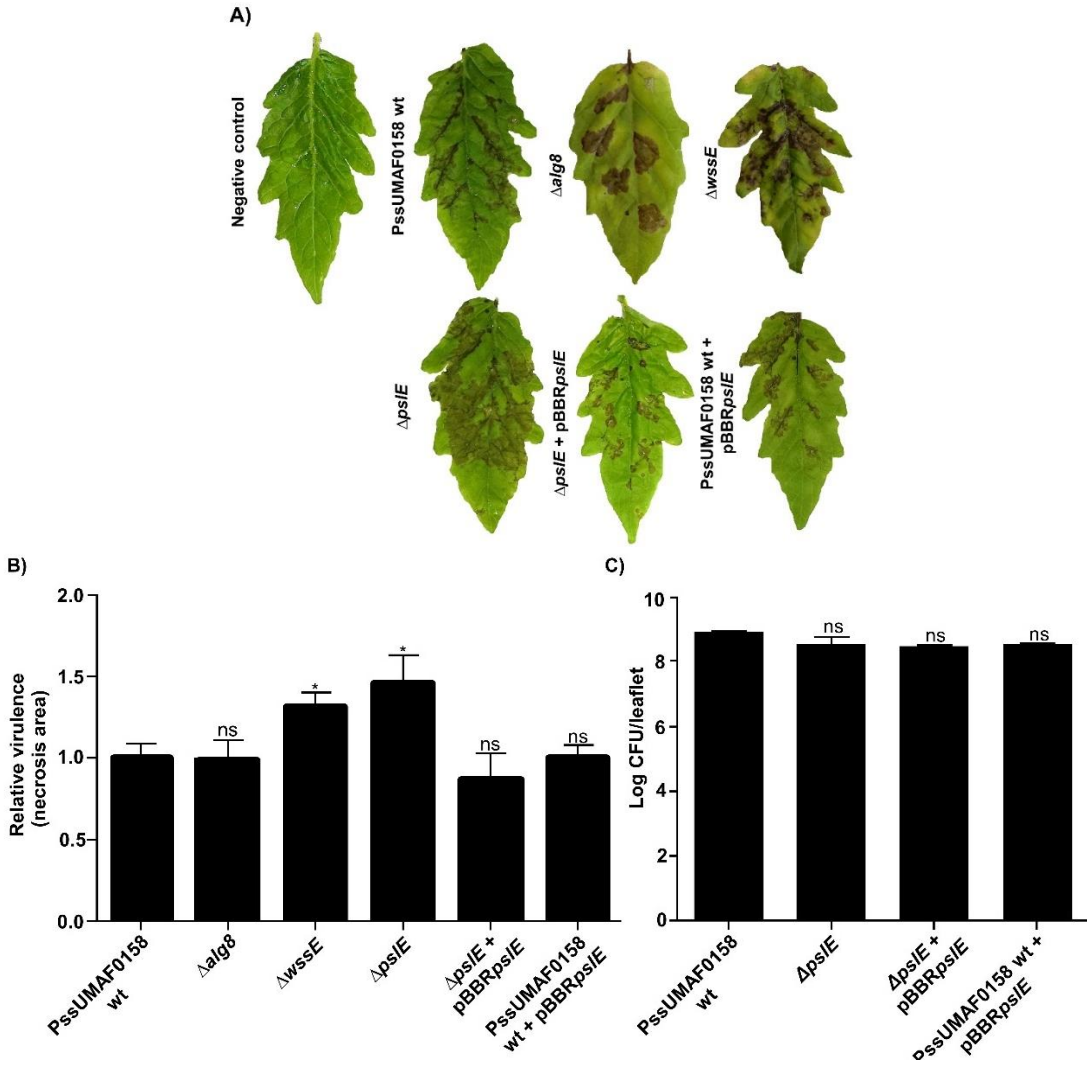

Figure 2.C1. Analysis of the Psl-like polysaccharide as a putative virulence factor for *P. syringae* pv. syringae UMAF0158. Virulence determination on inoculated tomato leaflets maintained *in vitro*; A) Representative symptoms developed on tomato leaflets at 6 days postinoculation; B) Relative virulence of PssUMAF0158 wild-type and Psl-like polysaccharide mutant in tomato leaflets measured by lesion size. The cellulose mutant was included as a positive control of virulence (Arrebola *et al.*, 2015). Four leaflets per experiment and three independent experiments were performed; C) Bacterial counts (log CFU/ml) after 6 days of inoculation; The PssUMAF0158 wild-type (PssUMAF0158 wt), PssUMAF0158 alginate mutant (*Δalg8*), PssUMAF0158 cellulose mutant (*ΔwssE*), PssUMAF0158 Psl-like polysaccharide mutant (*ΔpslE*), PssUMAF0158 Psl-like complemented strain (*ΔpslE*+pBBR*pslE*) and PssUMAF0158 *pslE* overexpressing strain (PssUMAF0158 wt+pBBR*pslE*) were tested. Statistical significance was assessed by two-tailed Mann–Whitney test (*p<0.05). Error bars correspond to the standard error of the mean (s.e.m).

Involvement of the Psl-like exopolysaccharide in the adhesion of *P. syringae* pv. syringae UMAF0158 to mango leaves. Adhesion experiments were performed on mango leaves using the PssUMAF0158 wild-type strain and derived mutant defective in Psl-like exopolysaccharide production (Figure 3.C1). The cellulose mutant was included as an impaired control of adhesion (Arrebola *et al.*, 2015). The results showed a significant reduction in adhesion to mango leaves in the Δ*pslE* mutant compared to the wild-type and that the Psl-like complemented strain restored adhesion to the wild-type levels (Figure 3.C1).

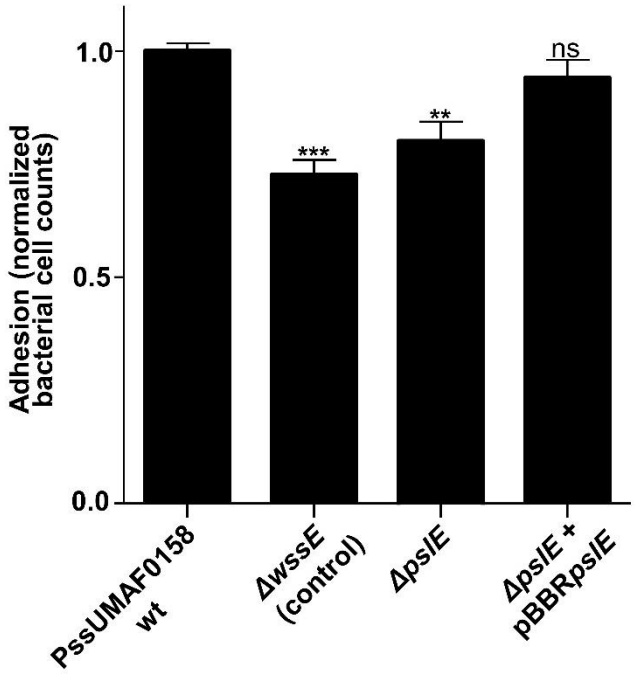

Figure 3.C1. Analysis of the Psl-like polysaccharide as a putative adhesion factor for *P. syringae* pv. syringae UMAF0158. Adhesion to mango leaves at 4h postinoculation. The cellulose mutant was included as a negative control of adhesion (Arrebola *et al.*, 2015). Normalized bacterial cell counts recovered from mango leaves of the different assayed mutants with respect to the wild-type strain counts. Two technical replicates per strain and experiment and at least four independent experiments were performed. The PssUMAF0158 wild-type (PssUMAF0158 wt), PssUMAF0158 cellulose mutant (*ΔwssE*), PssUMAF0158 Psl-like polysaccharide mutant (*ΔpslE*) and PssUMAF0158 Psl-like complemented strain (*ΔpslE*+pBBR*pslE*) were tested. Statistical significance was assessed by two-tailed Mann–Whitney test (**p<0.01, ***p<0.001). Error bars correspond to the standard error of the mean (s.e.m).

Effects of *alg8, wssE* and *pslE* mutations on colony morphology and Congo red binding. The Congo red (CR) binding observed in colonies of wild-type and derivative mutants suggests that these genes are involved in the production of exopolysaccharides. CR agar plates showed that PssUMAF0158 wild-type colonies were dark red, while colonies of the mutants were pale pink (Figure 4A.C1). Complemented strains restored the wild-type phenotype and no differences in colony morphology were observed. The pellicle CR binding experiments (Figure 4B.C1) showed some differences with plate CR binding experiments (Figure 4A.C1). The *Δalg8,pslE* double mutant, which was impaired in plate CR binding compared to the wild-type (Figure 4A.C1), restored the wild-type phenotype levels in pellicle CR binding (Figure 4B.C1). Increases of cellulose production were not observed in the *Δalg8,pslE* strain in the calcofluor staining experiments (Figure 4C.C1). Overexpression of the *wssE* gene was also not detected at 4-, 6- and 16 h postinoculation (Figure 5.C1). There were also differences between plate CR binding and pellicle CR binding in the alginate mutant. Cellulose mutant strain complemented with the *wssE* gene present on the pBBR1MCS5 plasmid fully restored to the wild-type phenotype, but the Psl-like mutant strain complemented with the *pslE* gene present on the same plasmid only partially restored CR binding in the pellicle. As observed in the CR binding phenotype of the pellicles of the vector control strain (wt + pBBR1MCS5), the plasmid is not affecting CR binding under these conditions. The decrease in CR binding observed in the wt + pBBR*pslE* strain suggests that expression of the *pslE* gene under the P_{lac} promoter present on the pBBR1MCS5 plasmid could affect CR binding in the pellicle. The *wssE* gene deletion completely impaired the ability to bind CR in the pellicle (Figure 4B.C1). The pellicle CR binding phenotypes observed (Figure 4B.C1) match with the ability of the tested strains to produce cellulose (Figure 4C.C1).

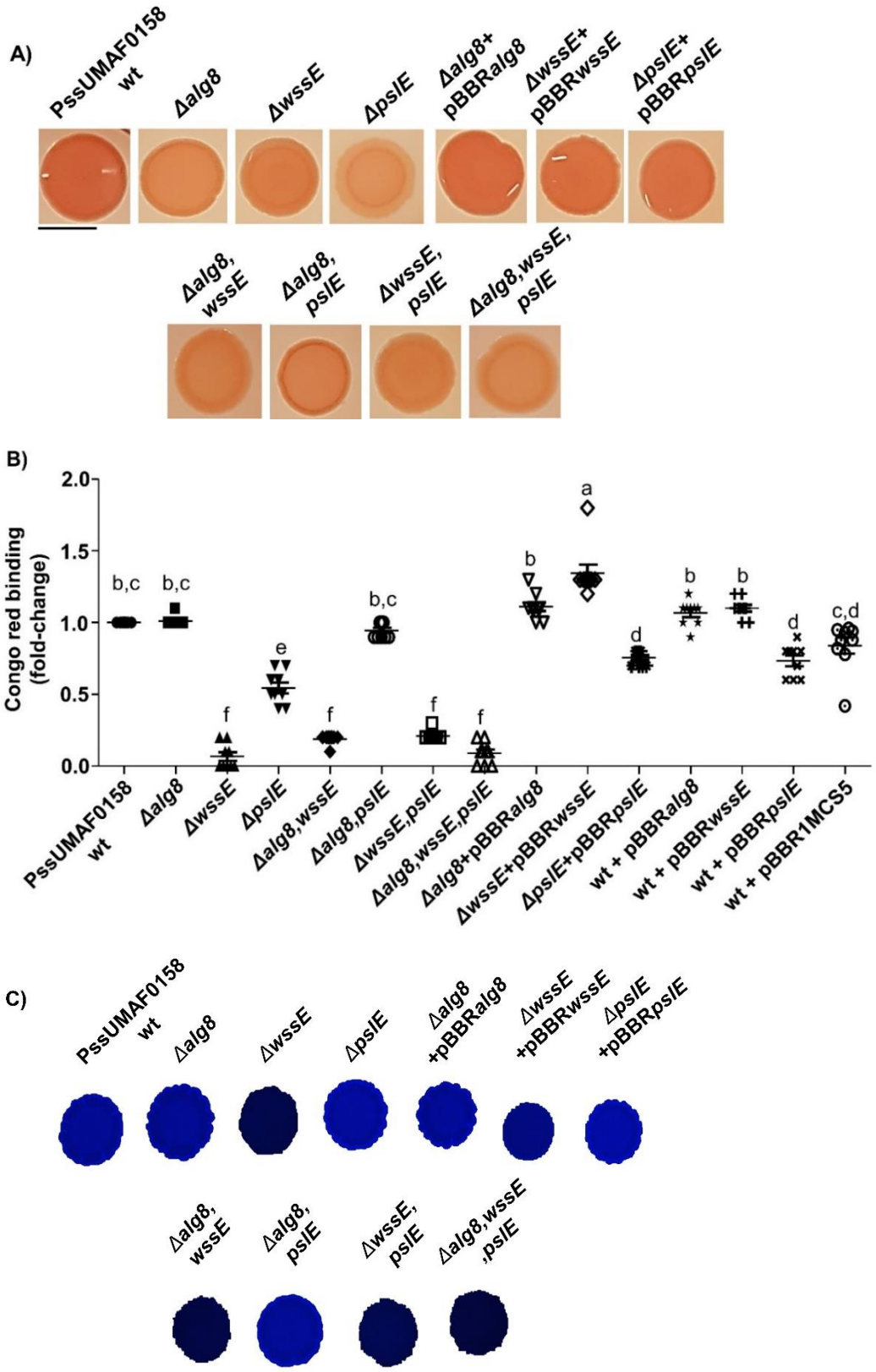

Figure 4.C1. Congo red binding and colony morphology. A) Plate CR binding assay and colony morphology of wild-type, mutants and complemented strains; B) Pellicle CR binding assay. The results show the CR binding levels of the pellicle in the form of a fold-change relative to the wild-type strain CR binding average; C) Plate calcofluor binding assay. The PssUMAF0158 wild-type (PssUMAF0158 wt), PssUMAF0158 alginate mutant (*Δalg8*), PssUMAF0158 cellulose mutant

(*ΔwssE*), PssUMAF0158 Psl-like polysaccharide mutant (*ΔpslE*), PssUMAF0158 *Δalg8,wssE* double mutant (*Δalg8,wssE*), PssUMAF0158 *Δalg8,pslE* double mutant (*Δalg8,pslE*), PssUMAF0158 *ΔwssE,pslE* double mutant (*ΔwssE,pslE*), PssUMAF0158 *Δalg8,wssE,pslE* triple mutant (*Δalg8,wssE,pslE*), alginate complemented strain (*Δalg8*+pBBR*alg8*), cellulose complemented strain (*ΔwssE*+pBBR*wssE*), Psl-like complemented strain (*ΔpslE*+pBBR*pslE*), *alg8* overexpression strain (wt+pBBR*alg8*), *wssE* overexpression strain (wt+pBBR*wssE*), *pslE* overexpression strain (wt+pBBR*pslE*) and vector control strain (wt + pBBR1MCS5) were tested. Statistical analysis was performed using ANOVA with the Bonferroni correction test. Three replicates and three independent experiments were performed. Different letters represent statistically significant differences, $p<0.05$. Error bars show the standard error of the mean (s.e.m). Scale bar 1 cm.

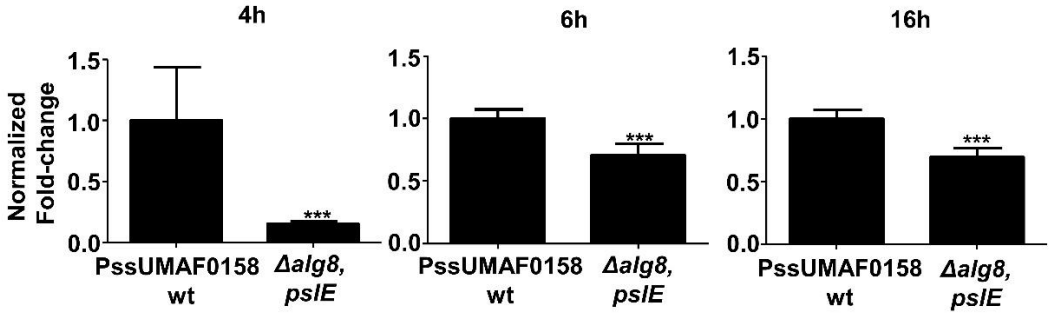

Figure 5.C1. qRT-PCR experiments of the *wssE* gene from pellicles after 4-, 6- and 16 h post-inoculation at 25ºC. Results are shown as the normalized fold-change expression of *wssE* in *Δalg8,pslE* strain compared to the wild-type. Expression of *wssE* is lower in the double mutant compared to the wild-type, which is not consistent with the phenotype observed in the *Δalg8,pslE* mutant strain regarding the Congo red binding in the pellicles. PssUMAF0158 wild-type (PssUMAF0158 wt) and PssUMAF0158 *Δalg8,pslE* double mutant (*Δalg8,pslE*) were tested. Statistical significance was assessed by two-tailed Mann–Whitney test (***$p<0.001$). Error bars correspond to the standard error of the mean (s.e.m).

The genes involved in the production of the cellulose and Psl-like polysaccharides are essential for biofilm formation. To investigate the role of alginate, cellulose and Psl-like exopolysaccharides in the biofilm architecture, flow-cell chamber experiments were performed in the wild-type and mutant bacteria, and confocal laser scanning microscopy (CLSM) was used to visualize live biofilms. A group of cells that were tightly joined together and motionless over the flow-cell chamber surface was considered a cell aggregate, as previously illustrated (Ghafoor *et al.*, 2011). Area and volume values in the field of view were calculated to evaluate the surface coverage and the overall biofilm architecture of each strain, respectively. After 48 h, the wild-type PssUMAF0158 formed thick biofilms with cell aggregates (Figure 6A.C1). The *Δalg8* mutant exhibited a significantly lower surface coverage

(Figure 6B.C1) and the overall biofilm architecture appeared to be flattened compared to that of the wild-type strain (Figure 6C.C1). The cellulose mutant showed an impairment in biofilm formation, characterized by the absence of cell aggregates (Figure 6A.C1). The PssUMAF0158 *ΔpslE* mutant produced a substantially altered biofilm characterized by scattered cell aggregates across the surface (Figure 6A.C1). As observed previously in the CR binding experiments of the pellicles, the biofilms formed by the *Δalg8,pslE* double mutant restored the wild-type phenotype in area and volume values. The PssUMAF0158 *Δalg8,wssE,pslE* triple mutant was almost completely impaired in biofilm formation (Figure S1).

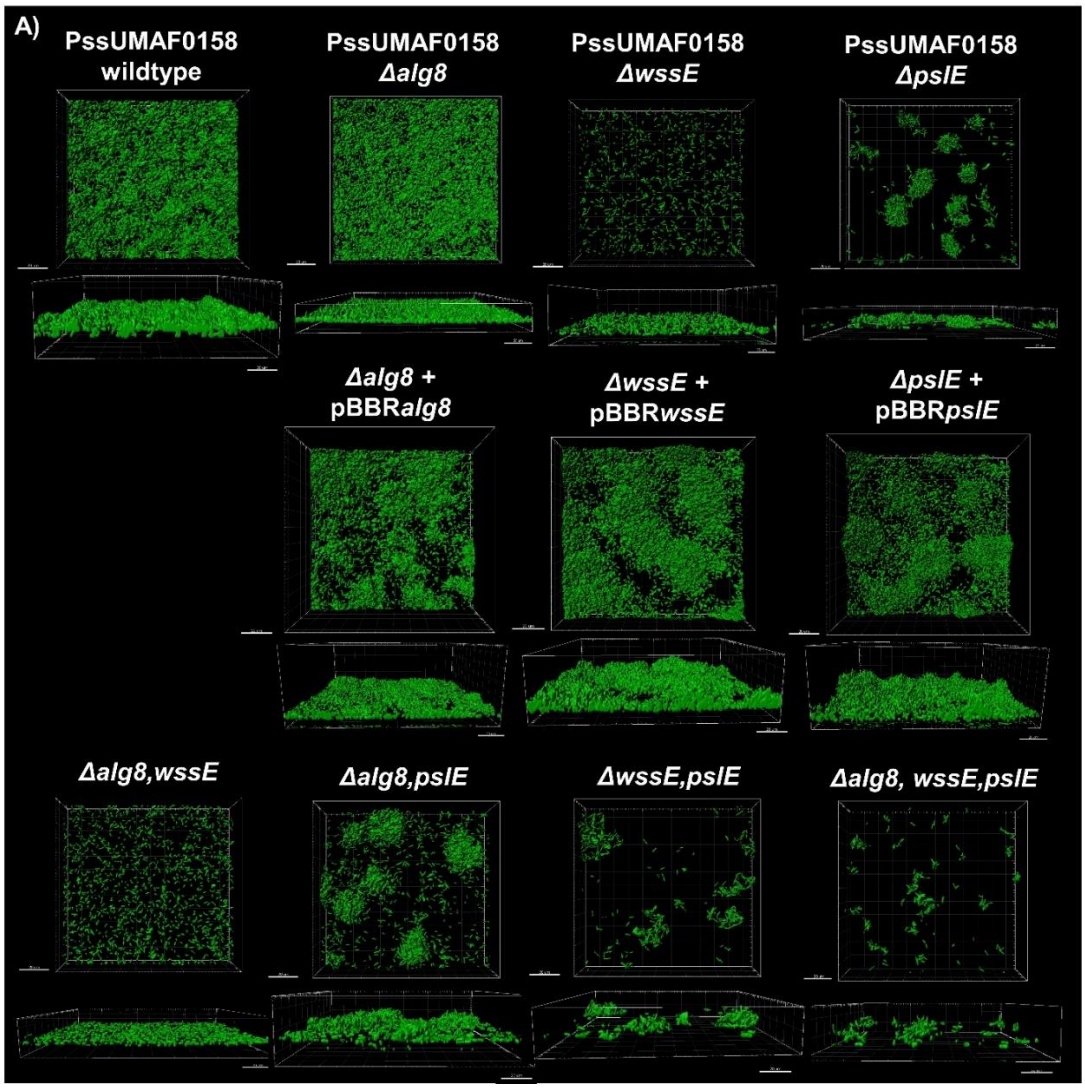

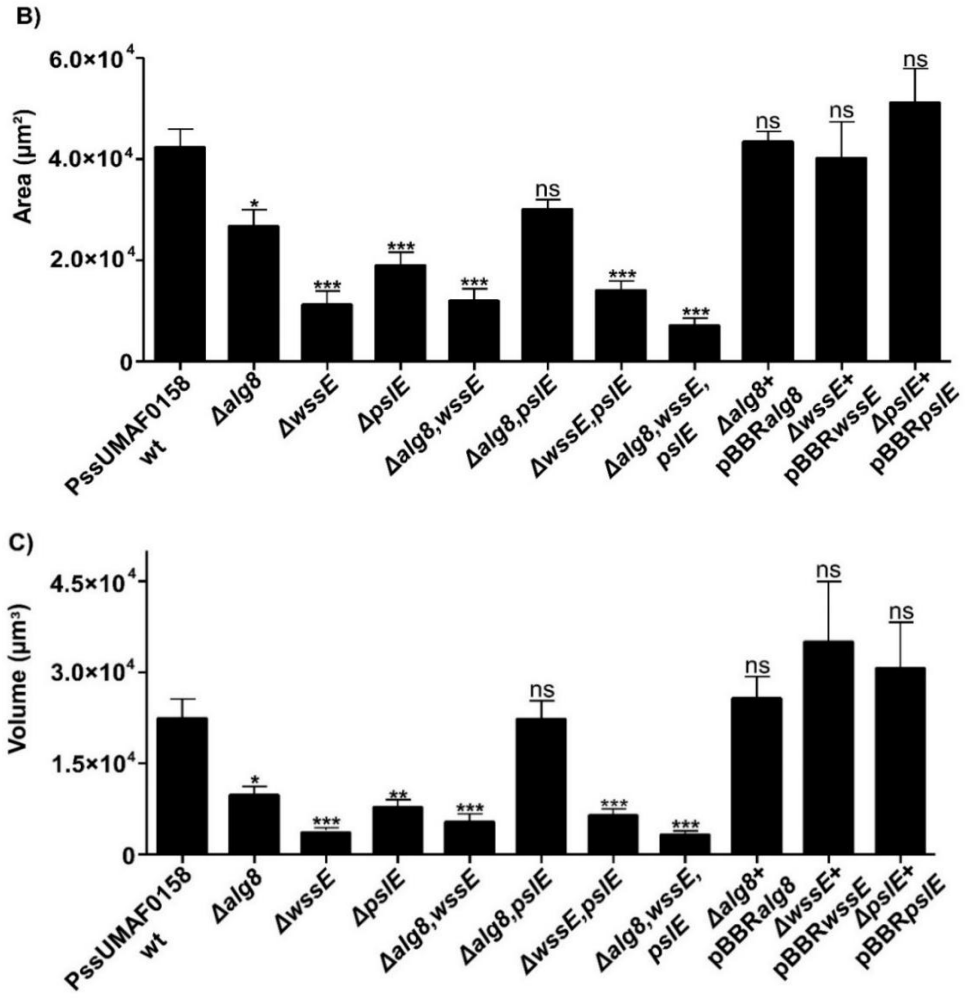

Figure 6.C1. Flow-cell chamber experiments of PssUMAF0158 wild-type and derived extracellular matrix mutants. A) Representative 48 h 3D biofilm images of GFP-tagged PssUMAF0158 wild-type and mutants are shown. The obtained images were analysed with the Leica Application Suite (Mannheim, Germany) and the IMARIS software package (Bitplane, Switzerland). Scale bar 20 µm; B) Area in the field of view covered by 48 h biofilms of the GFP-tagged PssUMAF0158 wild-type, extracellular matrix mutants and complemented strains; C) Volume in the field of view occupied by 48 h biofilms of the GFP-tagged PssUMAF0158 wild-type, extracellular matrix mutants and complemented strains. The area and volume values were calculated with the IMARIS software package (Bitplane, Switzerland). The following GFP-tagged strains were tested: PssUMAF0158 wild-type (PssUMAF0158 wt), PssUMAF0158 alginate mutant (*Δalg8*), PssUMAF0158 cellulose mutant (*ΔwssE*), PssUMAF0158 Psl-like polysaccharide mutant (*ΔpslE*), PssUMAF0158 *Δalg8,wssE* double mutant (*Δalg8,wssE*), PssUMAF0158 *Δalg8,pslE* double mutant (*Δalg8,pslE*), PssUMAF0158 *ΔwssE,pslE* double mutant (*ΔwssE,pslE*), PssUMAF0158 *Δalg8,wssE,pslE* triple mutant (*Δalg8,wssE,pslE*), alginate complemented strain (*Δalg8*+pBBR*alg8*), cellulose complemented strain (*ΔwssE*+pBBR*wssE*) and Psl-like complemented strain (*ΔpslE*+pBBR*pslE*). A minimal of three replicates and three independent experiments were performed. Statistical significance was assessed by two-tailed Mann–Whitney test (*p<0.05, **p<0.01, ***p<0.001). Error bars show the standard error of the mean (s.e.m).

Cellulose is a component of PssUMAF0158 biofilms. To observe the presence of cellulose polysaccharide in PssUMAF0158 biofilms, calcofluor staining was performed using flow-cell chambers (Figure 7.C1). As expected, cellulose staining was absent in the *ΔwssE* mutant. Flow-cell chamber experiments allowed us to observe that cellulose is located in the cell aggregates of the PssUMAF0158 wild-type strain (Figure 7.C1). In *trans* expression of the *wssE* gene restored cellulose mutant phenotype to the wild-type levels (Figure 4C.C1).

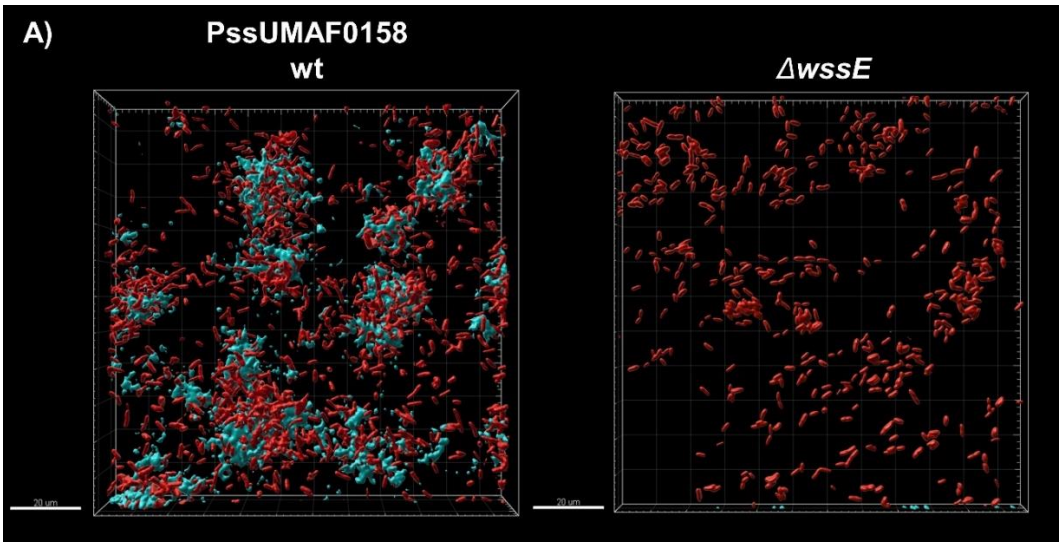

Figure 7.C1. Cellulose staining of the biofilm. Representative 12h 3D biofilm images of the dsRed-tagged *P. syringae* pv. syringae UMAF0158 wild-type (PssUMAF0158 wt) and dsRed-tagged cellulose mutant (*ΔwssE*) stained with calcofluor dye (blue) are shown. The obtained images were analysed with the Leica Application Suite (Mannheim, Germany) and the IMARIS software package (Bitplane, Switzerland). Scale bar 20 µm.

Both cellulose and Psl-like exopolysaccharides are necessary for the competition of *P. syringae* pv. syringae UMAF0158 in biofilm formation. To investigate the roles of the main exopolysaccharides implicated in biofilm formation in bacterial competition and niche colonization, mixed biofilms containing the dsRed-tagged wild-type and GFP-tagged mutants for cellulose and/or Psl-like gene clusters were assessed in flow-cell chambers (Figure 8.C1). When just one of the two most relevant polysaccharides were missing each strain occupied around fifty percent of the colonized space, which indicates that there was no impairment in niche colonization by the mutants compared to the wild-type strain (Figures 8B,C.C1). However, the double mutant was not able to compete with the wild-type, since it occupied about two percent of the colonized space compared to the nighty-

eight percent of the wild-type strain. This result suggests a synergistic role of the two polysaccharides during colonization.

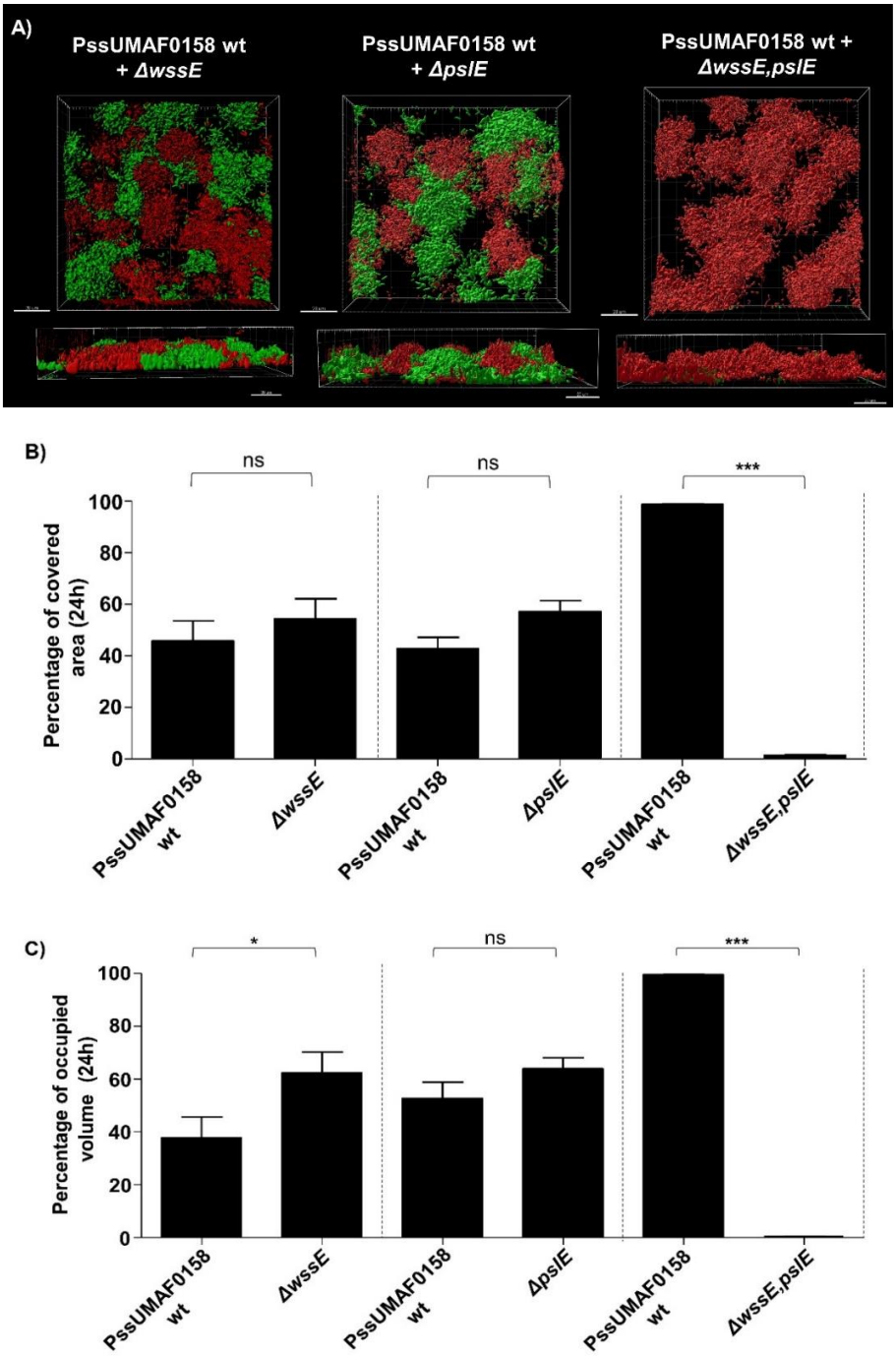

Figure 8.C1. Competition in mixed biofilms. Role of different polysaccharides in competition for biofilm formation. A) Representative 24 h 3D images of mixed biofilms including the dsRed-tagged PssUMAF0158 wild-type and GFP-tagged matrix mutants. The obtained images were analysed with the Leica Application Suite (Mannheim, Germany) and the IMARIS software package (Bitplane, Switzerland). Scale bar 20 µm; B) Percentage of the area occupied by the wild-type and the respective mutants after 24 h of competition calculated with IMARIS software; C) Percentage of the volume occupied by the wild-type and the respective mutants after 24 h of competition calculated

with IMARIS software. The dsRed-tagged PssUMAF0158 wild-type (PssUMAF0158 wt), GFP-tagged PssUMAF0158 cellulose mutant (*ΔwssE*), GFP-tagged PssUMAF0158 Psl-like polysaccharide mutant (*ΔpslE*) and GFP-tagged PssUMAF0158 *ΔwssE,pslE* double mutant (*ΔwssE,pslE*) were tested. A minimal of two replicates and three independent experiments were performed. Statistical significance was assessed by two-tailed Mann–Whitney test (*p<0.05, **p<0.01, ***p<0.001). Error bars show the standard error of the mean (s.e.m).

The Psl-like polysaccharide plays a role in swarming motility. Swarming experiments were performed using the PssUMAF0158 wild-type and extracellular matrix mutants. Swarming patterns occurred as migrating and branching tendrils from the point of inoculation. Among all the extracellular matrix mutants included in this study, only PssUMAF0158 *ΔpslE* mutant, and the double and triple mutants that included the *pslE* gene deletion, were impaired in swarming motility (Figure 9.C1). The Psl-like complemented strain did not exhibit significant restoration of the wild-type swarming motility phenotype in these conditions (Figure 10.C1). Analysis of transcript abundance of the *pslD* and *pslF* genes in the wild-type and *ΔpslE* mutant strains (Figure 11.C1) revealed differences in gene expression under the analysed conditions. Furthermore, *pslE* expression under the P_{lac} promoter present on the pBBR1MCS5 plasmid could also affect swarming in these conditions, as it was observed in the swarming phenotype of PssUMAF0158 wt + pBBR*pslE* control strain (Figure 10.C1). These facts could explain why swarming motility did not restore to the wild-type phenotype in the Psl-like complemented strain.

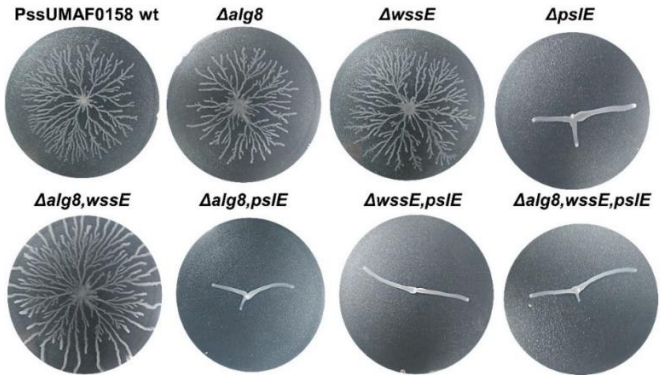

Figure 9.C1. Swarming motility. Representative images of swarming plates after 48 h of growth at 25ºC. The PssUMAF0158 wild-type (PssUMAF0158 wt), PssUMAF0158 alginate mutant (*Δalg8*), PssUMAF0158 cellulose mutant (*ΔwssE*), PssUMAF0158 Psl-like polysaccharide mutant (*ΔpslE*), PssUMAF0158 *Δalg8,wssE* double mutant (*Δalg8,wssE*), PssUMAF0158 *Δalg8,pslE* double mutant (*Δalg8,pslE*), PssUMAF0158 *ΔwssE,ΔpslE* double mutant (*ΔwssE,pslE*) and PssUMAF0158 *Δalg8,wssE,pslE* triple mutant (*Δalg8,wssE,pslE*) were tested. Three independent experiments and three technical replicates per experiment and strain were performed.

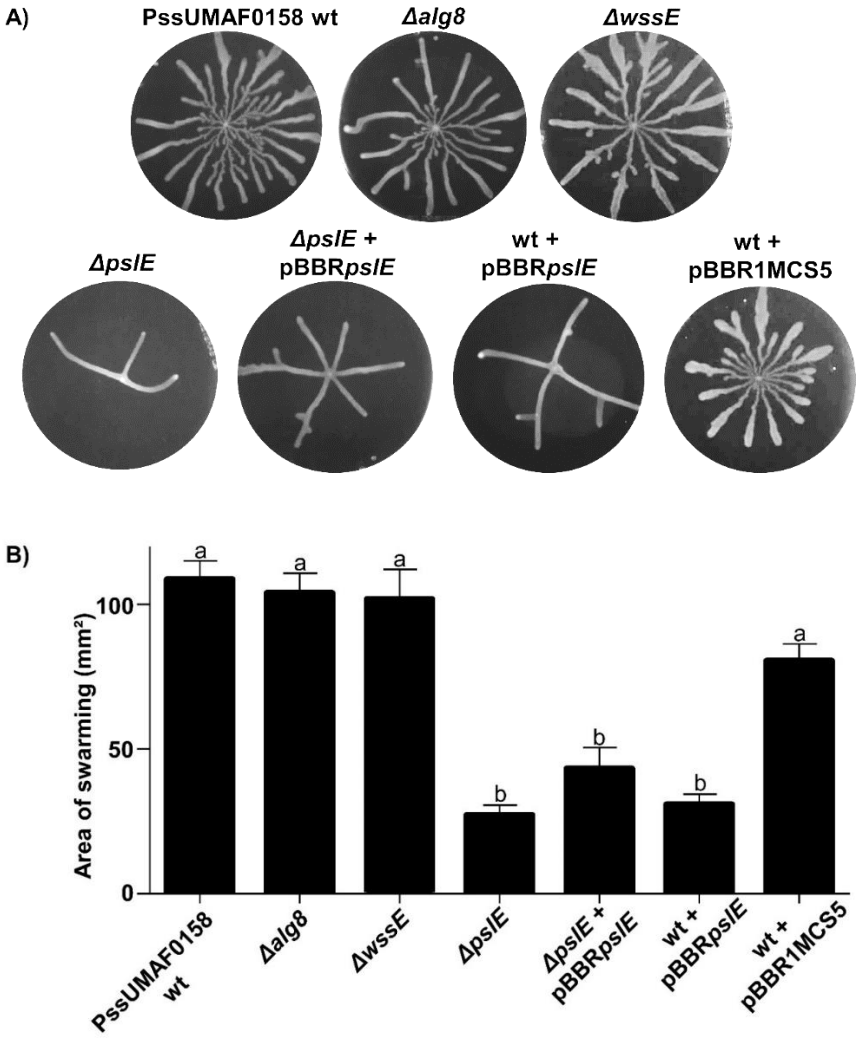

Figure 10.C1. Swarming motility. Effect of polysaccharide production on swarming motility. A) Representative images of swarming plates incubated at 25ºC at 48 h postinoculation; B) Swarm motility area after 48 h of growth at 25ºC. The PssUMAF0158 wild-type (PssUMAF0158 wt), PssUMAF0158 alginate mutant (*Δalg8*), PssUMAF0158 cellulose mutant (*ΔwssE*), PssUMAF0158 Psl-like polysaccharide mutant (*ΔpslE*), Psl-like complemented strain (*ΔpslE*+pBBR*pslE*), *pslE* overexpression strain (wt+pBBR*pslE*) and vector control (wt+pBBR1MCS5) were tested. Statistical analysis was performed using ANOVA with the Bonferroni correction test. Different letters represent statistically significant differences, $p<0.05$. Error bars show the standard error of the mean (s.e.m).

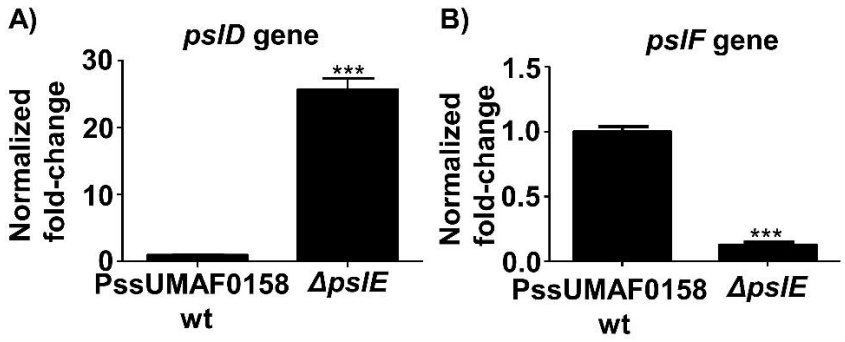

Figure 11.C1. qRT-PCR experiments of the *pslD* and *pslF* genes from TPG plates after 48 h of growth at 25ºC. Results are shown as the fold-change expression of the selected genes in the *ΔpslE* mutant strain compared to the wild-type. PssUMAF0158 wild-type (PssUMAF0158 wt) and PssUMAF0158 Psl-like mutant (*ΔpslE*) strains were tested. Three independent RNA extractions and two technical replicates per extraction were assessed. Statistical analysis was assessed by two-tailed Mann-Whitney test (***>0.001). Error bars correspond to the standard error of the mean (s.e.m).

The *P. syringae* pv. syringae UMAF0158 Psl-like polysaccharide might be similar in composition to the archetypal *P. aeruginosa*. The Psl exopolysaccharide of the *P. aeruginosa* supernatant has a molecular mass of 6,5 kDa (Kocharova *et al.,* 1998; Ma *et al.,* 2007). Therefore, the *P. aeruginosa* PAO1 F1 fraction (Figure 12A.C1), which includes exopolysaccharides with a molecular mass in the range of 6-72 kDa, was analysed as a control of Psl composition. The size exclusion chromatography (SEC) fractions conforming a peak that was present in the PssUMAF0158 Δ*alg8,wssE* strain (unaffected in Psl production) but not in PssUMAF0158 Δ*pslE* (impaired in Psl production) (Figure 12B,C.C1) were then separated by anion exchange chromatography (AEX) and chemically studied to determine their composition. The chemical analysis of the F1 fraction of PAO1 supernatant reported the presence of glucose, mannose, galactose and fucose (Table 2.C1). Cell-associated exopolysaccharide preparations exclusives of Δ*alg8,wssE* double mutant, unaffected in Psl-like production, contained primarily rhamnose and glucose (Table 2.C1). Furthermore, exopolysaccharide preparations of Δ*alg8,wssE* supernatant contained primarily galactose, glucose and mannose (Table 2.C1). Overall, considering all exopolysaccharide preparations of the Δ*alg8,wssE* peaks that are not present on Δ*pslE,* the predominant monosaccharides are rhamnose, glucose, galactose and mannose. Except for rhamnose, these sugar monomers were also detected in exopolysaccharide purified samples of *P. aeruginosa* PAO1 supernatant under the analysed conditions (Table 2.C1).

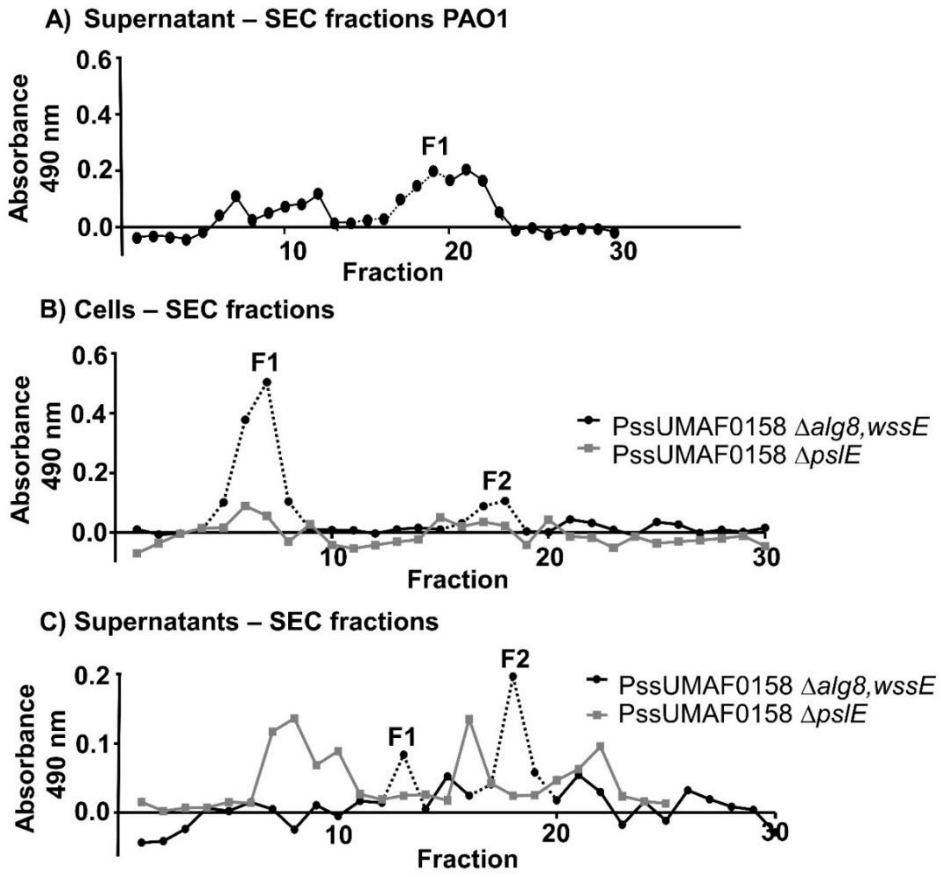

Figure 12.C1. Absorption spectra of polysaccharides in SEC fractions at 490 nm. A) Absorption spectra of polysaccharides in SEC fractions of PAO1 supernatant; B) Absorption spectra of polysaccharides in SEC fractions of cells of the PssUMAF0158 Δ*alg8,wssE* strain (black line; wild-type for Psl production) and PssUMAF0158 Δ*pslE* (grey line; impaired in Psl production); C) Absorption spectra of polysaccharides in SEC fractions of the PssUMAF0158 Δ*alg8,wssE* mutant (black line) and PssUMAF0158 Δ*pslE* mutant (grey line) supernatants. The dotted lines represent the peaks collected for chemical analysis.

Table 2.C1. Carbohydrate monomer composition. The table shows the sugar unities and proportions identified in the EPS fractions produced by the PssUMAF0158 Δ*alg8,wssE* mutant (unaffected in Psl production) that were not present in PssUMAF0158 Δ*pslE* (impaired in Psl production). The EPS fraction of *P. aeruginosa* PAO1 supernatant that putatively contains the Psl polysaccharide was included as a control of Psl composition. SEC = size exclusion chromatography, AEX = anion exchange chromatography; ; F = fraction; Glu (black) = glucose, Rha (blue) = rhamnose, Gal (yellow) = galactose, Man (pink) = mannose, Xil (green) = xylose, Ara (orange) = arabinose, Fuc (purple) = fucose; (×) neutral charge, (+) positive charge and (-) negative charge.

Strain	SEC Sample	Molecular weight (kDa)	AEX Fractions	Charge	Monosaccharides	Proportion (%)
PAO1	**Supernatant F1**	6-72	F1-SF1	× or +	Glu, Man, Gal, Fuc	75.6/11.9/11.3/1.2
			F1-SF2	× or +	Glu, Man, Gal, Fuc	57/23.9/17/2.1
Δ*alg8,wssE*	**Cells F1**	573-6817	F1-SF1	× or +	Rha, Glu, Gal	91.3/8.4/0.3
			F1-SF2	× or +	Rha, Glu	92.9/7.1
Δ*alg8,wssE*	**Cells F2**	9-48	F2-SF1	× or +	Rha, Glu, Xil, Gal	62.2/26/5.5/6.3
			F2-SF2	-	Glu, Gal, Xil, Man, Ara	52.4/18/11.7/10.5/7.4
Δ*alg8,wssE*	**Supernatant F1**	72-166	F1-SF1	× or +	Glu, Gal, Xil, Ara	60.3/26/9.6/4.1
			F1-SF2	× or +	Gal, Man, Glu, Rha	40.5/37.2/18.1/4.3
			F1-SF3	-	Glu, Man, Gal	75.7/13.1/11.2
Δ*alg8,wssE*	**Supernatant F2**	6-31	F2-SF1	× or +	Gal, Man, Glu, Ara	39.7/30.5/25.2/4.7
			F2-SF2	× or +	Gal, Man, Glu	42.8/39.2/18
			F2-SF3	-	Glu, Xil, Gal, Rha	45.8/26.4/21.6/6.2

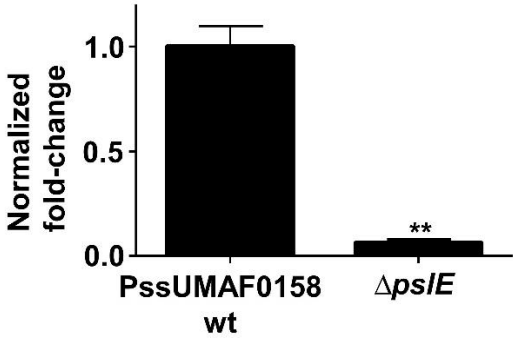

Figure 13.C1. qRT-PCR experiments of the *rhlA* gene from TPG plates after 24 h of growth at 25ºC. Results are shown as the fold-change expression of *rhlA* gene in the *ΔpslE* mutant compared to the wild-type. The expression of *rhlA* gene was lower in the mutant compared to the wild-type, which is consistent with the impairment in swarming motility observed in *ΔpslE*. PssUMAF0158 wild-type (PssUMAF0158 wt) and PssUMAF0158 *ΔpslE* mutant (*ΔpslE*) were tested. Statistical significance was assessed by two-tailed Mann–Whitney test (**p<0.01). Error bars correspond to the standard error of the mean (s.e.m).

4. Discussion

Biofilms play an important role in the lifestyle of the phytopathogenic bacterium *P. syringae* pv. syringae UMAF0158 (PssUMAF0158), particularly on mango tree surfaces (Arrebola *et al.*, 2015; Gutiérrez-Barranquero *et al.*, 2019). Beyond cellulose production by PssUMAF0158, little is known about the composition of PssUMAF0158 extracellular matrix. Therefore, we investigated the biological roles of two gene clusters other than those related to cellulose production that seem to be involved in the synthesis of alginate and a Psl-like exopolysaccharides in PssUMAF0158. The roles that Psl polysaccharide plays in nonaeruginosa *Pseudomonas* remain unknown. Then, it is noteworthy that the *psl*-like cluster was found in all the main plant-associated phylogenetic groups included in the *P. syringae* complex (Figure 1.C1). The phylogenetically maintained *psl*-like cluster suggests that this polysaccharide could be relevant not only for PssUMAF0158 lifestyle, but also among all the plant-associated phylogroups of the *P. syringae* complex. Taking this into account, we mainly concentrated our efforts on discerning the function of the *psl*-like gene cluster in PssUMAF0158.

Pss transitions between an epiphytic and a pathogenic lifestyle on mango surfaces (Cazorla *et al.*, 1998; Xin *et al.*, 2018; Gutiérrez-Barranquero *et al.*, 2019). Cellulose has proven to be an important component of the extracellular matrix that influences this transition, as the PssUMAF0158 cellulose-defective mutants are more virulent than the wild-type strain, and virulence is practically abolished in the cellulose-overproducing strain (Arrebola *et al.*, 2015). Thus, biofilm formation, through cellulose biosynthesis, could be favored in the epiphytic phase, and transition to the pathogenic phase could be promoted by a reduction in biofilm formation, led by a decrease in cellulose production (Gutiérrez-Barranquero *et al.*, 2019). Actually, something similar was observed in *Salmonella enterica*; when cellulose biosynthesis was repressed by MgtC, the bacteria became more virulent (Pontes *et al.*, 2015). Psl-like polysaccharide performed a role in virulence similar to that observed for cellulose (Figure 2.C1), which suggests that the transition between epiphytic and pathogenic lifestyles was not limited to a single component of the extracellular matrix. This redundancy might be important to rescue the epiphytic lifestyle when environmental conditions are adverse for cellulose production, and *vice versa*. In fact, redundant biological functions between biofilm components are not unusual

(Colvin *et al.,* 2012; Zapotoczna *et al.,* 2016). As previously observed for cellulose (Arrebola *et al.,* 2015), adhesion experiments on mango leaves reported the influence of Psl-like polysaccharide production on the PssUMAF0158 epiphytic lifestyle (Figure 3.C1). These results are consistent with other studies, in which several exopolysaccharides have been shown to play roles in cell-surface interactions (Ma *et al.,* 2006; Nielsen *et al.,* 2011; Limoli *et al.,* 2015). Alginate biosynthesis has been previously studied in Pss (Yu *et al.,* 1999; Fakhr *et al.,* 1999; Schenk *et al.,* 2008), but the role that it plays in the PssUMAF0158 strain, a mango tree pathogen, has not been investigated thus far. An essential role of alginate in virulence, biofilm formation or motility was not proven in this study (Figures 2.C1, 6.C1 and 10.C1, respectively). This first observation was in accord with other studies in which some alginate-defective mutants have been shown to be unaffected in the induction of symptoms (Peñaloza-Vázquez *et al.,* 1997; Schenk *et al.,* 2008).

The extracellular matrix of Pss includes the three polysaccharides analysed in this study – alginate, cellulose and Psl-like polysaccharide, as revealed the CR and calcofluor binding experiments (Figure 4.C1). The differences observed between plate CR binding (Figure 4A.C1) and pellicle CR binding (Figure 4B.C1) in the PssUMAF0158 *Δalg8* mutant suggest that this polysaccharide is more important to produce biofilms in agar plates than in broth medium. This is supported by previous works, where it was observed that alginate production in several *Pseudomonas* species, including *P. syringae*, was greater in agar plates than in broth medium (Darzins & Chakrabarty, 1984; Kidambi *et al.,* 1995).

In contrast to what had been previously reported for alginate in *P. syringae* (Laue *et al.,* 2006), our results revealed a slightly contribution of this polysaccharide to the biofilm matrix of the PssUMAF0158 strain (Figure 6.C1). As observed in PAO1 (Ghafoor *et al.,* 2011), the PssUMAF0158 *Δalg8* mutant formed fewer cell aggregates than the wild-type strain in flow-cell chamber experiments (Figure 6.C1). The cell aggregates formed by the PssUMAF0158 *ΔpslE* mutant were disrupted in PssUMAF0158 *ΔwssE,pslE* double mutant. This is similar to the *P. aeruginosa* E2, S54485 and 19660 flow-cell chamber phenotypes, in which the *Δpsl* mutants formed small aggregates and these aggregates were disrupted in the *Δpsl,pel* double mutants (Colvin *et al.,* 2012). The Pel polysaccharide, which is missing in PssUMAF0158, has been described in *P. aeruginosa* as a glucose-rich exopolysaccharide, similar to

cellulose (Friedman & Kolter, 2004). These aggregates were disrupted in both species when either cellulose or Pel were not produced, which suggest they could be performing similar roles in their biofilm architectures. The fact that the cellulose mutant was unable to form cell aggregates (Figure 6.C1), and that cellulose preferentially locates in them (Figure 7.C1), support this suggestion. Furthermore, the restoration of the wild-type phenotype in the *Δalg8,pslE* double mutant regarding CR binding experiments of the pellicles (Figure 4B.C1) and biofilm area and volume values (Figures 6B,C.C1), suggest that another polysaccharide, such as cellulose, could be being overexpressed in PssUMAF0158 *Δalg8,pslE* double mutant the same way Pel does in PAO1 *Δalg8,pslA* double mutant (Ghafoor *et al.,* 2011). Although our results lead to these suggestions, there was not noticeable cellulose overexpression in plate assays (Figures 4A,C.C1) or w*ssE* gene overexpression in the *Δalg8,pslE* pellicles (Figure 5.C1). However, cellulose biosynthesis can also be regulated at post-translational levels (Römling *et al.,* 2015). Besides, our results also indicate that cellulose and Psl-like polysaccharides cooperate for niche colonization in PssUMAF0158 strain, as the *ΔwssE,pslE* double but not the single mutants was outcompeted by the wild-type when they were coinoculated in flow-cell chambers (Figure 8.C1). This cooperation may explain why the *psl*-gene cluster is widely conserved among pseudomonads that also produce cellulose (Mann & Wozniak, 2012). In contrast to our findings, PAO1 *Δpsl* mutant was unable to compete for biofilm formation with PAO1 wild-type (Jackson *et al.,* 2004).

Swarming motility is related to biofilm formation, as the two processes are frequently co-regulated (Köler *et al.,* 2000; Caiazza *et al.,* 2007; Murray *et al.,* 2010; de la Fuente-Núñez *et al.,* 2012; Fünfhaus *et al.,* 2018). Biosurfactants have been frequently associated with bacterial motility, since for many strains swarming motility on semi-solid agar plates is dependent upon such compounds (Oschner *et al.,* 1994; Burch *et al.,* 2011; Kearns *et al.,* 2010). In fact, in *P. aeruginosa* PAO1, the production of Psl and/or Pel polysaccharides is correlated with rhamnolipid production (Wang *et al.,* 2014). We decided to analyse *rhlA* expression by q-RT-PCR in the *ΔpslE* mutant, which synthetizes the rhamnolipid precursor HAA, as PssUMAF0158 strain lacks the *rhlB* and *rhlC* genes. However, swarming motility does not strictly require rhamnolipid production, as HAA itself can act as wetting agent (Déziel *et al.,* 2003). We found downregulation of the *rhlA* gene in the *ΔpslE*

mutant compared to the wild-type strain (Figure 13.C1), which could explain the reduction of motility observed in the *ΔpslE* mutant (Figures 9.C1 and 10.C1). However, it is interesting to point out that the relationship between biofilm formation, rhamnolipid production and motility in PssUMAF0158 seems opposite to that described in *P. aeruginosa*, as PAO1 *Δpsl* mutant showed an increase in swarming motility due to a higher rhamnolipid production (Wang *et al.,* 2014). The swarming impairment observed in PssUMAF0158 *ΔpslE* mutant suggests a potential role of this polysaccharide in the movement of PssUMAF0158 over the plant surface. In fact, the Psl exopolysaccharide is also involved in surface colonization in *P. aeruginosa* (Zhao *et al.,* 2013). The increase in virulence in the mutant cannot be explained by its colonization ability, but once *ΔpslE* mutant penetrates the leaf, it shows the same phenotype as the cellulose mutant. This suggests that the Psl-like polysaccharide could act as an additional switch between the epiphytic-pathogenic lifestyles with respect to cellulose.

The first study regarding Psl composition in *P. aeruginosa* was performed using EPS samples of WFPA8001, a PAO1 Psl-inducible strain, and determined that it contained glucose, mannose and galactose, as well as trace amounts of xylose, rhamnose and N-acetylglucosamine (Ma *et al.,* 2007). Two years later, the structural analysis of Psl was published, indicating that it was likely composed of a pentasaccharide repeating unit of mannose, glucose and rhamnose in approximate ratios of 3:1:1 (Byrd *et al.,* 2009). Curiously, galactose, which was reported as a component of Psl in the first study (Ma *et al.,* 2007) was not detected in the structural analysis (Byrd *et al.,* 2009). However, different growth conditions were used in both studies, which could account for some variations in composition, as described previously (Flemming *et al.,* 2016). Be as it may, mannose has always been described as a characteristic component of the Psl structure in *P. aeruginosa* (Friedman & Kolter, 2004; Ma *et al.,* 2007; Byrd *et al.,* 2009). Preliminary results regarding the composition of the Psl-like exopolysaccharide of PssUMAF0158 determined that it might share a similar composition to that of *P. aeruginosa*, because out of all exopolysaccharide samples analysed (cell- and supernatant-derived), the main monosaccharides detected were rhamnose, glucose, galactose and mannose (Table 2.C1). Some hints exist regarding the existence of a polysaccharide that resembles Psl in *P. syringae*. It was reported that in addition to alginate and

levan, *P. syringae* PG4180 produces a third exopolysaccharide that constitutes a fibrous structure in its biofilms and binds to *Naja mossambica* lectin (NML; Laue *et al.,* 2006). Interestingly, the monosaccharide specificity of NML is mannose (Jiang *et al.,* 2016). If the mannose-containing polymer detected with NML in *P. syringae* PG4180 is actually Psl, we could suggest that PssUMAF0158 Psl-like polysaccharide could be likely composed of galactose, glucose and mannose, because mannose monosaccharide, which was just present in the supernatant samples, was always detected along with galactose and glucose monosaccharides (Table 2.C1). Interestingly, galactose, glucose and mannose were the Psl composition initially reported in *P. aeruginosa* (Ma *et al.,* 2007).

In summary, this work constitutes the first report of a Psl polysaccharide functioning in a phytopathogenic bacterium, and the obtained results reveal a clear role of this polysaccharide in biofilm formation, colonization and virulence, as well as suggest a potential general role during plant-bacteria interactions within the *P. syringae* complex, since the genomic region that encodes Psl is very well-conserved. The interconnection observed between the production of the Psl-like polysaccharide and swarming motility suggests a potential correlation between the expression of *psl* and rhamnolipid genes, but further investigation will be required to identify the mechanisms underlying this association.

CHAPTER 2

Environmental factors influence biofilm formation in *Pseudomonas syringae* pv. syringae

The results included in this chapter are under elaboration to be submitted for publication

1. Summary

P. syringae pv. syringae (Pss) is the causal agent of the bacterial apical necrosis (BAN) disease of mango trees, which is the most limiting factor for mango crop in the Mediterranean region. Previous studies have revealed a connection between weather conditions and the incidence and severity of disease symptoms, as the highest BAN disease symptoms always coincided with cool and wet periods. In this study, the role of some environmental factors, such as temperature and light, in biofilm formation of different Pss strains mainly associated with the mango host have been assessed. The results have shown that temperature and particularly light influence biofilm formation through exopolysaccharide biosynthesis. Thus, the different Pss strains show an oscillating pattern in biofilm formation and exopolysaccharide production depending on temperature. Noticeably, white light increases biofilm formation through exopolysaccharide biosynthesis in Pss. Furthermore, cellulose production phenotypes are congruent with the phylogenetic distribution of the Pss strains of this study regarding their cellulose clusters, which suggests this polysaccharide could be very important for the ecology of Pss over the mango host plant. Finally, as previously described in the model strain *P. syringae* pv. syringae UMAF0158, lower levels of exopolysaccharide production could be associated with higher virulence of Pss.

2. Introduction

Environmental factors have an enormous influence on biofilm formation (Toyofuku *et al.,* 2016; Rossi *et al.,* 2018). The environmental factors that modulate biofilm formation are usually species specific, which could enable each bacterial species to colonize their preferred niches more efficiently than others (Stanley & Lazazzera, 2004). Environmental factors include host- and external-derived signals, such as nutrients, temperature, light, humidity and pH. For instance, salt and nutrient content have been observed to influence biofilm formation in *Vibrio fischeri* (Marsden *et al.,* 2017). Recently, biofilm formation in *Pseudomonas aeruginosa* has been described to be highly dependent on temperature through the modulation of c-di-GMP synthesis (Kim *et al.,* 2020). Light has been reported to influence bacterial lifestyle choices (Gomelsky & Hoff, 2011), such as virulence, attachment and colonization in *Pseudomonas syringae* pv. tomato (Río-Álvarez *et al.,* 2014; Santamaría-Hernando *et al.,* 2018).

P. syringae pv. syringae (Pss) is the causal agent of bacterial apical necrosis (BAN) disease of mango trees (Cazorla *et al.,* 1998), which is the most limiting factor for mango crop in the Mediterranean region. Generally, the *P. syringae* species transits between an epiphytic and pathogenic stages on plants depending on environmental conditions (Xin *et al.,* 2018). Previous studies have revealed a connection between weather conditions and BAN disease symptoms (Cazorla *et al.,* 1998) and between biofilm formation and virulence in PssUMAF0158 strain (Arrebola *et al.,* 2015; Heredia-Ponce *et al.,* 2020a). The highest BAN disease symptoms coincide with cool and wet periods (Cazorla *et al.,* 1998) and the impairment in biofilm formation of the PssUMAF0158 cellulose and Psl-polysaccharide mutants increases virulence in tomato leaflets compared to the wild-type strain (Arrebola *et al.,* 2015; Heredia-Ponce *et al.,* 2020a). However, despite these evidences, it is unknown if environmental factors, such as temperature and light, can influence biofilm formation in Pss strains associated with the mango host.

In this study, biofilm formation, with a focus in the exopolysaccharidic component, was evaluated to determine the variability of this physiological trait and its involvement in virulence in different Pss strains mainly associated with the mango host. Besides, how temperature and light influence biofilm formation have been

evaluated and ultimately, based on the results obtained, the connection between environmental factors-biofilm formation-virulence is discussed.

3. Results

***P. syringae* pv. syringae strains mainly isolated from mango trees show heterogeneity in exopolysaccharide production.** Twenty Pss strains that had been mainly isolated from necrotic tissues of mango trees (Table 1.C2) were analysed for exopolysaccharide (EPS) production using two different approaches: two different plate assays (Figure 1.C2) and a biofilm formation assay on microwell plates (Figure 2.C2). Using the plate assays, the results obtained showed mucoid and nonmucoid phenotypes in YEM plates after 3 days of growth (Figure 1A.C2), which have been formerly associated with EPS and no EPS production in *Burkhordelia* spp., respectively (Zlosnik *et al.*, 2008). The PssUMAF0158 Δ*alg8* (alginate mutant) and PssUMAF0158 Δ*alg8*+*alg8* (alginate complemented) strains were used as controls of nonmucoid and mucoid phenotypes, respectively. Plate assays performed using TPG medium supplemented with 20 µg/ml of Congo red (CR) also showed mucoid and nonmucoid phenotypes (Figure 1B.C2) that correlate with the results previously obtained in YEM plates (Figure 1A.C2), except for the case of the PssUMAF2044 strain. The PssUMAF2044 strain showed a nonmucoid phenotype in YEM plates (Figure 1A.C2) and a mucoid phenotype in TPG+CR plates (Figure 1B.C2). In addition, all strains bound CR after 6 days of growth (Figure 1B.C2).

Quantification of the CR bound to the pellicles allowed estimation of their EPS production levels within biofilms, mainly cellulose according to Heredia-Ponce *et al.*, (2020a) (Figure 2.C2). The group 1 (G1) included those strains that produced similar amounts of EPS than PssUMAF0158, which was used as reference strain. This group was comprised by the PssUMAF0049, PssUMAF0176, PssUMAF1013 and PssUMAF2815 strains; the group 2 (G2) included those strains that produced higher amounts of EPS than PssUMAF0158, which comprised the PssUMAF0081, PssUMAF0170, PssUMAF0271, PssUMAF0273, PssUMAF2016, PssUMAF2600, PssUMAF7000, PssDAR77789 and PssEPS17a strains; finally, the group 3 (G3) included those strains that produced lower amounts of EPS than PssUMAF0158, which comprised the PssUMAF0291, PssUMAF0297, PssUMAF1029, PssUMAF2044, PssUMAF2801 and PssUMAF3028 strains.

Table 1.C2. *Pseudomonas syringae* pv. syringae strains used in this study.

Bacterial strains	Geographical origin	Host of isolation	Year of isolation	Reference
PssUMAF0049	Algarrobo, Malaga, Spain	Mango	1992	Cazorla *et al.*, 2002
PssUMAF0081	Algarrobo, Malaga, Spain	Mango	1992	Cazorla *et al.*, 2002
PssUMAF0158	Algarrobo, Malaga, Spain	Mango	1993	Arrebola *et al.*, 2003
PssUMAF0170	Estepona, Malaga, Spain	Mango	1993	Cazorla *et al.*, 2002
PssUMAF0176	Benajarafe, Malaga, Spain	Mango	1994	Arrebola *et al.*, 2003
PssUMAF0271	Algarrobo, Malaga, Spain	Mango	2016	Aprile *et al.*, 2021
PssUMAF0273	Algarrobo, Malaga, Spain	Mango	1990	Arrebola *et al.*, 2003
PssUMAF0291	Benajarafe, Malaga, Spain	Mango	2017	Aprile *et al.*, 2021
PssUMAF0297	Torrox, Malaga, Spain	Mango	2017	Aprile *et al.*, 2021
PssUMAF1013	Lepe, Huelva, Spain	Mango	2017	Aprile *et al.*, 2021
PssUMAF1029	Lepe, Huelva, Spain	Mango	1997	Cazorla *et al.*, 2002
PssUMAF2016	Faro, Portugal	Mango	1997	Cazorla *et al.*, 2002
PssUMAF2044	Faro, Portugal	Mango	2017	Aprile *et al.*, 2021
PssUMAF2600	Perth, Australia	Mango	2016	Aprile *et al.*, 2021
PssUMAF2801	La Palma, Canary Islands, Spain	Mango	2000	Gutiérrez-Barranquero *et al.*, 2008
PssUMAF2815	La Palma, Canary Islands, Spain	Mango	2016	Aprile *et al.*, 2021
PssUMAF3028	Algarrobo, Malaga, Spain	Mango	1990	Arrebola *et al.*, 2003
PssUMAF7000	Gerona, Spain	Pear	2017	Aprile *et al.*, 2021
PssDAR77789	Perth, Australia	Mango	2007	Young, 2008
PssEPS17a	Gerona, Spain	Pear	1987	Arrebola *et al.*, 2003

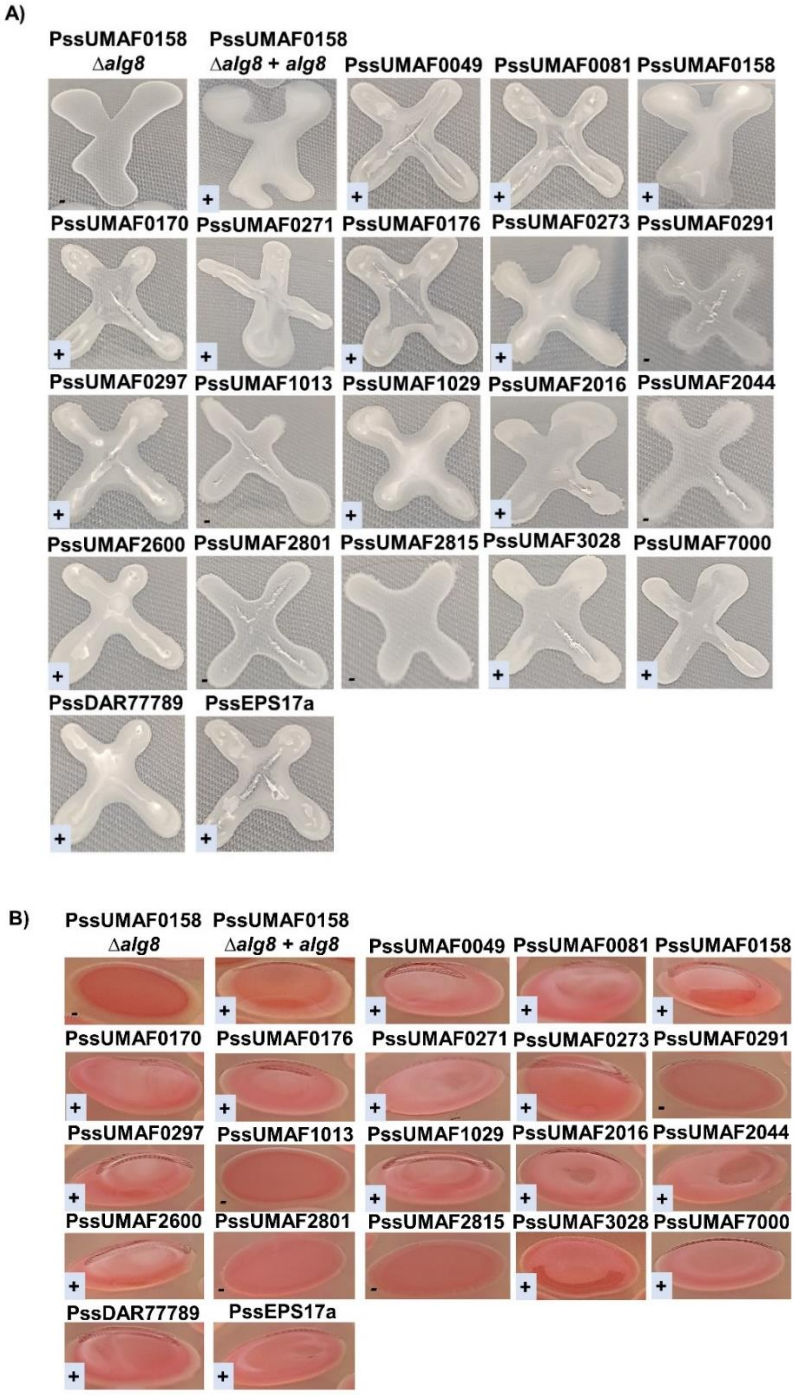

Figure 1.C2. Exopolysaccharide production phenotypes on agar plates of the 20 Pss strains included in this study. A) EPS production on YEM agar plates after 3 days of growth; EPS production was evaluated as follows: positive (+), which has been highlighted with a background, if the bacterial growth is mucoid and negative (-) if the bacterial growth is nonmucoid. B) EPS production on TPG+CR agar plates after 6 days of growth. EPS production was evaluated as follows: positive (+), which has been highlighted with a background, if the bacterial growth is mucoid and negative (-) if the bacterial growth is nonmucoid. The PssUMAF0158 Δ*alg8* (alginate mutant) and PssUMAF0158 Δ*alg8*+*alg8* (alginate complemented) strains were included as controls of nonmucoid

and mucoid phenotypes, respectively. Three replicates and three independent experiments were performed.

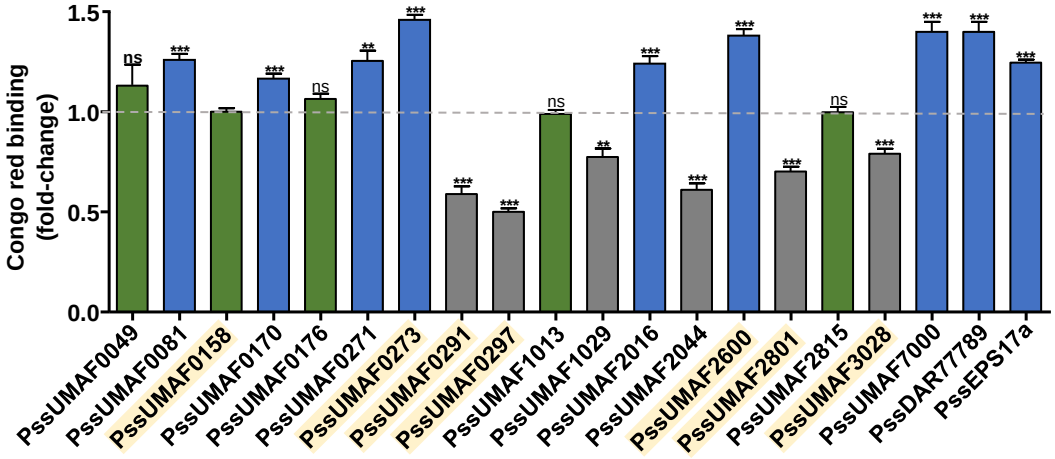

Figure 2.C2. Pellicle CR binding assay of the 20 Pss strains included in this study. The CR binding levels in the pellicle formed by each strain is represented in the form of a fold-change relative to the CR binding average of the PssUMAF0158 strain. Compared to PssUMAF0158, similar levels of CR binding are represented in green, higher in blue and lower in grey colors. Three replicates and three independent experiments were performed. Statistical significance was assessed by two-tailed Mann–Whitney test (**p<0.01, ***p <0.001). Error bars show the standard error of the mean (s.e.m.). The yellow-labeled strains were selected for the following experiments.

The phylogenetic distribution of the *P. syringae* pv. syringae strains regarding their cellulose-encoding clusters is congruent with their cellulose production phenotypes. The phylogenetic distribution of the Pss strains included in this study regarding the three main exopolysaccharide production clusters - alginate, Psl-like and cellulose clusters - was elucidated. The phylogenetic distribution of the strains included in this study regarding the *gyrB*, *rpoD*, *gapA* and *cts* housekeeping genes showed the presence of four main subgroups (Figure 3.C2) that generally coincided with the previously described phylogenetic subgroups within the Pss single mango phylotype, except for the PssEPS17a and PssUMAF7000 strains that were isolated from another host (Aprile *et al.*, 2021). The phylogenetic distribution of the Pss strains based on the housekeeping genes (Figure 3.C2) showed some incongruities with that regarding their alginate, Psl-like and cellulose encoding clusters (Figure 4.C2). Interestingly, the phylogenetic distribution of the Pss strains regarding the cellulose cluster (Figure 4C.C2) correlated with their cellulose production phenotypes within biofilms (Figure 2.C2). Thus, all the strains that produced similar, higher and lower amounts of cellulose than the model strain PssUMAF0158 grouped

together each forming different phylogroups regarding the cellulose cluster (Figure 4C.C2).

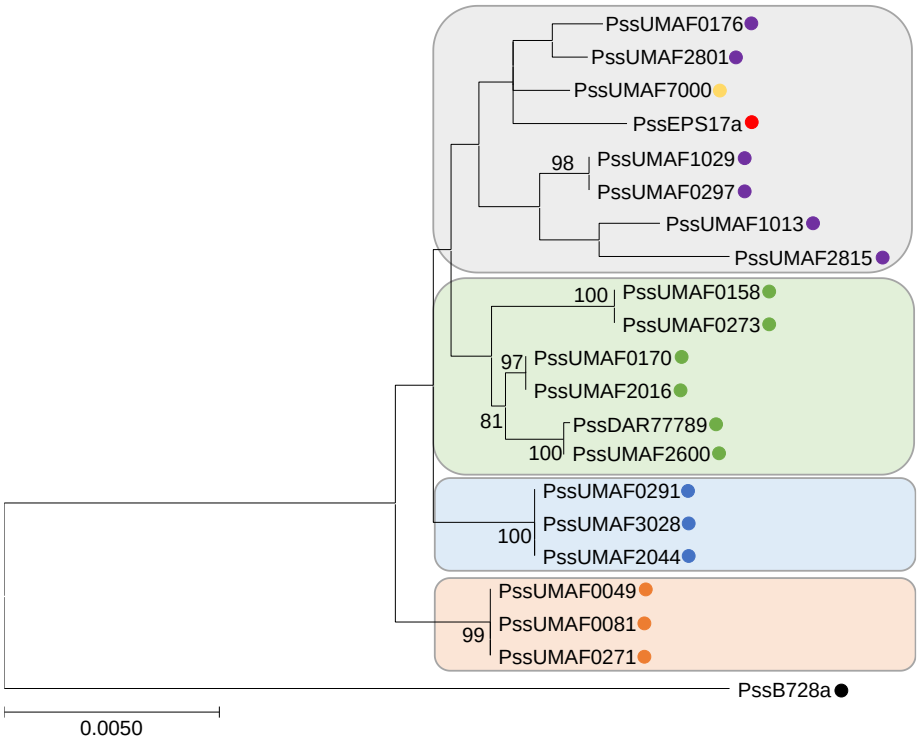

Figure 3.C2. Phylogeny of the 20 Pss strains included in this study based on housekeeping genes. Neighbour-joining tree generated with MEGAX using the combined sequences of the *gyrB*, *rpoD*, *gapA* and *cts* housekeeping genes. Four main subgroups resulted from the analysis: grey, green, blue and orange boxes. The Pss strains included in this study (Table 1.C2) belonged to the I (•blue circle), II (•orange circle), III (•yellow circle), IV (•purple circle), VI (•red circle) and VII (•green circle) phylogroups previously described within the Pss single mango phylotype (Aprile *et al.*, 2021). The PssB728a strain (•black circle) was included as outgroup.

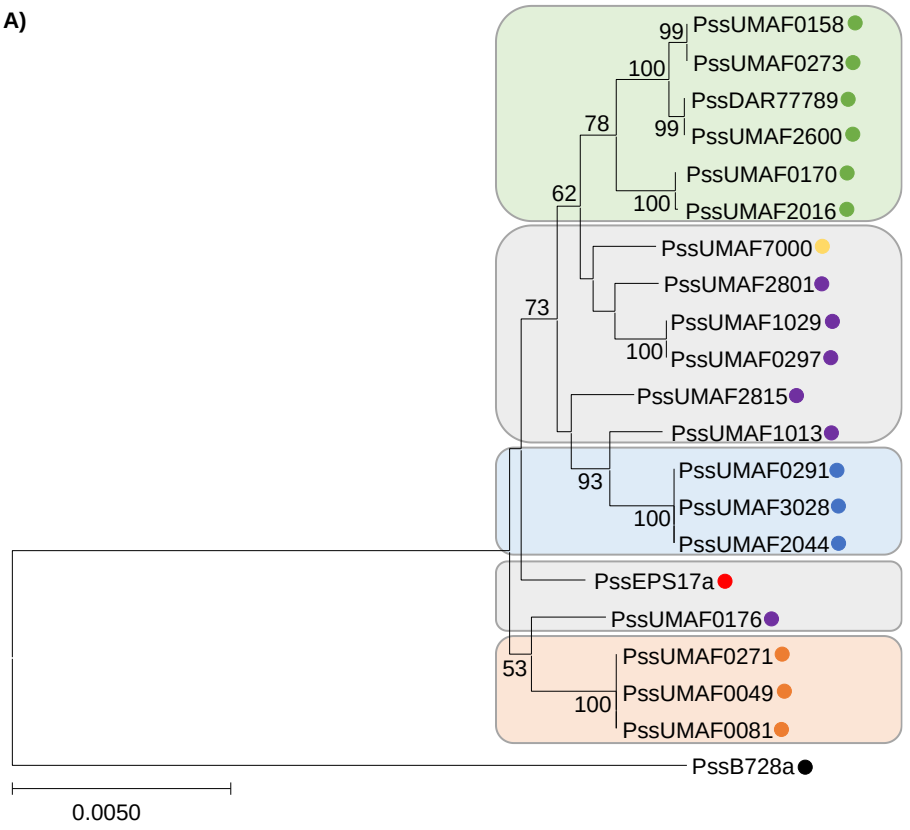

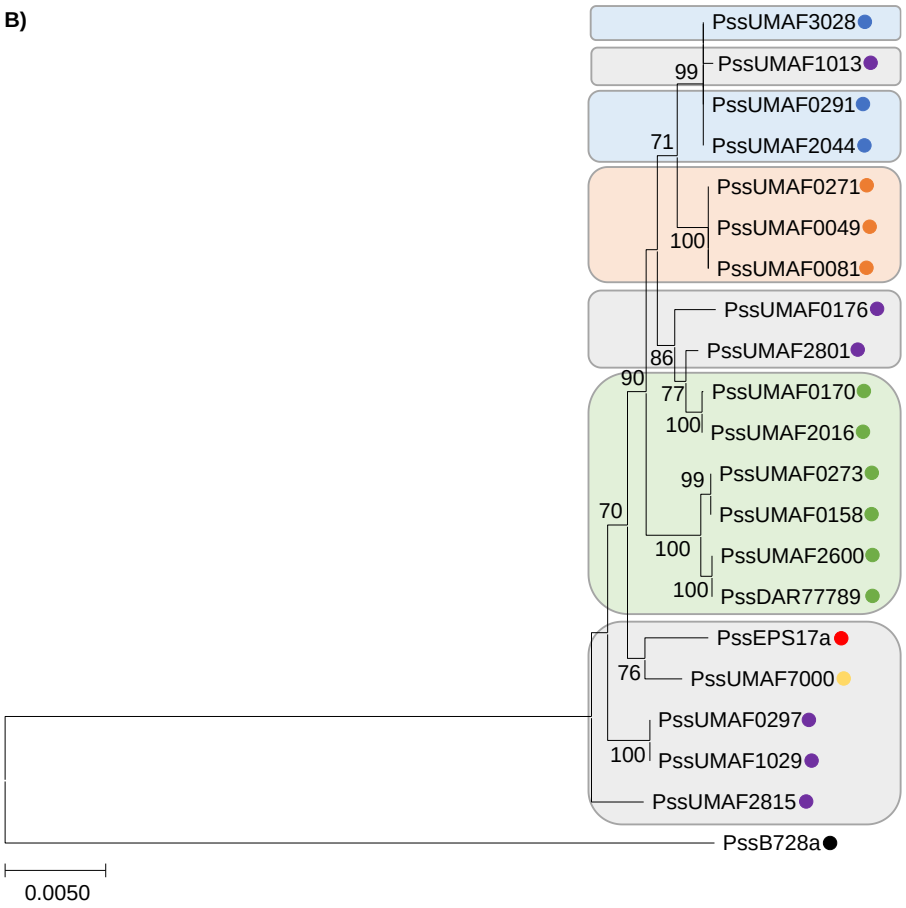

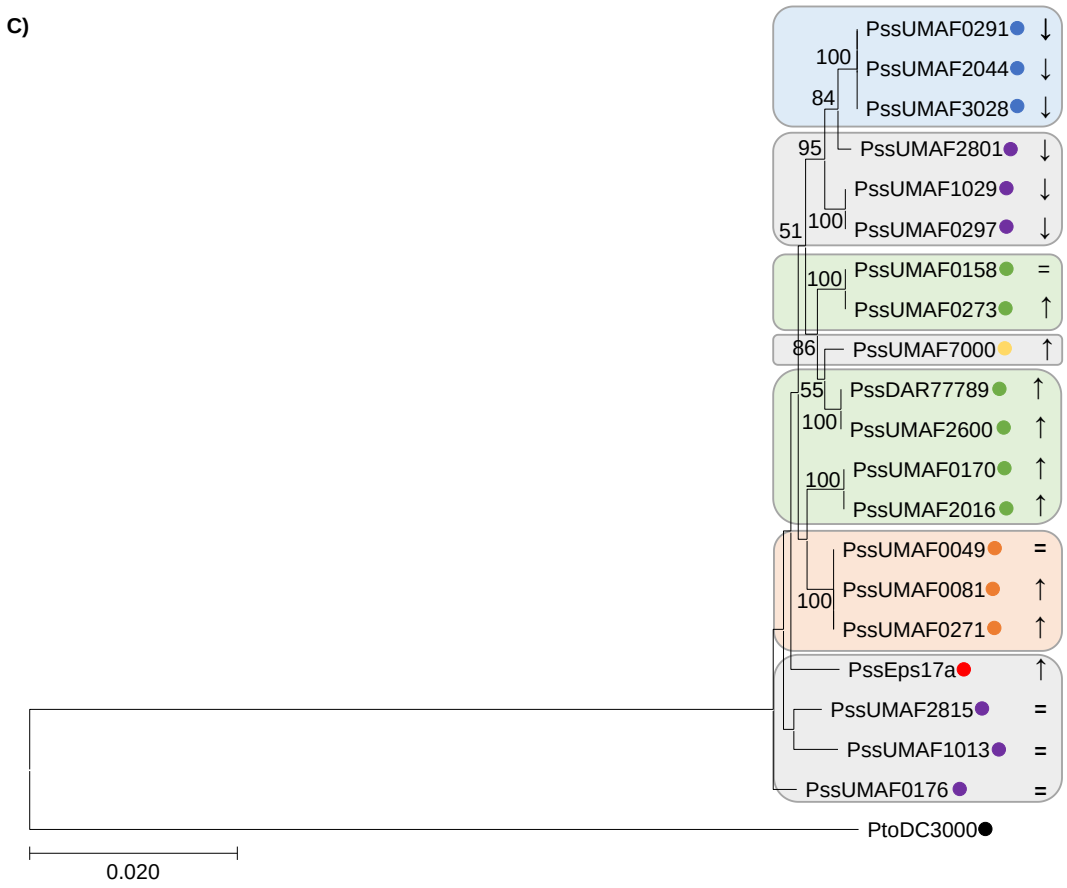

Figure 4.C2. Phylogeny of the 20 Pss strains included in this study based on three main exopolysaccharide synthesis clusters. A) Neighbour-joining tree generated with MEGAX using the alginate cluster nucleotide sequence; B) Neighbour-joining tree generated with MEGAX using the Psl-like cluster nucleotide sequence; C) Neighbour-joining tree generated with MEGAX using the cellulose cluster nucleotide sequence. The grey, green, blue and orange boxes represent the four main subgroups obtained regarding the *gyrB*, *rpoD*, *gapA* and *cts* housekeeping genes (Figure 3.C2). The Pss strains included in this study (Table 1.C2) belonged to the I (•blue circle), II (•orange circle), III (•yellow circle), IV (•purple circle), VI (•red circle) and VII (•green circle) phylogroups previously described within the Pss single mango phylotype (Aprile *et al.*, 2021). The symbols indicate higher (↑), lower (↓) and similar (=) amounts of cellulose within the pellicle of each strain compared to the PssUMAF0158 reference strain (Figure 2.C2). The PssB728a strain (•black circle) was used as outgroup in A and B and the PtoDC3000 strain (•black circle) was used as outgroup in C as PssB728a does not contain the cellulose cluster.

Exopolysaccharide production within *P. syringae* pv. syringae biofilms displays an oscillating pattern depending on the temperature. To assess whether temperature influences pellicle formation and EPS synthesis in Pss, representative strains belonging to G1 (PssUMAF0158), G2 (PssUMAF0273 and PssUMAF2600) and G3 (PssUMAF0291, PssUMAF0297, PssUMAF2801 and PssUMAF3028) were selected to screen their pellicles using microwell plate assays (Figure 5.C2) and to quantify the amount of CR bound to them (Figure 6.C2) at 15, 20, 25 and 30ºC. The results showed that all the Pss strains formed pellicles that contained polysaccharides, which were generally loosely attached to the wells surfaces and contained variable amounts of wrinkles on their surfaces (Figure 5.C2). Quantification of the CR bound to the pellicles determined that EPS production presented an oscillating pattern depending on the temperature that was consistent, although at different levels, in all the selected strains, which was characterized by lower levels of EPS production at 15 and 25ºC and higher levels at 20 and 30ºC (Figure 6.C2). Differences among strains at each temperature are displayed in Table 2.C2.

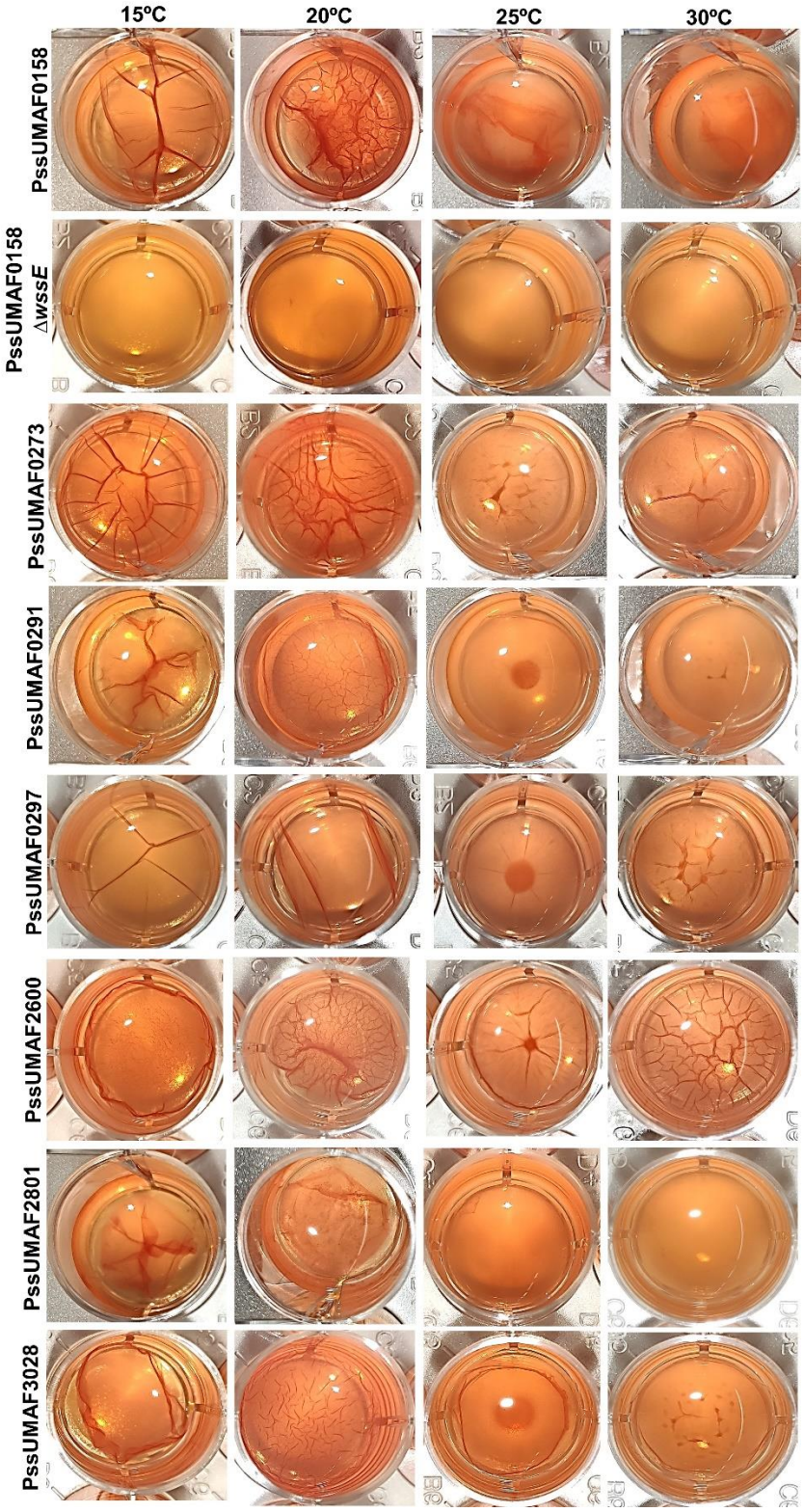

Figure 5.C2. Pellicle formation of the selected Pss strains at different temperatures. Representative images of the pellicles formed by the PssUMAF0158, PssUMAF0158 Δ*wssE* (cellulose mutant)- negative control of biofilm formation (Arrebola *et al.*, 2015)-, PssUMAF0291, PssUMAF3028, PssUMAF2801, PssUMAF2600, PssUMAF0273 and PssUMAF0297 strains at 15, 20, 25 and 30 ºC.

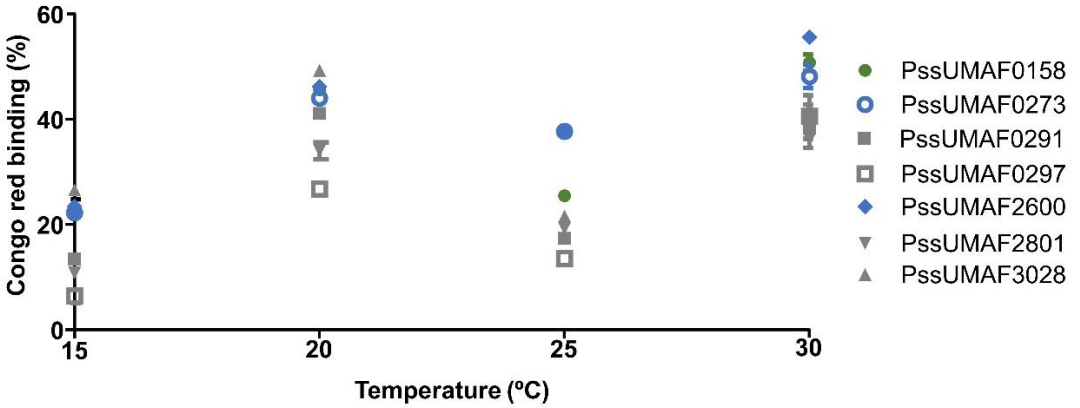

Figure 6.C2. Pellicle CR binding assay of the selected Pss strains at different temperatures. The results show the percentage of CR bound to the pellicles at 15, 20, 25 and 30ºC. The PssUMAF0158, PssUMAF0273, PssUMAF0291, PssUMAF0297, PssUMAF2600, PssUMAF2801 and PssUMAF3028 strains were tested. Three replicates and three independent experiments were performed.

Table 2.C2. Statistical analysis using one-way ANOVA with the Bonferroni correction test performed on Figure 6.C2 dataset. Different letters represent statistically significant differences among strains at each temperature.

Temperature (ºC)							
15		20		25		30	
Strains		Strains		Strains		Strains	
PssUMAF0158	a	PssUMAF0158	a,b	PssUMAF0158	b	PssUMAF0158	a
PssUMAF0273	a	PssUMAF0273	a,b	PssUMAF0273	a	PssUMAF0273	a
PssUMAF0291	b	PssUMAF0291	b	PssUMAF0291	d	PssUMAF0291	b
PssUMAF0297	c	PssUMAF0297	d	PssUMAF0297	e	PssUMAF0297	b
PssUMAF2600	a	PssUMAF2600	a,b	PssUMAF2600	a	PssUMAF2600	a
PssUMAF2801	b	PssUMAF2801	c	PssUMAF2801	c,d	PssUMAF2801	b
PssUMAF3028	a	PssUMAF3028	a	PssUMAF3028	c	PssUMAF3028	b

White light increases EPS production in *P. syringae* pv. syringae strains. White light contains a profile of distinct wavelengths across the visible spectrum (Santamaría-Hernando *et al.*, 2018). To assess whether white light influences biofilm formation in Pss, the percentage of CR bound to the pellicles formed under white light was compared to that retained under darkness after 24 h of incubation at 25ºC (Figure 7A.C2). The results showed higher EPS production in all the strains selected under white light, regardless of whether they belonged to G1, G2 or G3. To better illustrate this increase, the percentage of CR retained in the biofilms under

white light was compared to that retained under darkness (Figure 7B.C2). The results showed heterogeneity in the EPS increase among strains, but CR binding was always higher during white light exposure.

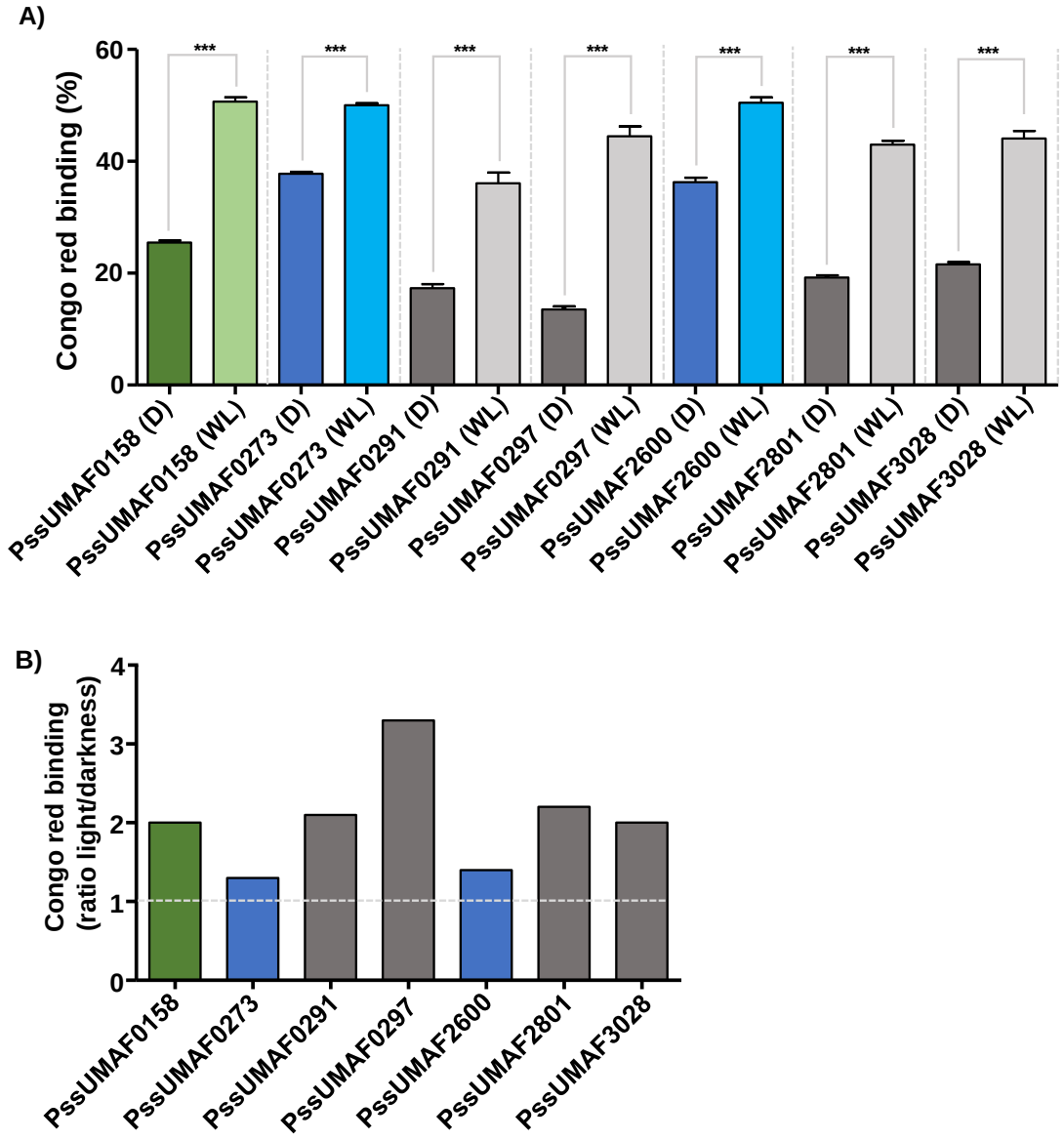

Figure 7.C2. EPS production under white light/darkness. A) CR binding in the biofilms formed under white light (WL; light colors) or darkness (D; dark colors) after 24 h at 25ºC; B) Ratio of EPS production white light (WL; light colors)/darkness (D; dark colors) after 24 h at 25ºC. The percentage of CR bound to the pellicle at 25ºC under white light was normalized to that bound in darkness. The PssUMAF0158, PssUMAF0291, PssUMAF3028, PssUMAF2600, PssUMAF0273, PssUMAF2801 and PssUMAF0297 strains were tested. Three replicates and three independent experiments were performed. Statistical significance was assessed by two-tailed Mann–Whitney test (*p<0.05, **p<0.01, ***p<0.001). Error bars correspond to the standard error of the mean (s.e.m.).

Lower levels of EPS production could be associated with a higher virulence of *P. syringae* pv. syringae. To assess whether exopolysaccharide synthesis has an impact in the virulence of other Pss strains isolated from mango trees different from PssUMAF0158, the virulence of PssUMAF0291 (lower EPS producer) and PssUMAF2600 (higher EPS producer) strains were assessed in tomato leaflets (Figure 8A,B.C2). The results showed that PssUMAF0291 virulence was similar to that of PssUMAF0158 *ΔwssE* cellulose mutant, being both higher than that of the PssUMAF0158 wild-type strain (Figure 8A,B.C2). The higher virulence observed in PssUMAF0291 was not due to an increase in its ability to growth on tomato leaflets (Figure 8C.C2). Otherwise, the PssUMAF2600 strain was as virulent as the PssUMAF0158 wild-type strain (Figure 8A,B.C2). The PssUMAF0158, PssUMAF0291 and PssUMAF2600 strains did not show significant differences in the attachment to mango leaves under the analysed conditions (Figure 9.C2).

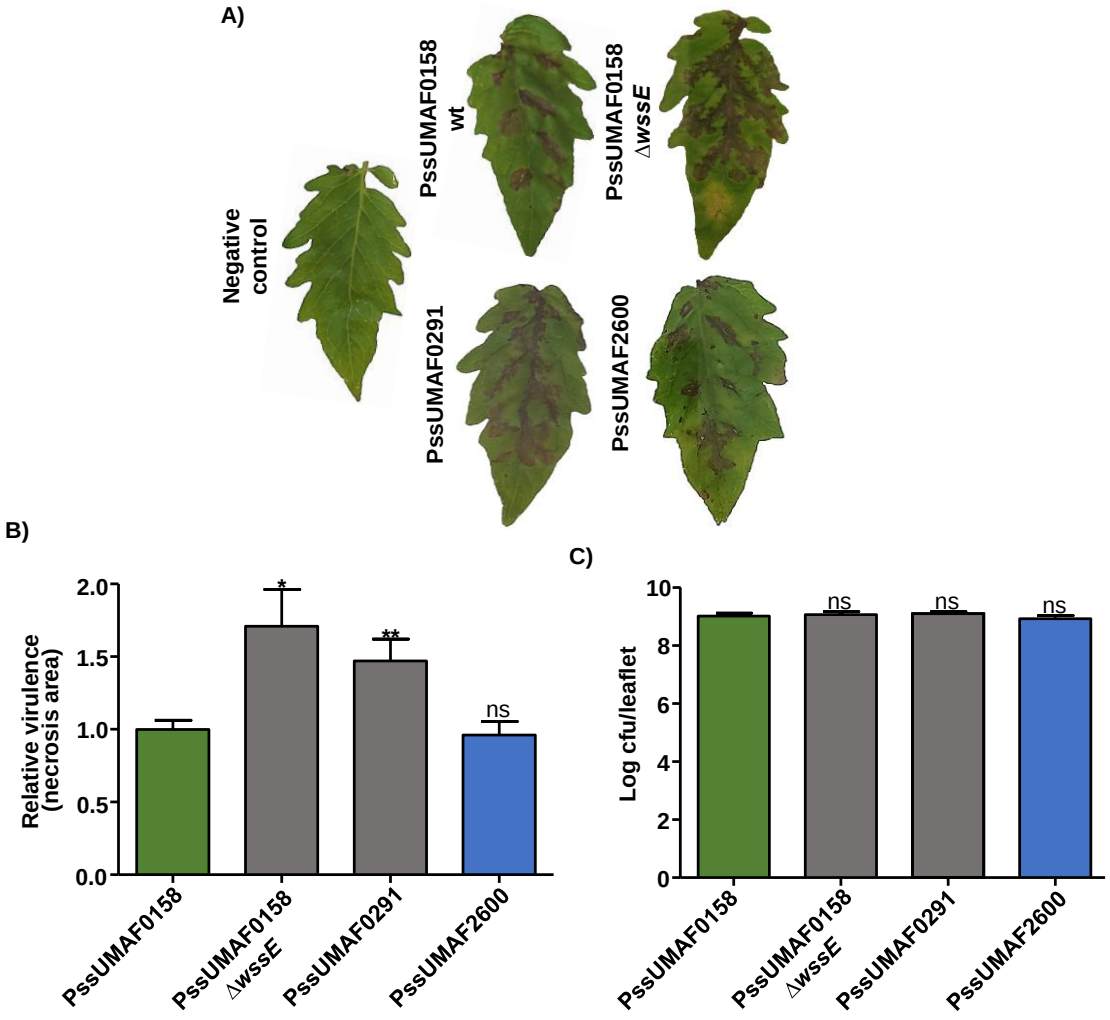

Figure 8.C2. Virulence of Pss strains with different EPS production levels. A) Representative symptoms developed on tomato leaflets at 6 days postinoculation; B) Relative virulence of PssUMAF0158 wild-type, PssUMAF0158 Δ*wssE* (cellulose mutant), PssUMAF0291 (lower EPS producer than PssUMAF0158 wild-type) and PssUMAF2600 (higher EPS producer than PssUMAF0158 wild-type) measured by lesion size. Statistical significance was assessed by two-tailed Mann–Whitney test (*p<0.05, **p<0.01, ***p<0.001). The PssUMAF0158 cellulose mutant was included as a positive control of virulence (Arrebola *et al.*, 2015). Three leaflets per experiment and three independent experiments were performed; C) Bacterial counts (log CFU/ml) after 6 days of inoculation.

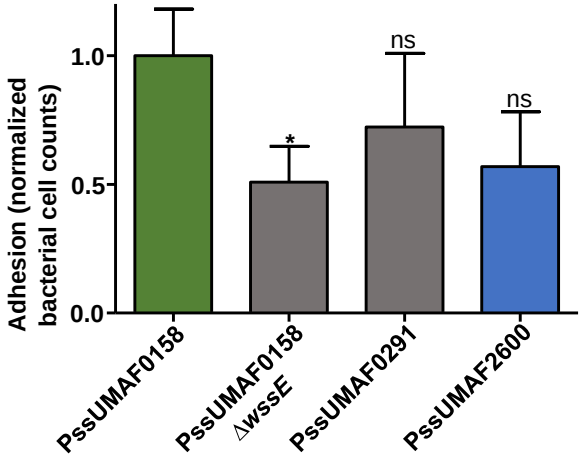

Figure 9.C2. Adhesion to mango leaves of Pss strains with different EPS production levels. Adhesion to mango leaves was assessed at 4 h postinoculation. The cellulose mutant was included as a negative control of adhesion (Arrebola *et al.*, 2015). The results are represented as normalized bacterial cell counts recovered from mango leaves with respect to the wild-type strain counts. The PssUMAF0158, PssUMAF0158 cellulose mutant (*ΔwssE*), PssUMAF0291 and PssUMAF2600 strains were tested. Statistical significance was assessed by two-tailed Mann–Whitney test (*p<0.05). Error bars correspond to the standard error of the mean (s.e.m.).

4. Discussion

The transition of *P. syringae* pv. syringae (Pss) between epiphytic and pathogenic stages is highly influenced by weather conditions and biofilm formation (Cazorla *et al.,* 1998; Arrebola *et al.,* 2015; Heredia-Ponce *et al.,* 2020a). The highest disease severity of Pss in mango trees was associated with cool and wet periods (Cazorla *et al.,* 1998). Former studies performed on PssUMAF0158 revealed that exopolysaccharide production plays key roles in the ecology of Pss (Arrebola *et al.,* 2015; Heredia-Ponce *et al.,* 2020a). The inability to produce some exopolysaccharides, such as cellulose and Psl-like exopolysaccharides, increases PssUMAF0158 virulence (Arrebola *et al.,* 2015; Heredia-Ponce *et al.,* 2020a). All these observations led to propose a life cycle for Pss on mango trees, in which biofilm formation, through exopolysaccharide production, would be predominant during the epiphytic stage (spring/summer), when bacteria are more exposed to the external environment and protection become crucial for survival (Gutiérrez-Barranquero *et al.,* 2019). During the pathogenic stage (autumn/winter), Pss reduces biofilm formation and increases the production of virulence factors that enhance the infection process (Gutiérrez-Barranquero *et al.,* 2019).

The Pss strains included in this study have shown heterogeneity in exopolysaccharide production (Figures 1.C2 and 2.C2). The mucoid phenotype of Pss could be due to the alginate polysaccharide, as mucoid phenotypes have been formerly associated with alginate production in *P. syringae* (Kidambi *et al.,* 1995). All the Pss strains included in this study bound CR in TPG agar plates (Figure 1B.C2), which is indicative of exopolysaccharide production (Zevenhuizen *et al.,* 1986; Wood *et al.,* 1988). Furthermore, although at different levels, all the Pss strains bound CR in their pellicles (Figure 2.C2), which could be mainly due to cellulose synthesis, as previously reported (Heredia-Ponce *et al.,* 2020a). The evolutionary history of the Pss strains included in this study based on the housekeeping genes (Figure 3.C2) showed some differences to that of the alginate, Psl-like and cellulose clusters (Figure 4.C2). Noticeable, the incongruities between the phylogeny based on the housekeeping genes (Figure 3.C2) to that based on the cellulose cluster (Figure 4C.C2) correlates with the phenotypes regarding cellulose production within biofilms (Figure 2.C2), which suggests that the evolution could have selected different Pss bacterial subpopulations with different levels of cellulose

production that could be important for their association with the mango and other host plants. In fact, cellulose has proven to be important for biofilm formation, adhesion to mango leaves and its production has an impact in the virulence of the PssUMAF0158 strain (Arrebola *et al.*, 2015; Heredia-Ponce *et al.*, 2020a).

There is a connection among transition through epiphytic and pathogenic stages, different environmental conditions and biofilm formation through exopolysaccharide production (Cazorla *et al.*, 1998; Arrebola *et al.*, 2015; Gutiérrez-Barranquero *et al.*, 2019; Heredia-Ponce *et al.*, 2020a). Therefore, the ability to produce EPS at different temperatures was assessed in seven Pss strains with different EPS production levels. The results showed an oscillating pattern of EPS production in their biofilms which was consistent, although at different levels, in all the strains tested (Figure 6.C2). In contrast, *P. aeruginosa* PAO1 and PA14 strains recognize different temperature ranges for biofilm formation (Kim *et al.*, 2020). The highest point of EPS production that correlates with the most intricate biofilm structures formed in microwell plates was 20ºC (Figure 5.C2 and 6.C2). This has been recently described in *P. aeruginosa*, in which the most intricate biofilms architectures formed in flow-cell chambers and highest EPS production were found at 20ºC (Kim *et al.*, 2020). In contrast to what has been described in *P. aeruginosa* (Kim *et al.*, 2020), the EPS production levels detected at 30ºC completely restored those at 20ºC (Figure 6.C2).

As an epiphyte, *P. syringae* requires adaptation mechanisms to cope with light (Vorholt *et al.*, 2012). This study has demonstrated that white light increases EPS synthesis in the Pss biofilms (Figure 7A.C2). This result goes in line with previous observations that reported up-regulation of polysaccharide synthesis genes, particularly belonging to the alginate cluster, in *P. syringae* pv. tomato DC3000 after white light exposure (Río-Álvarez *et al.*, 2014; Santamaría-Hernando *et al.*, 2018). The phyllosphere is an extremely unstable habitat where conditions can change abruptly in short distance/time ranges (Hirano & Upper, 2000). The fact that some strains can increase EPS synthesis more than others during white light exposure (Figure 7B.C2) and increase or decrease exopolysaccharide production within biofilms at different levels depending on the temperature (Figure 6.C2) suggests that when different Pss subpopulations interact over the plant surfaces and changes in

light and temperatures occur, some of these strains could cope better with these changes and take over regarding biofilm formation to favor community survival.

The PssUMAF0291 strain is a lower EPS producer than PssUMAF0158 and was more virulent on tomato leaflets than PssUMAF0158 (Figure 8.C2). This result correlates with previous studies, in which lower EPS derivatives of the PssUMAF0158 strain were more virulent than the wild-type (Arrebola *et al.*, 2015; Heredia-Ponce *et al.*, 2020a). The PssUMAF2600 strain produced higher levels of EPS than PssUMAF0158 and was as virulent as PssUMAF0158 (Figure 8.C2). Altogether, these results suggest that lower levels of EPS production could be associated with more virulent Pss strains. Noticeable, PssUMAF0291, but not PssUMAF0158, has been recently reported to contain a large Tn7-like transposon that confers hyper-resistance to copper (Aprile *et al.*, 2021). The higher virulence and hyper copper-resistance phenotype of PssUMAF0291 compared to the PssUMAF0158 strain could be a higher threat for mango crops. The differences in EPS production levels among PssUMAF0158, PssUMAF0291 and PssUMAF2600 strains did not have an impact in the adhesion to mango leaves (Figure 9.C2). This suggests that the amount of EPS produced by PssUMAF0291 could be enough to attach to the mango leaf surfaces as the PssUMAF0158 strain. Differences in adhesion between PssUMAF0158 and PssUMAF2600 were not found, which correlates with previous results in which cellulose overexpression in the PssUMAF0158 strain did not increase its ability to attach to mango leaves compared to the wild-type strain (Arrebola *et al.*, 2015).

In summary, the results obtained in this study show an interconnexion between environmental factors and biofilm formation, and between biofilm formation and the ecology of Pss strains. It has been described an oscillatory pattern of EPS production within biofilms depending on temperature and an increase of EPS production under white light exposure in Pss. Furthermore, lower EPS production seems to be associated with more virulent Pss strains, although more strains should be tested to obtain solid conclusions in this topic since disease severity is a multifactorial process that is mainly determined by the presence and expression levels of virulence factors and, as in all branches of biology, there could be exceptions.

CHAPTER 3

Role of extracellular matrix components in the formation of biofilms and their contribution to the biocontrol activity of *Pseudomonas chlororaphis* PCL1606

The results included in this chapter have been published:

Zaira Heredia-Ponce, José Antonio Gutiérrez-Barranquero, Gabriela Purtschert-Montenegro, Leo Eberl, Antonio de Vicente & Francisco M. Cazorla. Role of extracellular matrix components in the formation of biofilms and their contribution to the biocontrol activity of *Pseudomonas chlororaphis* PCL1606; ***Environmental Microbiology*** (2020)

1. Summary

Pseudomonas chlororaphis PCL1606 (PcPCL1606) displays plant-colonizing features and exhibits antagonistic traits against soil-borne phytopathogenic fungi. Biofilm formation could be relevant for the PcPCL1606 lifestyle, and in this study the role of some putative extracellular matrix components (EMC; Fap-like fibre, alginate and Psl-like polysaccharides) in the biofilm architecture and biocontrol activity of this bacterium were determined. EMC such as the Fap-like fibre and alginate polysaccharide play secondary roles in biofilm formation in PcPCL1606, because they are not fundamental to its biofilm architecture in flow-cell chamber, but synergistically they have shown to favour bacterial competition during biofilm formation. Conversely, studies on Psl-like polysaccharide have revealed that it may contain mannose, and that it is strongly involved in the PcPCL1606 biofilm architecture and niche competition. Furthermore, the Fap-like fibre and Psl-like exopolysaccharide play roles in early surface attachment and contribute to biocontrol activity against the white root rot disease caused by *Rosellinia necatrix* in avocado plants. These results constitute the first report regarding the study of the extracellular matrix of the PcPCL1606 strain and highlight the importance of a putative Fap-like fibre and Psl-like exopolysaccharide produced by PcPCL1606 in the biofilm formation process and interactions with the host plant root.

2. Introduction

Pseudomonas chlororaphis is a common inhabitant of the root environment that belongs to the *Pseudomonas fluorescens* complex (Garrido-Sanz *et al.,* 2017), one of the most diverse bacterial groups within the *Pseudomonas* genus. *P. chlororaphis* typically possesses plant-colonizing activities and exhibits antagonistic traits against soil-borne fungal pathogens (Arrebola *et al.,* 2019). In particular, the *P. chlororaphis* PCL1606 strain (PcPCL1606), isolated from the avocado rhizosphere, has protective features against the soil-borne phytopathogenic fungi *Rosellinia necatrix* and *Fusarium oxysporum*, which produce white root rot disease in avocado and foot and root rot in tomato, respectively (Cazorla *et al.,* 2006; González-Sanchez *et al,.* 2010; Calderón *et al.,* 2015). PcPCL1606 biocontrol activity is mediated by the action of antimicrobial compounds such as proteases and lipases, but mainly production of the compound 2-hexyl 5-propyl resorcinol (HPR), as a direct correlation between the ability to produce this metabolite and a strong inhibition activity against *R. necatrix* and *F. oxysporum* have been observed (Cazorla *et al.,* 2006; Calderón *et al.,* 2013).

The antifungal compound HPR is also involved in the multitrophic interaction avocado root-*R. necatrix*-PcPCL1606 (Calderón *et al.,* 2013, 2014), as well as in biofilm formation and root colonization (Calderón *et al.,* 2014, 2019). Biofilms are accretions of matrix-enclosed microorganisms that adhere to surfaces of biological or non-biological nature. Rhizosphere colonization is favored by the production of an extracellular matrix (Lasík *et al.,* 1989; Matthysse *et al.,* 1998; Lugtenberg *et al.,* 2001; Danhorn & Fuqua *et al.,* 2007; De Weert & Bloemberg, 2007), but the role that PcPCL1606 extracellular matrix components could play in biofilm formation and the lifestyle of this bacterium remain unknown. The formation of biofilms is a 3-stage process that includes the following steps: 1) attachment to a surface, 2) aggregation of cells, growth and maturation and 3) dispersion (Hall-Stoodley *et al.,* 2004). The first stage consists of adhesion to a surface, and proteinaceous structures such as bacterial adhesins and appendages are fundamental actors in this process. Regarding the protein component of the biofilm matrix of *Pseudomonas*, amyloid-like structures have been gaining importance during the last decade (Dueholm *et al.,* 2010, 2013a, b; Taglialegna *et al.,* 2016). In particular, Fap fimbriae could have environmental relevance due to their potential role in plant root colonization (Dueholm *et al.,* 2013b; Rouse *et al.,* 2018). Exopolysaccharides are the main matrix

components necessary for cell aggregation and biofilm maturation. In general, *Pseudomonas* spp. produces several polysaccharide biofilm matrix molecules, including alginate, levan, cellulose and Psl polysaccharide (Fuchs *et al.*, 1956; Conti *et al.*, 1994; Bianciotto *et al.*, 2001; Spiers *et al.*, 2003, 2005; Friedman & Kolter, 2004; Jackson *et al.*, 2004; Matsukawa & Greenberg, 2004). Alginate is composed of β-1,4 linked monomers of L-glucuronic and D-mannuronic acids (Evans & Linker, 1973), and although it is not fundamental for the constitution of biofilms in *Pseudomonas aeruginosa* and *Pseudomonas syringae* (Wozniak *et al.*, 2003; Laue *et al.*, 2006; McIntyre-Smith *et al.*, 2010; Heredia-Ponce *et al.*, 2020a), its participation in protection against stressors and biofilm structure have been proven in these species (Schnider-Keel *et al.*, 2001; Hentzer *et al.*, 2001; Pier *et al.*, 2001; Leid *et al.*, 2005; Heredia-Ponce *et al.*, 2020a). Levan polysaccharide, a polymer of β-2,6 linked fructose, has been mainly studied in *P. syringae*, where the involvement in biofilm architecture does not seem to be relevant (Laue *et al.*, 2006). Rather, levan accumulation in cell free areas of biofilms suggests a role as a storage molecule (Laue *et al.*, 2006). Cellulose is a glucose polymer with β-1,4 glycosidic linkages, which is considered to be an important biofilm matrix molecule in many environmental pseudomonads (Spiers *et al.*, 2002, 2003, 2005; Mann & Wozniak *et al.*, 2012). Although several biosynthesis and regulation mechanisms have been described for bacterial cellulose, a common role of this component is to facilitate the establishment of efficient host-bacteria interactions (Augimeri *et al.*, 2015). The described Psl polysaccharide, composed of D-mannose, D-glucose and L-rhamnose (Friedman & Kolter, 2004; Jackson *et al.*, 2004; Matsukawa & Greenberg, 2004; Byrd *et al.*, 2009), has been mainly studied in *P. aeruginosa* (Ma *et al.*, 2009; Zhao *et al.*, 2013; Wang *et al.*, 2013, 2014; Yang *et al.*, 2018). Recently, its involvement in the biofilm architecture, virulence and motility have also been described in the plant-associated bacterium *P. syringae* pv. syringae (Heredia-Ponce *et al.*, 2020a). Although the presence of the *psl*-like gene cluster has been reported in some environmentally relevant pseudomonads (Records & Gross, 2010; Mann & Wozniak *et al.*, 2012), including the biocontrol agent *P. fluorescens* Pf5, the biological participation of this polysaccharide in beneficial plant-bacteria interactions remains undetermined.

In this study, we identified a genomic region that putatively encodes a Fap-like amyloid fibre and two genomic regions that putatively encode alginate and Psl-like exopolysaccharides in the PcPCL1606 strain. Since biofilm formation could play a relevant role in the PcPCL1606 lifestyle, research regarding these biofilm components is explored in this work. Thus, the main aim of this work was to study the potential involvement of the Fap-like, alginate and Psl-like-encoding regions in biofilm formation and the lifestyle of PcPCL1606 during its interactions with the host plant root.

3. Results

Bioinformatics analysis of the *P. chlororaphis* PCL1606 genome revealed the presence of gene clusters encoding a putative Fap fibre, an alginate and Psl-like exopolysaccharides. The presence of Fap-like-, alginate- and Psl-like encoding clusters has never been assessed in PcPCL1606 strain. An *in-silico* analysis was performed to identify and characterize the genomic regions that might encode these components in PcPCL1606. Using the *P. aeruginosa* PAO1 (PAO1) PA1951-PA1956 genomic region as a template, which encodes the Fap system, the PCL1606_RS15320-PCL1606_RS15345 genomic region of PcPCL1606 was found to show similarity (Table S10). These similarities were even higher when the *fap* clusters of the *P. fluorescens* UK4 strain (PfUK4), the first strain in which the *fap* operon was described (Dueholm *et al.,* 2010), and PcPCL1606 were compared (Figure 1.C3). The FapC protein constitutes the main protein of the fibre and contains three proteinic repeat motifs (R1-R3; Dueholm *et al.,* 2010). Clustal alignments were performed between each of the three proteinic repeat motifs (R1-R3) present in the FapC protein of PfUK4 and the putative FapC protein of the PcPCL1606 strain (Figure 2.C3). These alignments revealed high conservation patterns among the amino acids present in those regions (Figure 2.C3).

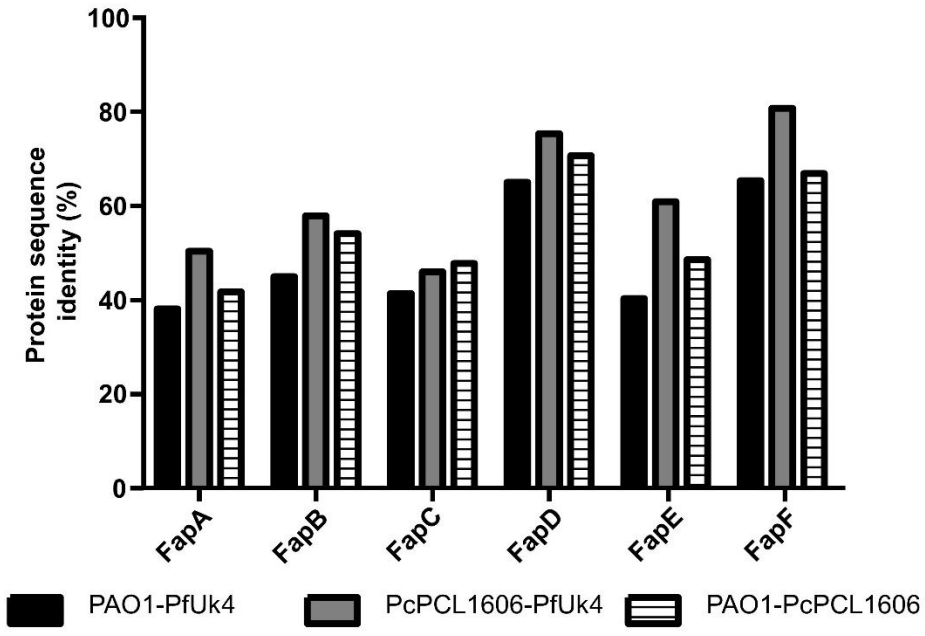

Figure 1.C3. Comparison of proteins encoded by the *fap* cluster between the *P. aeruginosa* PAO1, *P. fluorescens* UK4 and *P. chlororaphis* PCL1606 strains. Protein identity between the Fap proteins of the PAO1 and PfUK4 strains (black), of the PcPCL1606 and PfUK4 strains (grey) and of the PAO1 and PcPCL1606 strains (lined).

```
PfUK4_R1          NNAGANGSLSNSKGNLGANIAAGSGNQQDNAAAITSS
PcPCL1606_R1      NNAKADNSLNNSNGNMGANVAAGDGNQQDNAAALATA
                  *** *:.**.**:**:***:***.*********::::

PfUK4_R2          NNALLNNSANNSSGNVGVNVAAGQGNQQKNNLAIVTA
PcPCL1606_R2      NNATLNNAGNNGSGNIGINVTAGNFNQQKNNLAIAVS
                  *** ***:.**.***:*:**:**: *********..:

PfUK4_R3          NNAGLLNSANNASGNIGVNVAAGAGNQQSNTLTLGSG
PcPCL1606_R3      NNASLTNSLNGFSGNGGVNVSAGVGNQQSNSLSIAAG
                  ***.* ** *. *** ****:**.******:*::.:*
```

Figure 2.C3. Clustal alignment of the three repeat motifs (R1-R3) of the FapC protein of the PfUK4 and PcPCL1606 strains. The symbols used in the alignment are the following: "*" perfect alignment, ":" strong similarity, "." weak similarity and " " no similarity.

Regarding exopolysaccharide production clusters, the PFLU0300-PFLU0309 genomic region of the *P. fluorescens* SBW25 (SBW25) strain and the Psyrmg_RS20465–Psyrmg_RS20505 genomic region of the phytopathogen *P. syringae* pv. syringae UMAF0158 (PssUMAF0158) strain, which correspond to cellulose operon sequences, were not orthologous to any region located in the genome of the PcPCL1606 strain. The PCL1606_RS24735-PCL1606_RS24790 genomic region of PcPCL1606 was orthologous to the PA3540-PA3551 genomic region of PAO1, which encodes proteins of the alginate operon (Table S11). Additionally, the *psl* operon sequence of PAO1 allowed us to identify the orthologous PCL1606_RS04710-PCL1606_RS04765 genomic region in PcPCL1606 (Table S12). The gene that encodes the PslO protein is missing, and the PslM-like and PslN-like proteins (PCL1606_RS04265 and PCL1606_RS12970, respectively) seem to be encoded somewhere else in the chromosome outside the *psl*-like gene cluster (Table S12). Furthermore, the PAO1 PslL acyltransferase has not been associated with any protein encoded in the PcPCL1606 genome. However, the PCL1606_RS04715 gene, which is located within the *psl*-like gene cluster, encodes a putative acetyltransferase that might be performing a related function (Table S12). Most of the protein domains encoded within the *psl* cluster of PAO1 are conserved in PcPCL1606 (Tables S13 y S14).

Phylogenetic analysis revealed that the *psl*-like gene cluster has a random distribution within the *P. fluorescens* complex. To elucidate the phylogeny of the *psl*-like gene cluster within the *P. fluorescens* complex, a total of 50 strains belonging to the different phylogenetic groups included within the *P. fluorescens* complex and isolated from different habitats were selected and used for the analysis (Table S4). The *psl*-like gene cluster of PssUMAF0158 strain was also included in the analysis. The combined nucleotide sequences of the *gyrB* and *rpoD* housekeeping genes clearly supported the phylogenetic distribution in the different phylogroups included in the *P. fluorescens* complex (Garrido-Sanz *et al.*, 2016). The *psl*-like gene cluster was absent in the strains included in Garrido-Sanz *et al.*, (2017) as belonging to the *corrugata*, *jessenii* and *koreensis* phylogroups. Of all the strains included in the *mandelii* phylogroup, only *Pseudomonas* GM21 presented the *psl*-like gene cluster. Except for the *chlororaphis* phylogroup, in which the *psl*-like gene cluster was present in all the strains tested (Table S15), the rest of phylogroups contained strains that presented the cluster and strains that did not. The phylogenetic distribution of the strains selected based on the housekeeping genes (Figure 3A.C3) did not correlate with their phylogenetic distribution based on the *psl*-like gene cluster (Figure 3B.C3).

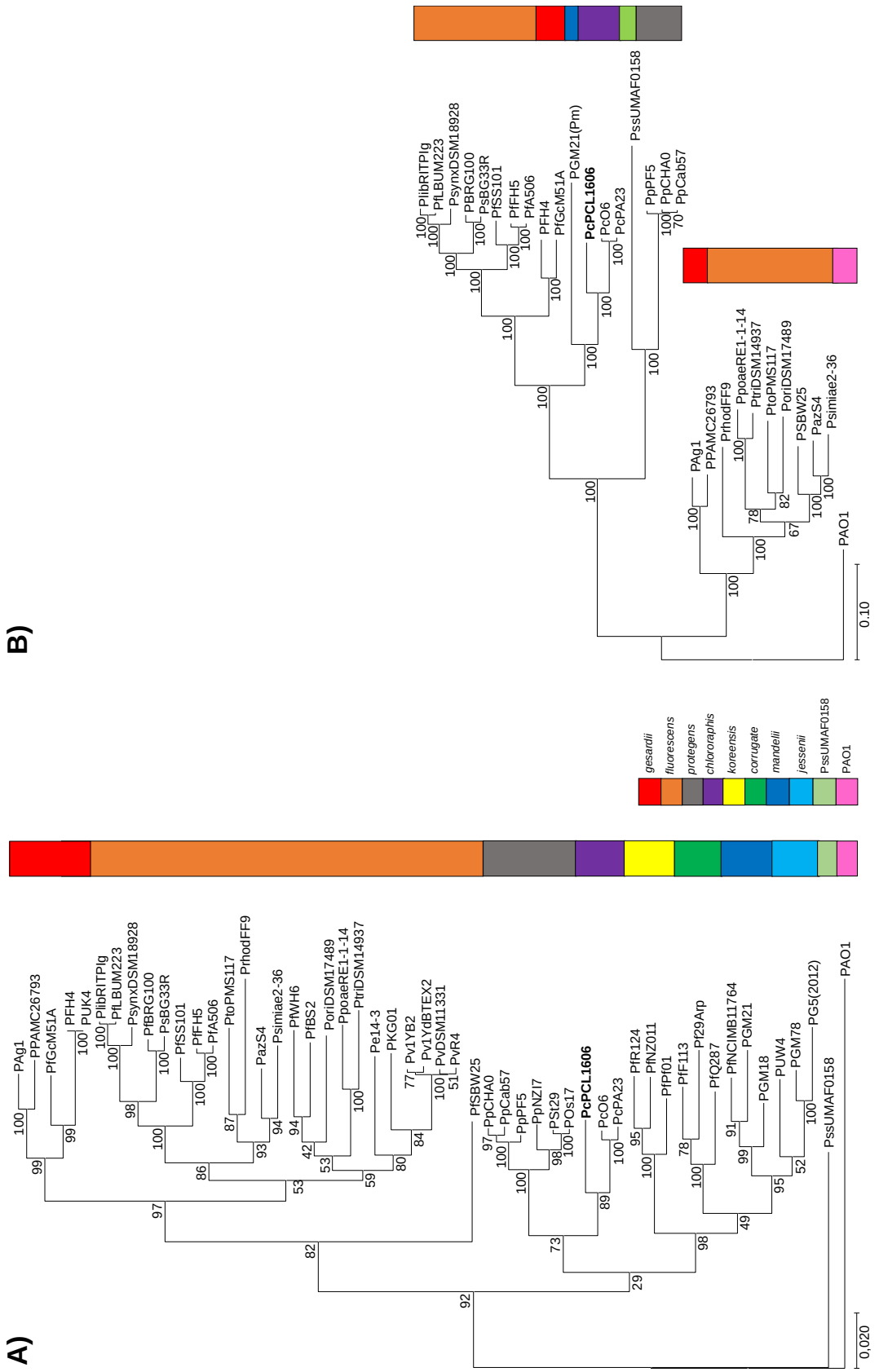

Figure 3.C3. Phylogeny of the *psl*-like genomic cluster into the *P. fluorescens* complex. A) Neighbour-joining tree generated with MEGAX using the combined sequences of the *gyrB* and *rpoD* housekeeping genes. The analysis included 50 strains belonging to the *fluorescens* (24 strains; orange), *gessardii* (5 strains; red), *mandelii* (3 strains; dark blue), *jessenii* (3 strains; light blue), *koreensis* (3 strains; yellow), *corrugata* (3 strains; dark green), *chlororaphis* (3 strains; purple) and *protegens* (6 strains; grey) phylogroups. The PcPCL1606 strain is highlighted in bold. The PssUMAF0158 strain (light green) was also included in the analysis. *P. aeruginosa* PAO1 was used as an outgroup (pink). B) Neighbour-joining tree generated with MEGAX using the *psl*-like cluster nucleotide sequence. The analysis included 27 strains belonging to the *fluorescens* (16 strains; orange), *gessardii* (4 strains; red), *mandelii* (1 strain; dark blue), *chlororaphis* (3 strains; purple) and *protegens* (3 strains; grey) phylogroups. The PcPCL1606 strain is highlighted in bold. PssUMAF0158 strain (light green) was also included in the analysis. *P. aeruginosa* PAO1 was used as outgroup (pink).

The putative Fap fibre and a Psl-like exopolysaccharide of *P. chlororaphis* PCL1606 are involved in the initial attachment to abiotic surfaces. To investigate the role of the extracellular matrix components under study at the initial stages of PcPCL1606 biofilm formation, short-term adhesion experiments to polystyrene microwell plates and Crystal violet staining were performed. The results showed that both the Fap-like fibre and the Psl-like exopolysaccharide, but not alginate, were involved in the initial surface attachment (Figure 4.C3). The impaired attachment values were not accumulative for the *ΔpslE* and *ΔfapBC* mutants, as we observed up to 60% reduction of the attachment levels for the single, double and triple mutants that included the *pslE* gene deletion and up to a 50% reduction for the single and double mutants that included the *fapBC* genes deletion. The complemented strains showed a restoration of the mutant phenotype to wild-type levels.

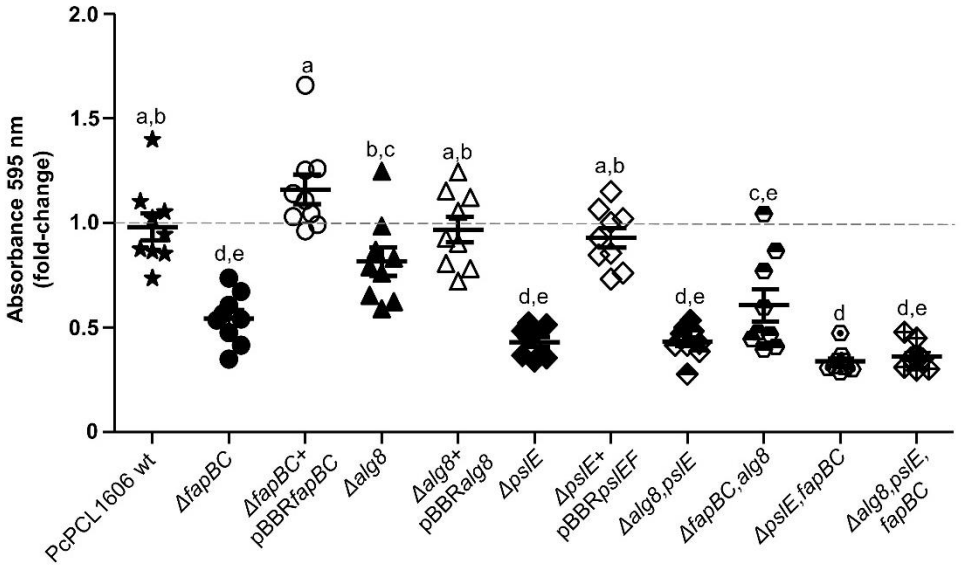

Figure 4.C3. Early bacterial attachment to abiotic surfaces. The initial attachment (4 h) to abiotic surfaces was assessed using a crystal violet (CV) staining assay. The results are displayed as the CV absorbance in the form of a fold-change relative to the wild-type average. The *P. chlororaphis* PCL1606 wild-type (PcPCL1606 wt), PcPCL1606 Fap-like fibre mutant (*ΔfapBC*), PcPCL1606 alginate mutant (*Δalg8*), PcPCL1606 Psl-like mutant (*ΔpslE*), PcPCL1606 *Δalg8,pslE* double mutant (*Δalg8,pslE*), PcPCL1606 *Δalg8,fapBC* double mutant (*ΔfapBC,alg8*), PcPCL1606 *ΔpslE,fapBC* double mutant (*ΔpslE,fapBC*), PcPCL1606 *Δalg8,pslE,fapBC* triple mutant (*Δalg8,pslE,fapBC*), Fap-like complemented strain (*ΔfapBC*+pBBR*fapBC*), alginate complemented strain (*Δalg8*+pBBR*alg8*) and Psl-like complemented strain (*ΔpslE*+pBBR*pslEF*) were tested. The complemented strains restored the mutant phenotypes to wild-type levels. The dotted line represents the wild-type average. Three technical replicates and three independent experiments were performed. Statistical analysis was performed using one-way ANOVA with the Bonferroni correction test. Different letters represent statistically significant differences. Error bars show the standard error of the mean (s.e.m.).

Production of the Psl-like exopolysaccharide is essential for biofilm formation in *P. chlororaphis* PCL1606. To investigate the roles of the Fap-like fibre, alginate and Psl-like exopolysaccharides in the biofilm architecture of the PcPCL1606 strain, flow-cell chamber experiments were performed and the biofilm architecture of the wild-type strain was compared to that of its derived extracellular matrix mutants (Figure 5.C3). Confocal laser scanning microscopy (CLSM) and IMARIS software reconstruction allowed us to display representative 3D images of the formed biofilms in the flow-cells. After 48 h, the *ΔfapBC* and *Δalg8* single mutants, as well as the *ΔfapBC,alg8* double mutant, formed biofilms that were undistinguishable from the wild-type strain (Figure 5A.C3). The biofilms formed by these strains were characterized by a multilayer of gathered cells that covered the flow-cell chamber

surface, and the presence of uncolonized space among the aggregating cells were barely noticeable (Figure 5A.C3). In contrast, the biofilms formed by the *ΔpslE* mutant consisted of a monolayer of loosely aggregated cells, where the amount of uncolonized space was more perceptible (Figure 5A.C3). The double and triple mutants that included the *pslE* gene deletion showed the same biofilm phenotype as the *ΔpslE* single mutant (Figure 5A.C3). The area and volume of the biofilms formed by the *ΔfapBC* and *Δalg8* single mutants, as well as the *ΔfapBC,alg8* double mutant, were not altered compared to the wild-type strain (Figure 5B,C.C3). All the mutants that contained the *pslE* gene deletion showed an impaired biofilm phenotype, which was characterized by a decrease in surface coverage and volume occupied (Figure 5B,C.C3).

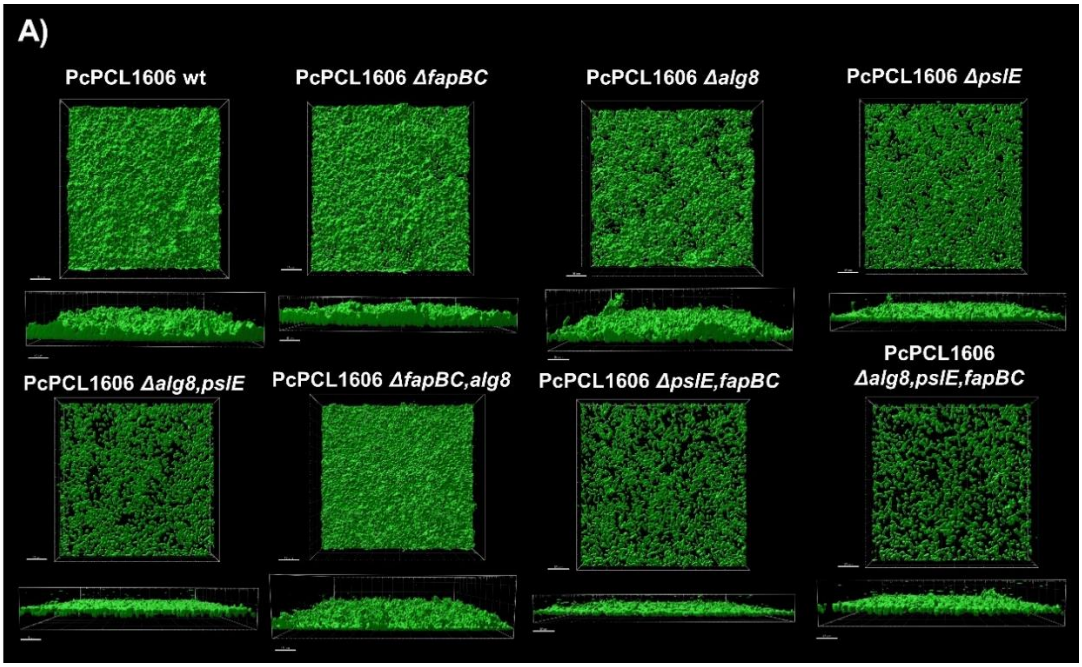

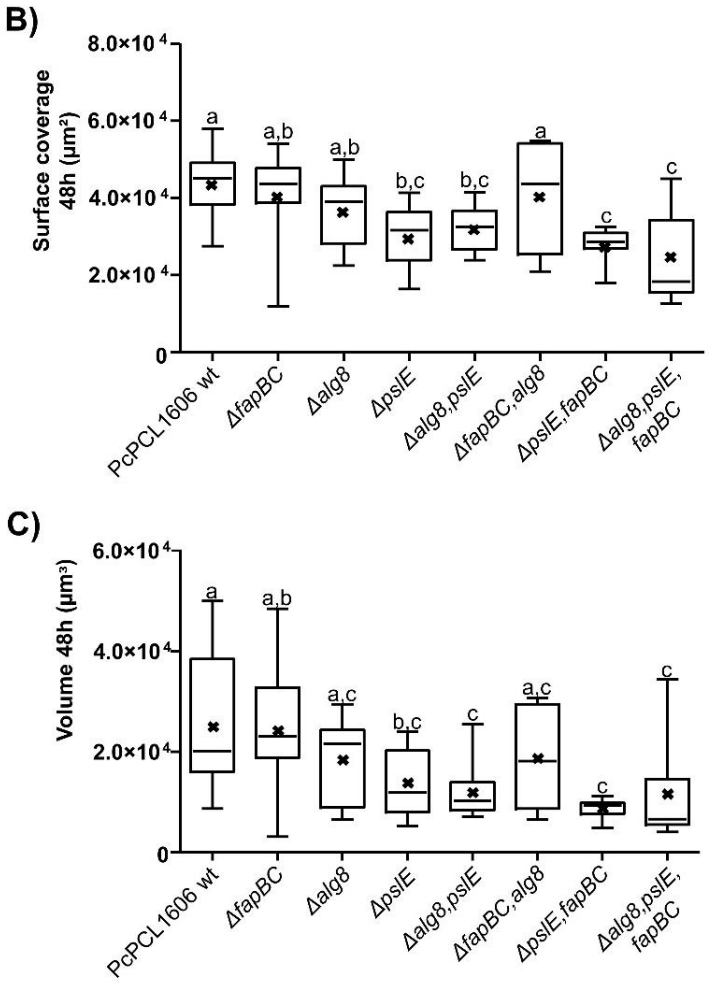

Figure 5.C3. Visualization of flow-cell chamber biofilms of the *P. chlororaphis* PCL1606 wild-type strain and its derived extracellular matrix mutants under CLSM. A) Representative 48 h 3D images of the biofilms formed by the GFP-tagged PcPCL1606 wild-type strain and its derived extracellular matrix mutants are shown. The obtained images were recorded and analysed with the Leica Application Suite (Mannheim, Germany) and the IMARIS software package (Bitplane, Switzerland). Scale bar: 20 µm. B) Box-and-Whisker plot showing the area in the field of view covered by 48 h biofilms of the GFP-tagged PcPCL1606 wild-type and GFP-tagged extracellular matrix mutants. The cross symbol (x) represents the arithmetic mean. C) Box-and-Whisker plot showing the volume in the field of view occupied by 48 h biofilms of the GFP-tagged PcPCL1606 wild-type and GFP-tagged extracellular matrix mutants. The cross symbol (x) represents the arithmetic mean. The *P. chlororaphis* PCL1606 wild-type (PcPCL1606 wt), PcPCL1606 Fap-like fibre mutant (*ΔfapBC*), PcPCL1606 alginate mutant (*Δalg8*), PcPCL1606 Psl-like mutant (*ΔpslE*), PcPCL1606 *Δalg8,pslE* double mutant (*Δalg8,pslE*), PcPCL1606 *Δalg8,fapBC* double mutant (*ΔfapBC,alg8*), PcPCL1606 *ΔpslE,fapBC* double mutant (*ΔpslE,fapBC*) and PcPCL1606 *Δalg8,pslE,fapBC* triple mutant (*Δalg8,pslE,fapBC*) were tested. Three technical replicates and a minimum of two independent experiments were performed with each strain. Statistical analysis was performed using one-way ANOVA with the Bonferroni correction test. Different letters represent statistically significant differences. Error bars show the distribution of the numerical data.

The Psl-like exopolysaccharide contains mannose and is allocated to the extracellular matrix of *P. chlororaphis* PCL1606. The Psl polysaccharide of the *P. aeruginosa* PAO1 strain is primarily composed of mannose (Ma *et al.*, 2007; Byrd *et al.*, 2009). Thus, to illustrate the presence of Psl-like exopolysaccharide in the extracellular matrix of PcPCL1606 biofilms, lectin staining of 48h-old biofilms formed by the wild-type strain and its derived Psl-like exopolysaccharide mutant was performed using FITC-labelled *Musa paradisiaca* lectin (BanLec), which binds to mannose residues (Figure 6.C3). The biofilm formed by the PcPCL1606 wild-type strain was able to bind lectin, while the *ΔpslE* mutant strain was not.

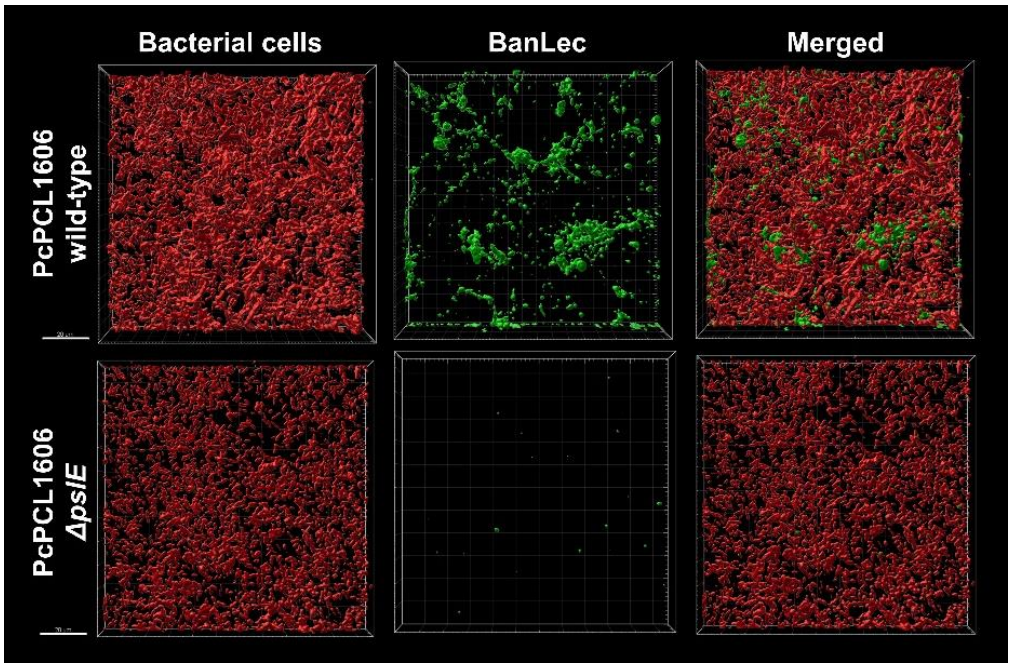

Figure 6.C3. *Musa paradisiaca* lectin (BanLec) staining of the *P. chlororaphis* PCL1606 extracellular matrix. Lectin staining of the extracellular matrix of the mCherry-tagged PcPCL1606 wild-type (red) and its mCherry-tagged Psl-like exopolysaccharide mutant (red) using FITC-tagged BanLec (green) was performed. The 48 h mCherry-tagged PcPCL1606 wild-type (PcPCL1606 wt) and mCherry-tagged PcPCL1606 Psl-like mutant (*ΔpslE*) biofilms were tested and observed under CLSM. Three technical replicates and three independent experiments were performed. Scale bar: 20 µm.

The putative Fap fibre, alginate and Psl-like exopolysaccharides provide a competitive advantage during biofilm formation in *P. chlororaphis* PCL1606. To investigate whether the extracellular matrix components under study participate in bacterial competition and niche colonization features displayed by PcPCL1606, competition experiments in flow-cell chambers were performed using mixed biofilms containing the mCherry-tagged wild-type bacterium and the corresponding GFP-tagged extracellular matrix mutant (Figure 7A.C3). The results were analysed as the percentage of colonized space (area and volume) occupied by the wild-type strain and each mutant (Figures 7B,C.C3). Competition assays between the *Δalg8* or *ΔfapBC* single mutants and the wild-type strain revealed equivalent fitness in niche competition due to the biofilm formed by the wild-type and each mutant occupied approximately 50% of the area and volume of the biofilm when both were coinoculated (Figure 7B,C.C3). However, the *Δalg8,fapBC* double mutant was significantly affected, as within the mixed biofilm, the wild-type strain occupied significantly higher area and volume than the *Δalg8,fapBC* strain. In addition, the *ΔpslE* single mutant, as well as the double and triple mutants containing the *pslE* gene deletion, were severely impaired in niche colonization compared with the wild-type strain (Figure 7A.C3). Thus, *pslE* gene deletion abrogated the ability of the PcPCL1606 strain to compete for biofilm formation with the wild-type equivalent, as the surface coverage and volume occupied by the mutants within the mixed biofilm were markedly reduced (Figure 7B,C.C3).

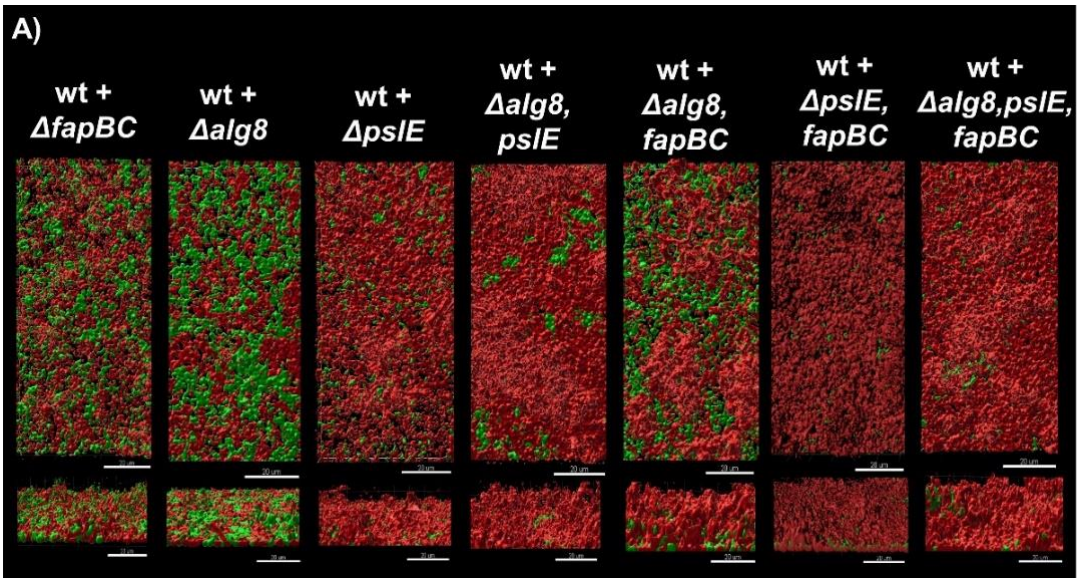

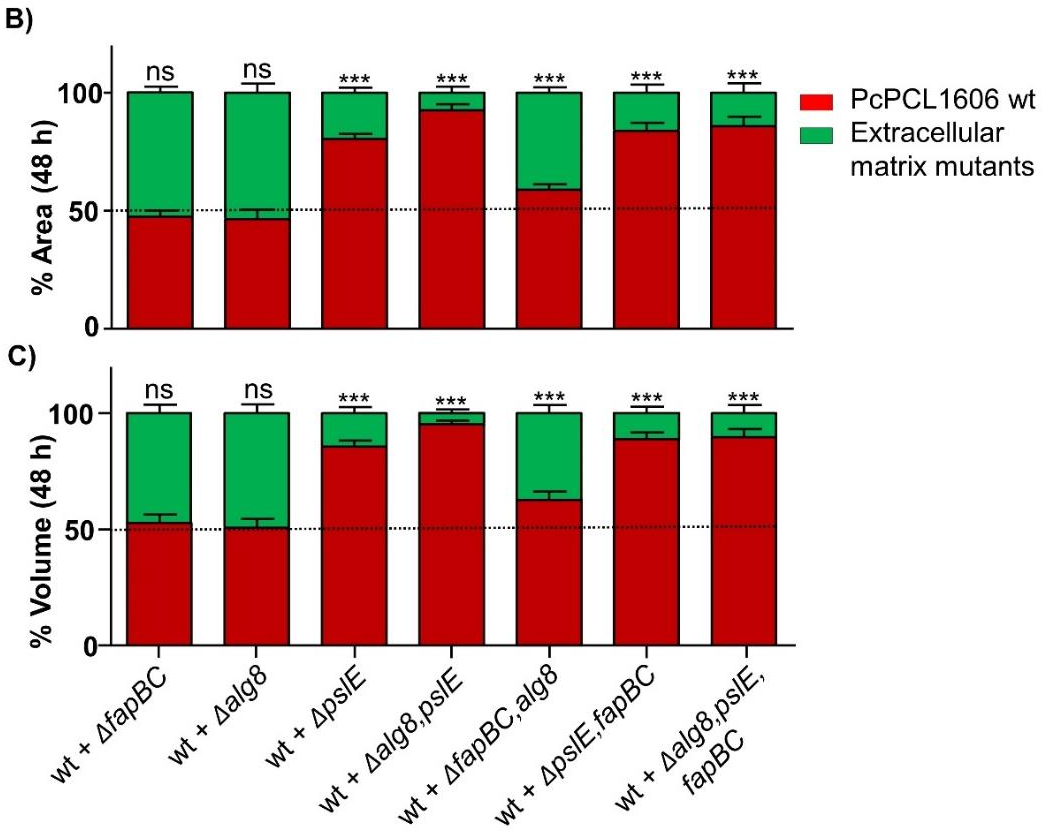

Figure 7.C3. Competition in mixed biofilms. The roles of the Fap-like fibre, alginate and Psl-like exopolysaccharides in competition during biofilm formation were analysed using the flow-cell system, and visualization was performed under CLSM. A) Representative 48 h 3D biofilm images of mixed biofilms including the mCherry-tagged PcPCL1606 wild-type and each GFP-tagged extracellular matrix mutant. B) Percentage of area occupied by the PcPCL1606 wild-type (red) and each extracellular matrix mutant (green) after 48 h of competition. C) Percentage of volume occupied by the PcPCL1606 wild-type (red) and each extracellular matrix mutant (green) after 48 h of competition. Both area and volume values were obtained with IMARIS software (Bitplane, Switzerland). The mCherry-tagged *P. chlororaphis* PCL1606 wild-type (PcPCL1606 wt) and GFP-tagged extracellular matrix PcPCL1606 Fap-like fibrils mutant (*ΔfapBC*), PcPCL1606 alginate mutant (*Δalg8*), PcPCL1606 Psl-like mutant (*ΔpslE*), PcPCL1606 *Δalg8,pslE* double mutant (*Δalg8,pslE*), PcPCL1606 *Δalg8,fapBC* double mutant (*ΔfapBC,alg8*), PcPCL1606 *ΔpslE,fapBC* double mutant (*ΔpslE,fapBC*) and PcPCL1606 *Δalg8,pslE,fapBC* triple mutant (*Δalg8,pslE,fapBC*) were tested. Three technical replicates, and a minimal of three independent experiments were performed. Statistical significance was assessed by two-tailed Mann–Whitney test (***p<0.001). Error bars correspond to the standard error of the mean (s.e.m.). Scale bar: 20 μm.

The Fap-like fibre and the Psl-like exopolysaccharide contribute to the biocontrol activity of the *P. chlororaphis* PCL1606 strain. Biocontrol assays against the avocado white root rot disease caused by *R. necatrix* were conducted on the *ΔpslE* and *ΔfapBC* single mutants because the putative Fap fibre and Psl-like exopolysaccharide showed the strongest effects in biofilm-related phenotypes (Figure 4.C3 and 5.C3). Aerial symptoms were evaluated using the previously described disease scale (Cazorla *et al.*, 2006). When no bacteria were applied to the avocado roots, the plants infected with *R. necatrix* reached a disease index value of approximately 76% on day 28 post-inoculation (Figure 8A.C3). However, when the plants were previously inoculated with the PcPCL1606 wild-type strain, the disease index reached approximately 48% on the same day (Figure 8A.C3). The plants that had been inoculated with the *ΔfapBC* and *ΔpslE* mutant strains prior to *R. necatrix* inoculation reached disease indices that were similar to those observed when the plants were not inoculated and subsequently higher than those observed when the plants were inoculated with the biocontrol wild-type strain (Figure 8A.C3). The area under the disease progress curve (AUDPC) showed that when the plants were inoculated with the PcPCL1606 wild-type strain, the disease severity was reduced by approximately 50% compared with those that were not previously inoculated (Figure 8B.C3). Instead, when the plants were inoculated with the *ΔfapBC* and *ΔpslE* mutants, disease development appeared similar to that observed in plants that were not previously inoculated (Figure 8B.C3). In summary, biocontrol activity was impaired in the *ΔfapBC* and *ΔpslE* mutants, and it was restored to wild-type levels in the *fapBC* and *pslEF* complemented strains (Figure 8B.C3). In addition, CLSM experiments revealed that the *ΔfapBC* and *ΔpslE* mutants showed alterations in their early attachment to avocado roots compared with the wild-type strain (Figure 8C.C3). The wild-type strain showed wider avocado root attachment than the *ΔfapBC* and *ΔpslE* mutants, with both individual and clumps of cells adhered to the avocado root cells. However, the *ΔfapBC* mutant showed less attachment of the root, the pattern of which was characterized by dispersed cell adhesion located among root cells. Finally, the *ΔpslE* mutant also showed less attachment to the roots, exhibiting an irregular pattern.

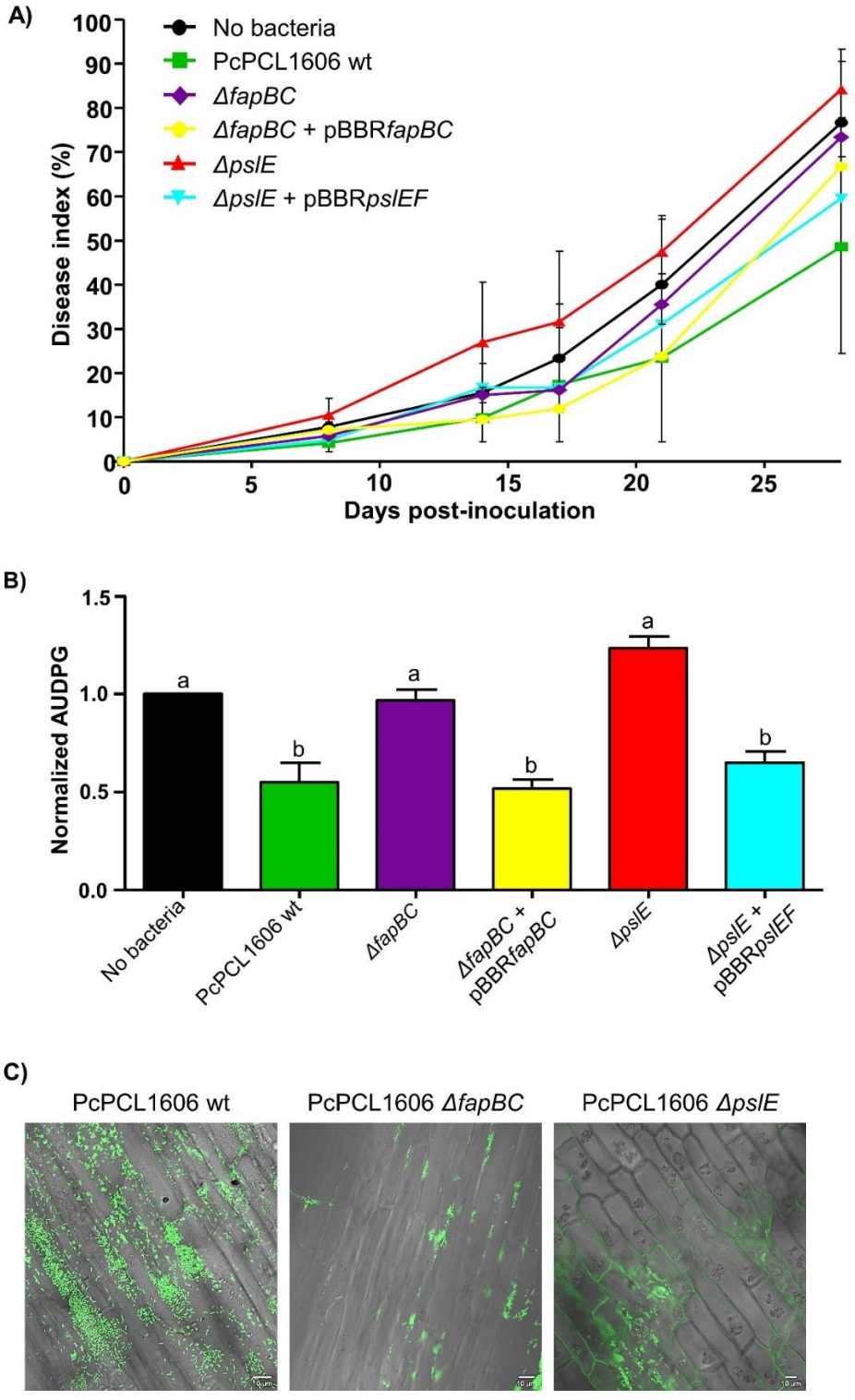

Figure 8.C3. Biocontrol of *R. necatrix*-induced white root rot on avocado plants. The PcPCL1606 wild-type strain and *ΔfapBC* and *ΔpslE* extracellular matrix mutants were tested in the *R. necatrix*-avocado test system. The roots of avocado seedlings were inoculated with each strain before being infected with *R. necatrix*. Plants that were not inoculated but were infected were included as negative controls for biocontrol activity. Aerial symptoms were recorded on a scale from 0 to 3 as described in Cazorla *et al.*, 2006. The data collected were used for calculation of the disease index (A) and area under the disease progress curve (B), as described in Cazorla *et al.*, 2006. A) Disease index

percentage. The graph shows the time course of the disease index of the avocado plants inoculated and infected with *R. necatrix* (green, red, purple, blue, yellow) and just infected with *R. necatrix* (● black). PcPCL1606 wild-type (■PcPCL1606 wt; green), PcPCL1606 Fap-like mutant strain (♦ *ΔfapBC*; purple), PcPCL1606 Psl-like mutant strain (▲*ΔpslE*; red), PcPCL1606 Fap-like mutant complemented strain (●*ΔfapBC* + pBBR*fapBC*; yellow) and PcPCL1606 Psl-like mutant complemented strain (▼*ΔpslE* + pBBR*pslEF*; blue) were tested. B) Area under the disease progress curve (AUDPC) calculated as described in Cazorla *et al.*, 2006. A minimum of seven plants per experiment and two independent experiments were performed. Statistical analysis was performed using one-way ANOVA with the Bonferroni correction test. Different letters represent statistically significant differences. Error bars show the standard error of the mean (s.e.m). C) Representative images of bacterial adherence to avocado roots 4 h postinoculation. The PcPCL1606 wild-type (PcPCL1606 wt), PcPCL1606 Fap-like mutant strain (*ΔfapBC*) and PcPCL1606 Psl-like mutant strain (*ΔpslE*) were tested. Three plants per experiment and strain, and three independent experiments were performed. Scale bar: 10 µm.

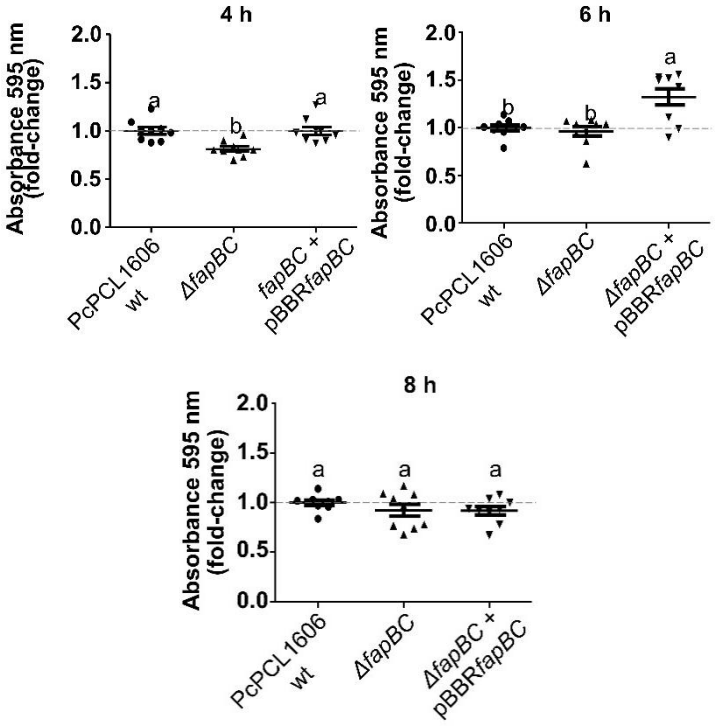

Figure 9.C3. Early bacterial attachment to abiotic surfaces. The attachment to abiotic surfaces after 4, 6 and 8 h post-inoculation was assessed using a crystal violet (CV) staining assay. The results are displayed as the CV absorbance in the form of a fold-change relative to the wild-type average. The *P. chlororaphis* PCL1606 wild-type (PcPCL1606 wt), PcPCL1606 Fap-like fibre mutant (*ΔfapBC*) and Fap-like complemented strain (*ΔfapBC*+pBBR*fapBC*), were tested. The complemented strain restored the mutant phenotype to wild-type levels. The dotted line represents the wild-type average. Three technical replicates, and three independent experiments were performed. Statistical analysis was performed using one-way ANOVA with the Bonferroni correction test. Different letters represent statistically significant differences. Error bars show the standard error of the mean (s.e.m).

4. Discussion

Biofilm formation plays an advantageous, if not essential, role in plant-bacteria interactions in many environmentally relevant *Pseudomonas* (Morris & Monier, 2003; Danhorn & Fuqua, 2007). Plant-associated bacteria can interact with the aerial parts, the rhizosphere or even the vascular system of the plant host using a great diversity of extracellular polymeric substances, including exopolysaccharides, proteins and DNA (Ramey *et al.,* 2004). Even though some *P. chlororaphis* strains have been reported as biofilm formers (Maddula *et al.* 2006; Poritsanos *et al.* 2006; Kim *et al.* 2014; Calderón *et al.,* 2019), little attention has been paid to the study of their extracellular matrix components. The *P. chlororaphis* PCL1606 strain (PcPCL1606) is a biofilm-forming bacterium with root-colonization and biocontrol activities (Cazorla *et al.,* 2006; Calderón *et al.* 2019; Arrebola *et al.,* 2019). The PcPCL1606 extracellular matrix could play a relevant role in these processes, and thereby, based on its lifestyle, the involvement of some putative extracellular matrix components in biofilm formation ability and biocontrol activity of this strain were explored in this work.

In this study, three genomic clusters were identified in the PcPCL1606 strain, which putatively encode a Fap amyloid-like fibre and two exopolysaccharides, alginate and Psl polysaccharide. These genomic regions might be involved in biofilm formation, as their relevance in other *Pseudomonas* has been previously revealed (Bianciotto *et al.,* 2001; Friedman & Kolter, 2004; Jackson *et al.,* 2004; Matsukawa & Greenberg, 2004; Franklin *et al.,* 2011; Dueholm *et al.,* 2013a, b; Marshall *et al.,* 2019). The genomic regions encoding the Fap fibre and alginate exopolysaccharide have been identified in several species of *Pseudomonas* (Conti *et al.,* 1994; Stapper *et al.,* 2004; Laue *et al.,* 2006; Rouse et *al.,* 2018; Marshall *et al.,* 2019). However, the genomic regions encoding a Psl-like exopolysaccharide have only been identified in *P. aeruginosa*, some strains of *P. syringae*, *P. mendocina* ymp and *P. fluorescens* Pf5 (Mann & Wozniak, 2012). Regardless, the biological role of Psl exopolysaccharide in beneficial plant-bacteria interactions is unknown to date. The results obtained in the phylogenetic analysis (Figure 3.C3) suggest that the distribution of the *psl*-like gene cluster within *P. fluorescens* complex is promiscuous. Additionally, the presence of the *psl*-like gene cluster in isolates of different sources (Table S4) further suggests that the ability to produce this

exopolysaccharide may not be habitat-dependent, but a more general feature of biofilm formation, and that this gene cluster could have been acquired by horizontal gene transfer. The *psl*-like cluster is widely distributed within the *chlororaphis* phylogroup (Table S15), which may explain why relevant roles in biofilm formation and related aspects have been observed in the PcPCL1606 strain in this study.

The initial stage in the biofilm formation process consists of attachment to a surface (Hall-Stoodley *et al.,* 2004). Proteinaceous structures, such as bacterial adhesins and appendages, play fundamental roles in this process (Berne *et al.,* 2015). Although exopolysaccharides were thought to be mainly required for later architectural development of the biofilms (Sutherland, 1999), implications in the initial attachment to the surfaces of roots have also been reported in several species (Wheatley & Poole, 2018). In agreement with previous studies (Colvin *et al.,* 2012; Berne *et al.,* 2015), the Fap-like fibre and Psl-like exopolysaccharide of the PcPCL1606 strain were found to be involved in the initial attachment to abiotic surfaces (Figure 4.C3). The finding that alginate did not play an important role in PcPCL1606 during initial surface attachment (Figure 4.C3) was also consistent with other studies performed in *P. aeruginosa*, in which this polysaccharide was not truly required for the early steps of biofilm formation (Wozniak *et al.,* 2003; McIntyre-Smith *et al.,* 2010).

Regarding later stages of biofilm development, the Psl-like exopolysaccharide was proven to be an essential component of the biofilm architecture of the PcPCL1606 strain (Figure 5.C3). This result was in line with previous studies, in which the Psl polysaccharide was reported to be important for adhesion and maintaining the biofilm structure post-attachment (Friedman & Kolter, 2004; Jackson *et al.,* 2004; Matsukawa & Greenberg, 2004; Ma *et al.,* 2006). After 48 h of incubation, the biofilm phenotype of the PcPCL1606 *ΔpslE* strain resembled that of the PAO1 Psl-like mutant (Jackson *et al.,* 2004; Ghafoor *et al.,* 2011), consisting of a monolayer of cells (Figure 5A,C.C3), which suggests that the Psl-like exopolysaccharide could be decisive for the constitution of the three-dimensional architecture of the PcPCL1606 biofilm. In *P. aeruginosa* PAO1, the most recent study determined that Psl polysaccharide is composed of a pentasaccharide subunit containing D-mannose, D-glucose and L-rhamnose, at approximate ratios of 3:1:1 (Byrd *et al.,* 2009). However, this result conflicts with previous reports, in which the presence of

galactose in the Psl structure was also reported (Ma *et al.*, 2007). In any case, mannose is described as the main monosaccharide of the polymer. BanLec staining of the Psl-like exopolysaccharide of the PcPCL1606 strain suggested that it also contained mannose (Figure 6.C3), which is in agreement with prior studies on *P. aeruginosa* and suggests that these polysaccharides might actually be similar in composition. The alginate mutants of *P. aeruginosa*, *P. syringae* and *P. fluorescens* retained the ability to form biofilms compared to their respective wild-types, but their biofilm architectures were different (Wozniak *et al.*, 2003; Stapper *et al.*, 2004; Laue *et al.*, 2006; Ghafoor *et al.*, 2011; Noirot-Gros *et al.*, 2019). However, no impairment in biofilm architecture was observed in the *Δalg8* mutant strain of PcPCL1606 (Figure 5.C3). The presence of the *fap* operon has been reported in several *Pseudomonas* species (Mann & Wozniak *et al.*, 2012; Dueholm *et al.*, 2013b), but its role in biofilm formation has been considered as secondary, because the PAO1 Fap mutant formed biofilms to the same extent as the wild-type strain (Dueholm *et al.*, 2013a). In line with the published data, and despite the differences observed in early adhesion in the *ΔfapBC* mutant (Figure 4.C3 and 9C.C3), similar surface coverage and volumes values of the biofilms formed by the PcPCL1606 wild-type strain and *ΔfapBC* mutant have been observed (Figure 7.C3), leading to a similar conclusion. Thus, similar to *P. aeruginosa* (Dueholm *et al.*, 2013a), the role of the PcPCL1606 Fap-like fibre seems to be more directed towards initial attachment of cells to surfaces, as the early adhesion deficiencies of the *ΔfapBC* mutant (4 h) were not observed at later time periods (6 and 8h; Figure 9.C3) and the developed biofilm architecture of the mutant was indistinguishable from that of the wild-type (Figure 5.C3).

The ability to produce Psl-like polysaccharide provided a selective advantage to synthesizing bacteria in competition for biofilm formation (Figure 7.C3). This result had been previously observed in *P. aeruginosa*, in which the *Δpsl* mutant of PAO1 strain could not be rescued by the parental strain when both were co-cultured (Jackson *et al.*, 2004; Irie *et al.*, 2016). Interestingly, these competition experiments suggest that Psl is acting as a private good in PcPCL1606, as it has been previously reported in *P. aeruginosa* (Irie *et al.*, 2016). Instead, the Fap-like fibre and the alginate exopolysaccharide were shown to play secondary roles in biofilm formation of the PcPCL1606 strain, as the biofilms formed by the mutant strains showed

surface coverage and volume values that were undistinguishable from those of the wild-type (Figure 5.C3), but together they contributed synergistically to biofilm architecture by providing colonization advantages during biofilm formation (Figure 7.C3). This result correlates with the impaired phenotype in early attachment observed in the *ΔfapBC,alg8* double mutant (Figure 4.C3). Cooperation between different extracellular matrix components is not uncommon, as some of them have been described to only function synergistically during biofilm formation (Saldaña *et al.,* 2009; Ostrowski *et al.,* 2011; Fong & Wildiz, 2015).

Colonization of the roots is one of the first steps in the establishment of beneficial plant-bacteria interactions (De Weert & Bloemberg, 2007). Since PcPCL1606 is a biocontrol agent of plant-fungal diseases, it was essential to ascertain the contribution of the Fap-like fibrils and the Psl-like exopolysaccharide, which showed the strongest effects in biofilm related phenotypes, in disease control. Both biofilm components were found to be relevant in white root rot disease suppression (Figures 8A,B.C3). The putative roles of Psl polysaccharide in the surface colonization of *P. aeruginosa* (Zhao *et al.,* 2013) and *P. syringae* (Heredia-Ponce *et al.,* 2020a), as well as the presence of a *psl*-like gene cluster in some pseudomonads that usually colonize the soil and roots of plants (Table S4), revealed the potential involvement of the PcPCL1606 Psl-like exopolysaccharide in root interaction. There is evidence suggesting that the Fap system could also play a role in root interaction (Dueholm *et al.,* 2013b; Rouse *et al.,* 2018). The obtained results revealed a clear influence of the Fap-like fibre and the Psl-like exopolysaccharide in PcPCL1606 biocontrol ability (Figures 8A,B.C3). Thus, the impairment in both initial abiotic and biotic surface attachment observed in the *ΔfapBC* and *ΔpslE* mutants (Figure 4.C3 and 8C.C3), as well as the contribution of the Psl-like exopolysaccharide to the PcPCL1606 overall biofilm architecture (Figures 5.C3 and 7.C3), could all indicate that inefficient root interaction by the mutants might lead to an impairment of disease suppression, probably by allowing a better access of the fungus to the plant root or by providing an ineffective delivery system of antifungal metabolites, as previously suggested (Chin-A-Woeng *et al.,* 2007). Thus, effective colonization of the rhizosphere appears as a prerequisite for the efficient disease control of PcPCL1606, in agreement with former studies performed in biocontrol agents (Bloemberg & Lugtenberg, 2001; Lugtenberg & Kamilova, 2009).

In conclusion, our work constitutes the first report regarding the presence of a *psl*-like gene cluster within the *P. chlororaphis* group, its role in biofilm formation and influence on the biocontrol lifestyle in the plant-beneficial bacterium PcPCL1606. Furthermore, the Fap-type system and alginate exopolysaccharide of PcPCL1606, although not fundamental for biofilm formation, seem to cooperatively contribute to biofilm formation in this bacterium by proving relevance during competitive colonization in biofilm formation experiments. Additionally, this is the first time that the role in early surface interactions and the biocontrol lifestyle has been demonstrated for a Fap-like fibre, in a manner similar to that of the Psl-like exopolysaccharide. These results contribute to a better understanding of the biofilm matrix of the PcPCL1606 biocontrol strain and its involvement in the multitrophic interactions that take place during the biological control of soil-borne plant pathogens.

GENERAL DISCUSSION

Biofilm formation has proven to be a very relevant trait in the ecology of the phytopathogen *P. syringae* pv. syringae UMAF0158 (PssUMAF0158) and the biocontrol agent *P. chlororaphis* PCL1606 (PcPCL1606) (Arrebola *et al.,* 2015, 2019; Calderón *et al.,* 2019). This observation was in agreement with previous studies performed in other plant-interacting bacteria, in which several extracellular matrix components that are important for biofilm formation are also involved in ecological traits such as colonization, adhesion, virulence, biocontrol or protection (Kidambi *et al.,* 1995; Yu *et al.,* 1999; Gal *et al.,* 2003; Morris & Monier, 2003; Chang *et al.,* 2007; Nielsen *et al.,* 2011; Nilsson *et al.,* 2011; Chen *et al.,* 2013; Pandin *et al.,* 2017). Therefore, the role of some extracellular matrix components, most of which were previously studied in *P. aeruginosa*, in the biofilm formation and bacterial ecology of PssUMAF0158 and PcPCL1606 were assessed in this dissertation.

Alginate polysaccharide does not play a critical role in the biofilm architecture of the PssUMAF0158 and PcPCL1606 strains, as the alginate mutants of both strains are slightly or not even impaired in their biofilm architectures, respectively, and they still retain the ability to form biofilms (Heredia-Ponce *et al.,* 2020a,b). Previous studies indicate that alginate is not a critical component for biofilm formation in some plant-associated *Pseudomonas*. Thus, the alginate mutants of the *P. syringae* PG4180 and *P. fluorescens* SBW25 strains, as that of the model strain *P. aeruginosa* PAO1, are slightly impaired in biofilm formation in flow-cell chambers compared to their wild-types but they still retain the ability to form biofilms (Laue et al., 2006; Ghafoor *et al.,* 2011; Noirot-Gros *et al.,* 2019). Other evidences indicate that the role of alginate could be more directed towards conferring protection against stressors, as it has been previously described in *P. syringae* and specially in *P. putida* (Kidambi *et al.,* 1995; Chang *et al.,* 2007; Nielsen *et al.,* 2011; Svenningsen *et al.,* 2018).

The genomic region that encodes the Pel exopolysaccharide in *P. aeruginosa* is absent in the PssUMAF0158 and PcPCL1606 genomes. However, a Psl-like gene cluster has been identified in the PssUMAF0158 and PcPCL1606 strains (Heredia-Ponce *et al.,* 2020a,b). The biofilm architecture of the PssUMAF0158 Δ*pslE* mutant, which is affected in the production of the Psl-like exopolysaccharide, consists of cell aggregates that are disrupted in the double mutant PssUMAF0158 *ΔwssE,pslE*, which does not produce both cellulose and Psl polysaccharides (Heredia-Ponce *et*

al., 2020a). These results are similar to the described *P. aeruginosa* E2, S54485 and 19660 flow-cell chamber phenotypes, in which the *Δpsl* mutants form small aggregates that are disrupted in the *Δpsl,pel* double mutants (Colvin *et al.,* 2012). The Pel polysaccharide was described as similar to cellulose, both the Pel and cellulose polysaccharides form pellicle biofilms (Friedman & Kolter, 2004; Jennings *et al.,* 2015), the PssUMAF0158 Δ*wssE* mutant is unable to produce cell aggregates and these aggregates are disrupted in *P. aeruginosa* and *P. syringae* when either cellulose or Pel are not produced, respectively (Colvin *et al.,* 2012; Heredia-Ponce *et al.,* 2020a). All these observations suggest that both exopolysaccharides could be performing similar structural roles within the biofilms in both species. Indeed, just 12 out of the 600 *Pseudomonas* strains that were analysed in a recent study, which belong to four different groups - *P. asplenii*, *P. fluorescens*, *P. fragi* and *P. oryzihabitans*- possess both the Pel and cellulose gene clusters (Blanco-Romero *et al.,* 2020; Heredia-Ponce *et al.,* 2021). Noticeably, none of these strains belong to the *P. syringae* or *P. aeruginosa* species.

Among the alginate, cellulose and Psl polysaccharides, Psl was the most interesting component because thus far research on this polysaccharide has been exclusively conducted in *P. aeruginosa,* despite the presence of a *psl*-like gene cluster has also been reported in some environmental nonaeruginosa *Pseudomonas* (Mann & Wozniak, 2012). In *P. aeruginosa* PAO1, Psl was formerly described to be encoded by the 15-gene operon *psl* (*pslA-O*), which corresponds to the PA2231-PA2245 genomic region (Friedman & Kolter, 2004; Jackson *et al.,* 2004; Matsukawa & Greenberg, 2004). However, later works have revealed that the last three genes of the operon (*pslMNO*) constitute an independent transcriptional unit (Goodman *et al.,* 2004; Hickman *et al.,* 2005; Starkey *et al.,* 2009) and that they are not truly required to produce Psl (Byrd *et al.,* 2009). Generally, the *psl*-like gene clusters found in nonaeruginosa *Pseudomonas* either lack orthologues to *pslMNO* genes or are found scattered in the genome outside the cluster (Mann & Wozniak, 2012), as it was observed in the PssUMAF0158 and PcPCL1606 strains (Heredia-Ponce *et al.,* 2020a,b). The PssUMAF0158 and PcPCL1606 strains lack orthologs to the acyltransferase protein PslL of *P. aeruginosa* (Heredia-Ponce *et al.,* 2020a,b). Instead, both strains encode a putative acetyltransferase between the *pslJ*- and *pslK*-like genes that might perform a related function to that of the acyltransferase PslL

(Heredia-Ponce *et al.,* 2020a,b). Among those environmental nonaeruginosa *Pseudomonas* strains that contain a *psl*-like gene cluster there are some plant-interacting pseudomonads with different lifestyles, including pathogenic and beneficial strains (Mann & Wozniak, 2012; Blanco-Romero *et al.,* 2020), which suggests this polysaccharide might constitute a general biofilm component in these bacteria. In this dissertation, a Psl-like exopolysaccharide has proven to be a biofilm component in the phytopathogenic bacterium PssUMAF0158 and the biocontrol agent PcPCL1606, playing roles in attachment and competition for biofilm formation, and in virulence and biocontrol, respectively (Heredia-Ponce *et al.,* 2020a,b). The roles of Psl in early attachment, biofilm formation, competition and virulence have also been reported in *P. aeruginosa* (Jackson *et al.,* 2004; Colvin *et al.,* 2012; Billings *et al.,* 2013; Irie *et al.,* 2016).

The first study regarding Psl composition in *P. aeruginosa* determined that this polysaccharide was a galactose- and mannose-rich exopolysaccharide (Ma *et al.,* 2007). Two years later, the structural analysis of Psl was published, indicating that it likely consisted of a pentasaccharide repeating unit of mannose, glucose and rhamnose in approximate ratios of 3:1:1 (Byrd *et al.,* 2009). Interestingly, galactose, which was reported as the major component of Psl in the first study (Ma *et al.,* 2007) was not detected in the structural analysis (Byrd *et al.,* 2009). The authors stated that different conditions were used in both studies, which could account for some variations in composition, as described previously (Flemming *et al.,* 2016). Therefore, there is some thought that different forms of Psl might be produced even in the same strain depending on the medium and growth conditions. Be as it may, mannose seems to be the most characteristic component of the Psl structure in *P. aeruginosa*. Preliminary results obtained in this dissertation have determined that the composition of the Psl-like exopolysaccharides of the PssUMAF0158 and PcPCL1606 strains could be similar to the archetypal *P. aeruginosa* (Chapter 1; Heredia-Ponce *et al.,* 2020b). This is because mannose monosaccharide was detected in the composition analysis performed in PssUMAF0158 (Chapter 1) and lectin staining analysis performed in PcPCL1606 (Heredia-Ponce *et al.,* 2020b). Curiously, there are some hints regarding the production of a Psl-like exopolysaccharide in *P. syringae* and *P. fluorescens* in the literature. Thus, Laue *et al.,* (2006) reported that in addition to alginate and levan, *P. syringae* PG4180

produces a third EPS that constitutes a fibrous structure and binds to the *Naja mossambica* lectin (NML). Interestingly, the monosaccharide specificity of NML is mannose (Jiang *et al.,* 2016). Furthermore, Fett *et al.,* (1989) reported that two *P. fluorescens* strains isolated from rotted bell pepper, PF-05-2 and PM-LB-1, produce a novel EPS composed of mannose, rhamnose and glucose (1:1:1 molar ratio) substituted with pyruvate and acetate.

Regarding the protein component of the pseudomonads biofilm matrix, amyloid-like structures have been gaining importance during the last decade (Dueholm *et al.,* 2010, 2013a,b). Expression of the Fap fibre results in aggregation and increased biofilm formation in *P. aeruginosa*, *P. fluorescens* and *P. putida* (Dueholm *et al.,* 2013b). The presence of a putative *fap* gene cluster was reported in the PcPCL1606 strain (Heredia-Ponce *et al.,* 2020b) but not in the PssUMAF0158 strain. Noticeably, the *fap* cluster has not been detected in the 98 *P. syringae* genomes included in a recent study but it is present in its closest relatives, including *Pseudomonas fragi*, the *P. fluorescens* complex and is widespread among another proteobacteria (Dueholm *et al.,* 2013b; Blanco-Romero *et al.,* 2020). Interestingly, a putative *fap* gene cluster is present in the *P. syringae* Riq4 strain but its role in adhesion and biofilm formation has not been assessed. In addition, 36% of the *fap* carrying bacteria have a rhizosphere lifestyle (Dueholm *et al.,* 2013b), which suggest this component plays a role in plant root interaction, as it has been demonstrated in the PcPCL1606 strain (Heredia-Ponce *et al.,* 2020b).

The importance of amyloid-like proteins for biofilm formation and/or plant-bacteria interaction has been described in other plant-interacting bacteria, such as *Bacillus cereus* and *Bacillus subtilis* (Caro-Astorga *et al.,* 2015; Cámara-Almirón *et al.,* 2020). Thus, the *Bacillus subtilis* NCIB3610 *ΔtasA* mutant, which is impaired in the production of the TasA amyloid-like fibre, reduces its biofilm structural integrity and adhesion to melon leaves at 4 h and 2 days post-inoculation (Romero *et al.,* 2010; Cámara-Almirón *et al.,* 2020). Something similar has been observed in the PcPCL1606 strain, in which the Fap-like fibre is not critical for biofilm formation but is involved in early adhesion to abiotic and biotic surfaces and biocontrol activity (Heredia-Ponce *et al.,* 2020b). However, in contrast to what it has been observed in PcPCL1606, the *Bacillus subtilis* NCIB3610 wild-type and its derived *ΔtasA* mutant showed comparable biocontrol activity against the fungal

phytopathogen *Podosphaera xanthii* because compared to the wild-type, the mutant overproduces fengycin and other antimicrobial molecules (Cámara-Almirón *et al.,* 2020). However, the authors demonstrated that if not for overproduction of these antimicrobial molecules, the *ΔtasA* mutant would result in a failure to manage *P. xanthii* infection (Cámara-Almirón *et al.,* 2020).

Biofilm formation contributes to the lifestyles displayed by the PssUMAF0158 and PcPCL1606 strains during interaction with their plant host (Heredia-Ponce *et al.,* 2020a,b). A reduction in exopolysaccharide synthesis seems to predispose PssUMAF0158 to the pathogenic lifestyle, because of the mutants impaired in cellulose and Psl-like exopolysaccharides production, which are impaired in biofilm formation compared to the wild-type strain, are significantly more virulent than the wild-type strain (Arrebola *et al.,* 2015; Heredia-Ponce *et al.,* 2020a). In line with this topic, results obtained in Chapter 2 have revealed that those observations in the PssUMAF0158 strain could be a general trait among Pss because unlike PssUMAF2600, which is a higher EPS producer than PssUMAF0158, the PssUMAF0291 strain, which is a lower EPS producer than PssUMAF0158, is more virulent than the PssUMAF0158 wild-type (Chapter 2). Therefore, a reduction in exopolysaccharide synthesis could generally predispose the Pss strains to a less biofilm and more virulent lifestyle. However, more strains would need to be tested to make stronger claims regarding this issue.

Biofilm formation is considered *per se* as a virulence factor in many phytopathogenic bacteria. However, this idea needs to be pondered, as it is strongly dependent on the phytopathogen lifestyle and mechanism of infection. The virulence of *E. amylovora*, *X. fastidiosa* and *R. solanacearum* is mainly determined by biofilm formation because its structure physically blocks the vascular system of plants (Sjulin *et al.,* 1978; Koczan *et al.,* 2009, 2011; Killiny *et al.,* 2013; Mori *et al.,* 2016; Marques *et al.,* 2020). However, this is not the case of *P. syringae*, in which virulence is mainly determined by phytotoxins and effectors secreted through the type III secretion system (Xie *et al.,* 2019). Biofilm formation in *P. syringae*, particularly some extracellular matrix components, could be considered a virulence factor only because it allows the attachment of this phytopathogenic bacterium to plant surfaces during the epiphytic stage and confers protection (Kidambi *et al.,* 1995; Peñaloza-Vázquez *et al.,* 1997; Arrebola *et al.,* 2015; Heredia-Ponce *et al.,*

2020a), but the biofilm structure *per se* does not seem to play a role in the infection process. Furthermore, biofilm formation by Pss is also influenced by temperature and particularly by light (Chapter 2), which are highly variable environmental factors affecting the phyllosphere (Hirano & Upper, 2000; Lindow & Brandl, 2003). White light increases biofilm formation in Pss (Chapter 2), which could be an important adaptive advantage in its epiphytic phase. Accordingly, environmental factors could influence the transition of Pss between epiphytic and pathogenic lifestyles by influencing the entering or exiting of the biofilm lifestyle, to either persist in the surface or colonize the internal plant tissues, respectively (Arrebola *et al.*, 2015; Heredia-Ponce *et al.*, 2020a; Chapter 2).

In summary, the results obtained in this dissertation reveal the role of some extracellular matrix components in biofilm formation and the bacterial ecology of two environmental pseudomonads with different lifestyles and for the first time reveal the role played by a Psl-like exopolysaccharide in other environmental pseudomonads besides *P. aeruginosa*. In addition, it has been proven an influence of environmental factors, especially light, in Pss biofilm formation.

CONCLUSIONS

From the results obtained in this doctoral thesis it can be concluded that:

- A Psl-like exopolysaccharide plays a role in the biofilm architecture of the phytopathogenic bacterium *Pseudomonas syringae* pv. syringae UMAF0158 and the biocontrol agent *Pseudomonas chlororaphis* PCL1606.

- Biofilm formation, through cellulose and Psl-like biosynthesis, plays a relevant role in the ecology of the phytopathogenic bacterium *P. syringae* pv. syringae UMAF0158 during the interaction with the plant by participating in biofilm formation, its association with the mango leaves and influencing transition between epiphytic and pathogenic lifestyles.

- Environmental factors, particularly white light, influence biofilm formation by controlling exopolysaccharide synthesis in *P. syringae* pv. syringae (Pss) strains. Furthermore, lower levels of exopolysaccharide production seem to be associated with more virulent strains.

- The Psl-like polysaccharide and the Fap-like amyloid fibre play relevant roles in the ecology of the biocontrol agent *P. chlororaphis* PCL1606, as they are involved in early attachment to surfaces, such as the avocado root, and their synthesis are related to the efficacy of the biocontrol activity.

De los resultados obtenidos en esta tesis doctoral se puede concluir que:

- Un polisacárido de tipo Psl forma parte de la arquitectura de la biopelícula de la bacteria fitopatógena *Pseudomonas syringae* pv. syringae UMAF0158 y el agente de control biológico *Pseudomonas chlororaphis* PCL1606.

- La formación de biopelículas, a través de la síntesis de celulosa y de un polisacárido similar a Psl, juega un papel relevante en la ecología de la bacteria fitopatógena PssUMAF0158 durante su interacción con la planta, participando en la formación de biopelículas, en la adhesión a las hojas e influyendo en la transición entre los estilos de vida epífito y patógeno.

- Los factores ambientales, particularmente la luz blanca, influyen en la formación de biopelículas al controlar la síntesis de polisacárido en cepas de *P. syringae* pv. syringae (Pss) aisladas de mango. Además, niveles más bajos de producción de polisacáridos parecen estar asociados a una mayor virulencia de Pss.

- Un polisacárido de tipo Psl y una putativa fibra amiloide juegan papeles relevantes en la ecología del agente de biocontrol *P. chlororaphis* PCL1606, al estar ambos implicados en la adhesión temprana a diferentes superficies, como la raíz de aguacate, y estar relacionada su producción con la eficacia de la actividad de control biológico.

BIBLIOGRAPHY

A

Abdulhaq, N., Nawaz, Z., Zahoor, M.A. & Siddique, A.B. (2020). Association of biofilm formation with multi drug resistance in clinical isolates of *Pseudomonas aeruginosa*. *EXCLI J* 19, 201-208.

An, D. & Parsek, M.R. (2007). The promise and peril of transcriptional profiling in biofilm communities. *Curr Opin Microbiol* 10(3), 292-296.

Anderson, A.J. & Kim, Y.C. (2020). Insights into plant-beneficial traits of probiotic *Pseudomonas chlororaphis* isolates. *J Med Microbiol* 69(3), 361-371.

Aprile, F., Heredia-Ponce, Z., Cazorla, F.M., de Vicente, A., Gutiérrez-Barranquero, J.A. (2020). A large Tn7-like transposon confers hyper-resistance to copper in *Pseudomonas syringae* pv. syringae. *Appl Environ Microbiol* 87, e02528-20.

Ardré, M., Dufour, D. & Rainey, P.B. (2019). Causes and biophysical consequences of cellulose production by *Pseudomonas fluorescens* SBW25 at the air-liquid interface. *J Bacteriol* 201(18), e00110-19.

Armbruster, C.R., Lee, C.K., Parker-Gilham, J., de Anda, J., Xia, A., Zhao, K., Murakami, K., Tseng, B.S., Hoffman, L.R., Jin, F., Harwood, C.S., Wong, G.C. & Parsek, M.R. (2020). Heterogeneity in surface sensing suggests a division of labor in *Pseudomonas aeruginosa* populations. *Elife* 8, e45084.

Armitano, J., Méjean, V. & Jourlin-Castelli, C. (2014). Floating biofilm in Gram-negative bacteria. *Environ Microbiol Rep* 6, 534-544.

Arrebola, E., Carrión, V.J., Gutiérrez-Barranquero, J.A., Rodríguez-Palenzuela, P., Cazorla, F.M., de Vicente, A. (2015). Cellulose production in *Pseudomonas syringae* pv. syringae: A compromise between epiphytic and pathogenic lifestyles. *FEMS Microbiol Ecol* 91(7), 1–12.

Arrebola, E., Cazorla, F.M., Codina, J.C., Gutiérrez-Barranquero, J.A., Pérez-García, A., de Vicente, A. (2009). Contribution of mangotoxin to the virulence and epiphytic fitness of *Pseudomonas syringae* pv. syringae. *Int Microbiol* 12(2), 87–95.

Arrebola, E., Cazorla, F.M., Durán, V.E., Rivera, E., Olea, F., Codina, J.C., Pérez-García, A., de Vicente, A. (2003). Mangotoxin: A novel antimetabolite toxin produced by *Pseudomonas syringae* inhibiting ornithine/arginine biosynthesis.

Physiol Mol Plant Pathol 63(3), 117–127.

Arrebola, E., Cazorla, F.M., Romero, D., Pérez-García, A. & de Vicente, A. (2007). A nonribosomal peptide synthetase gene (*mgoA*) of *Pseudomonas syringae* pv. syringae is involved in mangotoxin biosynthesis and is required for full virulence. *Mol Plant Microbe Interact* 20(5), 500-509.

Arrebola, E., Tienda, S., Vida, C., de Vicente, A., & Cazorla, F.M. (2019). Fitness features involved in the biocontrol interaction of *Pseudomonas chlororaphis* with host plants: the case study of PcPCL1606. *Front Microbiol* 10, 719.

Augimeri, R. V., Varley, A. J. & Strap, J. L. (2015). Establishing a role for bacterial cellulose in environmental interactions: lessons learned from diverse biofilm-producing *Proteobacteria*. *Front Microbiol* 6, 1282.

B

Bao, Y., Lies, D.P., Fu, H. & Roberts, G.P. (1991). An improved Tn7-based system for the single-copy insertion of cloned genes into chromosomes of gram-negative bacteria. *Gene* 109(1), 167–168.

Bar-On, Y.M. & Milo, R. (2019). Towards a quantitative view of the global ubiquity of biofilms. *Nat Rev Microbiol* 17(4), 199-200.

Berge, O., Monteil, C.L., Bartoli, C., Chandeysson, C., Guilbaud, C., Sands, D.C. & Morris, C.E. (2014). A user's guide to a data base of the diversity of *Pseudomonas syringae* and its application to classifying strains in this phylogenetic complex. *PLoS One* 9(9), e105547.

Berne, C., Ducret, A., Hardy, G. G., & Brun, Y.V. (2015). Adhesins involved in attachment to abiotic surfaces by Gram-negative bacteria. *Microbiol Spectr* 3(4), 1–45.

Bianciotto, V., Andreotti, S., Balestrini, R., Bonfante, P., & Perotto, S. (2001). Mucoid mutants of the biocontrol strain *Pseudomonas fluorescens* CHA0 show increased ability in biofilm formation on mycorrhizal and nonmycorrhizal carrot roots. *Mol Plant Microbe Interact* 14(2), 255–260.

Billings, N., Ramírez Millan, M., Caldara, M., Rusconi, R., Tarasova, Y., Stocker,

R. & Ribbeck, K. (2013). The extracellular matrix component Psl provides fast-acting antibiotic defense in *Pseudomonas aeruginosa* biofilms. *PLoS Pathog* 9(8), e1003526.

Blanco-Romero, E., Garrido-Sanz, D., Rivilla, R., Redondo-Nieto, M. & Martín, M. (2020). *In silico* characterization and phylogenetic distribution of extracellular matrix components in the model rhizobacteria *Pseudomonas fluorescens* F113 and other Pseudomonads. *Microorganisms* 8(11), 1740.

Bloemberg, G.V., & Lugtenberg, B.J.J. (2001). Molecular basis of plant growth promotion and biocontrol by rhizobacteria. *Curr Opin Plant Biol* 4(4), 343–350.

Bloemberg, G.V., Wijfjes, A.H.M., Lamers, G.E.M., Stuurman, N. & Lugtenberg, B.J.J. (2000). Simultaneous imaging of *Pseudomonas fluorescens* WCS365 populations expressing three different autofluorescent proteins in the rhizosphere: new perspectives for studying microbial communities. *Mol Plant Microbe Interact* 13(11), 1170–1176.

Bogino, P.C., Oliva, M., Sorroche, F.G. & Giordano, W. (2013). The role of bacterial biofilms and surface components in plant-bacterial associations. *Int J Mol Sci* 14(8), 15838-15859.

Boles, B.R., Thoendel, M. & Singh, P.K. (2005). Rhamnolipids mediate detachment of *Pseudomonas aeruginosa* from biofilms. *Mol Microbiol* 57(5), 1210-1223.

Boudarel, H., Mathias, J.D., Blaysat, B. & Grédiac, M. (2018). Towards standardized mechanical characterization of microbial biofilms: analysis and critical review. *npj Biofilms Microbiomes* 4, 17.

Boyd, A. & Chakrabarty, A.M. (1994). Role of alginate lyase in cell detachment of *Pseudomonas aeruginosa*. *Appl Environ Microbiol* 60(7), 2355-2359.

Branda, S.S., Vik, S., Friedman, L. & Kolter, R. (2005). Biofilms: the matrix revisited. *Trends Microbiol* 13(1), 20-26.

Bull, C.T., De Boer, S.H., Denny, T.P., Firrao, G., Fischer-Le S.M., Saddler G.S., Scortichini, M., Stead, D.E. & Takikawa, Y. (2010). Comprehensive list of names of plant pathogenic bacteria, 1980-2007. *J Plant Pathol* 92, 551–592.

Burch, A.Y., Browne, P.J., Dunlap, C.A., Price, N.P. & Lindow, S.E. (2011).

Comparison of biosurfactant detection methods reveals hydrophobic surfactants and contact-regulated production. *Environ Microbiol* 13(10), 2681–2691.

Byrd, M.S., Sadovskaya, I., Vinogradov, E., Lu, H., Sprinkle, A.B., Richardson, S.H., Ma, L., Ralston, B., Parsek, M.R., Anderson, E..M., Lam, J.S. & Wozniak, D.J. (2009). Genetic and biochemical analyses of the *Pseudomonas aeruginosa* Psl exopolysaccharide reveal overlapping roles for polysaccharide synthesis enzymes in Psl and LPS production. *Mol Microbiol* 73(4), 622–638.

C

Caiazza, N.C., Merritt, J.H., Brothers, K.M. & O'Toole, G.A. (2007). Inverse regulation of biofilm formation and swarming motility by *Pseudomonas aeruginosa* PA14. *J Bacteriol* 189(9), 3603–3612.

Calderón, C.E., de Vicente, A. & Cazorla, F.M. (2014). Role of 2-hexyl, 5-propyl resorcinol production by *Pseudomonas chlororaphis* PCL1606 in the multitrophic interactions in the avocado rhizosphere during the biocontrol process. *FEMS Microbiol Ecol* 89(1), 20–31.

Calderón, C. E., Pérez-García, A., de Vicente, A., & Cazorla, F. M. (2013). The *dar* genes of *Pseudomonas chlororaphis* PCL1606 are crucial for biocontrol activity via production of the antifungal compound 2-hexyl, 5-propyl resorcinol. *Mol Plant-Microbe Interact* 26(5), 554-565.

Calderón, C.E., Ramos, C., de Vicente, A., & Cazorla, F.M. (2015). Comparative genomic analysis of *Pseudomonas chlororaphis* PCL1606 reveals new insight into antifungal compounds involved in biocontrol. *Mol Plant Microbe Interact* 28(3), 249–260.

Calderón, C. E., Tienda, S., Heredia-Ponce, Z., Arrebola, E., Cárcamo-Oyarce, G., Eberl, L. & Cazorla, F.M. (2019). The compound 2-hexyl, 5-propyl resorcinol has a key role in biofilm formation by the biocontrol rhizobacterium *Pseudomonas chlororaphis* PCL1606. *Front Microbiol* 10, 369.

Cámara-Almirón, J., Navarro, Y., Díaz-Martínez, L. Magno-Pérez, C.M., Molina-Santiago, C., Pearson, J.R., de Vicente, A., Pérez-García, A. & Romero, D. (2020). Dual functionality of the amyloid protein TasA in *Bacillus* physiology and fitness on

the phylloplane. *Nat Commun* 11(1), 1859.

Cárcamo-Oyarce, G., Lumjiaktase, P., Kümmerli, R. & Eberl, L. (2015). Quorum sensing triggers the stochastic escape of individual cells from *Pseudomonas putida* biofilms. *Nat Commun* 6, 5945.

Carrión, V.J., Arrebola, E., Cazorla, F.M., Murillo, J. & de Vicente, A. (2012). The *mbo* operon is specific and essential for biosynthesis of mangotoxin in Pseudomonas syringae. *PLoS One* 7(5), e36709.

Carrión, V.J., van der Voort, M., Arrebola, E., Gutiérrez-Barranquero, J.A., de Vicente, A., Raaijmakers, J.M. & Cazorla, F.M. (2014). Mangotoxin production of *Pseudomonas syringae* pv. syringae is regulated by MgoA. *BMC Microbiol.* 14, 46.

Caro-Astorga, J., Frenzel, E., Perkins, J.R., Álvarez-Mena, A., de Vicente, A., Ranea, J.A.G., Kuipers, O.P. & Romero, D. (2020). Biofilm formation displays intrinsic offensive and defensive features of *Bacillus cereus*. *NPJ Biofilms Microbiomes* 6, 3.

Caro-Astorga, J., Pérez-García, A., de Vicente, A. & Romero, D. (2015). A genomic region involved in the formation of adhesin fibers in *Bacillus cereus* biofilms. *Front Microbiol* 5, 745.

Cazorla, F.M., Arrebola, E., Sesma, A., Pérez-García, A., Codina, J.C., Murillo, J. & de Vicente, A. (2002). Copper resistance in *Pseudomonas syringae* strains isolated from mango is encoded mainly by plasmids. *Phytopathology* 92(8), 909-916.

Cazorla, F.M., Duckett, S.B., Bergström, E.T., Noreen, S., Odijk, R., Lugtenberg, B.J.J., Thomas-Oates, J.E. & Bloemberg, G.V. (2006). Biocontrol of avocado dematophora root rot by antagonistic *Pseudomonas fluorescens* PCL1606 correlates with the production of 2-hexyl 5-propyl resorcinol. *Mol Plant Microbe Interact* 19(4), 418–428.

Cazorla, F.M., Torés, J.A., Olalla, L., Pérez-García, A., Farré, J.M. & de Vicente, A. (1998). Bacterial apical necrosis of mango in Southern Spain: A disease caused by *Pseudomonas syringae* pv. syringae. *Phytopathology* 88(7), 614–620.

Chang, W.S., van de Mortel, M., Nielsen, L., Nino de Guzman, G., Li, X. & Halverson, L.J. (2007). Alginate production by *Pseudomonas putida* creates a

hydrated microenvironment and contributes to biofilm architecture and stress tolerance under water-limiting conditions. *J Bacteriol* 189(22), 8290-8299.

Chen, Y., Yan, F., Chai, Y., Liu, H., Kolter, R., Losick, R. & Guo, J.H. (2013). Biocontrol of tomato wilt disease by *Bacillus subtilis* isolates from natural environments depends on conserved genes mediating biofilm formation. *Environ Microbiol* 15(3), 848-864.

Chin-A-Woeng, T.F.C, Bloemberg, G.V., Mulders, I.H.M, Dekkers, L.C. & Lugtenberg, B.J.J. (2007). Root colonization by phenazine-1-carboxamide-producing bacterium *Pseudomonas chlororaphis* PCL1391 is essential for biocontrol of tomato foot and root rot. *Mol Plant Microbe Interact* 13(12), 1340-1345.

Choi, K.H., Kumar, A. & Schweizer, H.P. (2006). A 10-min method for preparation of highly electrocompetent *Pseudomonas aeruginosa* cells: Application for DNA fragment transfer between chromosomes and plasmid transformation. *J Microbiol Methods* 64(3), 391–397.

Choi ,Y.C. & Morgenroth, E. (2003). Monitoring biofilm detachment under dynamic changes in shear stress using laser-based particle size analysis and mass fractionation. *Water Sci Technol* 47(5), 69-76.

Christensen, B.E. (1989). The role of extracellular polysaccharides in biofilms. *J. Biotech* 10(3-4), 181-202.

Christensen, B.B., Sternberg, C., Andersen, J.B., Palmer, R.J., Nielsen, A.T., Givskov, M. & Molin, S. (1999). Molecular tools for study of biofilm physiology. *Methods Enzymol* 310, 20–42.

Ciofu, O. & Tolker-Nielsen, T. (2019). Tolerance and resistance of *Pseudomonas aeruginosa* biofilms to antimicrobial agents - how *P. aeruginosa* can escape antibiotics. *Front Microbiol* 10, 913.

Clark, D.J. & Maaløe, O. (1967). DNA replication and the division cycle in *Escherichia coli*. *J Mol Biol* 23(1), 99–112.

Colvin, K.M., Gordon, V.D., Murakami, K., Borlee, B.R., Wozniak, D.J., Wong, G.C. & Parsek, M.R. (2011). The Pel polysaccharide can serve a structural and protective role in the biofilm matrix of *Pseudomonas aeruginosa*. *PLoS Pathog* 7(1),

e1001264.

Colvin, K.M., Irie, Y., Tart, C.S., Urbano, R., Whitney, J.C., Ryder, C., Howell, P.L., Wozniak, D.J. & Parsek, M.R. (2012). The Pel and Psl polysaccharides provide *Pseudomonas aeruginosa* structural redundancy within the biofilm matrix. *Environ Microbiol* 14(8), 1913-1918.

Conti, E., Flaibani, A., Regan, M.O., & Sutherland, I.W. (1994). Alginate from *Pseudomonas fluorescens* and *P. putida*: production and properties. *Microbiology* 140, 1125–1132.

Costa, O.Y.A., Raaijmakers, J.M. & Kuramae, E.E. (2018). Microbial extracellular polymeric substances: ecological function and impact on soil aggregation. *Front Microbiol* 9, 1636.

Costerton J.W. (1999). Introduction to biofilm. *Int J Antimicrob Agents* 11(3-4), 217-221.

Costerton, J.W & Lewandowski, Z. (1995). Microbial biofilms. *Annu Rev Microbiol* 49(1), 711-745.

Couillerot, O., Prigent-Combaret, C., Caballero-Mellado, J. & Moënne-Loccoz, Y. (2009). *Pseudomonas fluorescens* and closely-related fluorescent pseudomonads as biocontrol agents of soil-borne phytopathogens. *Lett Appl Microbiol* 48(5), 505-512.

D

Danhorn, T., & Fuqua, C. (2007). Biofilm formation by plant-associated bacteria. *Annu Rev Microbiol* 61, 401–22.

Darzins, A. & Chakrabarty, A.M. (1984). Cloning of genes controlling alginate biosynthesis from a mucoid cystic fibrosis isolate of *Pseudomonas aeruginosa*. *J Bacteriol* 159(1), 9-18.

Davey M.E. & O'Toole, G.A. (2000). Microbial biofilms: from ecology to molecular genetics. *Microbiol Mol Biol Rev* 64(4), 847-867.

De la Fuente-Núñez, C., Korolik, V., Bains, M., Nguyen, U., Breidenstein, E.B.M, Horsman, S., Lewenza, S., Burrows, L. & Hancock, R.E. (2012). Inhibition of bacterial biofilm formation and swarming motility by a small synthetic cationic

peptide. *Antimicrob Agents Chemother* 56(5), 2696–2704.

Del Pozo, J.L. (2018). Biofilm-related disease. *Expert Rev Anti Infect Ther* 16(1), 51-65.

De Pinto, M.C., Lavermicocca, P., Evidente, A., Corsaro, M.M., Lazzaroni, S. & de Gara, L. (2003). Exopolysaccharides produced by plant pathogenic bacteria affect ascorbate metabolism in *Nicotiana tabacum*. *Plant Cell Physiol* 44(8), 803–810.

De Weert S. & Bloemberg G.V. (2007). Rhizosphere competence and the role of root colonization in biocontrol. In: Gnanamanickam S.S. (eds) *Plant-Associated Bacteria* (pp. 317-333). Dordrecht (Netherlands): Springer.

Déziel, E., Lèpine, F., Milot, S. & Villemur, R. (2003). *rhlA* is required for the production of a novel biosurfactant promoting swarming motility in *Pseudomonas aeruginosa*: 3-(3-hydroxyalkanoyloxy)alkanoic acids (HAAs), the precursors of rhamnolipids. *Microbiology* 149(8), 2005–2013.

Diggle, S.P. & Whiteley, M. (2020). Microbe profile: *Pseudomonas aeruginosa*: opportunistic pathogen and lab rat. Microbiology 166(1), 30-33.

Dong, C.J., Wang, L.L., Li, Q., Shang, Q.M. (2019). Bacterial communities in the rhizosphere, phyllosphere and endosphere of tomato plants. *PLoS One* 14(11), e0223847.

Dubois, M., Gilles, K.A., Hamilton, J.K., Rebers, P.A. & Smith, F. (1956). Colorimetric method for determination of sugars and related substances. *Anal Chem* 28(3), 350-356.

Dueholm, M.S., Otzen, D., & Nielsen, P.H. (2013a). Evolutionary insight into the functional amyloids of the Pseudomonads. *PLoS ONE* 8(10), 1–9.

Dueholm, M.S., Petersen, S.V, Sønderkær, M., Larsen, P., Christiansen, G., Hein, K. L., Enghild, J.J., Nielsen, J.L., Nielsen, K.L., Nielsen, P.H. & Otzen, D.E. (2010). Functional amyloid in *Pseudomonas*. *Mol Microbiol* 77(4), 1009–1020.

Dueholm, M.S., Søndergaard, M.T., Nilsson, M., Christiansen, G., Stensballe, A., Overgaard, M.T., Givskov, M., Tolker-Nielsen, T., Otzen, D.E & Nielsen, P.H. (2013b). Expression of Fap amyloids in *Pseudomonas aeruginosa*, *P. fluorescens* and *P. putida* results in aggregation and increased biofilm formation.

MicrobiologyOpen 2(3), 365-382.

E

Elrod, R.P. & Braun, A.C. (1942). *Pseudomonas aeruginosa*: its role as a plant pathogen. *J Bacteriol* 44(6), 633-645.

Evans, L.R. & Linker, A. (1973). Production and characterization of the slime polysaccharide of *Pseudomonas aeruginosa*. *J Bacteriol* 116(2), 915–924.

F

Fageria, N. K. & Stone, L. F. (2006). Physical, chemical, and biological changes in the rhizosphere and nutrient availability. *J Plant Nutr* 29(7), 1327-1356.

Fakhr, M.K., Peñaloza-Vázquez, A., Chakrabarty, A.M. & Bender, C.L. (1999). Regulation of alginate biosynthesis in *Pseudomonas syringae* pv. syringae. *J Bacteriol* 181(11), 3478–3485.

Farias, G.A., Olmedilla, A. & Gallegos, M.T. (2019). Visualization and characterization of *Pseudomonas syringae* pv. tomato DC3000 pellicles. *Microb Biotechnol* 12(4), 688–702.

Fegan, M., Francis, P., Hayward, A.C., Davis, G.H. & Fuerst, J.A. (1990). Phenotypic conversion of *Pseudomonas aeruginosa* in cystic fibrosis. *J Clin Microbiol* 28(6), 1143-1146.

Fett, W.F. & Dunn, M.F. (1989). Exopolysaccharides produced by phytopathogenic *Pseudomonas syringae* pathovars in infected leaves of susceptible hosts. *Plant Physiol* 89, 5–9.

Fett, W.F., Osman, S.F. & Dunn, M.F. (1989). Characterization of exopolysaccharides produced by plant-associated fluorescent *Pseudomonads*. *Appl Environ Microbiol* 55, 579-583.

Flemming, H.C. & Wingender, J. (2010). The biofilm matrix. *Nat Rev Microbiol* 8(9), 623-633.

Flemming, H.C., Wingender, J., Szewzyk, U., Steinberg, P., Rice, S.A. & Kjelleberg, S. (2016). Biofilms: an emergent form of bacterial life. *Nat Rev*

Microbiol 14, 563–575.

Flemming, H.C. & Wuertz, S. (2019). Bacteria and archaea on Earth and their abundance in biofilms. *Nat Rev Microbiol* 17(4), 247-260.

Fong, J.N.C. & Yildiz, F.H. (2015). Biofilm matrix proteins. *Microbiol Spectr* 3(2).

Franklin, M.J., Nivens, D.E., Weadge, J.T. & Howell, L. (2011). Biosynthesis of the *Pseudomonas aeruginosa* extracellular polysaccharides, alginate, Pel and Psl. *Front Microbiol* 2, 167.

Friedman, L. & Kolter, R. (2004). Two genetic loci produce distinct carbohydrate-rich structural components of the *Pseudomonas aeruginosa* biofilm matrix. *J Bacteriol* 186(14), 4457–4465.

Freeman, S., Sztejnberg, A. & Chet, I. (1986). Evaluation of *Trichoderma* as a biocontrol agent for *Rosellinia necatrix*. *Plant Soil* 94, 163–170.

Fuchs, A. (1956). Synthesis of levan by *Pseudomonads*. *Nature* 178(4539), 921.

Fünfhaus, A., Göbel, J., Eberling, J., Knispel, H., García-Gonzalez, E. & Genersch, E. (2018). Swarming motility and biofilm formation of *Paenibacillus larvae*, the etiological agent of american foulbrood of honey bees (*Apis mellifera*). *Sci Rep* 8, 8840.

G

Gal, M., Preston, G.M., Massey, R.C., Spiers, A.J. & Rainey, P.B. (2003). Genes encoding a cellulosic polymer contribute towards the ecological success of *Pseudomonas fluorescens* SBW25 on plant surfaces. *Mol Ecol* 12(11), 3109-3121.

Ganeshan, G. & Kumar, A.M. (2005). *Pseudomonas fluorescens*, a potential bacterial antagonist to control plant diseases. *J Plant Interact* 1(3), 123-134.

Garrido-Sanz, D., Arrebola, E., Martínez-Granero, F., García-Méndez, S., Muriel, C., Blanco-Romero., E., Martín, M., Rivilla, R. & Redondo-Nieto, M. (2017). Classification of isolates from the *Pseudomonas fluorescens* complex into phylogenomic groups based in group-specific markers. *Front Microbiol* 8, 413.

Garrido-Sanz, D., Meier-Kolthoff, J. P., Göker, M., Martín, M., Rivilla, R. & Redondo-Nieto, M. (2016). Genomic and genetic diversity within the *Pseudomonas*

fluorescens complex. *PLoS ONE* 11(4), e0153733.

Ghafoor, A., Hay, I.D. & Rehm, B.H.A. (2011). Role of exopolysaccharides in *Pseudomonas aeruginosa* biofilm formation and architecture. *Appl Environ Microbiol* 77(15), 5238–5246.

González-Sánchez, M.A., Pérez-Jiménez, R.M., Pliego, C., Ramos, C., de Vicente, A. & Cazorla, F.M. (2010). Biocontrol bacteria selected by a direct plant protection strategy against avocado white root rot show antagonism as a prevalent trait. *J Appl Microbiol* 109(1), 65–78.

Goodman, A.L., Kulasekara, B., Rietsch, A., Boyd, D., Smith, R.S. & Lory, S. (2004). A signaling network reciprocally regulates genes associated with acute infection and chronic persistence in *Pseudomonas aeruginosa*. *Dev Cell* 7(5), 745-754.

Gutiérrez-Barranquero, J.A., Arrebola, E., Pérez-García, A., Codina, J.C., Murillo, J., de Vicente, A. & Cazorla, F.M. (2008). Evaluation of phenotypic and genetic techniques to analyze diversity of *Pseudomonas syringae* pv. syringae strains isolates from mango trees. In: Fatmi M. et al. (eds) *Pseudomonas syringae* pathovars and related pathogens – identification, epidemiology and genomics. Springer, Dordrecht.

Gutiérrez-Barranquero, J.A., Carrión, V.J., Murillo, J., Arrebola, E., Arnold, D.L., Cazorla, F.M. & de Vicente, A. (2013). A *Pseudomonas syringae* diversity survey reveals a differentiated phylotype of the pathovar syringae associated with the mango host and mangotoxin production. *Phytopathology* 103(11), 1115-1129.

Gutiérrez-Barranquero, J.A., Cazorla, F.M. & de Vicente, A. (2019). *Pseudomonas syringae* pv. syringae associated with mango trees, a particular pathogen within the "hodgepodge" of the *Pseudomonas syringae* complex. *Front Plant Sci* 10, 570.

Gutiérrez-Barranquero, J.A., Cazorla, F.M., de Vicente, A. & Sundin, G.W. (2017). Complete sequence and comparative genomic analysis of eight native *Pseudomonas syringae* plasmids belonging to the pPT23A family. *BMC Genomics* 18(1), 365.

Gutiérrez-Barranquero, J.A., de Vicente, A., Carrión, V.J., Sundin, G.W. & Cazorla, F.M. (2013). Recruitment and rearrangement of three different genetic determinants into a conjugative plasmid increase copper resistance in *Pseudomonas syringae*.

Appl Environ Microbiol 79(3), 1028-1033.

Gutiérrez-Barranquero, J.A., Reen, F.J. & O'Gara, F. (2015). Deciphering the role of coumarin as a novel quorum sensing inhibitor suppressing virulence phenotypes in bacterial pathogens. *Appl Microbiol Biotechnol* 99(7), 3303–3316.

H

Hall-Stoodley, L., Costerton, J. W., & Stoodley, P. (2004). Bacterial biofilms: from the natural environment to infectious diseases. *Nat Rev Microbiol* 2(2), 95-108.

Hanahan, D. (1983). Studies on transformation of *Escherichia coli* with plasmids. *J Mol Biol* 166(4), 557–580.

Helmann, T.C., Deutschbauer, A.M. & Lindow, S.E. (2019). Genome-wide identification of *Pseudomonas syringae* genes required for fitness during colonization of the leaf surface and apoplast. *Proc Natl Acad Sci USA* 116(38), 18900–18910.

Hentzer, M., Teitzel, G.M., Balzer, G.J., Heydorn, A., Molin, S., Givskov, M. & Parsek, M.R. (2001). Alginate overproduction affects *Pseudomonas aeruginosa* biofilm structure and function. *J Bacteriol* 183(18), 5395–5401.

Heredia-Ponce, Z., Gutiérrez-Barranquero, J.A., Purtschert-Montenegro, G., Eberl, L., de Vicente, A. & Cazorla, F.M. (2020b). Role of extracellular matrix components in the formation of biofilms and their contribution to the biocontrol activity of *Pseudomonas chlororaphis* PCL1606. *Environ Microbiol*.

Heredia-Ponce, Z., Gutiérrez-Barranquero, J.A., Purtschert-Montenegro, G., Eberl, L., Cazorla, F.M. & de Vicente, A. (2020a) Biological role of EPS from *Pseudomonas syringae* pv. syringae UMAF0158 extracellular matrix, focusing on a Psl-like polysaccharide. *NPJ Biofilms Microbiomes* 6(1), 37.

Heredia-Ponce, Z., de Vicente, A., Cazorla, F.M. & Gutiérrez-Barranquero, J.A. (2021). Beyond the wall: exopolysaccharides in the biofilm lifestyle of pathogenic and beneficial plant-associated *Pseudomonas*. *Microorganisms*, 9, 445.

Hickman, J.W., Tifrea, D.F. & Harwood, C.S. (2005). A chemosensory system that regulates biofilm formation through modulation of cyclic diguanylate levels. *Proc*

Natl Acad Sci USA 102(40), 14422-14427.

Hirano, S.S. & Upper, C.D. (2000). Bacteria in the leaf ecosystem with emphasis on *Pseudomonas syringae*-a pathogen, ice nucleus, and epiphyte. *Microbiol Mol Biol Rev* 64(3), 624-653.

Hoang, T.T., Karkhoff-Schweizer, R.R., Kutchma, A.J. & Schweizer, H.P. A broad-host-range Flp-*FRT* recombination system for site-specific excision of chromosomally-located DNA sequences: application for isolation of unmarked *Pseudomonas aeruginosa* mutants. *Gene*. 212(1), 77-86.

Hoffman, M.D., Zucker, L.I., Brown, P.J, Kysela, D.T., Brun, Y.V. & Jacobson, S.C. (2015). Timescales and frequencies of reversible and irreversible adhesion events of single bacterial cells. *Anal Chem* 87(24), 12032-12039.

Hogan, S., Zapotoczna, M., Stevens, N.T., Humphreys, H., O'Gara, J.P. & O'Neill, E. (2016). Eradication of *Staphylococcus aureus* catheter-related biofilm infections using ML:8 and citrox. *Antimicrob Agents Chemother* 60(10), 5968-5975.

Høiby, N., Bjarnsholt, T., Givskov, M., Molin, S. & Ciofu, O. (2010). Antibiotic resistance of bacterial biofilms. *Int J Antimicrob Agents* 35(4), 322-332.

Hunt, S.M., Werner, E.M., Huang, B., Hamilton, M.A. & Stewart, P. (2004). Hypothesis for the role of nutrient starvation in biofilm detachment. *Appl Environ Microbiol* 70(12), 7418-7425.

I

Ichinose, Y., Taguchi, F. & Mukaihara, T. (2013). Pathogenicity and virulence factors of *Pseudomonas syringae*. *J Gen Plant Pathol* 79, 285–296.

Irie, Y., Roberts, A. E. L., Kragh, K. N., Gordon, V. D., Hutchison, J., Allen, R. J. *et al* (2016). The *Pseudomonas aeruginosa* Psl polysaccharide is a social but non-cheatable trait in biofilms. *mBio* 8(3), e00374-17.

J

Jackson, K.D., Starkey, M., Kremer, S., Parsek, M.R. & Wozniak, D.J. (2004). Identification of *psl*, a locus encoding a potential exopolysaccharide that is essential for *Pseudomonas aeruginosa* PAO1 biofilm formation. *J Bacteriol* 186(14), 4466–4475.

Jagusiak, A., Piekarska, B., Chlopaś, K. & Bielańska, E. (2017). Congo red interactions with single-walled carbon nanotubes. In: Roterman I., Konieczny L. (eds) *Self-Assembled Mol.-New Kind of Protein Ligands* Krakow (Poland): Springer, Charm.

Jahn, C.E., Selimi, D.A., Barak, J.D. & Charkowski, A.O. (2011). The *Dickeya dadantii* biofilm matrix consists of cellulose nanofibres, and is an emergent property dependent upon the type III secretion system and the cellulose synthesis operon. *Microbiology* 157(10), 2733–2744.

Janssen, P.H. (2006). Identifying the dominant soil bacterial taxa in libraries of 16S rRNA and 16S rRNA genes. *Appl Environ Microbiol* 72(3), 1719-1728.

Jefferson, K.K. (2004). What drives bacteria to produce a biofilm? *FEMS Microbiol Lett* 136(2), 163–173.

Jennings, L.K., Storek, K.M., Ledvina, H.E., Coulon, C., Marmont, L.S., Sadovskaya, I., Secor, P.R., Tseng, B.S., Scian, M., Filloux, A., Wozniak, D.J., Howell, P.L. & Parsek, M.R. (2015). Pel is a cationic exopolysaccharide that cross-links extracellular DNA in the *Pseudomonas aeruginosa* biofilm matrix. *Proc Natl Acad Sci USA* 112(36), 11353-11358.

Jiang, K., Li, W., Zhang, Q., Yan, G., Guo, K., Zhang, S. & Liu, Y. (2016). GP_{73} N-glycosylation at Asn_{144} reduces hepatocellular carcinoma cell motility and invasiveness. *Oncotarget* 7(17), 23530-23541.

K

Kaplan, J.B. (2010). Biofilm dispersal: mechanisms, clinical implications and potential therapeutic uses. *J Dent Res* 89(3), 205-218.

Karygianni, L., Ren, Z, Koo, H. & Thurnheer, T. (2020). Biofilm matrixome:

extracellular components in structured microbial communities. *Trends Microbiol* 28(8), 668-681.

Kearns, D. B. (2010). A field guide to bacterial swarming motility. *Nat Rev Microbiol* 8, 634–644.

Kennelly, M.M, Cazorla, F.M., de Vicente, A., Ramos, C. & Sundin, G.W. (2007). *Pseudomonas syringae* diseases of fruit trees: progress towards understanding and control. *Plant Dis* 91(1), 4-17.

Kidambi, S.P., Sundin, G.W., Palmer, D.A., Chakrabarty, A.M. & Bender, C.L. (1995). Copper as a signal for alginate synthesis in *Pseudomonas syringae* pv. syringae. *Microbiology* 61(6), 2172–2179.

Killiny, N., Martinez, R.H., Dumenyo, C.K., Cooksey, D.A. & Almeida, R.P. (2013). The exopolysaccharide of *Xylella fastidiosa* is essential for biofilm formation, plant virulence, and vector transmission. *Mol Plant Microbe Interact* 26(9), 1044-1053.

Kim, J.S., Kim, Y.H., Park, J.Y., Anderson, A.J. & Kim, Y.C. (2014). The global regulator GacS regulates biofilm formation in *Pseudomonas chlororaphis* O6 differently with carbon source. *Can J Microbiol* 60(3), 133–138.

Kim, S., Li, X.H., Hwang, H.J. & Lee, J.H. (2020). Thermoregulation of *Pseudomonas aeruginosa* biofilm formation. *Appl Environ Microbiol* 86(22), e01584-20.

King E.O., Ward, M.K. & Raney, D.E. (1954). Two simple media for the demonstration of pyocyanin and fluorescein. *J Lab Clin Med*. 44(2), 301-307.

Kocharova, N.A., Knirel, Y.A., Shashkov, A.S., Kochetkov, N.K. & Pier, G.B. (1998). Structure of an extracellular cross-reactive polysaccharide from *Pseudomonas aeruginosa* immunotype 4. *J Biol Chem* 263(23), 11291-11295.

Koczan, J.M., Lenneman, B.R., McGrath, M.J. & Sundin, G.W. (2011). Cell surface attachment structures contribute to biofilm formation and xylem colonization by *Erwinia amylovora*. *Appl Environ Microbiol* 77(19), 7031-7039.

Koczan, J.M., McGrath, M.J., Zhao, Y. & Sundin, G.W. (2009). Contribution of *Erwinia amylovora* exopolysaccharides amylovoran and levan to biofilm formation:

implications in pathogenicity. *Phytopathology* 99(11), 1237-1244.

Köler, T., Curty, L.K., Barja, F., Van Delden, C. & Pechère, J.C. (2000). Swarming of *Pseudomonas aeruginosa* is dependent on cell-to-cell signaling and requires flagella and pili. *J Bacteriol* 182(21), 5990–5996.

Kovach, M.E., Elzer, P.H., Hill, D.S., Robertson, G.T., Farris, M.A., Roop, R.M and Peterson, K.M (1995). Four new derivatives of the broad-host-range cloning vector pBBR1MCS, carrying different antibiotic-resistance cassettes. *Gene* 166(1), 175–176.

L

Lambertsen, L., Sternberg, C. & Molin, S. (2004). Mini-Tn7 transposons for site-specific tagging of bacteria with fluorescent proteins. *Environ Microbiol* 6(7), 726–732.

Larkin, M.A., Blackshields, G., Brown, N.P., Chenna, R., McGettigan, P.A., McWilliam, H., Valentin, F., Wallace, I.M., Wilm, A., Lopez, R., Thompson, J.D., Gibson, T.J. & Higgins, D.G. (2007). Clustal W and Clustal X version 2.0. *Bioinformatics* 23(21), 2947–2948.

Lasík, J., Vancura, V., Hanzlikova, A. & Wurst, M. (1989). Polysaccharide compounds in the rhizosphere. In: Vancura V, Kunc F. (eds) *Interrelationships between microorganisms and plants in soil* (pp. 315-321). Oxford (UK): Elsevier.

Laue, H., Schenk, A., Li, H., Lambertsen, L., Neu, T.R., Molin, S. & Ullrich, M.S. (2006). Contribution of alginate and levan production to biofilm formation by *Pseudomonas syringae*. *Microbiology* 152(10), 2909–2918.

Lee, S.F., Li, Y.H. & Bowden, G.H. (1996). Detachment of *Streptococcus mutans* biofilm cells by an endogenous enzymatic activity. *Infect Immun* 64(3), 1035-1038.

Leid, J.G., Willson, C.J., Shirtliff, M.E., Hassett, D.J., Parsek, M.R. & Jeffers, A.K. (2005). The exopolysaccharide alginate protects *Pseudomonas aeruginosa* biofilm bacteria from IFN-γ-mediated macrophage killing. *J Immunol* 175(11), 7512-7518.

Leveau, J.H. (2019). A brief from the leaf: latest research to inform our understanding of the phyllosphere microbiome. *Curr Opin Microbiol* 49, 41-49.

Li, H. & Ullrich, M.S. (2001). Characterization and mutational analysis of three allelic *lsc* genes encoding levansucrase in *Pseudomonas syringae*. *J Bacteriol* 183(11), 3282–3292.

Limoli, D.H., Jones, C.J. & Wozniak, D.J. (2015). Bacterial extracellular polysaccharides in biofilm formation and function. *Microbiol Spectr* 3(3).

Lindow, S.E. & Brandl, M.T. (2003). Microbiology of the phyllosphere. *Appl Environ Microbiol* 69(4), 1875-1883.

López, D., Vlamakis, H. & Kolter, R. Biofilms. *Cold Spring Harb Perspect Biol* 2(7), a000398.

Lugtenberg, B.J.J., Dekkers, L. & Bloemberg, G.V. (2001). Molecular determinants of rhizosphere colonization by *Pseudomonas*. *Annu Rev Phytopathol* 39, 461-490.

Lugtenberg, B. & Kamilova, F. (2009). Plant-growth-promoting rhizobacteria. *Annu Rev Microbiol* 63(1), 541–556.

Lyczak, J.B., Cannon, C.L. & Pier, G.B. (2002). Lung infections associated with cystic fibrosis. *Clin Microbiol Rev* 15(2), 194-222.

Lynch, J.M. & de Leij, F. (2012). Rhizosphere. In eLS, (eds). Chichester (UK): John Wiley&Sons.

M

Ma, L., Conover, M., Lu, H., Parsek, M. R., Bayles, K. & Wozniak, D. J. (2009). Assembly and development of the *Pseudomonas aeruginosa* biofilm matrix. *PLoS Pathog* 5(3), e1000354.

Ma, L., Jackson, K.D., Landry, R.M., Parsek, M.R & Wozniak, D.J. (2006). Analysis of *Pseudomonas aeruginosa* conditional Psl variants reveals roles for the Psl polysaccharide in adhesion and maintaining biofilm structure postattachment. *J Bacteriol* 188(23), 8213–8221.

Ma, L., Lu, H., Sprinkle, A., Parsek, M.R. & Wozniak, D.J. (2007). *Pseudomonas aeruginosa* Psl is a galactose- and mannose-rich exopolysaccharide. *J Bacteriol* 189(22), 8353-8356.

Ma, L., Wang, S., Wang, D., Parsek, M.R. & Wozniak, D.J. (2012). The roles of

biofilm matrix polysaccharide Psl in mucoid *Pseudomonas aeruginosa* biofilms. *FEMS Immunol Med Microbiol* 65(2), 377-380.

Maddula, V.S.R.K, Zhang, Z., Pierson, E.A. & Pierson L.S. (2006). Quorum sensing and phenazines are involved in biofilm formation by *Pseudomonas chlororaphis* (*aureofaciens*) strain 30-84. *Microb Ecol* 52(2), 289-301.

Mann, E.E. & Wozniak, D.J. (2012). *Pseudomonas* biofilm matrix composition and niche biology. *FEMS Microbiol* 36(4), 893-916.

Marques, L.L.R., Ceri, H., Manfio, G.P., Reid, D.M. & Olson, M.E. (2002). Characterization of biofilm formation by *Xylella fastidiosa* in vitro. *Plant Dis* 86(6), 633-638.

Marshall K.C. (2006). Planktonic versus sessile life of prokaryotes. In: Dworkin M., Falkow S., Rosenberg E., Schleifer KH., Stackebrandt E. (eds) *The prokaryotes*. New York, NY: Springer.

Marshall, D.C., Arruda, B.E. & Silby, M.W. (2019). Alginate genes are required for optimal soil colonization and persistence by *Pseudomonas fluorescens* Pf0-1. *Access Microbiol* 1(3), 1–8.

Martínez-García, P.M., Rodríguez-Palenzuela, P., Arrebola, E., Carrión, V.J., Gutiérrez-Barranquero, J.A., Pérez-García, A., Ramos, C., Cazorla, F.M. & de Vicente, A. (2015). Bioinformatics analysis of the complete genome sequence of the mango tree pathogen *Pseudomonas syringae* pv. syringae UMAF0158 reveals traits relevant to virulence and epiphytic lifestyle. *PLoS One* 10(8), e0136101.

Matas, I.M., Castañeda-Ojeda, M.P., Aragón, I.M., Antúnez-Lamas, M., Murillo, J., Rodríguez-Palenzuela, P., López-Solanilla, E. & Ramos, C. (2014). Translocation and functional analysis of *Pseudomonas savastanoi* pv. savastanoi NCPPB 3335 type III secretion system effectors reveals two novel effector families of the *Pseudomonas syringae* complex. *Mol Plant-Microbe Interact* 27(5), 424–436.

Matthysse, A. N. N. G., Mahan, S. M. C., Carolina, N., Hill, C. & Carolina, N. (1998). Root colonization by *Agrobacterium tumefaciens* is reduced in *cel*, *attB*, *attD* and *attR* mutants. *Appl Environ Microbiol* 64(7), 2341–2345.

Matsukawa, M. & Greenberg, E.P. (2004). Putative exopolysaccharide synthesis

genese influence *Pseudomonas aeruginosa* biofilm development. *J Bacteriol* 186(14), 4449-4456.

McCarthy, R.R., Mooij, M.J., Reen, F.J., Lesouhaitier, O. & O' Gara, F. (2014). A new regulator of pathogenicity (*bvlR*) is required for full virulence and tight microcolony formation in *Pseudomonas aeruginosa*. *Microbiology* 160(7), 1488–1500.

McDougald, D., Rice, S.A., Barraud, N., Steinberg, P.D. & Kjelleberg, S. Should we stay or should we go: mechanisms and ecological consequences for biofilm dispersal. *Nat Rev Microbiol* 10(1), 39-50.

McIntyre-Smith, A., Schneiderman, J. & Zhou, K. (2010). Alginate does not appear to be essential for biofilm production by PAO1 *Pseudomonas aeruginosa*. *J Exp Microbiol Immunol* 14, 63–68.

Mercado-Blanco, J. & Bakker, P.A.H.M. (2007). Interactions between plants and beneficial *Pseudomonas* spp.: exploiting bacterial traits for crop protection. *Antonie Van Leeuwenhoek* 92(4), 367-89.

Monds, R.D. & O'Toole, G.A. (2009). The developmental model of microbial biofilms: ten years of a paradigm up for review. *Trends Microbiol* 17(2), 73-87.

Mori, Y., Inoue, K., Ikeda, K., Nakayashiki, H., Higashimoto, C., Ohnishi, K., Kiba, A. & Hikichi, Y. (2016). The vascular plant-pathogenic bacterium *Ralstonia solanacearum* produces biofilms required for its virulence on the surfaces of tomato cells adjacent to intercellular spaces. *Mol Plant Pathol* 17(6), 890-902.

Morris, C. E. & Monier, J. (2003). The ecological significance of biofilm formation by plant-associated bacteria. *Annu Rev Phytopathol* 41, 429-453.

Murray, T.S., Ledizet, M. & Kazmierczak, B.I. (2010). Swarming motility, secretion of type III effectors and biofilm formation phenotypes exhibited within a large cohort of *Pseudomonas aeruginosa* clinical isolates. *J Med Microbiol* 59(5), 511–520.

N

Neu, T. R. & Lawrence, J. R. (1999). Lectin-binding analysis in biofilm systems. *Methods Enzymol* 310, 145-150.

Nielsen, L., Li, X. & Halverson, L.J. (2011). Cell-cell and cell-surface interactions mediated by cellulose and a novel exopolysaccharide contribute to *Pseudomonas putida* biofilm formation and fitness under water-limiting conditions. *Environ Microbiol* 13(5), 1342–1356.

Nilsson, M., Chiang, W.C., Fazli, M., Gjermansen, M., Givskov, M. & Tolker-Nielsen, T. (2011). Influence of putative exopolysaccharide genes on *Pseudomonas putida* KT2440 biofilm stability. *Environ Microbiol* 13(5), 1357-1369.

Noirot-Gros, M.F., Forrester, S., Malato, G. Larsen, P.E. & Noirot P. (2019). CRISPR interference to interrogate genes that control biofilm formation in *Pseudomonas fluorescens*. *Sci Rep* 9(1), 15954.

Norris, M.H., Kang, Y., Wilcox, B. & Hoang, T.T. (2010). Stable, site-specific fluorescent tagging constructs optimized for *Burkholderia* species. *Appl Environ Microbiol* 76(22), 7635–7640.

O

Ochsner, U.A., Fiechter, A. & Reiser, J. (1994). Isolation, characterization, and expression in *Escherichia coli* of the *Pseudomonas aeruginosa rhlAB* genes encoding a rhamnosyltransferase involved in rhamnolipid biosurfactant synthesis. *J Biol Chem* 269(31), 19787–19795.

Osman, S.F., Fett, W.F. & Fishman, M.L. (1986). Exopolysaccharides of the phytopathogen *Pseudomonas syringae* pv. glycinea. *J. Bacteriol* 166(1), 66–71.

Ostrowski, A., Mehert, A., Prescott, A., Kiley, T.B. & Stanley-wall, N.R. (2011). YuaB functions synergistically with the exopolysaccharide and TasA amyloid fibres to allow biofilm formation by *Bacillus subtilis*. *J Bacteriol* 193(18), 4821–4831.

P

Palmer, J., Flint, S. & Brooks, J. (2007). Bacterial cell attachment, the begining of a biofilm. *J Ind Microbiol Biotechnol* 34(9), 577-588.

Pandin, C., Le Coq, D., Canette, A., Aymerich, S. & Briandet, R. (2017). Should the biofilm mode of life be taken into consideration for microbial biocontrol agents? *Microb Biotechnol* 10(4), 719-734.

Pandit, A., Adholeya, A., Cahill, D., Brau, L. & Kochar, M. (2020). Microbial biofilms in nature: unlocking their potential for agricultural applications. *J Appl Microbiol* 129(2), 199-211.

Paula, A.J., Hwang, G. & Koo, H. (2020) Dynamics of bacterial population growth in biofilms resemble spatial and structural aspects of urbanization. *Nat Commun* 11, 1354.

Percival, S.L., Suleman, L., Vuotto, C. & Donelli, G. (2015). Healthcare-associated infections, medical devices and biofilms: risk, tolerance and control. *J Med Microbiol* 64(4), 323-334.

Pérez-Mendoza, D., Aragón, I.M., Prada-Ramírez, H.A., Romero-Jiménez, L., Ramos, C., Gallegos, M.T. & Sanjuán, J. (2014). Responses to elevated c-di-GMP levels in mutualistic and pathogenic plant-interacting bacteria. *PLoS One* 9(3), e91645.

Pérez-Mendoza, D., Felipe, A., Ferreiro, M.D., Sanjuán, J., Gallegos, M.T. & Sanjuán, J. (2019). AmrZ and FleQ co-regulate cellulose production in *Pseudomonas syringae* pv. tomato DC3000. *Front Microbiol* 9(3), 1–16.

Periasamy, S., Nair, H.A.S., Lee, K.W.K., Ong, J., Goh, J.Q.J., Kjelleberg, S. & Rice, S.A. (2015). *Pseudomonas aeruginosa* PAO1 exopolysaccharides are important for mixed species biofilm community development and stress tolerance. *Front Microbiol* 6, 851.

Peñaloza-Vázquez, A., Kidambi, S.P., Chakrabarty, A.M. & Bender, C.L. (1997). Characterization of the alginate biosynthetic gene cluster in *Pseudomonas syringae* pv. syringae. *Microbiology* 179(4), 4464–4472.

Pier, G.B., Coleman, F., Grout, M., Franklin, M. & Ohman, D.E. (2001). Role of alginate O-acetylation in resistance of mucoid *Pseudomonas aeruginosa* to opsonic phagocytosis. *Infection and immunity* 69(3), 1895-1901.

Pontes, M.H., Lee, E.J., Choi, J. & Groisman, E.A. (2015). *Salmonella* promotes virulence by repressing cellulose production. *Proc Natl Acad Sci USA* 112(16), 5183–5188.

Poritsanos, N., Selin, C., Fernando, W. G., Nakkeeran, S. & de Kievit, T. R. (2006). A GacS deficiency does not affect *Pseudomonas chlororaphis* PA23 fitness when growing on canola, in aged batch culture or as a biofilm. *Can J Microbiol* 52(12), 1177–1188.

Prada-Ramírez, H.A., Pérez-Mendoza, D., Felipe, A., Martínez-Granero, F., Rivilla, R., Sanjuán, J. & Gallegos, M.T. (2016). AmrZ regulates cellulose production in *Pseudomonas syringae* pv. tomato DC3000. *Mol Microbiol* 99(5), 960-977.

Preston, L.A., Wong, T.Y., Bender, C.L. & Schiller, N.L. (2000). Characterization of alginate lyase from *Pseudomonas syringae* pv. syringae. *J Bacteriol* 182(21), 6268–6271.

R

Ramey, B.E., Koutsoudis, M., Bodman, S.B.V. & Fuqua, C. (2004). Biofilm formation in plant-microbe associations. *Curr Opin Microbiol* 7(6), 602–609.

Ramos-González, M.I., Campos, M.J. & Ramos, J.L. (2005). Analysis of *Pseudomonas putida* KT2440 gene expression in the maize rhizosphere: *in vivo* expression technology capture and identification of root-activated promoters. *J Bacteriol* 187(15), 5504.

Rainey, P.B. & Travisano, M. (1998). Adaptive radiation in a heterogeneous environment. *Nature* 394(6688), 69-72.

Records, A.R. & Gross, D.C. (2010). Sensor kinases RetS and LadS regulate *Pseudomonas syringae* type VI secretion and virulence factors. *J Bacteriol* 192(14), 3584-3506.

Reichhardt, C., Wong, C., Passos da Silva, D., Wozniak, D.J. & Parsek, M.R.

(2018). CdrA interactions within the *Pseudomonas aeruginosa* biofilm matrix safeguard it from proteolysis and promote cellular packing. *mBio* 9(5), e01376-18.

Rigano, L.A., Siciliano, F., Enrique, R., Sendín, L., Filippone, P., Torres, P.S., Qüesta, J., Dow, J.M., Castagnaro, A.P., Vojnov, A.A. & Marano, M.R. (2007). Biofilm formation, epiphytic fitness, and canker development in *Xanthomonas axonopodis* pv. citri. *Mol Plant Microbe Interact* 20(10), 1222-1230.

Río-Álvarez, I., Rodríguez-Herva, J.J., Martínez, P.M., González-Melendi, P., García-Casado, G., Rodríguez-Palenzuela, P. & López-Solanilla, E. (2014). Light regulates motility, attachment and virulence in the plant pathogen *Pseudomonas syringae* pv tomato DC3000. *Environ Microbiol* 16(7), 2072-2085.

Romero, D., Aguilar, C., Losick, R. & Kolter, R. (2010). Amyloid fibers provide structural integrity to *Bacillus subtilis* biofilms. *Proc Natl Acad Sci USA* 107 (5), 2230-2234.

Römling, U. & Galperin, M.Y. (2015). Bacterial cellulose biosynthesis: diversity of operons, subunits, products and functions. *Trends Microbiol* 23(9), 545-557.

Rouse, S. L., Matthews, S. J. & Dueholm, M.S. (2018). Ecology and biogenesis of functional amyloids in *Pseudomonas*. *J Mol Biol* 430(20), 3685-3695.

Rudolph, K.W.E., Gross, M., Ebrahim-Nesbat, F., Nöllenburg, M., Zomorodian, A., Wydra, K., Neugebauer, M., Hettwer, U., El-Shouny, W., Sonnerberg, B. & Klement, Z. (1994). The role of extracellular polysaccharides as virulence factors for phytopathogenic pseudomonads and xanthomonads. In: Kado C.I., Crosa J.H. (eds) Molecular Mechanisms of Bacterial Virulence. Developments in Plant Pathology, vol 3. Dordrech (Netherlands): Springer.

Rudrappa, T. & Biedrzycki, M.L. & Bais, H.P. (2008). Causes and consequences of plant-associated biofilms. *FEMS Microbiol Ecol* 64(2), 153-166.

S

Saldaña, Z., Xicohtencati-Cortes, J., Avelino, F., Phillips, A. D., Kaper, J. B., Puente, J. L. & Girón, J.A. (2009). Synergistic role of curli and cellulose in cell adherence and biofilm formation of attaching and effacing *Escherichia coli* and identification of Fis as a negative regulator of curli. *Environ Microbiol* 11(4), 992-

1006.

Sandhya, V. & Ali, S.Z. (2015). The production of exopolysaccharide by *Pseudomonas putida* GAP-P45 under various abiotic stress conditions and its role in soil aggregation. *Microbiology* 84(4), 512-519.

Santamaría-Hernando, S., Rodríguez-Herva, J.J., Martínez-García, P.M., Río-Álvarez, I., González-Melendi, P., Zamorano, J., Tapia, C., Rodríguez-Palenzuela, P. & López-Solanilla, E. (2018). *Pseudomonas syringae* pv. tomato exploits light signals to optimize virulence and colonization of leaves. *Environ Microbiol* 20(12), 4261-4280.

Schlechter, R.O, Miebach, M. & Remus-Emsermann, M.N.P. (2019). Driving factors of epiphytic bacterial communities: A review. *J Adv Res* 19, 57-65.

Schenk, A., Weingart, H. & Ullrich, M. (2008). The alternative sigma factor AlgT, but not alginate synthesis, promotes in planta multiplication of *Pseudomonas syringae* pv. glycinea. *Microbiology* 154(2), 413–421.

Schnider-Keel, U., Lejbølle, K. B., Baehler, E., Haas, D. & Keel, C. (2001). The sigma factor AlgU (AlgT) controls exopolysaccharide production and tolerance towards desiccation and osmotic stress in the biocontrol agent *Pseudomonas fluorescens* CHA0. *Appl Environ Microbiol* 67(12), 5683–5693.

Serra, D.O., Richter, A. & Hengge, R. (2013). Cellulose as an architectural element in spatially structured *Escherichia coli* biofilms. *J Bacteriol* 195(24), 5540–5554.

Sharma, G., Sharma, S., Sharma, P., Chandola, D., Dang, S., Gupta, S. & Gabrani, R. (2016). *Escherichia coli* biofilm: development and therapeutic strategies. *J Appl Microbiol* 121(2), 309-319.

Silby, M.W., Winstanley, C., Godfrey, S.A., Levy, S.B. & Jackson, R.W. (2011). *Pseudomonas* genomes: diverse and adaptable. *FEMS Microbiol Rev* 35(4), 652-680.

Simpson, J.A., Smith, S.E. & Dean, R.T. (1988). Alginate inhibition of the uptake of *Pseudomonas aeruginosa* by macrophages. *J Gen Microbiol* 134(1), 29-36.

Singh, S. S., Devi, S. K. & Ng, T. B. (2014). Banana lectin: A brief review. Molecules 19(11), 18817–18827.

Singh, R., Paul, D. & Jain, R.K. (2006). Biofilms: implications in bioremediation. *Trends Microbiol* 14(9), 389-397.

Sjulin, T.M. & Beer, S.V. (1978). Mechanism of wilt induction by amylovorin in *Cotoneaster* shoots and its relation to wilting of shoots infected by *Erwinia amylovora*. *Phytopathology* 68, 89.

Solano, C., García, B., Valle, J., Berasain, C., Ghigo, J.M., Gamazo, C. & Lasa, I. (2002). Genetic analysis of *Salmonella enteritidis* biofilm formation: Critical role of cellulose. *Mol Microbiol* 43(3), 793–808.

Spiers, A.J., Bohannon, J., Gehrig, S.M., & Rainey, P.B. (2003). Biofilm formation at the air-liquid interface by the *Pseudomonas fluorescens* SBW25 wrinkly spreader requires an acetylated form of cellulose. *Mol Microbiol* 50(1), 15–27.

Spiers, A.J., Deeni, Y.Y., Folorunso, A.O., Koza, A., Moshynets, O. & Zawadzki K. (2013). Cellulose expression in *Pseudomonas fluorescens* SBW25 and other environmental pseudomonads. Theo van de Ven and Louis Godbout. *Cellulose - Medical, Pharmaceutical and Electronic Applications*. IntechOpen.

Spiers, A.J., Kahn, S.G., Bohannon, J., Travisano, M. & Rainey, P.B. (2002). Adaptive divergence in experimental populations of *Pseudomonas fluorescens*. I. Genetic and phenotypic bases of wrinkly spreader fitness. *Genetics*, 161(1), 33–46.

Spiers, A.J. & Rainey, P.B. (2005). The *Pseudomonas fluorescens* SBW25 wrinkly spreader biofilm requires attachment factor, cellulose fibre and LPS interactions to maintain strength and integrity. *Microbiology* 151(9), 2829–2839.

Spormann, A.M. (2008). Physiology of microbes in biofilms. *Curr Top Microbiol Immunol* 322, 17-36.

Stanley, N.R. & Lazazzera, B.A. (2004). Environmental signals and regulatory pathways that influence biofilm formation. *Mol Microbiol* 52, 917-924.

Stapper, A. P., Narasimhan, G., Ohman, D. E., Barakat, J., Hentzer, M., Molin, S., Kharazmi, A., Høiby, N. & Mathee, K. (2004). Alginate production affects *Pseudomonas aeruginosa* biofilm development and architecture, but is not essential for biofilm formation. *J Med Microbiol* 53(7), 679–690.

Starkey, M., Hickman, J.H., Ma, L., Zhang, N., De Long, S., Hinz, A., Palacios, S.,

Manoil, C., Kirisits, M.J., Starner, T.D., Wozniak, D.J., Harwood, C.S. & Parsek, M.R. (2009). *Pseudomonas aeruginosa* rugose small-colony variants have adaptations that likely promote persistence in the cystic fibrosis lung. *J Bacteriol* 191(11), 3492-3503.

Stewart, P.S. Diffusion in biofilms. *J Bacteriol* 185(5), 1485-1491.

Sun, D., Zhuo, T., Hu, X. Fan, X. & Zou, H. (2017). Identification of a *Pseudomonas putida* as biocontrol agent for tomato bacterial wilt disease. *Biol Control* 114, 45-50.

Sundin, G.W., Kidambi, S.P., Ullrich, M. & Bender, C.L. (1996). Resistance to ultraviolet light in *Pseudomonas syringae*: sequence and functional analysis of the plasmid-encoded *rulAB* genes. *Gene* 177(1-2), 77-81.

Sutherland I.W. (1999) Biofilm Exopolysaccharides. In: Wingender J., Neu T.R., Flemming HC. (eds) *Microbial Extracellular Polymeric Substances.* Heidelberg (Germany): Springer, Berlin.

Sutherland, I.W. (2001). The biofilm matrix- an immobilized but dynamic microbial environment. *Trends Microbiol* 9(5), 222-227.

Svenningsen, N.B., Martínez-García, E., Nicolaisen, M.H., de Lorenzo, V. & Nybroe, O. (2018). The biofilm matrix polysaccharides cellulose and alginate both protect *Pseudomonas putida* mt-2 against reactive oxygen species generated under matric stress and copper exposure. *Microbiology* 164(6), 883-888.

T

Taglialegna, A., Lasa, I. & Valle, J. (2016). Amyloid structures as biofilm matrix scaffolds. *J Bacteriol* 198(19), 2579–2588.

Terry, J.M., Piña, S.E. & Mattingly, S.J. (1991). Environmental conditions which influence mucoid conversion *Pseudomonas aeruginosa* PAO1. *Infect Immun* 59(2), 471-277.

Thies, J.E & Grossman, J. M. (2008) The soil habitat and soil ecology. In: Nautiyal C.S., Dion P. (eds) *Molecular Mechanisms of Plant and Microbe Coexistence. Soil Biology, vol 15.* Heidelberg (Germany), Springer, Berlin.

Thornton & Basu *et al*. (2015). Preface: PCR primer design. *Methods Mol. Biol.* 1275, 173-9.

U

Ude, S., Arnold, D.L., Moon, C.D., Timms-Wilson, T. & Spiers, A.J. (2006). Biofilm formation and cellulose expression among diverse environmental *Pseudomonas* isolates. *Environ Microbiol* 8(11), 1997-2011.

V

Vishwakarma, V. (2020). Impact of environmental biofilms: Industrial components and its remediation. *J Basic Microbiol* 60, 198– 206.

Vorholt, J.A. Microbial life in the phyllosphere. (2012). *Nat Rev Microbiol* 10(12), 828-840.

W

Walker, T.S., Bais, H.P., Déziel, E., Schweizer, H.P., Rahme, L.G., Fall, R. & Vivanco, J.M. (2004). *Pseudomonas aeruginosa*-plant root interactions. Pathogenicity, biofilm formation, and root exudation. *Plant Physiol* 134(1), 320-331.

Wang, S., Parsek, M.R., Wozniak, D.J. & Ma, L.Z. (2013). A spider web strategy of type IV pili-mediated migration to build a fibre-like Psl polysaccharide matrix in *Pseudomonas aeruginosa* biofilms. *Environ Micriobiol* 15, 2238–2253.

Wang, S., Yu, S., Zhang, Z., Wei, Q., Yan, L., Ai, G., Liu, H., Ma, L.Z. (2014). Coordination of swarming motility, biosurfactant synthesis, and biofilm matrix exopolysaccharide production in *Pseudomonas aeruginosa*. *Appl Environ Microbiol* 80(21), 6724–6732.

Wheatley, R. M. & Poole, P. S. (2018). Mechanisms of bacterial attachment to roots. *FEMS Microbiol Rev* 42, 448–461.

Whitchurch, C.B., Tolker-Nielsen, T., Ragas, P.C. & Mattick, J.S. (2002). Extracellular DNA required for bacterial biofilm formation. *Science* 295(5559), 1487.

Willis, D.K., Holmstadt, J.J. & Kinscherf, T.G. (2001). Genetic evidence that loss of

virulence associated with *gacS* or *gacA* mutations in *Pseudomonas syringae* B728a does not result from effects on alginate production. *Appl Environ Microbiol* 67(3), 1400-1403.

Wood, P.J., Erfle, J.D. & Teather, R.M. (1988). Use of complex formation between Congo Red and polysaccharides in detection and assay of polysaccharide hydrolases. *Methods Enzymol* 160, 59-74.

Wozniak, D.J., Wyckoff, T.J.O., Starkey, M., Keyser, R., Azadi, P., O'Toole, G.A. & Parsek, M.R. (2003). Alginate is not a significant component of the extracellular polysaccharide matrix of PA14 and PAO1 *Pseudomonas aeruginosa* biofilms. *Proc Natl Acad Sci USA* 100(13), 7907–7912.

X

Xie, Y., Shao, X. & Deng, X. (2019). Regulation of type III secretion system in *Pseudomonas syringae*. *Environ Microbiol* 21(12), 4465-4477.

Xin, X.F., Kvitko, B. & He, S.Y. (2018). *Pseudomonas syringae*: what it takes to be a pathogen. *Nat Rev Microbiology.* 16(5), 139–148.

Y

Yang, S., Cheng, X., Jin, Z., Xia, A., Ni, L., Zhang, R. & Fan, J. (2018). Differential production of Psl in planktonic cells leads to two distinctive attachment phenotypes in *Pseudomonas aeruginosa*. *Appl Environ Microbiol* 84(14), 1–18.

Yin, W., Wang, Y., Liu, L. & He, J. (2019). Biofilms: the microbial "protective clothing" in extreme environments. *Int J Mol Sci* 20(14), 3423.

Ymele-Leki, P. & Ross, J.M. (2007). Erosion from *Staphylococcus aureus* biofilms grown under physiologically relevant fluid shear forces yields bacterial cells with reduced avidity to collagen. *Appl Environ Microbiol* 73(6), 1834-1841.

Young, A. 2008. Notes on *Pseudomonas syringae* pv. syringae bacterial necrosis of mango (*Mangifera indica*) in Australia. *Australas Plant Dis Notes* 3, 138-140.

Young, J. M. (2010). Taxonomy of *Pseudomonas syringae*. *J. Plant Pathol.* 92.

Yu, J., Peñaloza-Vázquez, A., Chakrabarty, A.M. & Bender, C.L. (1999).

Involvement of the exopolysaccharide alginate in the virulence and epiphytic fitness of *Pseudomonas syringae* pv. syringae. *Mol Microbiol* 33(4), 712–720.

Z

Zapotoczna, M., O'Neill, E. & O'Gara, J.P. (2016). Untangling the diverse and redundant mechanisms of *Staphylococcus aureus* biofilm formation. *PLoS Pathog* 12(7), e1005671.

Zevenhuizen, L.P.T.M., Bertocchi, C. & Van Neerven, A.R.W. (1986). Congo red absorption and cellulose synthesis by Rhizobiaceae. *Antonie van Leeuwenhoek* 52, 381–386.

Zeriouh, H., de Vicente, A., Pérez-García, A. & Romero, D. (2014). Surfactin triggers biofilm formation of *Bacillus subtilis* in melon phylloplane and contributes to the biocontrol activity. *Environ Microbiol* 16(7), 2196-2211.

Zhao, K., Tseng, B.S., Beckerman, B., Jin, F., Gibiansky, M.L., Harrison, J.J., Luijten, E., Parsek, M.R. & Wong, G.C.L. (2013). Psl trails guide exploration and microcolony formation in early *P. aeruginosa* biofilms. *Nature* 497(7449), 388–391.

Zlosnik, J.E.A., Hird, T.J., Fraenkel, M.C., Moreira, L.M., Henry, D.A. & Speert, D.P. (2008). Differential mucoid exopolysaccharide production by members of the *Burkholderia cepacia* complex. *J Clin Microbiol* 46(4), 1470-1473.

Zogaj, X., Nimtz, M., Rohde, M., Bokranz, W. & Römling, U. (2001). The multicellular morphotypes of *Salmonella typhimurium* and *Escherichia coli* produce cellulose as the second component of the extracellular matrix. *Mol Microbiol* 39(6), 1452–1463.

Zumaquero, A., Macho, A.P., Rufián, J.S. & Beuzón, C.R. (2010). Analysis of the role of the type III effector inventory of *Pseudomonas syringae* pv. phaseolicola 1448a in interaction with the plant. *J Bacteriol* 192(17), 4474–4488.

APPENDIX 1

Appendix 1

Table S1. Primers used in Chapter 1.

Primers code	Primers sequence 5'→3'	Use	Reference
*alg8*_fw_up	CGTCGTTATCCCGATTCTGG	To amplify *alg8* upstream sequence (1039 bp)	This study
*alg8*_HindIII_rv_up	*CCCTATAGTGAGTC*AAGCTTCGTATCCCTAAGTCAGTTGC		
*alg8*_HindIII_fw_down	AAGCTT*GACTCACTATAGGG*ATGAATACAGCCGTGAATGC	To amplify *alg8* downstream sequence (1044 bp)	This study
*alg8*_rv_down	CGCTCAGGTTGGTGCTGCTG		
*wssE*_fw_up	CAACCACAGCACCTCCGAAG	To amplify *wssE* upstream sequence (1022 bp)	This study
*wssE*_HindIII_rv_up	*CCCTATAGTGAGTC*AAGCTTGACGTCTCCCAGGATAATTTG		
*wssE*_HindIII_fw_down	AAGCTT*GACTCACTATAGGG*ATGCCTTCCGTTCTTGCCGG	To amplify *wssE* downstream sequence (1023 bp)	This study
*wssE*_rv_down	CTACCGTCGGACTGTGCGGT		
*pslE*_fw_up	CACACGCATCGTCTGGTCAA	To amplify *pslE* upstream sequence (1090 bp)	This study
*pslE*_HindIII_rv_up	*CCCTATAGTGAGTC*AAGCTTGTCTGTTTCCCTGACAATTA		
*pslE*_HindIII_fw_down	AAGCTT*GACTCACTATAGGG*CGGATCGGGAGCCGAGGCTG	To amplify *pslE* downstream sequence (1042 bp)	This study
*pslE*_rv_down	CATGCCGTTGCCATGCGAGA		
Check_*alg8*_fw	ACATCGTCTACCCGCACTTG	To amplify a fragment within *alg8* gene (1212 bp)	This study
Check_*alg8*_rv	TGTTGAACCAGCCCTGAAAG		
Check_*wssE*_fw	GTTAGTCATCGGGTTGGTTG	To amplify a fragment within *wssE* gene (1515 bp)	This study
Check_*wssE*_rv	TCGTCAGTCTTGAGGTACAG		

Appendix 1

Check_*pslE*_fw Check_*pslE*_rv	CGGTGAAGAACGGCATCAAG GCGGTGTTGAGGTTGTTGAG	To amplify a fragment within *pslE* gene (1549 bp)	This study
Check_Km_fw Check_Km_rv	GAAAGCCAGTCCGCAGAAAC CATCAGAGCAGCCGATTGTC	To amplify a fragment within kanamicine cassette (395 bp)	This study
Compl_HindIII_*alg8*_fw Compl_BamHI_*alg8*_rv	AAAAAGCTTGCTTGCAGCCTGGGGCTTGA AATCTAGATCAAACCATCGTCAACAGCA	To amplify the *alg8* gene and *rbs* sequence (1530 bp)	This study
Compl_HindIII_*wssE*_fw Compl_BamHI_*wssE*_rv	AAAAAGCTTCTATCAGTTCCGTGAAGACG AATCTAGATCAGTTGGAATAAGGTGAAC	To amplify the *wssE* gene and *rbs* sequence (3924 bp)	This study
Compl_HindIII_*pslE*_fw Compl_BamHI_*pslE*_rv	AAAAAGCTTCATGAATTACGAGCTGCGCA AATCTAGATCAGCCTCGGCTCCCGATCC	To amplify the *pslE* gene and *rbs* sequence (2040 bp)	This study
qRT-PCR158_*gyrB*_F qRT-PCR158_*gyrB*_R	TGCTGACCTTCTTCTTCCGT AGATACCTGGAGCCGATTCG	To amplify a fragment of the *gyrB* gene by q-RT-PCR (198 bp)	This study
qRT-PCR158_*rpoD*_F qRT-PCR158_*rpoD*_R	CGAAGAAGGCATCCGTGAAG CTCAGAACATCGGAAAGGCG	To amplify a fragment of the *rpoD* gene by q-RT-PCR (120 bp)	This study
qRT-PCR158_*rhlA*_F qRT-PCR158_*rhlA*_R	TCAGCCAGATTCGCCAACTA CCTTGCTTTCCAGGTCCAGA	To amplify a fragment of the *rhlA* gene by q-q-RT-PCR (198 bp)	This study
qRT-PCR_*pslD*_F qRT-PCR_*pslD*_R	TGTTTCAGGTGCTCAACGAC GGGAAATGTTGATGGTCAGC	To amplify a fragment of the *pslD* gene by q-RT-PCR (150 bp)	This study

Appendix 1

qRT-PCR_*pslF*_F	*CGTGATGGTTCTGCCCTATC*	*To amplify a fragment of the* pslF *gene by q-RT-PCR (154 pb)*	*This study*
qRT-PCR_*pslF*_R	GTTGCCATGCGAGACTTCTT		
B1	CTTTCCGTGGTCTTGATGAGG	To amplify a fragment of the *syrB* gene (752 pb)	Sorensen *et al.*, 1998
B2	TCGATTTTGCCGTGATGAGTC		

Nucleotide bases in italics show the sequences used for the phusion of the fragments amplified for mutation. Underlined bases show restriction sequences.

Appendix 1

Table S2. Primers used in Chapter 3.

Primers code	Primers sequence 5'→3'	Use	Reference
*alg8*_fw_up	CGATCAAGGACTACGACTTC	To amplify *alg8* upstream	
*alg8*_HindIII_rv_up	*CCCTATAGTGAGTCAAGCTT*CCGTCTCGATCTCGGGCGAG	sequence (1023 pb)	This study
*alg8*_HindIII_fw_down	*AAGCTTGACTCACTATAGGG*CCCGCCTTGCCTGAATTAAC	To amplify *alg8* downstream	
*alg8*_rv_down	GCTGACGATGGTGCCGCTGC	sequence (1040 bp)	This study
*pslE*_fw_up	CGGAGAAGGCAAGCGTTATG	To amplify *pslE* upstream	
*pslE*_HindIII_rv_up	*CCCTATAGTGAGTCAAGCTT*TGGTGGAGGCCGATCAAACG	sequence (1063 bp)	This study
*pslE*_HindIII_fw_down	*AAGCTTGACTCACTATAGGG*CCTGATGCGTATCGTCCTG	To amplify *pslE* downstream	
*pslE*_rv_down	GGACATCGCCTTGCTCGTAG	sequence (1026 bp)	This study
*fapBC*_fw_up	GCTGGCTGGAAAGCGAACTG	To amplify *fapBC* upstream	
*fapBC*_HindIII_rv_up	*CCCTATAGTGAGTCAAGCTT*CTCATTGGCCTCCGGCCAGC	sequence (1021 bp)	This study
*fapBC*_HindIII_fw_down	*AAGCTTGACTCACTATAGGG*AAAGCAACTCGCTGTCCATC	To amplify *fapBC* downstream	
*fapBC*_rv_down	GGTGCTGCTCATGACGATGC	sequence (1006 bp)	This study
Check_*alg8*_fw	GCTACATCATGAGCGAATGG	To amplify a fragment within	
Check_*alg8*_rv	ATAGAGAATCAGCGGGTAGG	*alg8* gene sequence (617 bp)	This study
Check_*pslE*_fw	GGAAGACCCTCAAGTTCTAC	To amplify a fragment within	This study
Check_*pslE*_rv	TTCTGCTCGATCTGCTTGAC	*pslE* gene sequence (655 bp)	
Check_*fapBC*_fw	CTCGGGAGCAACTGACATTC	To amplify a fragment within	This study
Check_*fapBC*_rv	TTATGCCCGCCATGGTTGTC	*fapBC* genes sequences (315 bp)	

Appendix 1

Km_fw Km_rv	GAAAGCCAGTCCGCAGAAAC CATCAGAGCAGCCGATTGTC	To amplify a fragment within the Km cassette sequence (395 bp)	This study
Compl_HindIII_*alg8*_fw Compl_XbaI_*alg8*_rv	AAAAAGCTTCCTTAACCCCATCGGGCCAC AATCTAGATCAGACCATCAGCAGCAGCG	To amplify the *alg8* gene and *rbs* sequence (1539 bp)	This study
Compl_HindIII_*pslEF*_fw Compl_XbaI_*pslEF*_rv	AAAAAGCTTTCGGCCTCCACCAGCCATGG AATCTAGATCATGACGACCGCTCCTTGC	To amplify the *pslEF* genes and *rbs* sequence (3212 bp)	This study
Compl_HindIII_*fapBC*_fw Compl_XbaI_*fapBC*_rv	AAGGATCCCAAGGGCTGAATGTCGTCAC AATCTAGATTACATGCAGGCCTTGCAGC	To amplify *fapBC* genes and *rbs* sequence (1816 bp)	This study
XbaI_Gm_fw BamHI_Gm_rv	AATCTAGAGTCGCCTTGCGTATAATATT AAGGATCCTTAGGTGGCGGTACTTGGGT	Gentamycin cassette of the pBBR1MCS5 plasmid (1816 bp) and clone it into pFLP2 plasmid	This study

Nucleotide bases in italics show the sequences used for the phusion of the fragments amplified for mutation. Underlined bases show restriction sequences.

Appendix 1

Table S3. Representative strains belonging to plant-associated phylogenetic groups of the *Pseudomonas syringae* complex.

Strain	Code	Isolation	Phylogroup	Accession number
Pseudomonas syringae pv. aceris strain ICMP2802	PsaICMP2802PG2	Acer sp.	2	NZ_LJPM00000000.1
Pseudomonas syringae pv. aceris strain A10853	PsaA10853PG2	-	2	NZ_LGAR00000000.1
Pseudomonas syringae pv. syringae B728a	PssB728aPG2	Bean	2	NZ_QJTV00000000.1
Pseudomonas syringae pv. syringae B301D	PssB301DPG2	Pear	2	NZ_CP005969.1
Pseudomonas syringae pv. aptata str. DSM50252	PsaDSM50252PG2	Sugar beet	2	AEAN00000000.1
Pseudomonas syringae pv. atrofaciens strain LMG5095	PsaLMG5095PG2	Common wheat	2	NZ_CP028490.1
Pseudomonas syringae pv. syringae UMAF0158	PssUMAF0158PG2	Mango	2	NZ_CP005970.1
Pseudomonas caricapapayae ICMP2855	PcICMP2855PG6	*Carica papaya*	6	NZ_LJPW00000000.1
Pseudomonas syringae pv. helianthi strain ICMP4531	PshICMP4531PG6	Sunflower	6	NZ_LJQM00000000.1
Pseudomonas syringae pv. tagetis strain ICMP4091	PstICMP4091PG6	*Tagetes erecta*	6	NZ_LJRM00000000.1
Pseudomonas savastanoi pv. savastanoi NCPPB 3335	PssNCPPB3335PG3	Olive	6	NZ_CP008742.1
Pseudomonas savastanoi pv. phaseolicola 1448A	Psp1448APG3	Bean	3	NC_005773.3
Pseudomonas savastanoi pv. glycinea strain ICMP2189	PsgICMP2189PG3	Soybean	3	NZ_LJQL00000000.1
Pseudomonas coronafaciens pv. coronafaciens strain 3113	Pc3113PG4	Oat	4	NZ_RBUJ00000000.1

Appendix 1

Pseudomonas coronafaciens pv. porri strain ICMP8961	PcpICMP8961PG4	Leek	4	NZ_LJRA00000000.1
Pseudomonas coronafaciens pv. oryzae strain I_6	Pc1_6PG4	Rice	4	NZ_CP046035.1
Pseudomonas coronafaciens pv. garcae strain ICMP4323	PcgICMP4323PG4	Coffee	4	NZ_LJQK00000000.1
Pseudomonas cannabina strain ICMP 2823	PcICMP2823PG5	Hemp	5	NZ_FNKU00000000.1
Pseudomonas cannabina strain ICMP 2821	PcICMP2821PG5	Hemp	5	NZ_RBOW00000000.1
Pseudomonas syringae pv. coriandricola strain ICMP12471	PscICMP12471PG5	Coriander	5	NZ_LJPZ00000000.1
Pseudomonas syringae CC1557	PsCC1557	Snow	10	NZ_CP007014.1
Pseudomonas syringae pv. actinidiae str. NCPPB 3871	PsaNCPPB3871PG1	Kiwi	1	NZ_LKEN00000000.1
Pseudomonas syringae pv. actinidiae str. NCPPB 3739	PsaNCPPB3739PG1	Kiwi	1	NZ_AFTH00000000.1
Pseudomonas syringae pv. delphinii strain ICMP529	PsdICMP529PG1	*Delphinium* sp.	1	NZ_LJQH00000000.1
Pseudomonas syringae pv. tomato str. DC3000	Pst3000PG1	Tomato	1	NC_004578.1
Pseudomonas syringae pv. apii strain ICMP2814	PsaICMP2814PG1	Celery	1	NZ_LJPR00000000.1
Pseudomonas syringae pv. tomato NCPPB 1108	PstNCPPB1108PG1	Tomato	1	NZ_ADGA00000000.1
Pseudomonas syringae pv. maculicola strain ICMP3935	PsmICMP3935PG1	Broccoli	1	NZ_LJQR00000000.1
Pseudomonas viridiflava strain CFBP 1590	PvCFBP1590PG7_8	Tomato	7	NZ_LT855380.1

Appendix 1

Pseudomonas syringae pv. primulae strain ICMP3956	PspICMP3956PG7	*Primula* sp.	7	NZ_LJRC00000000.1
Pseudomonas syringae pv. ribicola strain ICMP3882	PsrICMP3882PG7	Golden currant	7	NZ_LJRF00000000.1
Pseudomonas cichorii strain ICMP 3353	PcICMP3353PG11	Tomato	11	NZ_RBRE00000000.1
Pseudomonas cichorii strain ICMP 6917	PcICMP6917PG11	Safflower	11	NZ_RBRY00000000.1
Pseudomonas cichorii strain ICMP 1649	PcICMP1649PG11	Celery	11	NZ_RBPN00000000.1
Pseudomonas aeruginosa PAO1	PaPAO1	Outgroup	-	NC_002516.2

Table S4. Representative strains belonging to the *Pseudomonas fluorescens* complex.

Strain	Code	Isolation	Phylogroup	Accession number	Presence of a *psl*-like gene cluster
Pseudomonas fluorescens SBW25	>PfSBW25	-	*fluorescens*	NC_012660.1	Yes
Pseudomonas azotoformans S4	>PazS4	Soil	*fluorescens*	NZ_CP014546.1	Yes
Pseudomonas simiae 2-36	>Psimiae2-36	Soil	*fluorescens*	NZ_JRMC00000000.1	Yes
Pseudomonas tolaasii PMS117	>PtoPMS117	Mushroom cap	*fluorescens*	NZ_AJXG00000000.1	Yes
Pseudomonas rhodesiae FF9	>PrhodFF9	-	*fluorescens*	NZ_CCYI00000000.1	Yes
Pseudomonas orientalis DSM 17489	>PoriDSM17489	Water	*fluorescens*	NZ_JYLM00000000.1	Yes
Pseudomonas fluorescens WH6	>PfWH6	Rhizosphere	*fluorescens*	NZ_CM001025.1	No
Pseudomonas fluorescens BS2	>PfBS2	Soil	*fluorescens*	NZ_AMZG00000000.1	No
Pseudomonas poae RE*1-1-14	>PpoaeRE1-1-14	Endorhiza	*fluorescens*	NC_020209.1	Yes
Pseudomonas trivialis DSM14937	>PtriDSM14937	Phyllosphere	*fluorescens*	NZ_JYLK00000000.1	Yes
Pseudomonas extremaustralis 14-3	>Pe14-3	Water	*fluorescens*	NZ_AHIP00000000.1	No
Pseudomonas sp. KG01	>PKG01	Soil	*fluorescens*	NZ_LFMW00000000.1	No
Pseudomonas veronii DSM 11331	>PvDSM11331	Water	*fluorescens*	NZ_JYLL00000000.1	No
Pseudomonas veronii R4	>PvR4	Soil	*fluorescens*	NZ_JXWQ00000000.2	No
Pseudomonas veronii 1YB2	>Pv1YB2	Soil	*fluorescens*	NZ_JGYI00000000.1	No
Pseudomonas veronii 1YdBTEX2	>Pv1YdBTEX2	-	*fluorescens*	LT599583.1	No
Pseudomonas fluorescens FH5	>PfFH5	Water	*fluorescens*	NZ_AOJA00000000.1	Yes
Pseudomonas fluorescens A506	>PfA506	Leaf	*fluorescens*	NC_017911.1	Yes

Appendix 1

Pseudomonas fluorescens SS101	>PfSS101	Rhizosphere	*fluorescens*	NZ_AHPN00000000.1	Yes
Pseudomonas sp. BRG-100	>PBRG100	Soil	*fluorescens*	NZ_JPRX00000000.1	Yes
Pseudomonas synxantha BG33R	>PsBG33R	Rhizosphere	*fluorescens*	NZ_CM001514.1	Yes
Pseudomonas synxantha DSM18928	>PsynxDSM18928	Cream	*fluorescens*	NZ_JYLJ00000000.1	Yes
Pseudomonas libanensis strain RIT-PI-g	>PlibRITPIg	Steam	*fluorescens*	NZ_LHOY00000000.1	Yes
Pseudomonas fluorescens strain LBUM223	>PfLBUM223	-	*fluorescens*	NZ_CP011117.2	Yes
Pseudomonas sp. Ag1	>PAg1	Mosquito	*gessardii*	NZ_AKVH00000000.1	Yes
Pseudomonas sp. PAMC26793	>PPAMC26793	Grass	*gessardii*	NZ_AMXG00000000.1	Yes
Pseudomonas UK4	>PfUK4	-	*gessardii*	NZ_CP008896.1	No
P. sp. FH4	>PFH4	Water	*gessardii*	NZ_AOHN00000000.1	Yes
P. fluorescens GcM5-1A	>PfGcM5-1A	Nematode	*gessardii*	NZ_JJOE00000000.1	Yes
P. fluorescens NCIMB11764	>PfNCIMB11764	-	*mandelii*	NZ_CP010945.1	No
Pseudomonas GM21	>PGM21	Root	*mandelii*	NZ_AKJS00000000.1	Yes
Pseudomonas GM18	>PGM18	Root	*mandelii*	NZ_AKJT00000000.1	No
Pseudomonas GM78	>PGM78	Root	*jessenii*	NZ_AKJF00000000.1	No
Pseudomonas G5(2012)	>PG5(2012)	-	*jessenii*	NZ_APIO00000000.1	No
Pseudomonas UW4	>PUW4	Fermentation liquor	*jessenii*	NC_019670.1	No
Pseudomonas fluorescens Pf0-1	>PfPf01	-	*koreensis*	NC_007492.2	No
Pseudomonas fluorescens R124	>PfR124	Orthoquartzite cave surface	*koreensis*	NZ_CM001561.1	No

Appendix 1

Pseudomonas fluorescens NZ011	>PfNZ011	-	*koreensis*	NZ_AJXJ00000000.1	No
Pseudomonas chlororaphis O6	>PcO6	-	*chlororaphis*	NZ_CM001490.1	Yes
Pseudomonas chlororaphis PA23	>PcPA23	Root	*chlororaphis*	NZ_CP008696.1	Yes
Pseudomonas chlororaphis PCL1606	>PcPCL1606	Root	*chlororaphis*	NZ_CP011110.1	Yes
Pseudomonas protegens CHA0	>PpCHA0	-	*protegens*	NC_021237.1	Yes
Pseudomonas protegens Cab57	>PpCab57	-	*protegens*	NZ_AP014522.1	Yes
Pseudomonas protegens Pf-5	>PpPf5	-	*protegens*	NZ_CP032358.1	Yes
Pseudomonas fluorescens NZI7	>PpNZI7	Mushroom	*protegens*	NZ_AJXF00000000.1	No
Pseudomonas PSt29	>PSt29	Soil	*protegens*	NZ_AP014628.1	No
Pseudomonas Os17	>POs17	Soil	*protegens*	NZ_AP014627.1	No
Pseudomonas fluorescens F113	>PfF113	-	*corrugata*	NC_016830.1	No
Pseudomonas fluorescens Q2-87	>PfQ287	-	*corrugata*	NZ_CM001558.1	No
Pseudomonas fluorescens Pf29Arp	>Pf29Arp	-	*corrugata*	NZ_ANOR00000000.1	No
Pseudomonas syringae pv. syringae UMAF0158	>PssUMAF0158	Mango	-	NZ_CP005970.1	Yes
Pseudomonas aeruginosa PAO1	>PAO1	-	outgroup	NC_002516.2	Yes

Appendix 1

Table S5. Comparison of proteins encoded by the alginate gene cluster of *Pseudomonas syringae* pv. syringae B728a and *Pseudomonas syringae* pv. syringae UMAF0158.

***P. syringae* pv. syringae B728a**			***P. syringae* pv. syringae UMAF0158**			
Protein	**Protein size (aa)**	**Function**	**Protein**	**Identity PssB728a (%)**	**Protein size (aa)**	**Function**
AlgD Psyr_1063	438	GDP-mannose 6-dehydrogenase	**Psyrmg_RS21330**	99.09	438	GDP-mannose 6-dehydrogenase
Alg8 Psyr_1062	493	Alginate biosynthesis protein Alg8	**Psyrmg_RS21325**	100	493	Glycosyltransferase
Alg44 Psyr_1061	390	Alginate biosynthesis protein Alg44	**Psyrmg_RS21320**	99.23	390	Hemolysin D
AlgK Psyr_1060	470	Sel1 repeat-containing protein	**Psyrmg_RS21315**	99.94	470	Alginate biosynthesis protein AlgK
AlgE Psyr_1059	494	Alginate biosynthesis protein AlgE	**Psyrmg_RS21310**	99.39	494	Alginate biosynthesis protein AlgE
AlgG Psyr_1058	536	Parallel beta-helix repeat-containing protein	**Psyrmg_RS21305**	98.32	536	Poly (beta-D-mannuronate) C5 epimerase
AlgX Psyr_1057	479	Alginate biosynthesis protein	**Psyrmg_RS21300**	98.75	479	Alginate O-acetyltransferase

Appendix 1

AlgL Psyr_1056	378	Poly (beta-D-mannuronate) O-acetylase	**Psyrmg_RS21295**	98.68	378	Alginate lyase
AlgI Psyr_1055	518	Membrane bound O-acyltransferase	**Psyrmg_RS21290**	98.84	518	Poly (beta-D-mannuronate) O-acetylase
AlgJ Psyr_1054	391	Alginate biosynthesis protein	**Psyrmg_RS21285**	97.95	391	Alginate O-acetyltransferase
AlgF Psyr_1053	221	Alginate biosynthesis protein	**Psyrmg_RS21280**	96.85	222	Alginate O-acetyltransferase
AlgA Psyr_1052	483	Mannose-1-phosphate guanylyltransferase	**Psyrmg_RS21275**	100	483	Mannose-1-phosphate guanylyltransferase

The Psyr_1052-Psyr_1063 region of PssB728a encodes alginate polysaccharide, and the Psyrmg_RS21275-Psyrmg_RS21330 region of PssUMAF0158 was identified as an orthologue. The table shows the sizes of the proteins as the number of amino acids, their putative functions and the percentage of identity between the two strains being compared. Putative functions have been obtained from the Pseudomonas Genome Database (https://www.pseudomonas.com/).

Table S6. Comparison of proteins encoded by the *psl* gene cluster of *P. aeruginosa* PAO1 and *P. syringae* pv. syringae UMAF0158.

***P. aeruginosa* PAO1**			***P. syringae* pv. syringae UMAF0158**			
Protein	**Protein size (aa)**	**Function**	**Protein**	**Identity PAO1 (%)**	**Protein size (aa)**	**Function**
PslA PA2231	478	Putative glycosyl transferase	**Psyrmg_RS06720**	65.48	478	Capsular polysaccharide biosynthesis protein
PslB PA2232	488	Mannose-1-phosphate guanylyltransferase/ 6-phosphate isomerase	**Psyrmg_RS06725**	72.03	485	Mannose-1-phosphate guanylyltransferase
PslC PA2233	303	Glycosyltransferase family 2 protein	**Psyrmg_RS00890***	48.84	308	Rhamnosyltransferase
PslD PA2234	256	Polysaccharide biosynthesis/ export protein	**Psyrmg_RS06730**	50.39	259	Sugar ABC transporter substrate-binding protein
PslE PA2235	662	Lipopolysaccharide biosynthesis protein	**Psyrmg_RS06735**	53.32	663	Exopolysaccharide biosynthesis protein
PslF PA2236	395	Glycosyltransferase	**Psyrmg_RS06740**	63.64	392	Glycosyl transferase family 1
PslG PA2237	442	β-xylosidase	**Psyrmg_RS06745**	51.71	437	β-xylosidase
PslH PA2238	402	Glycosyltransferase	**Psyrmg_RS06750**	58.17	405	Glycosyltransferase

PslI PA2239	367	Glycosyltransferase family 4 protein	**Psyrmg_RS06755**	55.19	366	Group 1 glycosyltransferase
PslJ PA2240	478	O-antigen ligase-like membrane family protein	**Psyrmg_RS06760**	53.74	471	Hypothetical protein
PslK PA2241	469	Murein biosynthesis integral membrane protein MurJ	**Psyrmg_RS06770**	67.95	471	Hypothetical protein
PslL PA2242	355	Acyltransferase family protein	**Psyrmg_RS06765**	0	273	Acetyltransferase
PslM PA2243	577	FAD-dependent oxidoreductase	-	-	-	-
PslN PA2244	333	DNA topoisomerase B	**Psyrmg_RS04445***	59.28	356	DNA topoisomerase
PslO PA2245	101	Hypothetical protein	-	-	-	-

*These genes are located outside the putative *psl*-like cluster.

The PA2231-PA2245 region of PAO1 encodes a Psl polysaccharide, and the Psyrmg_RS06720-Psyrmg_RS06770 region of PssUMAF0158 was identified as similar. The PslC-like and PslN-like proteins seem to be encoded outside the *psl*-like cluster at Psyrmg_RS00890 and Psyrmg_RS04445. The *pslM* and *pslO* genes are missing, although they are not required to produce the polysaccharide (Byrd *et al.*, 2009). The *pslL* gene of PAO1 encodes for an acyltransferase that has no identity with any protein encoded in the PssUMAF0158 genome. However, the Psyrmg_RS06765 gene, located within the *psl*-like cluster, encodes an acetyltransferase that may replace the role of PslL in PssUMAF0158. In fact, this has already been illustrated in the *P. syringae* B728a strain, in which the acetyltransferase Psyr_3310 encoded by a gene located between *pslJ* and *pslK* may fulfil the normal function of *pslL* in *P. aeruginosa* strains (Mann *et al.*, 2012). The table shows the sizes of the proteins as the number of amino acids, their putative functions and the percentage of identity between the two strains being compared. Putative functions have been obtained from the Pseudomonas Genome Database (https://www.pseudomonas.com/).

Table S7. Protein domains encoded by the *psl*-like gene cluster of *Pseudomonas syringae* pv. syringae UMAF0158 strain.

Protein	Domains	Domain position	Domain description
Psyrmg_RS06720 (PslA-like)	CoA_binding_3 Bac_transf	70-248 284-472	CoA binding Bacteria sugar transferase
Psyrmg_RS06725 (PslB-like)	NTP_transf MannoseP_isomer	6-294 323-473	Nucleotidyl transferase Mannose-6-phosphate isomerase
Psyrmg_RS00890* (PslC-like)	Glyco_transf_2_3	9-173	Glycosyltransferase like family 2
Psyrmg_RS06730 (PslD-like)	Poly_export	47-130	Polysaccharide biosynthesis/export protein
Psyrmg_RS06735 (PslE-like)	No domains predicted	-	-
Psyrmg_RS06740 (PslF-like)	Glyco_transf_1	189-367	Glycosyl transferase group 1
Psyrmg_RS06745 (PslG-like)	Cellulase	47-279	Glycosyl hydrolase family 5
Psyrmg_RS06750 (PslH-like)	Glyco_trans_4_4 Glyco_trans_1_4	16-205 221-359	Glycosyl transferase 4-like domain Glycosyl transferase group 1
Psyrmg_RS06755 (PslI-like)	Glyco_trans_1	200-308	Glycosyl transferase group 1
Psyrmg_RS06760 (PslJ-like)	Wzy_C	252-380	O-Antigen ligase
Psyrmg_RS06765	Hexapep	202-235	Bacterial transferase hexapeptide (six repeats)
Psyrmg_RS06770 (PslK-like)	MurJ	28-434	Lipid II flippase MurJ
***Psyrmg_RS04445 (PslN-like)**	Topoisom_I	94-292	Eurkaryotic DNA topoisomerase I, catalytic core

*These genes are located outside the putative *psl*-like cluster.

Table S8. Protein domains encoded by the *psl* gene cluster of *Pseudomonas aeruginosa* PAO1.

Protein	Domains	Domain position	Domain description
PslA	CoA_binding_3 Bac_transf	70-248 284-472	CoA binding Bacteria sugar transferase
PslB	NTP_transf MannoseP_isomer	9-296 325-475	Nucleotidyl transferase Mannose-6-phosphate isomerase
PslC	Glyco_transf_2_3	3-220	Glycosyltransferase like family 2
PslD	Poly_export	49-129	Polysaccharide biosynthesis/export protein
PslE	GNVR	403-479	G-rich domain on putative tyrosine kinase
PslF	Glyco_transf_1	192-365	Glycosyltransferase group 1
PslG	Cellulase	48-285	Glycosyl hydrolase family 5
PslH	Glyco_trans_4_4 Glyco_trans_1_4	16-206 222-359	Glycosyltransferase 4-like domain Glycosyltransferase group 1
PslI	Glyco_trans_4 Glyco_trans_1_4	17-183 204-308	Glycosyltransferase family 4 Glycosyltransferase group 1
PslJ	No domains predicted	-	-
PslK	MurJ	30-442	Lipid II flippase MurJ
PslL	Acyl_trans_3	7-322	Acyltransferase family
PslM	FAD_binding_2	14-549	FAD binding domain
PslN	Topoisom_I	94-266	Eukaryotic DNA topoisomerase I, catalytic core
PslO	No domains predicted	-	-

Table S9. Comparison of proteins encoded by the cellulose operon of *P. syringae* pv. tomato DC3000 and *P. syringae* pv. syringae UMAF0158.

***P. syringae* pv. tomato DC3000**			***P. syringae* pv. syringae UMAF0158**			
Protein	**Protein size (aa)**	**Function**	**Protein**	**Identity DC3000 (%)**	**Protein size (aa)**	**Function**
WssA (Ptpto_1026)	381	Cellulose biosynthesis protein BcsQ	**Psyrmg_RS20465**	76.38	379	Cellulose biosynthesis protein BcsQ
WssB (Ptpto_1027)	739	Cellulose synthase (catalytic subunit)	**Psyrmg_RS20470**	95.13	739	Cellulose synthase (catalytic subunit)
WssC (Ptpto_1028)	751	Bacterial cellulose synthase subunit	**Psyrmg_RS20475**	94.54	751	Bacterial cellulose synthase subunit
WssD (Ptpto_1029)	403	Glycosyl hydrolase family 8	**Psyrmg_RS20480**	88.34	403	Glycosyl hydrolase family 8
WssE (Ptpto_1030)	1133	Cellulose synthase subunit BcsC	**Psyrmg_RS20485**	95.65	1291	Cellulose synthase subunit BcsC
WssF (Ptpto_1031)	221	O-acetyltransferase BcsX	**Psyrmg_RS20490**	98.19	221	O-acetyltransferase BcsX
WssG (Ptpto_1032)	224	O-acetyltransferase AlgF	**Psyrmg_RS20495**	87.95	224	O-acetyltransferase AlgF
WssH (Ptpto_1033)	471	Membrane bound O-acetyltransferase family	**Psyrmg_RS20500**	92.78	471	Membrane bound O-acetyltransferase family
WssI (Ptpto_1034)	383	Acetyltransferase AlgX	**Psyrmg_RS20505**	86.79	383	Acetyltransferase AlgX

The Pspto_1026-Pspto_1034 region of PtDC3000 encodes cellulose polysaccharide, and the Psyrmg_RS20465-Psyrmg_RS20505 region of PssUMAF0158 was identified as an orthologue. The table shows the sizes of the proteins as the number of amino acids, their putative functions and the percentage of identity between the two strains being

Appendix 1

compared. Putative functions have been obtained from the Pseudomonas Genome Database (https://www.pseudomonas.com/) and the Protein Family Software (PFAM) (https://pfam.xfam.org/).

Appendix 1

Table S10. Comparison of proteins encoded by the *fap* gene cluster between the *P. aeruginosa* PAO1 and *P. chlororaphis* PCL1606 strains.

***P. aeruginosa* PAO1**			***P. chlororaphis* PCL1606**			
Protein	**Protein size (aa)**	**Function**	**Protein**	**Identity PAO1 (%)**	**Protein size (aa)**	**Function**
FapA PA1956	162	Hypothetical protein	**PCL1606_RS15320**	41.67	150	Hypothetical protein
FapB PA1955	189	Hypothetical protein	**PCL1606_RS15325**	54.12	192	Autotransporter adhesin
FapC PA1954	340	Heme utilization or adhesion protein	**PCL1606_RS15330**	47.75	340	Heme utilization protein
FapD PA1953	226	Peptidase C39	**PCL1606_RS15335**	70.71	226	Peptidase C39
FapE PA1952	250	Hypothetical protein	**PCL1606_RS15340**	48.58	248	Hypothetical protein
FapF PA1951	421	Hypothetical protein	**PCL1606_RS15345**	66.90	429	Hypothetical protein

The PA1951-PA1956 genomic region of PAO1 encodes the Fap system, and the PCL1606_RS15320-PCL1606_RS15345 genomic region of PcPCL1606 was found to be similar. The table shows the percentage of identity between the proteins of the strains being compared, the size of the proteins as the number of amino acids (aa) and their putative function. Putative functions have been obtained from the Pseudomonas Genome Database (https://www.pseudomonas.com/).

Appendix 1

Table S11. Comparison of proteins encoded by the alginate gene cluster between the *P. aeruginosa* PAO1 and *P. chlororaphis* PCL1606 strains.

***P. aeruginosa* PAO1**			***P. chlororaphis* PCL1606**			
Protein	**Protein size (aa)**	**Function**	**Protein**	**Identity PAO1 (%)**	**Protein size (aa)**	**Function**
AlgD PA3540	436	GDP-mannose 6-dehydrogenase	**PCL1606_RS24735**	77.85	438	GDP-mannose dehydrogenase
Alg8 PA3541	494	Alginate biosynthesis protein	**PCL1606_RS24740**	84.01	496	Glycosyl transferase
Alg44 PA3542	389	Alginate biosynthesis protein	**PCL1606_RS24745**	57.92	389	Hemolysin D
AlgK PA3543	475	Alginate biosynthetic protein precursor	**PCL1606_RS24750**	59.69	456	Alginate biosynthesis protein
AlgE PA3544	490	Alginate production outer membrane protein precursor	**PCL1606_RS24755**	58.60	507	Alginate regulatory protein
AlgG PA3545	543	Alginate-C5-mannuronan-epimerase	**PCL1606_RS24760**	68.53	534	Poly(β-D-mannuronate) C5 epimerase

Appendix 1

AlgX PA3546	474	Alginate biosynthesis protein	**PCL1606_RS24765**	51.70	487	Alginate O-acetyltransferase
AlgL PA3547	367	Poly(β-D-mannuronate) lyase precursor	**PCL1606_RS24770**	64.74	374	Poly(β-D-mannuronate) lyase
AlgI PA3548	520	Alginate O-acetyltransferase	**PCL1606_RS24775**	78.48	521	Poly(β-D-mannuronate) O-acetylase
AlgJ PA3549	391	Alginate O-acetyltransferase	**PCL1606_RS24780**	55.18	391	Alginate O-acetyltransferase
AlgF PA3550	216	Alginate O-acetyltransferase	**PCL1606_RS24785**	64.65	218	Alginate O-acetyltransferase
AlgA PA3551	481	Phosphomannose isomerase/guanosine 5'-diphospho-D-mannose pyrophosphorylase	**PCL1606_RS24790**	80.64	483	Mannose-1-phosphate guanylyltransferase

The PA3540-PA3551 genomic region of PAO1 encodes alginate polysaccharide, and the PCL1606_RS24735-PCL1606_RS24790 genomic region of the PcPCL1606 strain was found to be similar. The conservation patterns between the proteins encoded by these regions are higher of 50 percent. The table shows the percentage of identity between the proteins of the strains being compared, the size of the proteins as the number of amino acids (aa) and their putative function. Putative functions have been obtained from the Pseudomonas Genome Database (https://www.pseudomonas.com/).

Appendix 1

Table S12. Comparison of proteins encoded by the *psl* cluster between the *P. aeruginosa* PAO1 and *P. chlororaphis* PCL1606 strains.

***P. aeruginosa* PAO1**			***P. chlororaphis* PCL1606**			
Protein	**Protein size (aa)**	**Function**	**Protein**	**Identity PAO1 (%)**	**Protein size (aa)**	**Function**
PslA PA2231	478	Putative glycosyl transferase	**PCL1606_RS04765**	68.83	478	Capsular biosynthesis protein
PslB PA2232	488	Mannose-1-phosphate guanylyl transferase/ 6-phosphate isomerase	**PCL1606_RS04760**	76.56	482	Mannose-1-phosphate guanylyl transferase
PslC PA2233	303	Glycosyl transferase family 2 protein	**PCL1606_RS04755**	74.83	302	Glycosyl transferase
PslD PA2234	256	Polysaccharide biosynthesis/ export protein	**PCL1606_RS04750**	45.38	276	Polysaccharide biosynthesis protein
PslE PA2235	662	Lipopolysaccharide biosynthesis protein	**PCL1606_RS04745**	54.45	660	LPS biosynthesis protein
PslF PA2236	395	Glycosyl transferase	**PCL1606_RS04740**	66.07	393	Glycosyl transferase family 1
PslG PA2237	442	β-xylosidase	**PCL1606_RS04735**	57.59	449	β-xylosidase

PslH PA2238	402	Glycosyl transferase	**PCL1606_RS04730**	63.28	404	Glycosyl transferase
PslI PA2239	367	Glycosyl transferase family 4 protein	**PCL1606_RS04725**	52.46	367	Glycosyl transferase family 1
PslJ PA2240	478	O-antigen ligase-like membrane family protein	**PCL1606_RS04720**	55.03	465	Membrane protein
PslK PA2241	469	Murein biosynthesis integral membrane protein MurJ	**PCL1606_RS04710**	65.56	468	Membrane protein
PslL PA2242	355	Acyltransferase family protein	**PCL1606_RS04715**	0	273	Acetyltransferase
PslM PA2243	577	FAD-dependent oxidoreductase	***PCL1606_RS04265**	67.79	575	FAD binding protein
PslN PA2244	333	DNA topoisomerase B	***PCL1606_RS12970**	63.55	344	Eukaryotic DNA topoisomerase I, catalytic core
PslO PA2245	101	Hypothetical protein	-	-	-	-

*These genes are located outside the putative *psl*-like cluster.

The PA2231-PA2245 region of PAO1 encodes a Psl polysaccharide, and the PCL1606_RS04765-PCL1606_RS04710 region of PcPCL1606 was identified as similar. The PslM-like and PslN-like proteins seem to be encoded outside the *psl*-like cluster at PCL1606_RS04265 and PCL1606_RS12970, respectively. The *pslO* gene is missing,

Appendix 1

although it is not required to produce Psl in *P. aeruginosa* (Byrd *et al.*, 2009). The *pslL* gene of PAO1 encodes for an acyltransferase that has no identity with any protein encoded in the PcPCL1606 genome. However, the PCL1606_RS04710 gene, located within the *psl*-like cluster, encodes an acetyltransferase that may replace the role of PslL in PcPCL1606. In fact, this has already been illustrated in the *P. syringae* B728a strain, in which the acetyltransferase Psyr_3310 encoded by a gene located between *pslJ* and *pslK* may fulfil the normal function of *pslL* in *P. aeruginosa* strains (Mann *et al.*, 2012). The table shows the percentage of identity between the proteins of the strains being compared, the size of the proteins as the number of amino acids (aa) and their putative function. Putative functions have been obtained from the Pseudomonas Genome Database (https://www.pseudomonas.com/).

Table S13. Protein domains encoded by the *psl*-like gene cluster of *Pseudomonas chlororaphis* PCL1606.

Protein	Domains	Domain position	Domain description
PCL1606_RS04765 (PslA-like)	CoA_binding_3 Bac_transf	70-248 284-472	CoA binding Bacteria sugar transferase
PCL1606_RS04760 (PslB-like)	NTP_transf MannoseP_isomer	9-295 325-475	Nucleotidyl transferase Mannose-6-phosphate isomerase
PCL1606_RS04755 (PslC-like)	Glyco_transf_2_3	5-171	Glycosyltransferase like family 2
PCL1606_RS04750 (PslD-like)	Poly_export	59-129	Polysaccharide biosynthesis/export protein
PCL1606_RS04745 (PslE-like)	No domains predicted	-	-
PCL1606_RS04740 (PslF-like)	Glyco_transf_1	190-365	Glycosyl transferase group 1
PCL1606_RS04735 (PslG-like)	Glyco_hydro_35	53-130	Glycosyl hydrolase family 5
PCL1606_RS04730 (PslH-like)	Glyco_trans_4_4 Glyco_trans_1_4	16-206 222-357	Glycosyl transferase 4-like domain Glycosyl transferase group 1

Appendix 1

PCL1606_RS04725 (PslI-like)	Glyco_trans_1	198-307	Glycosyl transferase group 1
PCL1606_RS04720 (PslJ-like)	Wzy_C	252-380	O-Antigen ligase
PCL1606_RS04715	Hexapep	201-236	Bacterial transferase hexapeptide (six repeats)
PCL1606_RS04710 (PslK-like)	MurJ	28-443	Lipid II flippase MurJ
PCL1606_RS04265 (PslM-like)	FAD_binding_2	15-554	FAD binding domain
***PCL1606_RS12970 (PslN-like)**	DNA topoisomerase	95-295	Eukaryotic DNA topoisomerase I, catalytic core

*These genes are located outside the putative *psl*-like cluster.

Table S14. Protein domains encoded by the *psl* gene cluster of *Pseudomonas aeruginosa* PAO1.

Protein	Domains	Domain position	Domain description
PslA	CoA_binding_3 Bac_transf	70-248 284-472	CoA binding Bacteria sugar transferase
PslB	NTP_transf MannoseP_isomer	9-296 325-475	Nucleotidyl transferase Mannose-6-phosphate isomerase
PslC	Glyco_transf_2_3	3-220	Glycosyltransferase like family 2
PslD	Poly_export	49-129	Polysaccharide biosynthesis/export protein
PslE	GNVR	403-479	G-rich domain on putative tyrosine kinase
PslF	Glyco_transf_1	192-365	Glycosyltransferase group 1
PslG	Cellulase	48-285	Glycosyl hydrolase family 5
PslH	Glyco_trans_4_4 Glyco_trans_1_4	16-206 222-359	Glycosyltransferase 4-like domain Glycosyltransferase group 1
PslI	Glyco_trans_4 Glyco_trans_1_4	17-183 204-308	Glycosyltransferase family 4 Glycosyltransferase group 1

PslJ	No domains predicted	-	-
PslK	MurJ	30-442	Lipid II flippase MurJ
PslL	Acyl_trans_3	7-322	Acyltransferase family
PslM	FAD_binding_2	14-549	FAD binding domain
PslN	Topoisom_I	94-266	Eukaryotic DNA topoisomerase I, catalytic core
PslO	No domains predicted	-	-

Table S15. Strains belonging to the *Pseudomonas chlororaphis* species that contain a *psl*-like gene cluster. The strains used in the phylogenetic analysis have been highlighted in bold.

Strain	Isolation	Accession number
***Pseudomonas chlororaphis* PCL1606**	Rhizosphere	NZ_CP011110.1
Pseudomonas chlororaphis FW305-25	-	NZ_FMCZ00000000.1
Pseudomonas chlororaphis HT66	Root	NZ_ATBG00000000.1
Pseudomonas chlororaphis 189	Soil	NZ_CP014867.1
***Pseudomonas chlororaphis* O6**	-	NZ_CM001490.1
Pseudomonas chlororaphis 48B8	Soil	NZ_MOAO00000000.1
Pseudomonas chlororaphis ATCC 13985	-	NZ_LT629738.1
Pseudomonas chlororaphis ATCC 17415	Soil	NZ_CP027714.1
Pseudomonas chlororaphis B25	White and red clover	NZ_CP027753.1
Pseudomonas chlororaphis L19	Soil	NZ_LNTS00000000.1
Pseudomonas chlororaphis LBS 160603	Soil	NZ_QJRW00000000.1
Pseudomonas chlororaphis LMG 21630	-	NZ_LT629747.1
Pseudomonas chlororaphis strain LZHT5	Soil	NZ_CP025309.1
Pseudomonas chlororaphis NCTC 7357	-	NZ_LR134334.1
Pseudomonas chlororaphis NCTC 10686	-	NZ_UGUQ00000000.1
***Pseudomonas chlororaphis* PA23**	Root	NZ_CP008696.1
Pseudomonas chlororaphis PbSt2	Rhizosphere	NZ_CP027716.1
Pseudomonas chlororaphis PCL1601	Rhizosphere	NZ_MSCT00000000.1
Pseudomonas chlororaphis TAMOak81	-	NZ_CP027713.1
Pseudomonas chlororaphis YL1	Rhizosphere	NZ_AWWJ00000000.1
Pseudomonas chlororaphis subsp. aurantiaca StFRB508	Leaf	NZ_AP014623.1
Pseudomonas chlororaphis subsp. aurantiaca 449	Rhizosphere	NZ_CP027741.1
Pseudomonas chlororaphis subsp. aurantiaca CW2	Rhizosphere	NZ_CP027743.1

Pseudomonas chlororaphis subsp. aurantiaca M12	Rhizosphere	NZ_CP027715.1
Pseudomonas chlororaphis subsp. aurantiaca PCM2210	Rhizosphere	NZ_CP027717.1
Pseudomonas chlororaphis subsp. aurantiaca JD37	Soil	NZ_CP009290.1
Pseudomonas chlororaphis subsp. aurantiaca PB-St2	Sugar cane	NZ_AYUD00000000.1
Pseudomonas chlororaphis subsp. aureofaciens 66	Rhizosphere	NZ_CP027747.1
Pseudomonas chlororaphis subsp. aureofaciens C50	Rhizosphere	NZ_CP027722.1
Pseudomonas chlororaphis subsp. aureofaciens P2	Root	NZ_CP027719.1
Pseudomonas chlororaphis subsp. aureofaciens ChPhzTR38	Root	NZ_CP027752.1
Pseudomonas chlororaphis subsp. aureofaciens ChPhzS23	Rhizosphere	NZ_CP027748.1
Pseudomonas chlororaphis subsp. aureofaciens NBRC 3521	Bulk soil	NZ_CP027738.1
Pseudomonas chlororaphis subsp. aureofaciens 30-84	Bulk soil	NZ_CP027738.1
Pseudomonas chlororaphis subsp. chlororaphis GP72	Rhizosphere	NZ_AHAY00000000.1
Pseudomonas chlororaphis subsp. chlororaphis DSM50083	Plate contaminant	NZ_CP027712.1
Pseudomonas chlororaphis subsp. chlororaphis LMG5004	Plate contaminant	NZ_LHVC00000000.1
Pseudomonas chlororaphis subsp. chlororaphis NBRC3904	Rhizosphere	NZ_BCZX00000000.1
Pseudomonas chlororaphis subsp. chlororaphis ATCC9446	Root	NZ_NBAT00000000.1
Pseudomonas chlororaphis subsp. piscium ATCC17809	-	NZ_CP027709.1
Pseudomonas chlororaphis subsp. piscium DSM21509	European perch intestine	NZ_CP027707.1
Pseudomonas chlororaphis subsp. piscium ZJU60	-	NZ_CP027656.1
Pseudomonas chlororaphis subsp. piscium ChPhzS140	Bulk soil	NZ_CP027740.1
Pseudomonas chlororaphis subsp. piscium DTR133	Rhizosphere	NZ_CP027735.1

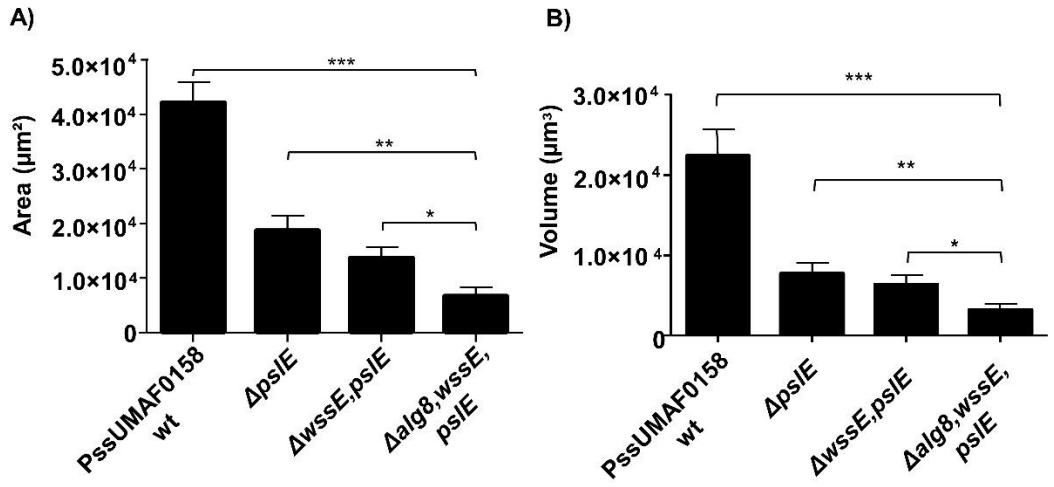

Figure S1. Flow-cell chamber experiments. a) Area covered (µm²) by 48 h biofilms; b) Volume covered (µm³) by 48 h biofilms. PssUMAF0158 wild-type (PssUMAF0158 wt), PssUMAF0158 *ΔpslE* single mutant (*ΔpslE*), PssUMAF0158 *ΔwssE,pslE* double mutant (*ΔwssE,pslE*) and PssUMAF0158 *Δalg8,wssE,pslE* triple mutant (*Δalg8,wssE,pslE*) were tested. Statistical significance was assessed by two-tailed Mann–Whitney test (*p<0.05, **p<0.01, ***p<0.001). Error bars correspond to the standard error of the mean (s.e.m).

APPENDIX 2

Published papers included in this dissertation

Heredia-Ponce, Z., de Vicente, A., Cazorla, F.M. & Gutiérrez-Barranquero, J.A. (2021). Beyond the wall: exopolysaccharides in the biofilm lifestyle of pathogenic and beneficial plant-associated *Pseudomonas*. ***Microorganisms***, 9, 445.

Heredia-Ponce, Z., Gutiérrez-Barranquero, J.A., Purtschert-Montenegro, G., Eberl, L., de Vicente, A. & Cazorla, F.M. (2021). Role of extracellular matrix components in the formation of biofilms and their contribution to the biocontrol activity of *Pseudomonas chlororaphis* PCL1606. ***Environmental Microbiology***.

Heredia-Ponce, Z., Gutiérrez-Barranquero, J.A., Purtschert-Montenegro, G., Eberl, L., Cazorla, F.M. & de Vicente, A. (2020) Biological role of EPS from *Pseudomonas syringae* pv. syringae UMAF0158 extracellular matrix, focusing on a Psl-like polysaccharide. ***NPJ Biofilms Microbiomes*** 6(1), 37.

Other contributions during PhD related to the dissertation's topic

Aprile, F., **Heredia-Ponce, Z**., Cazorla, F.M., de Vicente, A., Gutiérrez-Barranquero, J.A. (2020). A large Tn7-like transposon confers hyper-resistance to copper in *Pseudomonas syringae* pv. syringae. ***Applied and Environmental Microbiology*** 87, e02528-20

Calderón, C. E., Tienda, S., **Heredia-Ponce, Z**., Arrebola, E., Cárcamo-Oyarce, G., Eberl, L. & Cazorla, F.M. (2019). The compound 2-hexyl, 5-propyl resorcinol has a key role in biofilm formation by the biocontrol rhizobacterium *Pseudomonas chlororaphis* PCL1606. ***Frontiers in Microbiology*** 10, 369.

Caro-Astorga, J., Álvarez-Mena, A., Hierrezuelo, J., Guadix, J.A., **Heredia-Ponce, Z**., Arboleda-Estudillo, Y., González-Munoz, E., de Vicente, A. & Romero, D. (2020). Two genomic regions encoding exopolysaccharide production systems have complementary functions in *B. cereus* multicellularity and host interaction. ***Scientific Reports*** 10(1), 1000.

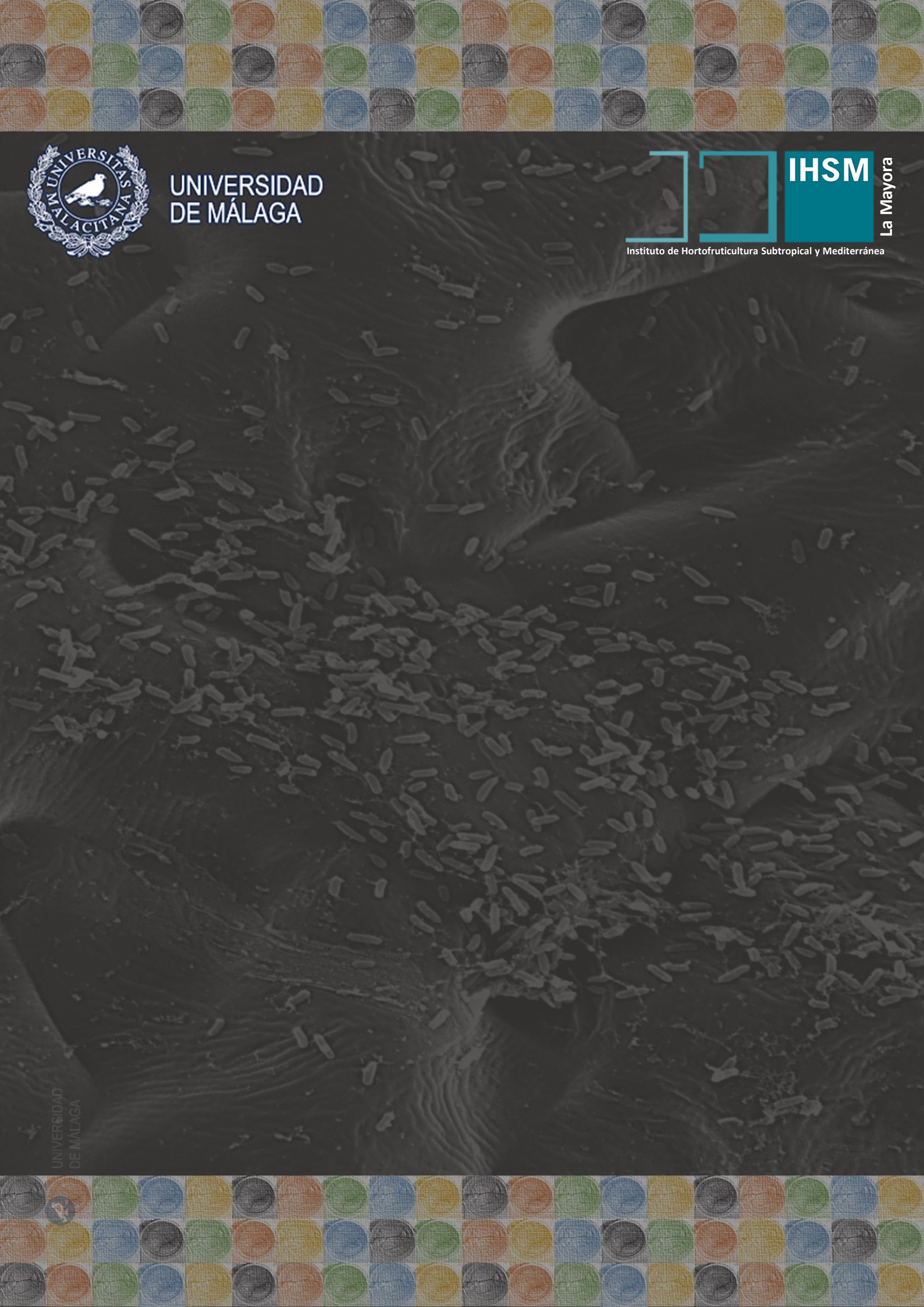
UNIVERSIDAD
DE MÁLAGA
IHSM
La Mayora
Instituto de Hortofruticultura Subtropical y Mediterránea
UNIVERSIDAD
DE MÁLAGA